UNIVERSIDADE FEDERAL DE SÃO CARLOS
CENTRO DE CIÊNCIAS BIOLÓGICAS E DA SAÚDE
PROGRAMA DE PÓS-GRADUAÇÃO EM GENÉTICA EVOLUTIVA E BIOLOGIA MOLECULAR

WELLISON JARLES DA SILVA DINIZ

IDENTIFICAÇÃO DE REDES GÊNICAS DE COEXPRESSÃO E DOS MECANISMOS REGULATÓRIOS ASSOCIADOS À COMPOSIÇÃO MINERAL E QUALIDADE DE CARNE EM BOVINOS

SÃO CARLOS - SP
2019

WELLISON JARLES DA SILVA DINIZ

IDENTIFICAÇÃO DE REDES GÊNICAS DE COEXPRESSÃO E DOS MECANISMOS REGULATÓRIOS ASSOCIADOS À COMPOSIÇÃO MINERAL E QUALIDADE DE CARNE EM BOVINOS

Thesis submitted in partial fulfillment of the requirements for the Doctor of Philosophy degree in Evolutionary Genetics and Molecular Biology from the Graduation Program of Evolutionary Genetics and Molecular Biology, Center for Biological and Health Sciences in the Federal University of São Carlos.

Advisor: Prof. Dr. Luciana Correia de Almeida Regitano

São Carlos-SP
2019

UNIVERSIDADE FEDERAL DE SÃO CARLOS

Centro de Ciências Biológicas e da Saúde
Programa de Pós-Graduação em Genética Evolutiva e Biologia Molecular

Folha de Aprovação

Assinaturas dos membros da comissão examinadora que avaliou e aprovou a Defesa de Tese de Doutorado do candidato Wellison Jarles da Silva Diniz, realizada em 11/10/2019:

Luciana

Profa. Dra. Luciana Correia de Almeida Regitano
EMBRAPA

Prof. Dr. Marcos Roberto Chiaratti
UFSCar

Lisandra Marques Gava Borges

Profa. Dra. Lisandra Marques Gava Borges
UFSCar

p/ Luciana

Profa. Dra. Sonia Cristina da Silva Andrade
USP

Profa. Dra. Mirele Daiana Poleti
USP

This thesis is **dedicated** to my family for all the encouragement and support to pursue my dreams, and to my dearest wife, Priyanka, for all the love and abetting through the Ph.D. path.

ACKNOWLEDGMENTS

Through these four years of Ph.D. course, I was lucky to meet and have had the pleasure to collaborate with exceptional professionals who guided me to make great personal and scientific achievements.

I am profoundly grateful to all of those who contributed to my learning, direct or indirectly, and unfortunately, I'm not able to name all of them here. However, be sure that you were important and are part of this achievement.

I am grateful to my advisor, Prof. Dr. Luciana C. A. Regitano, for all the guidance, mentoring, friendship, support, and trust during the Ph.D. process.

I am also grateful to Prof. Dr. Haja N. Kadarmideen and the Quantitative Genomics, Bioinformatics and Computational (Systems) Biology (QBC) group, DTU Compute at the Technical University of Denmark (DTU), for all the support and guidance during my internship abroad.

Thank you to Prof. Dr. Luiz L. Coutinho and his research group (Aline Cesar, Mierele Poleti, and Bárbara Vignato) for this fruitful collaboration.

I want to thank the financial support grants 2015/09158-1, 2017/20761-7, and 2012/23638-8 from the São Paulo Research Foundation (FAPESP) and the Coordenação de Aperfeiçoamento de Pessoal de Nível Superior - Brasil (CAPES) - Finance Code 001.

I am also grateful to the Federal University of São Carlos and Embrapa Pecuária Sudeste staff for all the support.

A very special thanks goes out to my friends who collaboratively shared the challenges and achievements: Andressa Lima, Carlos Buss, Juliana Afonso, Marina Ibelli, Priscila Neubern, Tainã Cardoso, Bruno Nascimento, Jéssica Malheiros, Karina, Jennifer, Adriana Somavilla, Polyana Tizioto, and Marcela de Souza. Also, those who were not directly working with me, but were part of this challenge: Leandro, Lívia, Verônica, Paulo, Monalisa, Pedro, and Laís…

I owe profound gratitude to my friend Ludwig Geistlinger, who have been so supportive and always available to guide me through R codes and programming challenges.

Heartfelt thanks go to Gianluca Mazzoni, this great friend who worked hard with me and has always been generous by sharing his knowledge. Thank you so much for the enjoyable and memorable moments in Copenhagen.

I also would like to thank all the friends from QBC group: Victor, Xiao, and Marcus.

To my Italian friends Claudia, Francesca, Mattia, Monica, and Felice for all the amazing moments that we shared.

To Flavia Aline and João Paulo for the friendship and the opportunity to be part of your family, my warmest thank you.

With a lovely thank you to Priyanka Banerjee, my wife, my partner in life and researcher to all the support, great moments, and constant encouragement.

Finally, to my family for their support, belief, encouragement, and help on this Ph.D. mission, thank you so much.

Thanks to you all for the support and to make it real!!

"Like musicians, like mathematicians—like elite athletes—scientists peak early and dwindle fast. It isn't creativity that fades, but stamina: science is an endurance sport. To produce that single illuminating experiment, a thousand nonilluminating experiments have to be sent into the trash; it is battle between nature and nerve".

Mukherjee, S.

(The Gene: An Intimate History)

RESUMO

De caráter complexo, as características de qualidade de carne e composição mineral são reguladas geneticamente. Evidências crescentes sugerem que os minerais têm papel central em funções regulatórias e fisiológicas relacionadas à maciez e deposição de gordura em bovinos. Além disso, miRNAs e genes têm sido apontados como potenciais reguladores desses fenótipos. No entanto, ainda pouco se sabe a respeito dessa interação e seu efeito sobre a qualidade da carne em bovinos. Desse modo, a fim de explorar vias regulatórias, genes e miRNAs candidatos e suas relações com o metabolismo muscular e mineral em novilhos Nelore, nós integramos dados de expressão de genes e miRNAs, eQTLs, conteúdo de minerais e características de qualidade de carne baseados em redes de coexpressão. Para tanto, os perfis de expressão global de mRNAs (n = 200) e miRNAs (n = 50), obtidos por meio de RNA-Seq, foram utilizados separadamente para construir redes de coexpressão utilizando o pacote do R WGCNA (*Weighted gene co-expression network analysis*). Os dados fenotípicos de macro (Ca, K, Mg, Na, P, S) e micro minerais (Co, Cr, Cu, Fe, Mn, Se, Zn), assim como de qualidade de carne (gordura intramuscular, maciez, e pH da carne) foram também integrados a fim de identificar módulos de genes/miRNAs associados a estas características. Mediante a clusterização de 11.996 genes e 343 miRNAs, nós identificamos, com base em um modelo linear, 15 módulos de genes e nove de miRNAs associados a pelo menos um dos fenótipos ($p \leq 0,05$). Nós identificamos 82 genes candidatos potenciais reguladores dos módulos associados aos fenótipos avaliados. A partir da análise funcional, nós identificamos vias biológicas enriquecidas relacionadas ao metabolismo energético e protéico, tais como AMPK, mTOR, insulina e hormônio da tireoide. Nós também integramos os módulos gênicos com os de miRNAs e apontamos 1.815 genes únicos, alvos de 41 miRNAs. Ca e Fe mostraram-se fortemente regulados, principalmente pelos miRNAs da família miR-29. Além das vias previamente apontadas, o enriquecimento funcional dos genes alvo também indicou a participação de vias como o fator 1 induzido por hipóxia, ferroptose e p53. Genes chave envolvidos na homeostase do Fe, tais como receptor da transferrina (*TFRC*), proteina de ligação do elemento responsivo ao ferro (*IREB2*) e transferrina (*TF*) foram identificados, bem como envolvidos com metabolismo de lipídeos. De modo geral, existe uma intricada relação entre qualidade de carne e metabolismo mineral, bem como destaca-se o papel fundamental dos miRNAs regulando os genes alvo. Estudos adicionais são necessários para investigar o efeito de diferentes níveis de suplementação mineral na expressão gênica e na qualidade de carne.

Palavras-chaves: Análise de redes, genômica integrativa, maciez da carne, metabolismo mineral.

ABSTRACT

Identification of co-expression gene networks and regulatory mechanisms related to mineral composition and meat quality in bovine

Meat quality and mineral composition are complex traits genetically regulated. Growing evidence suggests that minerals play a central role in regulatory and physiological functions related to meat tenderness and fat deposition in cattle. Furthermore, miRNAs and genes have been identified as potential regulators of these traits. However, there is a lack of knowledge regarding the interplay among miRNA-gene expression-mineral metabolism in cattle. Thus, to explore regulatory pathways, candidate genes and miRNAs, and their relationships to muscle and mineral metabolism in Nelore steers, we integrated gene and miRNA expression data, eQTLs, mineral content, and meat quality traits based on coexpression networks. To this end, the muscle genome-wide expression profiles of mRNAs (n = 200) and miRNAs (n = 50), obtained by RNA-Seq, were used separately to construct co-expression networks using the WGCNA (Weighted gene co-expression network analysis) R package. Phenotypic data of macro (Ca, K, Mg, Na, P, S) and micro minerals (Co, Cr, Cu, Fe, Mn, Se, Zn), as well as meat quality (intramuscular fat, meat pH, and tenderness) were also integrated to identify gene/miRNAs modules associated to these traits. By clustering 11,996 genes and 343 miRNAs, we identified, based on a linear model, 15 and nine modules, respectively, associated with at least one trait ($p \leq 0.05$). We identified 82 potential candidate genes based on the module-phenotype association analysis. From the functional analysis, we identified as over-represented biological pathways related to energy and protein metabolism, such as AMPK, mTOR, insulin, and thyroid hormone. We also integrated the gene and miRNA modules, and pointed out 1,815 unique genes targets of 41 miRNAs. Among the minerals, Ca and Fe were strongly regulated, mainly by the miR-29 family. In addition to the pathways previously mentioned, the target genes functional over-representation analysis highlighted signaling pathways such as hypoxia-inducible factor 1, ferroptosis, and p53. Key genes involved in Fe homeostasis, such as transferrin receptor (*TFRC*), iron responsive element binding protein 2 (*IREB2*), and transferrin (*TF*) were identified, as well as those underlying lipid metabolism. Overall, there is a complex relationship between meat quality and mineral metabolism, as well as the fundamental role of miRNAs regulating target genes. Further studies are needed to investigate the effect of different levels of mineral supplementation in gene expression and meat quality traits.

Keywords: Integrative genomics, meat tenderness, mineral metabolism, network analysis.

LIST OF TABLES

LIST OF FIGURES

TABLE OF CONTENTS

INTRODUCTION

Animal breeding is based on the selection of individuals with high breeding values for economically important traits. However, most of the traits in livestock are controlled by many genes, each one with a small additive effect, along with the environment. Despite the progress in animal breeding based on the phenotypic records and pedigrees (GODDARD; HAYES, 2009), high-throughput “omics” technologies like genomics, transcriptomics, epigenomics, proteomics, and metabolomics have provided large amount of biological data to shed light on the genetic architecture of these complex traits (RITCHIE et al., 2015).

These approaches have provided new opportunities to select for difficult-to-improve traits (MATEESCU et al., 2013) such as nutrient profile and meat quality. Although genome-wide association studies (GWAS) have shown several chromosomal regions affecting those traits (MATEESCU et al., 2013; TIZIOTO et al., 2013, 2015; AHLBERG et al., 2014), it still challenging to identify the causal genes. Likewise, genome-wide transcriptomic analyses have identified genes with significant changes in its expression between experimental conditions (DINIZ et al., 2016; GONÇALVES et al., 2018). Also, miRNAs have emerged as modulators of the gene expression under different biological contexts as meat tenderness (KAPPELER et al., 2019) and fat deposition (OLIVEIRA et al., 2018). However, biological systems are a result of multiple and complex regulatory layers that contribute to determining the phenotype (DINIZ; CANDURI, 2017). To address the limitations from single-data-type approach (RITCHIE et al., 2015) systems biology methodologies have been proposed (SURAVAJHALA; KOGELMAN; KADARMIDEEN, 2016).

Systems biology presents a holistic approach to reach complete and informative questions about the genotype-phenotype relationship (DINIZ; CANDURI, 2017). The methods based on systems biology focuses on the integration of different ‘omics’ layers (SURAVAJHALA; KOGELMAN; KADARMIDEEN, 2016) by modeling the interactions among them (*e.g.,* DNA variation, gene expression and methylation, miRNA expression, etc.) to identify key genomics factors and shed light on the mechanism or causal relationships of complex-trait architecture (RITCHIE et al., 2015). Among the approaches, Weighted Gene Co-expression Network Analysis (WGCNA) are increasingly being employed to identify the connection among genes and to detect subsets (modules) of tightly connected genes (ZHAO et al., 2010). Based on the concept of a scale-free network, WGCNA general framework is composed by the following steps: (i) network construction, (ii) module detection, (iii) module-trait association, and (iv) network visualization (LANGFELDER; HORVATH, 2008).

Herein, we combined multiple omics data under a systems biology framework to identify putative drivers (miRNAs and genes) associated with muscle mineral concentration (macro and micro minerals), regulatory networks, as well as the role of minerals in pathways underpinning meat quality traits (intramuscular fat content, meat pH, and tenderness). Both muscle mineral metabolism and meat quality traits are interrelated (DINIZ et al., 2019), genetically determined (AHLBERG et al., 2014), and the heritability ranges from moderate to high (TIZIOTO et al., 2015). Growing evidence has shown an interplay among genes, miRNAs, and mineral content in pathways involved with protein synthesis and fatty acid metabolism (DAUNCEY; KATSUMATA; WHITE, 2004; BECKETT et al., 2014). Additionally, genes and miRNAs have a putative role in mineral homeostasis based on a bi-directional regulatory circuit (DAVIS; CLARKE, 2013; BECKETT et al., 2014). However, to date it is still unclear not only the genetic basis of mineral homeostasis in muscle and its interplay with meat quality but also the miRNA-gene-mineral relationship in Nelore cattle, the major breed to beef production in Brazil.

The present Ph.D. was based on the hypothesis that gene-miRNA co-expression networks underly both muscle mineral homeostasis and meat quality traits in Nelore cattle. To elucidate this hypothesis, from muscle expression profile, we first built gene and miRNA co-expression modules relying on WGCNA approach. Then, a linear association was fitted to identify modules biologically associated with the phenotypes. As phenotypes, we evaluated the concentration of macro minerals [calcium (Ca), magnesium (Mg), phosphorus (P), potassium (K), sodium (Na), sulfur (S)], and micro minerals [chromium (Cr), cobalt (Co), copper (Cu), manganese (Mn), selenium (Se), iron (Fe), and zinc (Zn)], meat pH, tenderness, and intramuscular fat content. Further, we carried out a multi-level miRNA-gene module integration, selected the anticorrelated modules, intersected it with the target miRNA prediction, and carried out a functional over-representation analysis on the miRNA target genes.

Based on state of the art, the **first chapter** consists of a literature review (Cross talk between mineral metabolism and meat quality: a systems biology overview) addressing the following questions: (i) Are the meat quality traits and mineral content interdependent and under the same regulatory mechanisms? (ii) How do the genes, miRNAs, and minerals interact with each other? (iii) Which are the modulated pathways, how it can affect muscle growth, lipid metabolism, mineral homeostasis, and consequently, meat quality traits?

The findings from the data analysis carried out through this Ph.D. comprises chapters 2 and 3 (scientific papers), as follows:

Chapter 2 *(Detection of co-expressed pathway modules associated with mineral concentration and meat quality in Nelore cattle)*: To explore regulatory pathways, putative gene regulators, and to study their relationship with muscle and mineral metabolism in Nelore skeletal muscle, we integrated gene expression, eQTL variation, mineral concentration (macro and micro minerals), and meat quality traits (intramuscular fat content, tenderness, and meat pH) based on a network approach.

As the hypothesis for this study, we stated: Co-expressed genes are associated with the mineral concentration in muscle and meat quality traits such as tenderness, meat pH, and intramuscular fat content;

Chapter 3 *(Interplay among miR-29 family, mineral metabolism, and gene regulation in Bos indicus muscle)*: We carried out a miRNA co-expression and multi-level miRNA-mRNA integration analyses to uncover the pathways and regulatory networks underlying mineral concentration in Nelore cattle muscle.

As the hypothesis for this study, we stated: Regulatory gene-miRNA networks underly mineral concentration in muscle and meat quality related-pathways.

REFERENCES

AHLBERG, C. M. et al. Genome wide association study of cholesterol and poly- and monounsaturated fatty acids, protein, and mineral content of beef from crossbred cattle. **Meat Science**, v. 98, n. 4, p. 804–814, dez. 2014.

BECKETT, E. L. et al. The role of vitamins and minerals in modulating the expression of microRNA. **Nutrition research reviews**, v. 27, p. 94–106, 2014.

DAUNCEY, M. J.; KATSUMATA, M.; WHITE, P. Nutrition, hormone receptor expression and gene interactions: implications for development and disease. In: PAS, M. F. W.; EVERTES, M. E.; HAAGSMAN, H. P. (Ed.). **Muscle development of livestock animals: physiology, genetics and meat quality**. Wallingford: CABI, 2004. p. 419.

DAVIS, M.; CLARKE, S. Influence of microRNA on the maintenance of human iron metabolism. **Nutrients**, v. 5, p. 2611–2628, 2013.

DINIZ, W. J. da S. et al. Iron Content Affects Lipogenic Gene Expression in the Muscle of Nelore Beef Cattle. **PLOS ONE**, v. 11, n. 8, p. e0161160, 17 ago. 2016.

DINIZ, W. J. S.; CANDURI, F. REVIEW-ARTICLE Bioinformatics: an overview and its applications. **Genetics and Molecular Research**, v. 16, n. 1, p. 1–21, 2017

DINIZ, W. J. S. da S. et al. Detection of Co-expressed Pathway Modules Associated with Mineral Concentration and Meat Quality in Nelore Cattle. **Frontiers in Genetics**, v. 10, p. 210, 13 mar. 2019.

GODDARD, M. E.; HAYES, B. J. Mapping genes for complex traits in domestic animals and their use in breeding programmes. **Nature Reviews Genetics**, v. 10, n. 6, p. 381–391, jun. 2009.

GONÇALVES, T. M. et al. Gene Co-expression Analysis Indicates Potential Pathways and Regulators of Beef Tenderness in Nellore Cattle. **Frontiers in Genetics**, v. 9, p. 441, 5 out. 2018.

KAPPELER, B. I. G. et al. MiRNAs differentially expressed in skeletal muscle of animals with divergent estimated breeding values for beef tenderness. **BMC Molecular Biol**, v. 20, p. 1, 2019.

LANGFELDER, P.; HORVATH, S. WGCNA: An R package for weighted correlation network analysis. **BMC Bioinformatics**, v. 9, 2008.

MATEESCU, R. G. et al. Genome-wide association study of concentrations of iron and other minerals in longissimus muscle of Angus cattle. **Journal of Animal Science**, v. 91, p. 3593–3600, 2013.

OLIVEIRA, G. B. et al. Integrative analysis of microRNAs and mRNAs revealed regulation of composition and metabolism in Nelore cattle. **BMC Genomics**, v. 19, n. 1, p. 126, 7 dez. 2018.

RITCHIE, M. D. et al. Methods of integrating data to uncover genotype–phenotype interactions. **Nature Reviews Genetics**, v. 16, n. 2, p. 85–97, 2015.

SURAVAJHALA, P.; KOGELMAN, L. J. A.; KADARMIDEEN, H. N. Multi-omic data integration and analysis using systems genomics approaches: methods and applications in animal production, health and welfare. **Genetics Selection Evolution**, v. 48, n. 1, p. 38, 29 dez. 2016.

TIZIOTO, P. C. et al. Genome scan for meat quality traits in Nelore beef cattle. **Physiological Genomics**, v. 45, n. 21, p. 1012–1020, 1 nov. 2013.

TIZIOTO, P. C. et al. Detection of quantitative trait loci for mineral content of Nelore longissimus dorsi muscle. **Genetics Selection Evolution**, v. 47, n. 1, p. 15, 2015.

ZHAO, W. et al. Weighted gene coexpression network analysis: state of the art. **Journal of biopharmaceutical statistics**, v. 20, n. June 2013, p. 281–300, 2010.

Chapter 1

Cross talk between mineral metabolism and meat quality: a systems biology overview[1]

ABSTRACT

Meat quality has an inherent complexity due to the multiple interrelated causative factors and the layers of feedback regulation. Understanding the key factors and their interactions has been challenging, despite the availability of remarkable high throughput tools and techniques that have provided insights on muscle metabolism and the genetic basis of meat quality. Likewise, we have deepened our knowledge about mineral metabolism and its role in cell functioning. Regardless of these facts, complex traits like mineral content and meat quality have been studied under reductionist approaches. However, as these phenotypes arise from complex interactions among different biological layers (genome, transcriptome, proteome, epigenome, *etc.*), along with environmental effects, a holistic view and systemic-level understanding of the genetic basis of complex phenotypes is in demand. Based on state of the art, we addressed some of the questions regarding the interdependence of meat quality traits and mineral content. Furthermore, we sought to highlight potential regulatory mechanisms arising from the genes, miRNAs and mineral interactions, as well as the pathways modulated by this interplay affecting muscle, mineral metabolism, and meat quality. By answering these questions, we did not intend to give an exhaustive review, but to identify the key biological points, the challenges and benefits of integrative genomic approaches.

Keywords: calcium, iron, marbling, muscle, mineral, regulatory network, tenderness

---

[1] Diniz, WJS; Banerjee, P; Regitano, LCA. (2019). Cross talk between mineral metabolism and meat quality: a systems biology overview. *Physiological genomics*. 10.1152/physiolgenomics.00072.2019.

1.1. INTRODUCTION

Meat plays an essential role in the human diet. With an increasing consumption of animal protein, there has been a considerable pressure on the livestock sector to meet the growing demand for high-value animal protein. As the consumers are becoming more health-conscious about food and because the meat is a major source of several nutrients, including minerals, vitamins, proteins, and lipids, by improving its nutritional value it can meet the consumers' requirements (MATEESCU, 2014). Although all these nutrients are fundamental for biological processes, herein, we will focus on the role of minerals and its interplay with meat quality. Minerals are not only vital for humans but also have a recognized role in livestock systems, emphasized by their relevance in animal performance. They are essential for normal animal health, growth, reproduction, and production, acting in structural, physiological, catalytic, and regulatory functions (NRC, 2001; MCDOWELL, 2003; SUTTLE, 2010), working collaboratively as components of proteins, enzymes, or as enzymatic cofactors, in a range of biochemical processes (MCDOWELL, 2003; FLEET; REPLOGLE; SALT, 2011). Despite their essentiality, both mineral deficiency and overload are harmful (SUTTLE, 2010). Thereby, a balance among uptake, transport, metabolism, and storage processes are required to maintain narrow concentrations in the body (MCDOWELL, 2003).

The knowledge about mineral metabolism in livestock has improved over the years, mainly due to the advent of molecular biology, biochemistry tools, and nutritional science (SUTTLE, 2010). Based on that, a wide range of metabolic processes in which the minerals take part has been unveiled. Furthermore, the measurement and integration of environmental, physiological, and genomic information are now possible using high-throughput technologies and bioinformatic tools (FLEET; REPLOGLE; SALT, 2011; SURAVAJHALA; KOGELMAN; KADARMIDEEN, 2016). These approaches allow us to capture the functional knowledge of an organism and trace it back to the genome variation to understand the mineral homeostasis and their interplay with cell biology (FLEET; REPLOGLE; SALT, 2011).

Genomic approaches have shed light on the relationship among mineral content, muscle development, fat deposition, and meat quality traits (MATEESCU et al., 2013a; AHLBERG et al., 2014; DINIZ et al., 2016). These approaches have identified genomic regions affecting these traits (MATEESCU et al., 2013b; AHLBERG et al., 2014; TIZIOTO et al., 2015). However, there is a lack of knowledge concerning the genetic architecture, the metabolic process and the relationship among these traits. In this regard, new regulatory layers have been added to fill these gaps. A growing number of studies have pointed out minerals as modulators of genes (mRNA) and microRNAs (miRNA) expression, which in turn regulate mineral homeostasis in a feedback loop system (DAVIS; CLARKE, 2013; BECKETT et al., 2014).

Mineral content, genes, miRNAs, and several other environmental factors are part of the multifactorial system involved in the modulation of meat quality traits. By applying the available genomic tools, the nutritional composition of meat can be improved, impacting both human nutrition (MATEESCU, 2014) and animal performance. This review describes the role of minerals in meat quality traits, highlighting the putative mechanisms by which minerals interact with intramuscular fat content and tenderness. Additionally, we review the pathways underlying muscle development and lipid metabolism and their interaction with minerals, genes, and miRNAs.

1.2. MEAT QUALITY: A MULTIFACTORIAL SYSTEM

The most common definition of meat quality is the measure of characteristics like tenderness, fatness, juiciness, flavor, and color (MUCHENJE et al., 2009; MATEESCU; GARRICK; REECY, 2017) sought and valued by the consumer. By affecting the consumer’s acceptance, these attributes have an economic impact on the demand for the product. Among them, tenderness and fatness are the most impacting on consumer’s preference and will be focused here.

Biochemical, physical, histological, and nutritional factors may affect meat quality and were discussed elsewhere (MUCHENJE et al., 2009). The former, including the postmortem metabolic changes, are the main events affecting meat tenderness (MALTIN et al., 2003). For example, stress hormones, pH, and muscle glycolysis are interdependent and affect meat color, tenderness, water-holding capacity, and drip loss (MALTIN et al., 2003; MUCHENJE et al., 2009). Also, the calpain proteolytic system is central in postmortem proteolysis and meat tenderization process (MALTIN et al., 2003; BHAT et al., 2018). Regarding histological attributes, the type of muscle fiber is related to its metabolic properties, oxidative or glycolytic (DAUNCEY; KATSUMATA; WHITE, 2004), and eating quality (MALTIN et al., 2003). Concerning nutritional factors, intramuscular fat content (IMF) and fatty acid composition are involved in sensorial traits like flavor, taste, juiciness, and meat tenderness (MALTIN et al., 2003), besides their putative association with cardiovascular disease, stroke, and diabetes in humans (MICHA; WALLACE; MOZAFFARIAN, 2010).

The different processes affecting meat quality are dynamic, interdependent, and not fully understood. Factors such as age, sex, breed, muscle type, nutritional, and sanitary status (MALTIN et al., 2003; DAUNCEY; KATSUMATA; WHITE, 2004) must be considered in both muscle development and quantitative/qualitative meat attributes. While all these factors play a role in determining meat quality, diet is one factor that can be easily manipulated and has significant effects on meat nutritional composition (MALTIN et al., 2003). Thereby, elucidating the role of minerals on meat quality is of foremost relevance.

1.3. MINERALS IN LIVESTOCK: A GENERAL OVERVIEW

Mineral biochemistry and metabolic aspects were extensively reviewed in textbooks (MCDOWELL, 2003; SUTTLE, 2010), as well as in other papers used in this review. Thereby, we do not intend to address the biochemistry of each one of the minerals, which goes beyond the scope of this work. However, we will highlight the biological aspects necessary to understand the role of the minerals affecting meat quality in livestock.

1.3.1. Factors affecting mineral requirements

Significant differences are observed in mineral metabolism inherent to species, breed, and individual variation (MCDOWELL, 2003). Furthermore, age, sex, organ or tissue, and production system affects the nutritional requirements and mineral metabolism (NRC, 2001; GIUFFRIDA-MENDOZA et al., 2007; HOLLÓ et al., 2007; CABRERA et al., 2010). Variation in muscle mineral deposition from different crossbred, age, and sex was reported for beef cattle (GIUFFRIDA-MENDOZA et al., 2007). Also, increased storage of iron (Fe) and zinc (Zn) was described as a function of age in lambs (PANNIER et al., 2010), as well as calcium (Ca), Fe, and sodium (Na) in beef (BARGE et al., 2005). According to Pannier et. al. (2010), muscle development affects mineral deposition in lambs as the older animals have an increased proportion of oxidative fiber type. However, mineral variation across ages could be a confounding effect of growth rate, physiological state, and feeding system (TAJIK et al., 2010).

Among all the over-mentioned factors, nutritional management has a pivotal role in muscle mineral composition and growth. Although the diet is the primary source of minerals for livestock, some of its constituents can affect mineral uptake. Minerals interact among themselves, which can impair their absorption and bioavailability (SUTTLE, 2010). Nutritional status can modulate intrinsic muscle properties such as the number and type of myofibers (ODDY et al., 2001) and consequently, the mineral requirements. Slow-twitch fibers (type 1) have a predominant oxidative capacity and requires more mitochondria and Fe/cooper (Cu)-dependent proteins, which are involved with the electron transfer chain (CHOI; KIM, 2009). Thereby, factors affecting fiber type are also likely to affect mineral concentration (PANNIER et al., 2014).

1.3.2. Biological role of minerals in meat quality

Mineral-dependent enzymes with catalytic and regulatory roles have been a research focus as new functions are being unveiled in gene transcription and signaling regulation (SUTTLE, 2010). Growing evidence has pointed out the role of minerals in muscle metabolism, mainly related to energy production (MCDOWELL, 2003). Several mineral-dependent enzymes acting in the electron transfer chain were reported (CAMMACK; WRIGGLESWORTH; BAUM, 1990; SUTTLE, 2010). Fe-deficient rats decreased the cytochrome c and cytochrome oxidase activity, negatively affecting the aerobic metabolism muscle-skeletal capacity (MCLANE et al., 1981). Likewise, Van Dronkelaar et al. (2018) reported a significant mineral association [Ca, Fe, potassium (K), magnesium (Mg), phosphorus (P), selenium (Se), and Zn] with muscle mass and physical performance in elderly humans.

Besides the role in muscle energy metabolism, mineral-dependent enzymes are also involved in the post-mortem meat tenderization (MUCHENJE et al., 2009; BHAT et al., 2018). This process has been extensively studied and evidence suggests that myofibrillar protein proteolysis, mediated by proteases, is the key cause of meat tenderization (MALTIN et al., 2003). Calpains are endogenous calcium-dependent proteases pointed out as the primary drivers of protein turnover and aging tenderization (MALTIN et al., 2003; BHAT et al., 2018). Furthermore, genetic markers in the calpain (*CAPN*) gene were associated with Ca (TIZIOTO et al., 2014) and Fe (CASAS et al., 2014) content in beef. The genotypes of animals with tougher meat showed higher levels of Fe muscle content (CASAS et al., 2014). Genetic polymorphisms in the myostatin (*MST*) gene, which is involved with muscle fibers formation and adipogenic regulation (BAGATOLI et al., 2013), have also been associated with mineral content in different bovine tissues (MORRIS et al., 2013) and meat tenderness in lambs (BAGATOLI et al., 2013).

The interplay between minerals and IMF content was reported in lambs selected for lean meat yield, which showed reduced IMF, Fe, and Zn levels (PANNIER et al., 2014). Likewise, a moderate correlation of Fe and P with IMF was reported in beef (HOLLÓ et al., 2007). Moderate to strong correlations were identified among K and Fe with cholesterol, mono- (MUFA), and poly-unsaturated fatty acid (PUFA) in Angus cattle (AHLBERG et al., 2014). However, no significant genetic correlation was described among Fe, marbling score, and rib eye area in cattle (MATEESCU et al., 2013a). From these studies, it has been suggested that genomic selection could improve meat Fe content and fatty acid profile with no effect on carcass traits.

Growing evidence has suggested beneficial effects on adipogenesis based on chromium (Cr) supplementation (NAJAFPANAH et al., 2014; SUNG et al., 2015). Najafpanah et al. (2014) reported a reduced backfat thickness and increased muscle deposition on Cr-supplemented goats. Similar results were identified in crossbred pigs (PAMEI et al., 2014), whereas in cattle, Cr supplementation has shown discordant results. Sung et al. (2015) described positive effects of Cr supplementation on meat quality traits of Hanwoo cattle, while no effect was identified on backfat thickness, marbling score, and loin-eye area in Charolais (CHANG; MOWAT; SPIERS, 2010) or Angus (KNEESKERN et al., 2016) crossed steers.

Although the role of minerals, such as Cu, Zn, and Se, is well known in lipid metabolism (ENGLE, 2011; MEHDI; DUFRASNE, 2016), their supplementation have shown inconsistent results. No effect on fatty acid composition in Brangus cattle supplemented with Cu and Se was identified, despite a reduction in cholesterol levels (NETTO et al., 2014). Besides effects on cholesterol, a reduced backfat and increased PUFA levels were described in Cu-supplemented steers (ENGLE et al., 2000). Furthermore, Cu-supplemented goats showed a linear increase of shear force and IMF, but no effect on cholesterol levels (HUANG et al., 2014). Zn supplementation did not affect carcass traits nor growth performance of finishing steers (MCBETH et al., 2001; KESSLER et al., 2003). Likewise, Se supplementation had no effect on meat color and pH in sheep (LIBIÉN-JIMÉNEZ et al., 2015) nor in backfat thickness, MUFA or PUFA in Nelore steers (PEREIRA et al., 2012). Additionally, no effect was reported on growth performance, thawing, cooking or drip losses, and pH in cattle fed with different Se sources (SGOIFO ROSSI et al., 2015).

Sensorial traits such as taste, flavor, juiciness, and tenderness have been associated with Fe, Mg, manganese (Mn), P, and Se content (GARMYN et al., 2011; HERNANDEZ-CALVA et al., 2013). However, Nour et al. (1983) suggested that mineral concentration is a poor predictor of meat sensorial attributes. Despite varying with species/breed, form of the dietary mineral and supplementation levels, the results of mineral supplementation on meat quality traits in livestock do not deny their importance on these phenotypes. Furthermore, it is also necessary to pay attention that minerals do not act alone and most of these reported papers focused on single mineral analysis. Fleet, Replogle, and Salt (2011) highlighted that minerals are part of a complex network in which direct and indirect relationship happen and many functions are carried out simultaneously. Thereby, it is necessary to consider multiple mineral interactions when supplementing or testing their effect on meat quality.

1.3.3. Minerals on transcriptional regulation: a nutrigenomics viewpoint

Revolution on high-throughput technologies increased our understanding of the transcriptional gene regulation once information on multiple regulatory elements has been added to this process. Transcriptomic approaches have shed light on the complexity of mammalian transcriptome by unrevealing transcriptional and post-transcriptional mechanisms, including noncoding regulatory elements. Noncoding RNAs such as microRNAs (miRNAs) have ~22 nucleotides, and modulate gene translation by mRNA degradation and translational repression mechanisms (O'BRIEN et al., 2018). Although the canonical regulatory role of miRNAs is downregulating the translation of target genes, some studies have suggested that miRNAs can also increase gene expression (RITCHIE et al., 2009; SU; KLEINHANZ; SCHADT, 2014). By acting cooperatively and/or redundantly, miRNAs can regulate hundreds of gene targets and function as key sensors on gene expression networks (SU; KLEINHANZ; SCHADT, 2014; DAS; SEN, 2015).

Nutrigenomics has emerged showing the responsiveness of the genome to nutritional elements (DAS; SEN, 2015) and adding a new regulatory level on gene expression. As a branch of nutrigenomics, nutrimiRomics has also shown that nutrients, including minerals, can modulate the miRNA biogenesis (DAVIS; CLARKE, 2013; DAS; SEN, 2015). Moreover, interacting with responsive regulatory elements, minerals may change gene transcription by different mechanisms (COUSINS, 1999). Pathways underlying this complex regulatory system are still under study. To the best of our knowledge, minerals may have a direct effect on responsive transcription factors leading to gene activation or repression (COUSINS, 1999). Minerals indirectly regulate gene expression through miRNA synthesis, which may regulate their targets (DAVIS; CLARKE, 2013; BECKETT et al., 2014). In addition to these mechanisms, transition metals like Cu, Fe, and Zn can catalyze the production of reactive oxygen species (ROS), which in turn drives the gene expression and miRNA biogenesis (PEÑA and KISELYOV, 2015; MAGENTA et al., 2016).

Responsive genes like transcription factor EB, hypoxia-inducible factor 1-alpha and 3-alpha (*TFEB, HIF1A, HIF3A*) have been reported as metal-modulated and miRNA regulated (LI et al., 2006; PEÑA and KISELYOV, 2015). The HIF family is under thyroid hormone (TH) regulation (OTTO; FANDREY, 2008) and have also been associated with miRNA biogenesis (AZZOUZI et al., 2013; MAGENTA et al., 2016) by interacting with metals like Cu and Fe (LI et al., 2006). From this redundant regulation and pathway overlap, arises a complex feedback loop system to keep the mineral levels within a narrow range (Figure 1.1).

Mineral nutrigenomic studies in livestock have focused only on a reduced number of candidate genes (BENÍTEZ; NÚÑEZ; ÓVILO, 2018), mainly on those related to fat metabolism and mineral homeostasis (Table 1.1). However, the gene expression seems to be mineral/species/tissue-dependent. For example, the expression of peroxisome proliferator-activated receptor γ (*PPARγ*) gene was increased by Ca, Cr, and Zn supplementation, either *in vivo* or *in vitro* assays, in cattle or pig muscle (TOKACH et al., 2015; ZHANG et al., 2015; HERGENREDER et al., 2016). Mineral supplementation not only affects the genes involved in its homeostasis but also modulates the uptake of other minerals. Hansen et al. (2009) reported that pigs fed with high-Fe diet showed reduced absorption of Mn as a result of reduced expression of *DMT1* (divalent metal transporter 1) and *ZIP14* (zinc transporter ZIP14) genes, which code the transporters for both minerals. Se supplementation, besides affecting the expression of selenoproteins, increased the expression of apolipoprotein E (*APOE*) and lipoprotein lipase (*LPL*) genes in lambs *Longissimus dorsi* muscle (JUSZCZUK-KUBIAK et al., 2016). RNA-Seq results suggested reduced lipogenic activity in Nelore steers with low genetic values for muscle Fe content (DINIZ et al., 2016). Alike, Zn supplemented piglets showed higher IMF deposition due to the up-regulation of lipogenic and fatty acid transport genes (ZHANG et al., 2014b).

Figure 1.1. Overview of the potential mechanisms by which minerals can modulate gene expression.

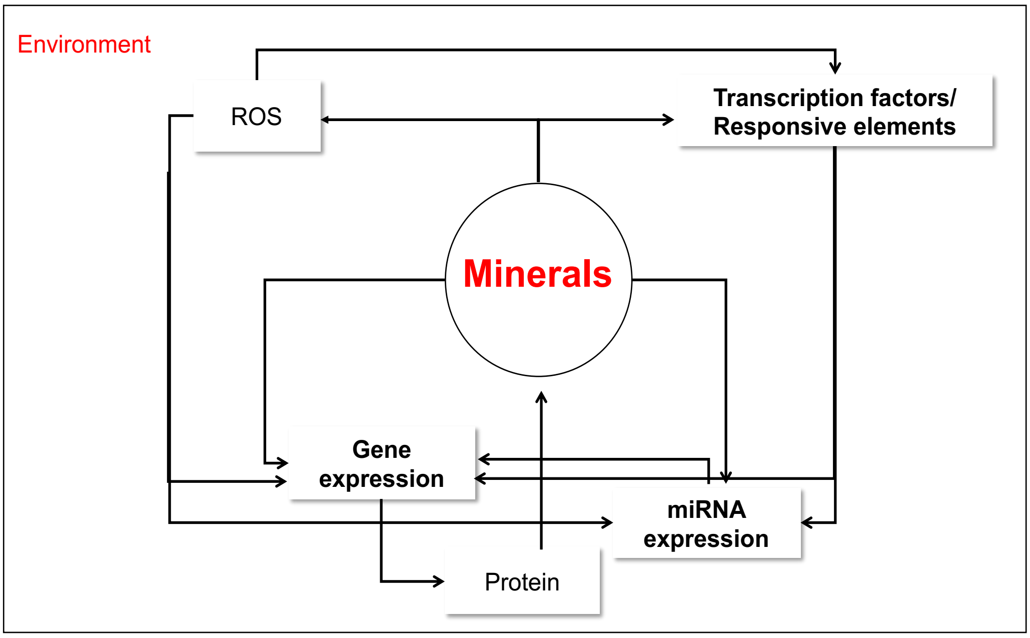

Minerals can activate or inhibit gene expression by interacting directly with mineral-responsive genes, miRNAs, and transcription factors (TFs). Indirectly, minerals can catalyze the reactive oxygen species (ROS) production leading to the activation of responsive TFs, miRNA biosynthesis, and gene expression. Increased miRNA biosynthesis is expected to downregulate target genes, which may change the protein abundance and mineral uptake. This redundant regulation suggests an intricate and complex feedback loop system to keep mineral levels at a narrow range.

Regarding minerals modulating miRNAs, most of the studies were carried out in animal models and focused on Ca (HARADA et al., 2014; MAGENTA et al., 2016), Fe (LI et al., 2012; DAVIS; CLARKE, 2013; RIPA et al., 2017) and Zn (RYU et al., 2011; ZHAO et al., 2016), with some reports on Mg (LOUVET et al., 2016) and Se (XING et al., 2015; FENG et al., 2018). In livestock, Jacometo et al. (2015) reported that organic trace minerals (Co, Cu, Mn, and Zn) modulated the expression of bta-miR-155 and bta-miR-125b in calves born from supplemented cows. Additionally, Ripa et al. (2017) showed that miR-29 was induced by Fe load and its repression is followed by increased expression of *TFRC* (transferrin receptor) and *IRP2* (iron-responsive element-binding protein), as well as increased Fe uptake. The miR-29 family also targets *YY1* and *SP1* transcription factors, which, in turn, modulate the *TF* (transferrin) gene expression (ADRIAN et al., 1996).

Table 1.1. Mineral nutrigenomics in livestock.

Mineral	Species	Tissue	Genes involved	Trait	Description/Reference
Ca	bovine	*l. muscle*	*PPARγ, CEBPA*	adipogenesis	Ca propionate supplementation effects on gene expression in Wagyu steers (ZHANG et al., 2015).
Cr	caprine	*l. muscle*, liver, visceral fat & subcutaneous	*ACC, DGAT1, FABP4, FAS, HSL, LEP*	lipid biosynthesis	Cr supplementation effects on gene expression in young male goats (SADEGHI et al., 2015).
	bovine	intramuscular adipocytes	*PPARγ, GLUT4*	adipogenesis	Cr propionate effects on gene expression in cultured bovine preadipocytes (TOKACH et al., 2015).
Cu	bovine	adipose	*ACC, LEP, SCD, UCP2*	lipid metabolism	Cu supplementation effects on gene expression in growing and finishing Angus steers (LEE; ENGLE; HOSSNER, 2002).
Fe	swine	duodenum, liver	*DMT1, SLC39A14 HAMP, FPN, ACO1 IRP2*	Fe and Mn metabolism	Fe effects on gene expression and the relationship with Mn and Cu in piglets (HANSEN et al., 2009).
	swine	duodenum, liver	16*	Fe uptake and homeostasis	Fe effects on the expression of candidate genes for Fe homeostasis (HANSEN et al., 2010).
Mg	swine	*l. muscle*	*CAPN1, CAST*	drip loss, meat color and tenderness	Mg aspartate supplementation and short-term transportation stress effects on gene expression (TANG et al., 2008).
Se	ovine	liver, *l. dorsi*	17*	lipid metabolism	Se effects on selenoproteins and lipid metabolism genes expression in growing lambs (JUSZCZUK-KUBIAK et al., 2016).
	chicken	liver	21*	regulation of selenoprotein	Se deficiency effects on selenoprotein gene expression in layer chickens (LIU et al., 2014).
Zn	swine	*l. muscle*	9*	fat metabolism	Zn effects on fat metabolism related gene expression in piglets (ZHANG et al., 2014b).
	bovine	culture cells	*PPARγ, SCD*	carcass traits, adipocyte differentiation	Zn source and level effects on gene expression from cultured stromal-vascular cells harvested from subcutaneous and intramuscular adipocytes (MCBETH et al., 2001).
	bovine	*semimembranosus*, subcutaneous muscle	13*	feedlot, carcass performance	Zn methionine and zilpaterol hydrochloride effects on myogenic and lipogenic gene expression in skeletal and adipose tissue (HERGENREDER et al., 2016).

*L, Longissimus muscle;**Numbers represent the amount of evaluated candidate genes.

Despite these studies, there is still a lack of knowledge concerning the interplay between miRNAs and minerals in livestock species. MiRNAs have a regulatory role in a wide range of biological functions including those related to fatty acid composition (OLIVEIRA et al., 2018; DE OLIVEIRA et al., 2019) and meat tenderness (KAPPELER et al., 2019). Considering all the facts that miRNAs can regulate several genes, affect multiple biological processes, and the mineral-gene-miRNA relationship, it opens up new opportunities to investigate the modulation of complex traits in animals. The results from this interplay, so far, suggest an intricate and complex process, affecting central signaling pathways in cellular and organismal metabolism.

1.3.4. Pathways underlying muscle growth and lipid metabolism

Molecular mechanisms underlying skeletal muscle maintenance involves an interplay among multiple signaling pathways (SMITH; MEYER; LIEBER, 2013). Mammalian target of rapamycin (mTOR) along with protein kinase B (Akt) are the main regulators of muscle cell development. Akt controls muscle growth through mTOR and GSK3 (glycogen synthase kinase 3), along with muscle protein degradation, via FoxO family and AMP-activated protein kinase (AMPK) (DU et al., 2009). Among other factors, thyroid hormone T_3 (triiodothyronine) can activate AMPK (YAMAUCHI et al., 2008) and mTOR by phosphorylation mediated by phosphatidylinositol 3-kinase (P13K)-Akt signaling cascade (CAO et al., 2005).

The interaction among these signaling pathways modulates gene expression and muscle development (DU et al., 2009). TH has a role in muscle growth, gene expression regulation, energy homeostasis, and metabolism (YAO et al., 2014). Moreover, TH negatively regulates mice muscle fiber type conversion indirectly via miR-133a (ZHANG et al., 2014a). Yao et al. (2014) pointed out several genes, either positively or negatively affected by TH. Likewise, the IGF/ growth hormone (GH) system affects body weight via muscle accretion (DAUNCEY; KATSUMATA; WHITE, 2004). Insulin also interacts with IGF1 and both stimulate protein synthesis (DØRUP, 2004). The major role of IGF1 modulating skeletal muscle growth is mediated by PI3K/Akt along with mTOR and AMPK pathways (DU et al., 2009; SCHIAFFINO; MAMMUCARI, 2011), whose interaction with minerals will be discussed below.

AMPK has a pivotal role in energy homeostasis by mediating muscle insulin sensitivity (DU et al., 2009), energy balance regulation, and lipid metabolism (MIHAYLOVA; SHAW, 2011). Its activation increases fatty acid oxidation by downregulating acetyl CoA carboxylase (*ACC*), which encodes a rate-limiting enzyme for long-chain fatty acid synthesis (JE et al., 2006). Under low energy levels, AMPK activates *PPARGC1A* (peroxisome proliferator-activated receptors GC1A) (SMITH; MEYER; LIEBER, 2013) and stimulates fatty acid oxidation in skeletal muscle (JE et al., 2006).

1.3.4.1. How minerals can affect muscle growth?

As previously discussed, TH has a wide range of metabolic functions, mainly driving gene transcription (DAUNCEY; KATSUMATA; WHITE, 2004), and has been pointed out as crucial for muscle growth (MEHDI; DUFRASNE, 2016). Among the minerals, Se, Fe, I (iodine), and Zn are essential for TH synthesis (ZIMMERMANN; KÖHRLE, 2002). Suboptimal Se, Fe, and Zn supplementation leads to a decreased activity of glutathione peroxidase (GOYENS et al., 1987), thyroperoxidase (HESS et al., 2002), and 1,5’-deiodinase (MAXWELL; VOLPE, 2007), respectively, and impairs TH synthesis and action (ZIMMERMANN; KÖHRLE, 2002). These authors also pointed out that Fe deficiency, with or without anemia, decreases the TH activity. Freake et al. (2001) evaluated the interactions between T_3 and Zn status in rats and found that both of them affect growth and reduce the serum IGF-1 levels.

According to Dørup (2004), minerals like K, Mg, in addition to Zn, have been associated with impaired IGF system function in rats. Likewise, reduced weight gain, feed intake, insulin, and IGF-1 plasma levels were reported in calves Fe-deficient (CEPPI; BLUM, 1994). Flyvbjerg et al. (1991) reported a strong correlation between K-deficiency and IGF-1 serum level in young rats, followed by a reduced weight gain. Growth inhibition, as well as reduced levels of IGF-1, were identified in Mg and Zn-deficient rats (DØRUP et al., 1991). Altogether, the deficiency of the over-mentioned minerals is related to growth retardation, which can be reversible by the supplementation of the lacking element (DØRUP, 2004).

mTOR and GSK3 signaling pathways are nutritional and hormonal regulated, and stimulate protein synthesis (SCHIAFFINO; MAMMUCARI, 2011). Also, some minerals have been associated with their activation. Ndong et al. (2009) reported a down-regulation in the Akt/mTOR pathway caused by Fe deficiency both in rats and COS-1 cells. Accordingly, Fe depletion was shown to decrease protein synthesis via mTOR downregulation and reduced Akt phosphorylation (WATSON et al., 2016). Akt phosphorylation inhibits GSK3 activity, which is also involved with muscle hypertrophy via inhibition of the eukaryotic translation initiation factor 2B (eIF2B) (SCHIAFFINO; MAMMUCARI, 2011). In addition to other nutrients, Liu and Yao (2016) pointed out minerals like Ca, Cl (chlorine), Cr, Fe, K, Na, Mn, Se and Zn among the factors modulating PI3K/Akt and/or GSK3 activities. It is noteworthy that among the pathways discussed here, mTOR plays a role in cellular Fe homeostasis based on the modulation of the transferrin receptor 1 (*TfR1*) stability (BAYEVA et al., 2012).

1.3.4.2. How minerals can affect lipid metabolism?

Due to the pleiotropic effect, AMPK and mTOR signaling pathways are also pivotal in lipid and carbohydrate metabolism (MIHAYLOVA; SHAW, 2011). Energy homeostasis is crucial not only for cell functioning but also dictates whether lipids will be synthesized or catabolized (CARON; RICHARD; LAPLANTE, 2015). Concerning meat quality, lipids affect consumers health perception, as well as juiciness and meat tenderness (MUCHENJE et al., 2009). Thus, understanding the role of the over-mentioned pathways and their interplay with minerals can be a tool to design nutritional strategies to improve meat quality and nutritional composition.

mTOR signaling regulates lipid synthesis through multiple effectors such as the sterol regulatory element-binding proteins (SREBPs), PPAR-γ, and Lipin1 (LAMMING; SABATINI, 2013). Once AMPK negatively modulates mTOR, it is feasible that AMPK activator may reduce fat deposition based on the mTORC1/SREBP mechanism affecting the lipogenic genes' expression (CARON; RICHARD; LAPLANTE, 2015). The interplay between mTORC1 and SREBPs is critical for the activation of lipogenic genes in response to nutrient intake (CARON; RICHARD; LAPLANTE, 2015). SREBPs are transcription factors that modulate *ACC* and *FASN* (fatty acid synthase) involved with fatty acid synthesis (MIHAYLOVA; SHAW, 2011). Additionally, stearoyl-CoA desaturase 1 (*SCD*) and lipoprotein lipase (*LPL*) have been considered as the rate-limiting enzymes for the de novo fatty acid synthesis (ROPKA-MOLIK et al., 2017). Tang et al. (2000) reported that Cu-deficient rats showed an increased expression of *FASN* and cholesterol 7-α hydroxylase genes through increased hepatic translocation of mature SREBP-1. Zn mediates the regulation of the SREBP-SCD axis in lipid metabolism, which is also affected by the antagonistic relationship between Zn and Fe (ZHANG et al., 2017). *SREBP1*, *FASN*, *SCD1,* and *FAD1* (fatty acid desaturase 1) genes were also downregulated in Fe-deficient rats (KAMEI et al., 2010). *SCD1* is an iron-containing enzyme and had its expression up-regulated in muscle under Fe overload conditions (RODRIGUEZ et al., 2007). Huang et al. (2017) reported PPAR as a key pathway regulating fat deposition and metabolism in cattle. These authors also pointed out candidate genes belonging to this pathway like *FABP4* (fatty acid-binding protein 4), *ACC, ELOVL5* (ELOVL fatty acid elongase 5), and *PLIN2* (perilipin 2).

The AMPK and mTOR pathways are pivotal in energy homeostasis and muscle growth. Despite the knowledge gained from the role of minerals in gene expression, the direction of these regulations and consequences on the signaling pathways are not exhaustively explored. Thereby, to elucidate the functional relationship between mineral metabolism and the IGF-1/PIK3/Akt/mTOR system represents a significant challenge to comprehend protein, energy metabolism, and mineral homeostasis.

1.4. SYSTEMS BIOLOGY OF COMPLEX PHENOTYPES

As broadly discussed heretofore, there are multiple interrelated factors and layers of feedback regulation involved in the relationship among minerals, genes, and miRNAs. Although it is known that this interplay affects important biological processes and phenotypes, it is still unclear how meat quality traits can be affected by these multiple interactions. New opportunities to understand the genetic basis of meat quality and to select for difficult-to-improve traits (MATEESCU et al., 2013a) - such as nutrient profile, have been provided by the emerging high-throughput “omics” technologies, like genomics and transcriptomics. These approaches have shown chromosomal regions and candidate genes affecting mineral and meat quality traits based on genome-wide association (MATEESCU et al., 2013a; MORRIS et al., 2013; TIZIOTO et al., 2013, 2015; AHLBERG et al., 2014) and transcriptomic analyses (DINIZ et al., 2016; GONÇALVES et al., 2018; OLIVEIRA et al., 2018; KAPPELER et al., 2019). However, these are reductionist approaches, which rely on a single regulatory layer without considering the interactions among themselves.

To address the limitations from single-data-type analysis (RITCHIE et al., 2015), systems biology approaches have been proposed (SURAVAJHALA; KOGELMAN; KADARMIDEEN, 2016). These approaches focus on the integration of different ‘omics’ layers by modeling the interactions among them (*e.g.,* DNA variation, gene expression, and methylation, miRNA expression, *etc.*) to identify key genomic factors and clarify the mechanisms or causal relationships of complex-trait architecture (RITCHIE et al., 2015). Different methodologies and analytical tools have been proposed for data integration [reviewed in (RITCHIE et al., 2015; VAN DAM et al., 2017)], mainly based on network correlation assumptions, including Weighted Gene Co-expression Network Analysis (WGCNA) (LANGFELDER; HORVATH, 2008), Partial Correlation with Information Theory (PCIT) (REVERTER; CHAN, 2008), and Association Weight Matrix (FORTES et al., 2010).

Although data integration studies based on systems biology approaches have increased and been fruitful, it is still emerging on the mineral nutrigenomics field. Nonetheless, a growing literature shows promising results by adopting integrative approaches to uncover the role of minerals and the relationship with miRNAs and gene expression. Based on data integration network approach, Feng et al. (2018) carried out an mRNA/miRNA expression profile assay unraveling miRNAs-target gene interactions in Se deficient rats. These authors reported, among other processes, the lipid metabolism and heart development as affected by the differentially expressed genes, as well as the interaction of Se deficiency and miRNA in cardiovascular disease development. Also, to overcome the limitations from the genome-wide association studies (GWAS) approach, Mateescu, Garrick, and Reecy (2017) adopted a combination of GWAS, Association Weight Matrix (AWM) and Partial Correlation and Information Theory (PCIT). Relying on this integrated approach, the authors explored the genetic basis of the carcass, meat quality, and composition traits, including the concentration of Ca, Fe, K, Mg, Na, P, and Zn. These authors highlighted among the over-represented functions calcium-related processes, apoptosis, and TGF-beta signaling underlying these traits. Genes like *CAPN*, *CAST*, among others*,* were pointed out as the main nodes in the networks, supporting their relevance to muscle growth, Ca metabolism, and adipogenesis (MATEESCU; GARRICK; REECY, 2017).

Also, our research group had directed efforts to integrate the muscle gene expression, expression quantitative trait loci variation, mineral concentration (macro and micro minerals) and meat quality traits (IMF, shear force, and meat pH) from Nelore steers to uncover the common pathways underlying these phenotypes (DINIZ et al., 2019). We described co-expressed modules potentially co-regulating meat tenderness, IMF, and minerals. Hub genes identified, including *ACC, FASN, PDE3B,* and *TGFB3*, were mainly acting in energy and protein metabolism (AMPK and mTOR) pathways (DINIZ et al., 2019). By adopting a multi-level miRNA-mRNA integrative approach, we reported for the first time a complex interplay between miRNAs and mRNAs to maintain mineral cellular homeostasis in *Bos indicus* muscle (DINIZ et al., under review)[2]. Based on WGCNA framework, we identified the interaction among 41

---

[2] Diniz, WJS; Banerjee, P; Mazzoni, G; Coutinho, LL; Cesar, ASM; Afonso, J; Gromboni, CF; Nogueira, ARA; Kadarmideen, HN; Regitano, LCA. Interplay among miR-29 family, mineral metabolism, and gene regulation in muscle. **Under review on Molecular Genetics and Genomics Journal** (MGAG-D-19-00536).

hub miRNAs, mainly from the bta-mir-29 and mir-154 families, and 1,185 target genes acting in the AMPK, insulin, mTOR, and thyroid hormone signaling pathways.

These few reports applying integrative approaches provide new insights regarding the several metabolic processes modulated by the relationship among genes, miRNAs, and minerals. However, in the face of the multiple factors and regulatory mechanisms, it is still essential to add new biochemical layers like protein and metabolites to uncover the regulators underpinning complex phenotypes.

1.5. FUTURE PERSPECTIVES

The understanding of complex phenotypes has increased over the years, mainly driven by the high throughput technologies emerged in the last decade. Additionally, the availability of omics data and the development of analytical methodologies have provided new insights on the black box underlying polygenic traits like meat quality and nutritional composition. Overall, the mineral role on nutrigenome and nutrimiRome are being elucidated. It has provided evidence of an intricated process able to modulate not only protein and energy metabolism but also those related with miRNA biosynthesis and mineral homeostasis. Although challenging to identify the major drivers affecting complex traits and the interplay among these regulatory levels, the opportunities provided by the systems biology approaches have changed our perception from a one-dimensional to a systems-level analysis. By considering the multilayer interaction, it has been possible to uncover major players not identified under reductionist approaches.

The genetic basis of meat quality and mineral nutrigenomics in livestock species is at its early stage. Several candidate genes and miRNAs have been identified both in livestock and animal models, and are already considered for animal breeding. Although genome-wide and high throughput analytical methods have increased our knowledge, we still need to improve our ability to deal with the amount and the complexity of the generated data. Beyond the need for cost reduction in data generation and storage, it is also important to improve the sensitivity and accuracy of analytical techniques. The development of practical application of methods like mass spectrometry, X-ray fluorescence, and next generation sequencing holds great impact in “omics” analyses and knowledge advances. Also, the development of statistical methods for earlier breeding value prediction for polygenic traits considering the impact of genetic mutations and distortions from the Mendelian inheritance model are still incipient. Some open questions need to be addressed in future studies concerning the minerals affecting the histochemical and biochemical meat quality traits. Additionally, mineral interaction with themselves and with other dietary components could help to elucidate their bioavailability and absorption. Thus, *in vitro* cell culture systems coupled with omics approaches (genomic, transcriptomic, metabolomic, proteomic, epigenomic, and lipidomic) can provide opportunities to shed light on these questions, and overcome the limitations for *in vivo* studies. Also, dose-response essays could be useful to determine the best level of supplementation and mineral combination to achieve beneficial effects on meat quality traits. Further research on comparative genomics and regulatory elements under a systems genomics level will allow a better understanding of the relationship among minerals, genome, and environment, as well as the individual response to mineral supplementation.

ACKNOWLEDGMENTS

The authors thank Simone C. Meo Niciura, Ph.D.; Tainã F. Cardoso, Ph.D.; and Juliana Afonso, Ph.D., for their critical comments and suggestions about the manuscript.

DISCLOSURES

No conflicts of interest, financial or otherwise, are declared by the authors.

GRANTS

This work was partly supported by the Coordenação de Aperfeiçoamento de Pessoal de Nível Superior – Brasil (CAPES) – Finance Code 001. LCAR was granted CNPq fellowship. WJSD was granted by São Paulo Research Foundation (FAPESP) grant# 2015/09158-1.

AUTHOR CONTRIBUTIONS

WJSD and PB wrote the first draft and prepared the figures. LCAR contributed ideas to the manuscript. WJSD, PB and LCAR edited and revised the manuscript. All authors read and approved the final manuscript.

1.6. REFERENCES

ADRIAN, G. S. et al. YY1 and Spl Transcription Factors Bind the Human Transferrin Gene in an Age-Related Manner. **The Journals of Gerontology Series A: Biological Sciences and Medical Sciences**, v. 51A, n. 1, p. B66–B75, 1 jan. 1996.

AHLBERG, C. M. et al. Genome wide association study of cholesterol and poly- and monounsaturated fatty acids, protein, and mineral content of beef from crossbred cattle. **Meat Science**, v. 98, n. 4, p. 804–814, dez. 2014.

AZZOUZI, H. El et al. The Hypoxia-Inducible MicroRNA Cluster miR-199a~214 Targets Myocardial PPARδ and Impairs Mitochondrial Fatty Acid Oxidation. **Cell Metabolism**, v. 18, n. 3, p. 341–354, 3 set. 2013.

BAGATOLI, A. et al. Expression of calpastatin and myostatin genes associated with lamb meat quality. **Genetics and Molecular Research**, v. 12, n. 4, p. 6168–6175, 2013.

BARGE, M. T. et al. Preliminary results on mineral content of some beef muscles. **Italian Journal of Animal Science**, v. 4, n. sup2, p. 272–274, 3 jan. 2005.

BAYEVA, M. et al. mTOR Regulates Cellular Iron Homeostasis through Tristetraprolin. **Cell Metabolism**, v. 16, n. 5, p. 645–657, nov. 2012.

BECKETT, E. L. et al. The role of vitamins and minerals in modulating the expression of microRNA. **Nutrition research reviews**, v. 27, p. 94–106, 2014.

BENÍTEZ, R.; NÚÑEZ, Y.; ÓVILO, C. Nutrigenomics in Farm Animals. **Journal of Investigative Genomics**, v. 4, n. 1, 2018.

BHAT, Z. F. et al. Role of calpain system in meat tenderness: A review. **Food Science and Human Wellness**, v. 7, n. 3, p. 196–204, set. 2018.

CABRERA, M. C. et al. Selenium, copper, zinc, iron and manganese content of seven meat cuts from Hereford and Braford steers fed pasture in Uruguay. **Meat Science**, v. 84, n. 3, p. 518–528, 2010.

CAMMACK, R.; WRIGGLESWORTH, J. M.; BAUM, H. Iron-dependent enzymes in mammalian systems. In: PONKA, P. et al. (Ed.). **Iron:transport and storage**. United States of America: CRC Press, 1990. p. 17–39.

CAO, X. et al. Thyroid Hormone Induces Rapid Activation of Akt/Protein Kinase B-Mammalian Target of Rapamycin-p70 S6K Cascade through Phosphatidylinositol 3-Kinase in Human Fibroblasts. **Molecular Endocrinology**, v. 19, n. 1, p. 102–112, jan. 2005.

CARON, A.; RICHARD, D.; LAPLANTE, M. The Roles of mTOR Complexes in Lipid Metabolism. **Annual Review of Nutrition**, v. 35, n. 1, p. 321–348, 17 jul. 2015.

CASAS, E. et al. Polymorphisms in calpastatin and mu-calpain genes are associated with beef iron content. **Animal Genetics**, v. 45, n. 2, p. 283–284, abr. 2014.

CEPPI, A.; BLUM, J. W. Effects of Growth Hormone on Growth Performance, Haematology, Metabolites and Hormones in Iron-Deficient Veal Calves*. **Journal of Veterinary Medicine Series A**, v. 41, n. 1–10, p. 443–458, 12 fev. 1994.

CHANG, X.; MOWAT, D. N.; SPIERS, G. A. Carcass characteristics and tissue-mineral contents of steers fed supplemental chromium. **Canadian Journal of Animal Science**, v. 72, n. 3, p. 663–669, 2010.

CHOI, Y. M.; KIM, B. C. Muscle fiber characteristics, myofibrillar protein isoforms, and meat quality. **Livestock Science**, v. 122, n. 2–3, p. 105–118, 2009.

COUSINS, R. J. Nutritional regulation of gene expression. **The American Journal of Medicine**, v. 106, n. 1, p. 20–23, jan. 1999.

DAS, A.; SEN, C. K. NutrimiRomics. In: BAGCHI, D.; SWAROOP, A.; MANASHI BAGCHI (Ed.). **Genomics, Proteomics and Metabolomics in Nutraceuticals and Functional Foods**. Chichester, UK: John Wiley & Sons, Ltd, 2015. p. 53–60.

DAUNCEY, M. J.; KATSUMATA, M.; WHITE, P. Nutrition, hormone receptor expression and gene interactions: implications for development and disease. In: PAS, M. F. W.; EVERTES, M. E.; HAAGSMAN, H. P. (Ed.). **Muscle development of livestock animals: physiology, genetics and meat quality**. Wallingford: CABI, 2004. p. 103–124.

DAVIS, M.; CLARKE, S. Influence of microRNA on the maintenance of human iron metabolism. **Nutrients**, v. 5, p. 2611–2628, 2013.

DE OLIVEIRA, P. S. N. et al. Co-Expression Networks Reveal Potential Regulatory Roles of miRNAs in Fatty Acid Composition of Nelore Cattle. **Frontiers in Genetics**, v. 10, p. 651, 11 jul. 2019.

DINIZ, W. J. da S. et al. Iron Content Affects Lipogenic Gene Expression in the Muscle of Nelore Beef Cattle. **PLOS ONE**, v. 11, n. 8, p. e0161160, 17 ago. 2016.

DINIZ, W. J. S. da S. et al. Detection of Co-expressed Pathway Modules Associated with Mineral Concentration and Meat Quality in Nelore Cattle. **Frontiers in Genetics**, v. 10, p. 210, 13 mar. 2019.

DØRUP, I. et al. Role of insulin-like growth factor-1 and growth hormone in growth inhibition induced by magnesium and zinc deficiencies. **British Journal of Nutrition**, v. 66, n. 03, p. 505, 9 nov. 1991.

DØRUP, I. The impact of minerals and micronutrients on growth control. In: PAS, M. F. W.; EVERTS, M. E.; HAAGSMAN, H. P. (Ed.). **Muscle development of livestock animals: physiology, genetics and meat quality**. Wallingford: CABI, 2004. p. 125-136.

DU, M. et al. AMP-Activated Protein Kinase in Muscle Growth, Fat Deposition, and Meat Quality. In: DU, M.; MCCORMICK, R. J. (Ed.). **Applied Muscle Biology and Meat Science**. 1. ed. Boca Raton: CRC Press, 2009. p. 195-216.

ENGLE, T. E. et al. Effects of dietary copper source and concentration on carcass characteristics and lipid and cholesterol metabolism in growing and finishing steers.

Journal of Animal Science, v. 78, n. 4, p. 1053, 2000.

ENGLE, T. E. Copper and lipid metabolism in beef cattle: A review. **Journal of Animal Science**, v. 89, n. 2, p. 591–596, 2011.

FENG, Y. et al. Integrated analysis of microRNA and mRNA expression profiles in rats with selenium deficiency and identification of associated miRNA-mRNA network. **Scientific Reports**, v. 8, n. 1, p. 1–9, 2018.

FLEET, J. C.; REPLOGLE, R.; SALT, D. E. Systems Genetics of Mineral Metabolism. **The Journal of Nutrition**, v. 141, p. 520–525, 2011.

FLYVBJERG, A. et al. Evidence that potassium deficiency induces growth retardation through reduced circulating levels of growth hormone and insulin-like growth factor I. **Metabolism**, v. 40, n. 8, p. 769–775, 1 ago. 1991.

FORTES, M. R. S. et al. Association weight matrix for the genetic dissection of puberty in beef cattle. **Proceedings of the National Academy of Sciences of the United States of America**, v. 107, n. 31, p. 13642–7, 3 ago. 2010.

FREAKE, H. C. et al. Actions and Interactions of Thyroid Hormone and Zinc Status in Growing Rats. **The Journal of Nutrition**, v. 131, n. 4, p. 1135–1141, 1 abr. 2001.

GARMYN, A. J. et al. Estimation of relationships between mineral concentration and fatty acid composition of longissimus muscle and beef palatability traits. **Journal of Animal Science**, v. 89, p. 2849–2858, 2011.

GIUFFRIDA-MENDOZA, M. et al. Mineral content of longissimus dorsi thoracis from water buffalo and Zebu-influenced cattle at four comparative ages. **Meat Science**, v. 75, p. 487–493, 2007.

GONÇALVES, T. M. et al. Gene Co-expression Analysis Indicates Potential Pathways and Regulators of Beef Tenderness in Nellore Cattle. **Frontiers in Genetics**, v. 9, p. 441, 5 out. 2018.

GOYENS, P. et al. Selenium deficiency as a possible factor in the pathogenesis of myxoedematous endemic cretinism. **Acta Endocrinologica**, v. 114, n. 4, p. 497–502, abr. 1987.

HANSEN, S. L. et al. Iron Transporters Are Differentially Regulated by Dietary Iron, and Modifications Are Associated with Changes in Manganese Metabolism in Young Pigs. **The Journal of Nutrition**, v. 139, n. 8, p. 1474–1479, 1 ago. 2009.

HANSEN, S. L. et al. Age and Dietary Iron Affect Expression of Genes Involved in Iron Acquisition and Homeostasis in Young Pigs. **The Journal of Nutrition**, v. 140, n. 2, p. 271–277, 1 fev. 2010.

HARADA, M. et al. MicroRNA Regulation and Cardiac Calcium Signaling. **Circulation Research**, v. 114, n. 4, p. 689–705, 14 fev. 2014.

HERGENREDER, J. E. et al. Zinc Methionine Supplementation Impacts Gene and Protein Expression in Calf-Fed Holstein Steers with Minimal Impact on Feedlot

Performance. **Biological trace element research**, v. 171, n. 2, p. 315–327, jun. 2016.

HERNANDEZ-CALVA, L. M. et al. Influence of dietary magnesium and selenium levels in finishing diets on growth performance and carcass meat quality of feedlot Pelibuey lambs. **Archives Animal Breeding**, v. 56, n. 1, p. 303–314, 2013.

HESS, S. Y. et al. Iron Deficiency Anemia Reduces Thyroid Peroxidase Activity in Rats. **The Journal of Nutrition**, v. 132, n. 7, p. 1951–1955, 1 jul. 2002.

HOLLÓ, G. et al. Effect of feeding on the composition of longissmus muscle of Hungarian Grey and Holstein Friesian bulls. **Archiv Tierzucht**, v. 50, n. 6, p. 575–586, 2007.

HUANG, W. et al. Global transcriptome analysis identifies differentially expressed genes related to lipid metabolism in Wagyu and Holstein cattle. **Scientific Reports**, v. 7, n. 1, p. 1–11, 2017.

HUANG, Y. et al. Effects of supplemental copper on the serum lipid profile, meat quality, and carcass composition of goat kids. **Biological Trace Element Research**, v. 159, n. 1–3, p. 140–146, 2014.

JACOMETO, C. B. et al. Maternal consumption of organic trace minerals alters calf systemic and neutrophil mRNA and microRNA indicators of inflammation and oxidative stress. **Journal of Dairy Science**, v. 98, n. 11, p. 7717–7729, nov. 2015.

JUSZCZUK-KUBIAK, E. et al. Effect of Inorganic Dietary Selenium Supplementation on Selenoprotein and Lipid Metabolism Gene Expression Patterns in Liver and Loin Muscle of Growing Lambs. **Biological Trace Element Research**, v. 172, n. 2, p. 336–345, 23 ago. 2016.

KAMEI, A. et al. Dietary iron-deficient anemia induces a variety of metabolic changes and even apoptosis in rat liver: a DNA microarray study. **Physiological Genomics**, v. 42, p. 149–156, 2010.

KAPPELER, B. I. G. et al. MiRNAs differentially expressed in skeletal muscle of animals with divergent estimated breeding values for beef tenderness. **BMC Molecular Biol**, v. 20, p. 1, 2019.

KESSLER, J. et al. Effect of organic zinc sources on performance, zinc status and carcass, meat and claw quality in fattening bulls. **Livestock Production Science**, v. 81, n. 2–3, p. 161–171, 2003.

KNEESKERN, S. G. et al. Effects of chromium supplementation to feedlot steers on growth performance, insulin sensitivity, and carcass characteristics. **Journal of Animal Science**, v. 94, n. 1, p. 217–226, 2016.

LAMMING, D. W.; SABATINI, D. M. A central role for mTOR in lipid homeostasis. **Cell Metabolism**, v. 18, n. 4, p. 465–469, 2013.

LANGFELDER, P.; HORVATH, S. WGCNA: An R package for weighted correlation network analysis. **BMC Bioinformatics**, v. 9, 2008.

LEE, S. H.; ENGLE, T. E.; HOSSNER, K. L. Effects of dietary copper on the expression of lipogenic genes and metabolic hormones in steers. **Journal of Animal Science**, v. 80, n. 7, p. 1999–2005, 2002.

LEE, W. J. et al. AMPK activation increases fatty acid oxidation in skeletal muscle by activating PPAR. v. 340, **Biochemical and Biophysical Research Communications,** v.340, p. 291–295, 2006.

LI, Q. et al. Effects of 12 metal ions on iron regulatory protein 1 (IRP-1) and hypoxia-inducible factor-1 alpha (HIF-1α) and HIF-regulated genes. **Toxicology and Applied Pharmacology**, v. 213, n. 3, p. 245–255, 15 jun. 2006.

LI, Y. et al. Iron Homeostasis Regulates the Activity of the MicroRNA Pathway through Poly(C)-Binding Protein 2. **Cell Metabolism**, v. 15, n. 6, p. 895–904, jun. 2012.

LIBIÉN-JIMÉNEZ, Y. et al. Effect of organic selenium supplementation in the diets of finishing sheep on meat color and pH during shelf life. **Indian Journal of Animal Research**, v. 49, n. 5, p. 652–657, 2015.

LIU, C. P. et al. Effects of dietary selenium deficiency on mRNA levels of twenty-one selenoprotein genes in the liver of layer chicken. **Biological Trace Element Research**, v. 159, n. 1–3, p. 192–198, 2014.

LIU, X.; YAO, Z. Chronic over-nutrition and dysregulation of GSK3 in diseases. **Nutrition & Metabolism**, v. 13, n. 1, p. 49, 4 dez. 2016.

LOUVET, L. et al. Magnesium Attenuates Phosphate-Induced Deregulation of a MicroRNA Signature and Prevents Modulation of Smad1 and Osterix during the Course of Vascular Calcification. **BioMed Research International**, v. 2016, p. 1–11, 22 jun. 2016.

MAGENTA, A. et al. Oxidative stress, microRNAs and cytosolic calcium homeostasis. **Cell Calcium**, v. 60, n. 3, p. 207–217, 1 set. 2016.

MALTIN, C. et al. Determinants of meat quality: tenderness. **Proceedings of the Nutrition Society**, v. 62, n. 02, p. 337–347, 5 maio 2003.

MATEESCU, R. It is possible to genetically change the nutrient profile of beef. (Beef Improvement Federation, Ed.) In: Beef improvement Federation Research Symposium & Annual Meeting, Lincoln, Nebraska. **Anais**... Lincoln, Nebraska: 2014. Disponível em: <http://www.bifconference.com/bif2014/newsroom.html>.

MATEESCU, R. G. et al. Genome-wide association study of concentrations of iron and other minerals in longissimus muscle of Angus cattle. **Journal of Animal Science**, v. 91, p. 3593–3600, 2013a.

MATEESCU, R. G. et al. Genetic parameters for concentrations of minerals in longissimus muscle and their associations with palatability traits in Angus cattle. **Journal of Animal Science**, v. 91, n. 3, p. 1067–75, mar. 2013b.

MATEESCU, R. G.; GARRICK, D. J.; REECY, J. M. Network analysis reveals putative genes affecting meat quality in Angus cattle. **Frontiers in Genetics**, v. 8, n. Nov, 2017.

MAXWELL, C.; VOLPE, S. L. Effect of Zinc Supplementation on Thyroid Hormone Function. **Annals of Nutrition and Metabolism**, v. 51, n. 2, p. 188–194, 2007.

MCBETH, L. J. et al. Effect of Zinc Source and Level on Finishing Cattle Performance , Carcass Characteristics , and Adipocyte Differentiation. 2001. Disponível em: < http://afs.okstate.edu/research/reports/2004/2004-1%20McBeth%20Research%20Report.pdf>.

MCDOWELL, L. R. **Minerals in Animal and Human Nutrition**. 2. ed. Wallingford: Elsevier, 2003.

MCLANE, J. A. et al. Physiological and biochemical effects of iron deficiency on rat skeletal muscle. **The American Journal of Physiology**, v. 241, n. 27, p. C47–C54, 1981.

MEHDI, Y.; DUFRASNE, I. Selenium in Cattle: A Review. **Molecules**, v. 21, n. 5, p. 545, 23 abr. 2016.

MICHA, R.; WALLACE, S. K.; MOZAFFARIAN, D. Red and Processed Meat Consumption and Risk of Incident Coronary Heart Disease, Stroke, and Diabetes Mellitus. **Circulation**, v. 121, n. 21, p. 2271–2283, 1 jun. 2010.

MIHAYLOVA, M. M.; SHAW, R. J. The AMPK signalling pathway coordinates cell growth, autophagy and metabolism. **Nature Cell Biology**, v. 13, n. 9, p. 1016–1023, 1 set. 2011.

MORRIS, C. A. et al. Effects of quantitative trait loci and the myostatin locus on trace and macro elements (minerals) in bovine liver, muscle and kidney. **Animal Genetics**, v. 44, n. 4, p. 361–8, ago. 2013.

MUCHENJE, V. et al. Some biochemical aspects pertaining to beef eating quality and consumer health: A review. **Food Chemistry**, v. 112, n. 2, p. 279–289, jan. 2009.

NAJAFPANAH, M. J. et al. Chromium downregulates the expression of Acetyl CoA Carboxylase 1 gene in lipogenic tissues of domestic goats : a potential strategy for meat quality improvement. **Gene**, v. 543, n. 2, p. 253–258, 2014.

NDONG, M. et al. Iron deficiency down-regulates the Akt/TSC1-TSC2/mammalian Target of Rapamycin signaling pathway in rats and in COS-1 cells. **Nutrition Research**, v. 29, n. 9, p. 640–647, set. 2009.

NETTO, A. S. et al. Effects of Copper and Selenium Supplementation on Performance and Lipid Metabolism in Confined Brangus Bulls. **Asian-Australasian Journal of Animal Sciences**, v. 27, n. 4, p. 488–494, 1 abr. 2014.

NOUR, a. Y. M. et al. Muscle Mineral Concentrations as Predictors of Taste Panel Sensory Attributes of Beef. **Journal of Food Science**, v. 48, p. 1170–1171, 1983.

NRC. **Nutrient requirements of dairy cattle**. 7. ed. Washington: National Academy Press, 2001.

O'BRIEN, J. et al. Overview of MicroRNA Biogenesis, Mechanisms of Actions, and Circulation. **Frontiers in Endocrinology**, v. 9, p. 402, 3 ago. 2018.

ODDY, V. H. et al. Nutritional and developmental effects on the intrinsic properties of muscles as they relate to the eating quality of beef. **Australian Journal of Experimental Agriculture**, v. 41, p. 921–942, 2001.

OLIVEIRA, G. B. et al. Integrative analysis of microRNAs and mRNAs revealed regulation of composition and metabolism in Nelore cattle. **BMC Genomics**, v. 19, n. 1, p. 126, 7 dez. 2018.

OTTO, T.; FANDREY, J. Thyroid Hormone Induces Hypoxia-Inducible Factor 1α Gene Expression through Thyroid Hormone Receptor β/Retinoid X Receptor α-Dependent Activation of Hepatic Leukemia Factor. **Endocrinology**, v. 149, n. 5, p. 2241–2250, 1 maio 2008.

PAMEI, G. et al. Influence of dietary supplementation of chromium on the carcass traits of crossbred pigs. **Journal of Advanced Veterinary and Animal Research**, v. 1, n. September, p. 1, 2014.

PANNIER, L. et al. Prime Australian lamb supplies key nutrients for human health. **Animal Production Science**, v. 50, p. 1115–1122, 2010.

PANNIER, L. et al. Associations of genetic and non-genetic factors with concentrations of iron and zinc in the longissimus muscle of lamb. **Meat Science**, v. 96, n. 2, p. 1111–1119, 2014.

PEÑA, K. A.; KISELYOV, K. Transition metals activate TFEB in overexpressing cells. **Biochemical Journal**, v. 470, n. 1, p. 65–76, 15 ago. 2015.

PEREIRA, A. S. C. et al. Lipid and selenium sources on fatty acid composition of intramuscular fat and muscle selenium concentration of Nellore steers. **Revista Brasileira de Zootecnia**, v. 41, n. 11, p. 2357–2363, nov. 2012.

REVERTER, A.; CHAN, E. K. F. Combining partial correlation and an information theory approach to the reversed engineering of gene co-expression networks. **Bioinformatics**, v. 24, n. 21, p. 2491–2497, 2008.

RIPA, R. et al. MicroRNA miR-29 controls a compensatory response to limit neuronal iron accumulation during adult life and aging. **BMC Biology**, v. 15, n. 1, p. 9, 13 dez. 2017.

RITCHIE, M. D. et al. Methods of integrating data to uncover genotype–phenotype interactions. **Nature Reviews Genetics**, v. 16, n. 2, p. 85–97, 2015.

RITCHIE, W. et al. Conserved Expression Patterns Predict microRNA Targets. **PLoS Comput Biol**, v. 5, n. 9, p. 1000513, 2009.

RODRIGUEZ, A. et al. Effects of iron loading on muscle: genome-wide mRNA expression profiling in the mouse. **BMC Genomics**, v. 8, p. 379, jan. 2007.

ROPKA-MOLIK, K. et al. Nutritional modification of SCD, ACACA and LPL gene expressions in different ovine tissues. **Arch. Anim. Breed**, v. 60, p. 243–250, 2017.

RYU, M.-S. et al. Genomic analysis, cytokine expression, and microRNA profiling reveal biomarkers of human dietary zinc depletion and homeostasis. **Proceedings of the National Academy of Sciences**, v. 108, n. 52, p. 20970–20975, 27 dez. 2011.

SADEGHI, M. et al. Transcription analysis of genes involved in lipid metabolism reveals the role of chromium in reducing body fat in animal models. **Journal of Trace Elements in Medicine and Biology**, v. 32, p. 45–51, 2015.

SCHIAFFINO, S.; MAMMUCARI, C. Regulation of skeletal muscle growth by the IGF1-Akt/PKB pathway: insights from genetic models. **Skeletal Muscle**, v. 1, n. 1, p. 4, 2011.

SGOIFO ROSSI, C. et al. The effect of different selenium sources during the finishing phase on beef quality. **Journal of Animal and Feed Sciences**, v. 24, n. 2, p. 93–99, 2015.

SMITH, L. R.; MEYER, G.; LIEBER, R. L. Systems analysis of biological networks in skeletal muscle function. **Wiley Interdisciplinary Reviews: Systems Biology and Medicine**, v. 5, n. 1, p. 55–71, 1 jan. 2013.

SU, W.-L.; KLEINHANZ, R. R.; SCHADT, E. E. Characterizing the role of miRNAs within gene regulatory networks using integrative genomics techniques. **Molecular Systems Biology**, v. 7, n. 1, p. 490–490, 16 abr. 2014.

SUNG, K.-I. et al. Effects of forage level and chromium-methionine chelate supplementation on performance, carcass characteristics and blood metabolites in Korean native (Hanwoo) steers. **Journal of Animal Science and Technology**, v. 57, n. 1, p. 1–7, 2015.

SURAVAJHALA, P.; KOGELMAN, L. J. A.; KADARMIDEEN, H. N. Multi-omic data integration and analysis using systems genomics approaches: methods and applications in animal production, health and welfare. **Genetics Selection Evolution**, v. 48, n. 1, p. 38, 29 dez. 2016.

SUTTLE, N. **Mineral nutrition of livestock**. 4^a ed. Wallingford: CABI, 2010.

TAJIK, H. et al. Mineral Contents of muscle (Longissimus dorsi thoracis) and liver in river buffalo (Bubalus bubalis). **Journal of Muscle Foods**, v. 21, n. 3, p. 459–473, 16 jun. 2010.

TANG, R. et al. Effects of supplementing two levels of magnesium aspartate and transportation stress on pork quality and gene expression of µ-calpain and calpastatin of finishing pigs. **Archives of Animal Nutrition**, v. 62, n. 5, p. 415–425, 2008.

TANG, Z. R. et al. Copper deficiency induces hepatic fatty acid synthase gene transcription in rats by increasing the nuclear content of mature sterol regulatory element binding protein 1. **Journal of Nutrition**, v. 130, n. 12, p. 2915–2921, 2000.

TIZIOTO, P. C. et al. Genome scan for meat quality traits in Nelore beef cattle. **Physiological Genomics**, v. 45, n. 21, p. 1012–1020, 1 nov. 2013.

TIZIOTO, P. C. et al. Calcium and potassium content in beef: influences on tenderness and associations with molecular markers in Nellore cattle. **Meat science**, v. 96, n. 1, p. 436–40, jan. 2014.

TIZIOTO, P. C. et al. Detection of quantitative trait loci for mineral content of Nelore longissimus dorsi muscle. **Genetics Selection Evolution**, v. 47, n. 1, p. 15, 2015.

TOKACH, R. J. et al. Chromium Propionate Enhances Adipogenic Differentiation of Bovine Intramuscular Adipocytes. **Frontiers in Veterinary Science**, v. 2, n. September, p. 1–11, 2015.

VAN DAM, S. et al. Gene co-expression analysis for functional classification and gene–disease predictions. **Briefings in Bioinformatics**, n. September 2016, p. bbw139, 10 jan. 2017.

VAN DRONKELAAR, C. et al. Minerals and Sarcopenia; The Role of Calcium, Iron, Magnesium, Phosphorus, Potassium, Selenium, Sodium, and Zinc on Muscle Mass, Muscle Strength, and Physical Performance in Older Adults: A Systematic Review. **Journal of the American Medical Directors Association**, v. 19, n. 1, p. 6- 11.e3, jan. 2018.

WATSON, A. et al. Iron depletion suppresses mTORC1-directed signalling in intestinal Caco-2 cells via induction of REDD1. **Cellular Signalling**, v. 28, n. 5, p. 412–424, 1 maio 2016.

XING, Y. et al. MicroRNA expression profiles in rats with selenium deficiency and the possible role of the Wnt/β-catenin signaling pathway in cardiac dysfunction. **International Journal of Molecular Medicine**, v. 35, n. 1, p. 143–152, 1 jan. 2015.

YAMAUCHI, M. et al. Thyroid Hormone Activates Adenosine 5′-Monophosphate-Activated Protein Kinase via Intracellular Calcium Mobilization and Activation of Calcium/Calmodulin-Dependent Protein Kinase Kinase-β. **Molecular Endocrinology**, v. 22, n. 4, p. 893–903, 2008.

YAO, X. et al. Thyroid Hormone Receptor Coregulators in Metabolic Regulation. **Journal of Endocrinology, Diabetes & Obesity**, v. 2, n. 3, p. 1051, 2014.

ZHANG, D. et al. Thyroid hormone regulates muscle fiber type conversion via miR-133a1. **Journal of Cell Biology**, v. 207, n. 6, p. 753–766, 2014a.

ZHANG, H. B. et al. Supplementation Dietary Zinc Levels on Growth Performance, Carcass Traits, and Intramuscular Fat Deposition in Weaned Piglets. **Biological Trace Element Research**, v. 161, n. 1, p. 69–77, 23 out. 2014b.

ZHANG, J.-J. et al. Zinc mediates the SREBP-SCD axis to regulate lipid metabolism in Caenorhabditis elegans. **Journal of Lipid Research**, v. 58, n. 9, p. 1845–1854, set. 2017.

ZHANG, X. et al. The effect of calcium propionate supplementation on performance, meat quality, and mRNA expression of finishing steers fed a high-concentrate diet. **Journal of Animal and Feed Sciences**, v. 24, n. 2, p. 100–106, 2015.

ZHAO, Y. et al. Regulation of MicroRNAs, and the Correlations of MicroRNAs and Their Targeted Genes by Zinc Oxide Nanoparticles in Ovarian Granulosa Cells. **PLOS ONE**, v. 11, n. 5, p. e0155865, 19 maio 2016.

ZIMMERMANN, M. B.; KÖHRLE, J. The impact of iron and selenium deficiencies on iodine and thyroid metabolism : biochemistry and relevance to public health. **Thyroid**, v. 12, n. 10, p. 867–878, 2002.

Chapter 2

frontiers
in Genetics

ORIGINAL RESEARCH
published: 13 March 2019
doi: 10.3389/fgene.2019.00210

Detection of Co-expressed Pathway Modules Associated With Mineral Concentration and Meat Quality in Nelore Cattle

*Wellison J. S. Diniz[1,2,3], Gianluca Mazzoni[4], Luiz L. Coutinho[5], Priyanka Banerjee[2], Ludwig Geistlinger[3,6], Aline S. M. Cesar[5], Francesca Bertolini[7], Juliana Afonso[1], Priscila S. N. de Oliveira[3], Polyana C. Tizioto[5], Haja N. Kadarmideen[2] and Luciana C. A. Regitano[3]**

[1] Department of Genetics and Evolution, Federal University of São Carlos, São Carlos, Brazil, [2] Department of Applied Mathematics and Computer Science, Technical University of Denmark, Kongens Lyngby, Denmark, [3] Embrapa Pecuária Sudeste, Empresa Brasileira de Pesquisa Agropecuária, São Paulo, Brazil, [4] Department of Health Technology, Technical University of Denmark, Kongens Lyngby, Denmark, [5] Department of Animal Science, Luiz de Queiroz College of Agriculture, University of São Paulo, Piracicaba, Brazil, [6] Graduate School of Public Health and Health Policy, The City University of New York, New York, NY, United States, [7] Department of Aquaculture, Technical University of Denmark, Kongens Lyngby, Denmark

Edited by:
*Robert J. Schaefer,
University of Minnesota Twin Cities,
United States*

Reviewed by:
*Martin Johnsson,
Swedish University of Agricultural Sciences, Sweden
Fabyano Fonseca Silva,
Universidade Federal de Viçosa, Brazil*

***Correspondence:**
*Luciana C. A. Regitano
luciana.regitano@embrapa.br*

Specialty section:
*This article was submitted to
Livestock Genomics,
a section of the journal
Frontiers in Genetics*

***Received**: 03 December 2018*
***Accepted**: 26 February 2019*
***Published**: 13 March 2019*

***Citation**:*
Diniz WJS, Mazzoni G, Coutinho LL, Banerjee P, Geistlinger L, Cesar ASM, Bertolini F, Afonso J, de Oliveira PSN, Tizioto PC, Kadarmideen HN and Regitano LCA (2019) Detection of Co-expressed Pathway Modules Associated With Mineral Concentration and Meat Quality in Nelore Cattle. Front. Genet. 10:210. doi:10.3389/fgene.2019.00210

Meat quality is a complex trait that is influenced by genetic and environmental factors, which includes mineral concentration. However, the association between mineral concentration and meat quality, and the specific molecular pathways underlying this association, are not well explored. We therefore analyzed gene expression as measured with RNA-seq in *Longissimus thoracis* muscle of 194 Nelore steers for association with three meat quality traits (intramuscular fat, meat pH, and tenderness) and the concentration of 13 minerals (Ca, Cr, Co, Cu, Fe, K, Mg, Mn, Na, P, S, Se, and Zn). We identified seven sets of co-expressed genes (modules) associated with at least two traits, which indicates that common pathways influence these traits. From pathway analysis of module hub genes, we further found an over-representation for energy and protein metabolism (AMPK and mTOR signaling pathways) in addition to muscle growth, and protein turnover pathways. Among the identified hub genes *FASN, ELOV5*, and *PDE3B* are involved with lipid metabolism and were affected by previously identified eQTLs associated to fat deposition. The reported hub genes and over-represented pathways provide evidence of interplay among gene expression, mineral concentration, and meat quality traits. Future studies investigating the effect of different levels of mineral supplementation in the gene expression and meat quality traits could help us to elucidate the regulatory mechanism by which the genes/pathways are affected.

Keywords: AMPK pathway, co-expression analysis, intramuscular fat, RNA sequencing, tenderness

---

Abbreviations: AMPK, AMP-activated protein kinase; CPM, Counts *per* million; ECM, Extra Cellular Matrix; IMF, Intramuscular Fat Content; ME, Module eigengene; MM, Module Membership; QC, Quality Control; WBSF7, Warner- Bratzler Shear Force after 7 days of meat aging; WGCNA, Weighted Gene Co-expression Network Analysis.

2.1. INTRODUCTION

Meat is an important source of nutrients in the human diet. Meat quality traits such as intramuscular fat content (IMF), mineral concentration, and fatty acid profile influence consumer purchase decision (AHLBERG et al., 2014; MATEESCU, 2014) and human health (PIGHIN et al., 2016). Mineral deficiency, mainly iron and zinc (RITCHIE; ROSER, 2018), and protein deficiency (CLUGSTON and SMITH, 2002), have been reported as worldwide health hazards. In addition, IMF, meat pH, and muscle mineral concentration also affect meat tenderness, flavor, and juiciness, which are major sensory traits related to eat satisfaction (AHLBERG et al., 2014; ENGLE et al., 2000; PANNIER et al., 2014).

Brazil is one of the largest exporters of meat and meat products, and the Brazilian cattle herd is mainly composed of Nelore and its crosses (ABIEC, 2018). Despite being well adapted to tropical climate, Nelore cattle has typically less tender and marble meat when compared with European breeds due to several genetic and environmental factors (CESAR et al., 2015; TIZIOTO et al., 2015). Genome-wide association (GWAS) of SNPs (TIZIOTO et al., 2013, 2015; CESAR et al., 2014) and copy-number variations (CNVs) (SILVA et al., 2016) in conjunction with transcriptomic studies (DINIZ et al., 2016; SILVA-VIGNATO et al., 2017; GEISTLINGER et al., 2018; GONÇALVES et al., 2018), have illustrated the genetic factors affecting complex traits in Nelore. However, growing evidence suggested interplay among gene expression, mineral concentration, and meat quality traits, which are still unclear.

Multi-omic data integration has been useful to reveal potential causal and regulatory mechanisms underlying complex animal production, reproduction and welfare traits (reviewed in Suravajhala et al. (2016)). Integrating genomic, transcriptomic, and phenotype data has contributed to an improved understanding of complex traits by identifying regulatory candidate genes and biological functions (PONSUKSILI et al., 2013; CESAR et al., 2018; GEISTLINGER et al., 2018; GONÇALVES et al., 2018). Based on that, Mateescu; Garrick; and Reecy (2017) carried out a GWAS combined with gene network analysis for association with the carcass, meat quality traits and mineral concentration. Among the identified pathways, the authors pointed out calcium-related processes, apoptosis, and TGF-beta signaling involved with these traits.

GWAS and differential gene expression analyses have been fruitful in investigating the role of genes in complex phenotypes. However, biological systems are a result of complex interactions among genes and multiple regulatory mechanisms, which are not explored in the above-mentioned studies. To address the relationship between transcriptome and traits, co-expression networks have been successfully employed. This approach allows to identify and cluster highly connected genes and associate them to the phenotypes, shedding light on the common pathways underlying these traits as well as the main regulators (LANGFELDER; HORVATH, 2008). To date, there is no information about this approach integrating meat quality traits and mineral concentration in beef cattle. In addition, we still have a lack of knowledge about the interplay among gene expression, mineral concentration, and meat quality traits. Thus, to explore regulatory pathways, putative gene regulators, and to study their relationship with muscle and mineral metabolism in Nelore skeletal muscle, we integrated gene expression, eQTL variation, mineral concentration (macro and micro minerals), and meat quality traits (intramuscular fat, shear force, and meat pH) based on a network approach.

2.2. MATERIALS AND METHODS

2.2.1. Ethics Statement

The Institutional Animal Care and Use Committee (IACUC) from the Empresa Brasileira de Pesquisa Agropecuária (EMBRAPA – Pecuária Sudeste) approved all experimental procedures involving the animals used in this study.

2.2.2. Animals and Phenotyping

A total of two hundred Nelore steers (produced at Embrapa Pecuária Sudeste, São Carlos – Brazil) were used in this study. The experimental design, production system, and animal management were previously described (TIZIOTO et al., 2015; DINIZ et al., 2016). Briefly, animals were raised in the grazing system until 21 months of age when they were taken to three feedlots under similar nutritional and sanitary management. The Nelore steers with an average age of 25 months were harvested at commercial facilities after about 90 days of feeding and the *Longissimus thoracis* (LT) muscle samples were collected.

The steaks (2.5 cm) harvested as a cross-section of the LT muscle (11th and 13th ribs) collected at slaughter were used to measure the beef quality traits as described (TIZIOTO et al., 2013; CESAR et al., 2014). The traits evaluated were tenderness (Warner-Bratzler shear force - WBSF7, kg) measured seven days after slaughter, meat pH measured 24 hours after slaughter along with intramuscular fat (IMF %) (TIZIOTO et al., 2013).

Tissue samples were used for total RNA extraction (DINIZ et al., 2016) and mineral measurement (TIZIOTO et al., 2014). The concentration of macro minerals [Calcium (Ca), Magnesium (Mg), Phosphorus (P), Potassium (K), Sodium (Na), Sulphur (S)] and micro minerals [Chromium (Cr), Cobalt (Co), Copper (Cu), Manganese (Mn), Selenium (Se), Iron (Fe) and Zinc (Zn)] were measured using inductively coupled plasma-optical emission spectrometry (ICP OES; Vista Pro-CCD ICP OES1, radial view, Varian, Mulgrave, Australia) as described by Tizioto et al. (2014).

2.2.3. Genome Expression Profile, Sequencing, and Data Processing

The LT muscle samples were collected immediately after slaughter, snap frozen in liquid nitrogen and kept at -80 ºC until RNA extraction. To extract RNA, approximately 100 mg of frozen tissue was used, and total RNA was purified using Trizol® standard protocol (Life Technologies, Carlsbad, CA). The mRNA concentration and quality were evaluated in the Bioanalyzer 2100® (Agilent, Santa Clara, CA, USA).

The Illumina TruSeq® RNA Sample Preparation Kit v2 Guide (San Diego, CA) protocol was used to generate cDNA libraries for each sample using 2 µg of total RNA as input. Library preparation and sequencing were conducted by ESALQ Genomics Center (Piracicaba, São Paulo, Brazil). cDNA libraries were purified and validated using Agilent 2100 Bioanalyzer (Santa Clara, CA). Paired-end (PE) sequencing was performed on Illumina Hiseq 2500® (San Diego, CA) platform following the standard protocols. The samples were multiplexed and run on multiple lanes to obtain 2 X 100 bp reads.

The PE reads were filtered using the Seqyclean package version 1.4.13 (https://github.com/ibest/seqyclean; ZHBANNIKOV et al., 2017), which removed all reads with a mean quality under 24, length under 65 bp, as well as the adapter sequences. Quality control (QC) of raw RNA-Seq reads was carried out with FastQC version 0.11.2

(https://www.bioinformatics.babraham.ac.uk/projects/fastqc/; ANDREWS, 2010) and MultiQC version1.4 (http://multiqc.info/; EWELS et al., 2016).

Read mapping and gene counting were carried out by STAR aligner version 2.5.4b (DOBIN et al., 2013) using a reference genome (*Bos taurus,* ARS-UCD1.2) and gene annotation file (release 106) obtained from NCBI (NCBI, 2018). One sample with mapping rate lower than 70% was removed out for further analyses.

The data editing was done using the Bioconductor package edgeR version 3.20.9 (ROBINSON; MCCARTHY; SMYTH, 2010). Taking into account that low expressed genes are less reliable and indistinguishable from sampling noise (TARAZONA et al., 2015), the read counts per gene were normalized to counts per million (*cpm* function). The genes with less than one *cpm* in more than 90% of the samples were filtered out. Gene counts were normalized applying the variance stabilizing transformation (*VST*) from DESeq2 version 1.18.1 (ANDERS AND HUBER, 2010).

Potential biases due to technical variation in gene expression among samples were evaluated by applying a Principal Component Analysis (PCA) and hierarchical clustering on normalized data using NOISeq version 2.22.1 (TARAZONA et al., 2015). A linear model was fitted in order to adjust the gene expression matrix for batch effect (flow cell). To this end, the *removeBacthEffect* function from Limma (version 3.34.9) R package (RITCHIE et al., 2015) was used. Three samples were identified as outliers. Thus, 12 known housekeeping genes were selected based on the literature (*ACTB, API5, EIF2B2, GAPDH, GUSB, HMBS, PGK1, PPIA, RPS18, VAPB, YWHAZ*) to evaluate their variability on the samples. The housekeeping genes expression confirmed these samples as outliers, and therefore, they were filtered out.

2.2.4. Network Gene Co-Expression Analysis

A co-expression approach was applied using the Weighted Gene Co-expression Network Analysis (WGCNA) R package version 1.63 (LANGFELDER; HORVATH, 2008). The method adopted for constructing the networks included two steps: First, a similarity co-expression network was calculated with Pearson’s correlation for all genes, followed by transformation to a signed adjacency matrix (AM) by using the soft thresholding power β, to which co-expression similarity is raised. Based on the criteria of approximating scale-free topology, we chose the power of $\beta = 12$ such that the resulting network satisfies the scale-free topology (linear regression model fitting index $R^2 = 0.80$).

Outlier animals (n = 2) were identified based on hierarchical clustering and filtered out (as they had a lower number of counts compared to other samples) after WGCNA quality control, as suggested by the WGCNA authors. Accordingly, 194 animals and 11,996 genes were used to construct an undirected, signed network. Topological overlap measure (TOM) was computed from AM where TOM was converted to dissimilarity TOM. Based on TOM dissimilarity, we used the dynamic tree cut v.1.63.1 (LANGFELDER; ZHANG; HORVATH, 2008) to identify the modules as the branches of the resulting dendrogram. As parameters, the minimum size per module was set to 50 genes with a high sensitivity to split the clusters (deepSplit = 4). Genes with a similar expression pattern across samples were grouped into the same module and arbitrarily labeled by number.

WGCNA was used for summarizing the obtained modules by a concept of eigengene. Eigengenes are the first principal component of the expression matrix for each module and represent the weighted average of expression profile for each module. Modules highly correlated were merged based on the module eigengene (ME) dissimilarity threshold of 0.2 leading to the final set of modules for constructing the network.

2.2.5. Trait Association Analysis and Module Selection

After the phenotypic data were mean-centered and scaled, a linear model was fitted to analyze the association between the expression profiles of the modules (MEs) and the phenotypes (LI et al., 2018). The model included the place of birth, the season of production, and animal's age, according to the equation:

$$y_{ijkl} = \mu + C_i + G_j + A_k + T_l + \varepsilon_{ijkl}$$

Where:

y_{ijkl}: is the expression level of the eigengene in each module (n = 23);

μ: is the intercept of ME;

C_i: is the fixed effect for the place of birth (3 levels = CPPSE, IMA, NOHO);

G_j: is the fixed effect for the season of production (3 levels = 2009, 2010, 2011);

A_k: is the covariate for the animal's age, in days;

T_l: is the trait observation for each animal;

ε_{ijkl}: is the random residual effect associated with each observation.

Modules associated with at least two beef quality or mineral traits ($p \leq 0.05$) were selected for further analyses.

2.2.6. Pathway Over-representation Analysis

Pathway analysis was performed using ClueGO version 2.5.1 to identify gene KEGG pathways over-represented in the selected modules (BINDEA et al., 2009). Redundant terms were grouped based on the kappa score = 0.4 (BINDEA et al., 2009). The p-value was calculated and corrected with a Bonferroni step down. Only pathways with a p-value (pV) $\leq$ 0.05 were selected. These analyses were carried out based on the *B. taurus* annotation, and the network visualization was performed on Cytoscape version 3.6.1 (SHANNON et al., 2003).

2.2.7. Hub Gene Selection

Highly connected genes (hub genes) are supposed to be the main regulators in the network and have a pivotal biological role concerning the associated trait (LANGFELDER; HORVATH, 2007, 2008). Hub genes in the associated modules were selected based on the module membership $\geq$ 0.8 (LANGFELDER; HORVATH, 2008). Among them, hub genes partaking in over-represented biological pathways previously identified were retained. Moreover, over-representation pathway analysis including all hub genes was applied following the approach previously described.

2.2.8. Integration of eQTL and Co-expression Modules

A list of eQTLs from the same population and dataset (CESAR et al., 2018) evaluated in this work was provided. The dataset included 1,268 cis- and 10,334 trans-eQTLs based on the association between 461,466 SNPs and the expression level of 11,808 genes from 192 animals. Since the eQTLs have a known effect on gene expression, the eQTLs that target the hub genes (MM $\geq$ 0.8) in the selected modules were evaluated. A Fisher's exact test was applied to assess the module under/ over-representation (FDR $\geq$ 0.05).

2.3. RESULTS

We applied a network-based approach to identify relevant genes and pathways associated with meat quality and mineral concentration in Nelore cattle (Figure 2.1). Based on the transcriptomic profiles of skeletal muscle samples of 194 steers, we constructed a signed weighted gene co-expression network with WGCNA (LANGFELDER; HORVATH, 2008). From co-expressed modules and pathway analysis, we thereby identified several hub genes significantly associated with meat quality traits and mineral concentration.

Figure 2.1. Workflow.

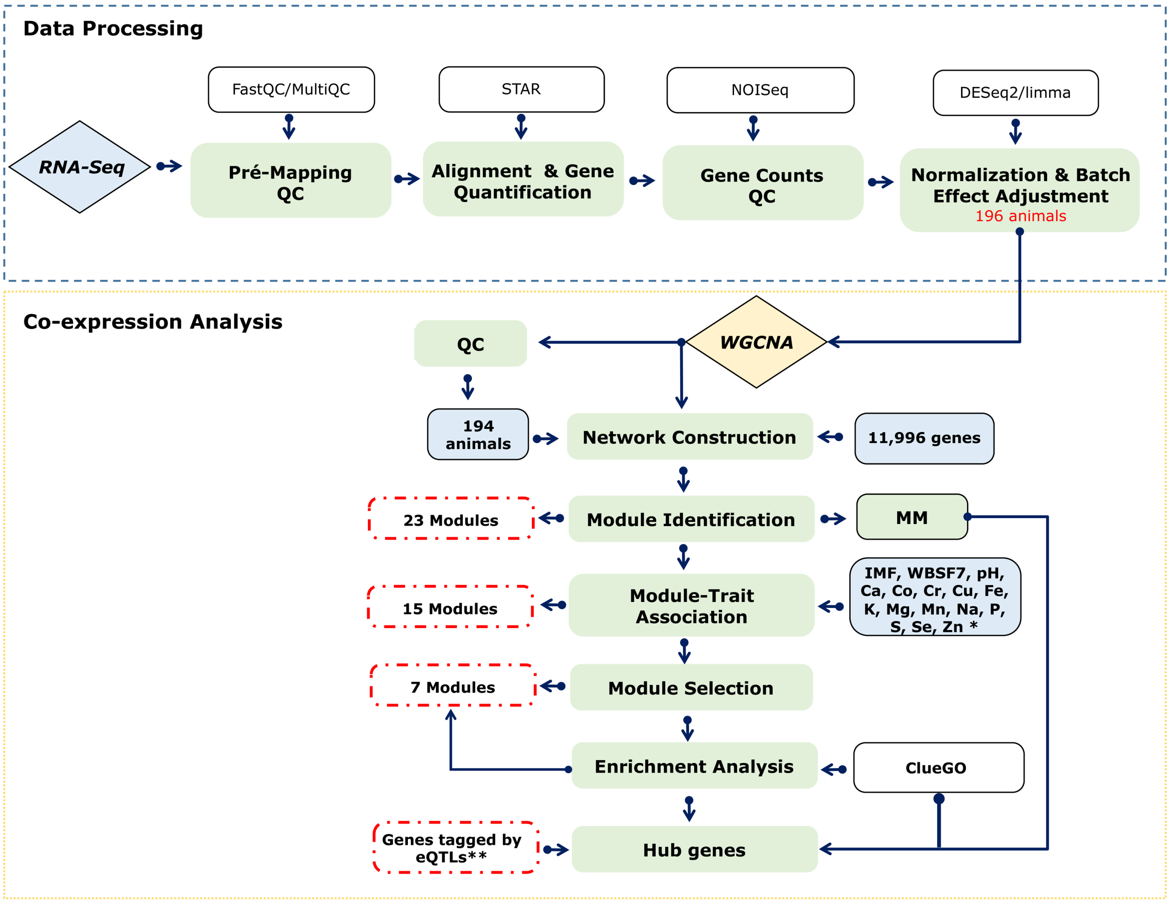

Green boxes represent the main analysis steps that were involved in data processing and co-expression analysis.Tools applied in each step are shown in white boxes. Inputs and outputs are shown in blue and dashed red boxes, respectively. *A varying number of samples was analyzed for each trait (Supplementary Table 1). **Data from an eQTL analysis carried out for the same population used in this study (CESAR et al., 2018).

2.3.1. Descriptive Statistics and Correlation Estimates

We analyzed gene expression levels as measured with RNA-seq for association with three meat quality traits (intramuscular fat, meat pH, and tenderness) and the concentration of 13 minerals (Ca, Cr, Co, Cu, Fe, K, Mg, Mn, Na, P, S, Se, and Zn) available for a varying number of samples (ranging from 57 to 194, Supplementary Table 1). The genetic variance and heritability for the traits evaluated here, obtained from this population, ranged from low to moderate as previously published (TIZIOTO et al., 2013, 2015). A summary of descriptive statistics for each trait is in Supplementary Table 1 and Figure 2.2.

Figure 2.2. Box plot of mineral concentration (macro and micro) and meat quality traits.

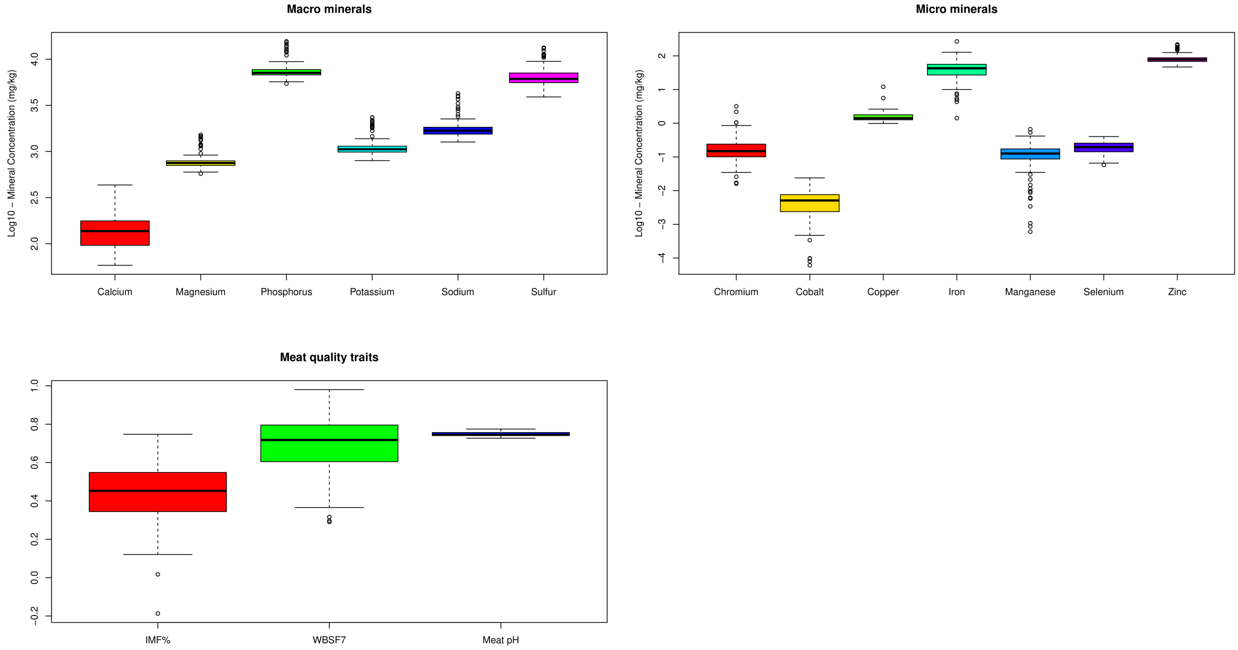

IMF% - Percentage of intramuscular fat content; WBSF7 - Warner-Bratzler Shear Force after seven days of meat aging; The data are in log10 scale.

We performed clustering analysis to identify similarities between traits (Figure 2.3 - top). We identified four clusters as follows: cluster 1 (WBSF7 and Cr), cluster 2 (Co, Cu, Mn, and IMF), cluster 3 (Fe, Ca, S, Zn, Na, P, Mg, and K), and cluster 4 (pH and Se). The pair-wise correlation within all traits is provided in Supplementary Figure 1. Significant and strong correlation ranged from 0.45 to 0.99 among minerals in the cluster 3 ($p \leq 0.05$). We identified positive correlation among IMF with some minerals (Ca = 0.25, Cu = 0.23, Mn = 0.24, K = 0.17, Na = 0.3, S = 0.18 and Zn = 0.23) ($p \leq 0.05$). Meat pH was positively correlated with Se (r = 0.29), whereas negatively associated with Fe (-0.17), Mg (-0.22), P (-0.25), K (-0.21), Na (-0.26), S (-0.17), and Zn (-0.22) (Supplementary Figure 1). No significant correlation was observed between tenderness (WBSF7), IMF, and meat pH.

Figure 2.3. Hierarchical clustering of phenotypic correlation between traits (top) and module-trait association analysis (bottom).

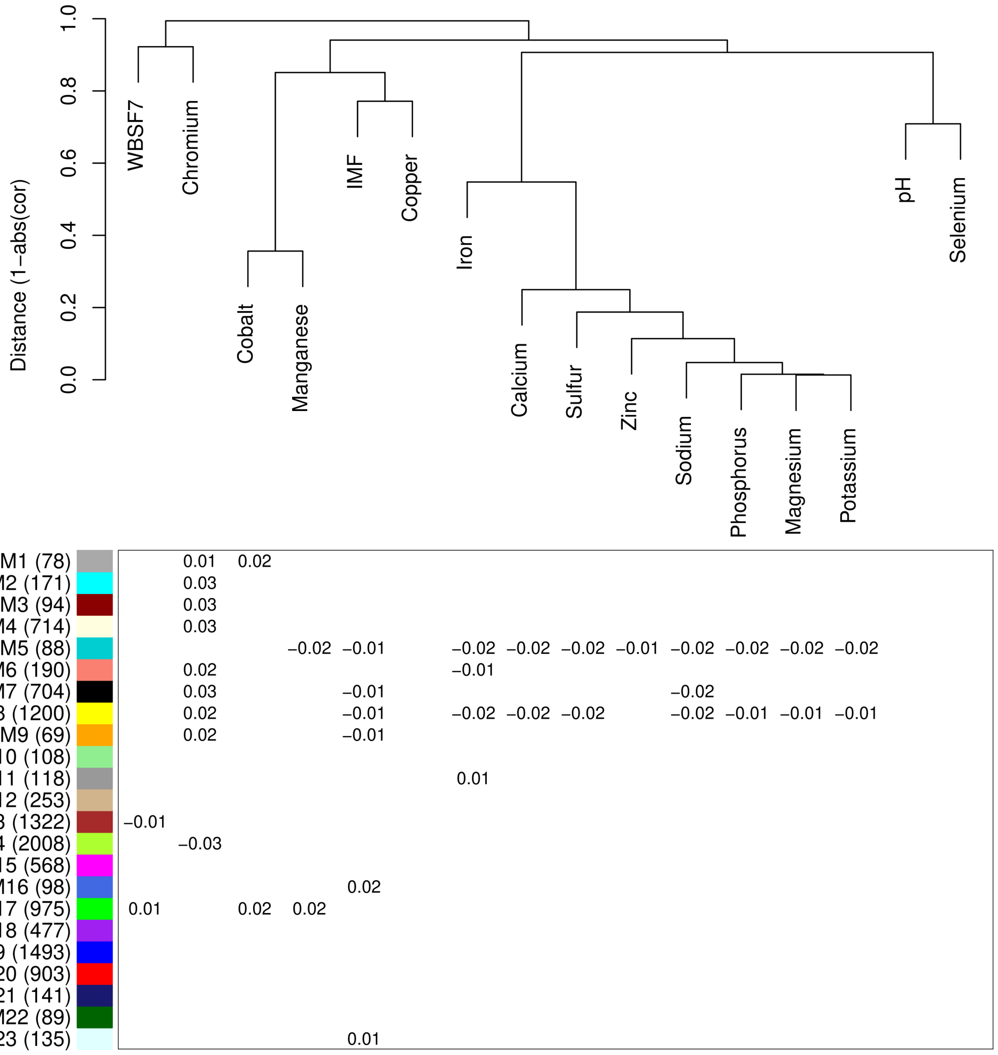

Modules are labeled by number on the y-axis with the number of contained genes in parenthesis. Each column represents a trait as indicated on the corresponding dendrogram branch. For significantly associated modules, the coefficient from the linear model is given within the cell.

2.3.2. Data Processing and Co-expression Network Construction

On average, a total of 13 million of 100 bp paired-end reads per sample were generated. Around 96.71% of unique reads were mapped to the reference *Bos taurus* genome (ARS-UCD1.2). Taking into account that low expressed genes are less reliable and indistinguishable from sampling noise (TARAZONA et al., 2015), we filtered out the genes with less than one *cpm* in more than 90% of the samples. In addition, four samples were removed because they had a mapping rate lower than 70% or showed high variability on the housekeeping genes expression (see methods). Thus, we used 11,996 genes and 194 samples for the co-expression analysis.

Considering the WGCNA assumptions, the weighted network starts from the level of thousands of genes, identifies modules of co-expressed genes, summarizes the module expression profile as the first principal component (module eigengene - ME), and relates the MEs with the trait of interest (LANGFELDER; HORVATH, 2008). The module membership (MM) value quantifies the degree of co-expression of a gene with other genes within a module, thereby enabling the identification of intramodular hub genes.

From clustering 11,996 genes with WGCNA, we obtained 23 modules labeled by number (Figure 2.3). The module size ranged from 69 genes (M9) to 2,008 genes (M14) (Figure 2.3 - lower block). The proportion of variance explained by the eigengenes ranged from 0.18 (M20) to 0.53 (M5) (Supplementary Table 2).

2.3.3. Trait Association and Pathway Enrichment Analysis

We performed an association analysis to identify the relationship between network and traits. This analysis measures the strength of the effect and the direction of the association between the module (eigengenes) and the trait. Thus, if the association is positive, it means the trait increases with increasing “eigengene expression” or vice-versa. We selected seven modules (M1, M5, M6, M7, M8, M9, and M17), associated with at least two traits ($p \leq 0.05$) (Figure 2.3 - bottom) once we also want to point out shared pathways among traits. We found the highest number of significant associated modules between M5 (ten associations; negative with IMF, and the concentration of Mn, Fe, Ca, S, Zn, Na, P, Mg, and K), followed by M8 (nine associations; positive with Cr, negative with IMF, and the minerals of cluster 3, except Zn). The average expression profile of M17 module showed association with three traits (positive with WBSF7, Co, and Mn) along with M7 (negative with Na and IMF, and positive with Cr concentration). For the modules M1, M6, and M9, we found an association with two traits. We identified a positive association among M6 and M9 with Cr concentration while a negative association was observed between M9 with IMF, and M6 with Fe concentration. M1 was positively associated with the concentration of Cr and Co. The modules with none or only one trait association were not included for further analysis.

The module membership values for all the genes for selected modules are given in Supplementary Table 3. We carried out a pathway over-representation analysis on ClueGo version 2.5.1 for the seven selected modules (Table 2.1, Supplementary Table 4) to identify meaningful metabolic pathways involved with meat quality traits and mineral concentration. We detected several pathways (pV $\leq$ 0.05, group p-value corrected with Bonferroni step down) mainly related to energy and protein metabolism, such as AMPK and mTOR signaling pathways.

2.3.4. Hub Gene Selection, Pathway Analysis, and Integration with eQTLs

Highly connected genes are likely to play an important role both in the network's topology and biological pathways. In this way, we combined a pathway-based gene analysis for each selected module (Supplementary Table 4) and gene connectivity measure (MM $\geq$ 0.8) (Supplementary Table 3) selecting 82 hub genes (Table 2.1, see methods). Further, taking advantage of an eQTL study carried out in the same population (CESAR et al., 2018), we screened whether the genes in the modules were underlying eQTLs, and applied a Fisher's exact test to assess the module overrepresentation. We identified 323 genes targeted by 760 unique eQTLs (Table 2.1, Supplementary Table 5) into the seven modules. In addition, we identified 24 out of 323 genes with a MM $\geq$ 0.8, and six of them are part of the hub gene list (Table 2.1). However, based on the Fisher's exact test (FDR $\geq$ 0.05) no significant over-/underrepresentation was detectable in these modules.

To gain further insights into their functions as well as to integrate the pathways among the modules, we carried out a KEGG pathway analysis. Considering a kappa score = 0.4 and pV $\leq$ 0.05 (Figure 2.4, Supplementary Table 6), we clustered the identified pathways into eight groups. The pathways related to energy metabolism were clustered together and included AMP-activated protein kinase (AMPK), peroxisome proliferator-activated receptors (PPAR), insulin, glucagon, and adipocytokine signaling pathways. We also identified ubiquitin-mediated proteolysis and biosynthesis of fatty acids pathways overrepresented in this network.

Figure 2.4. Network clusters based on over-represented KEGG pathways of hub genes associated with mineral concentration and meat quality traits.

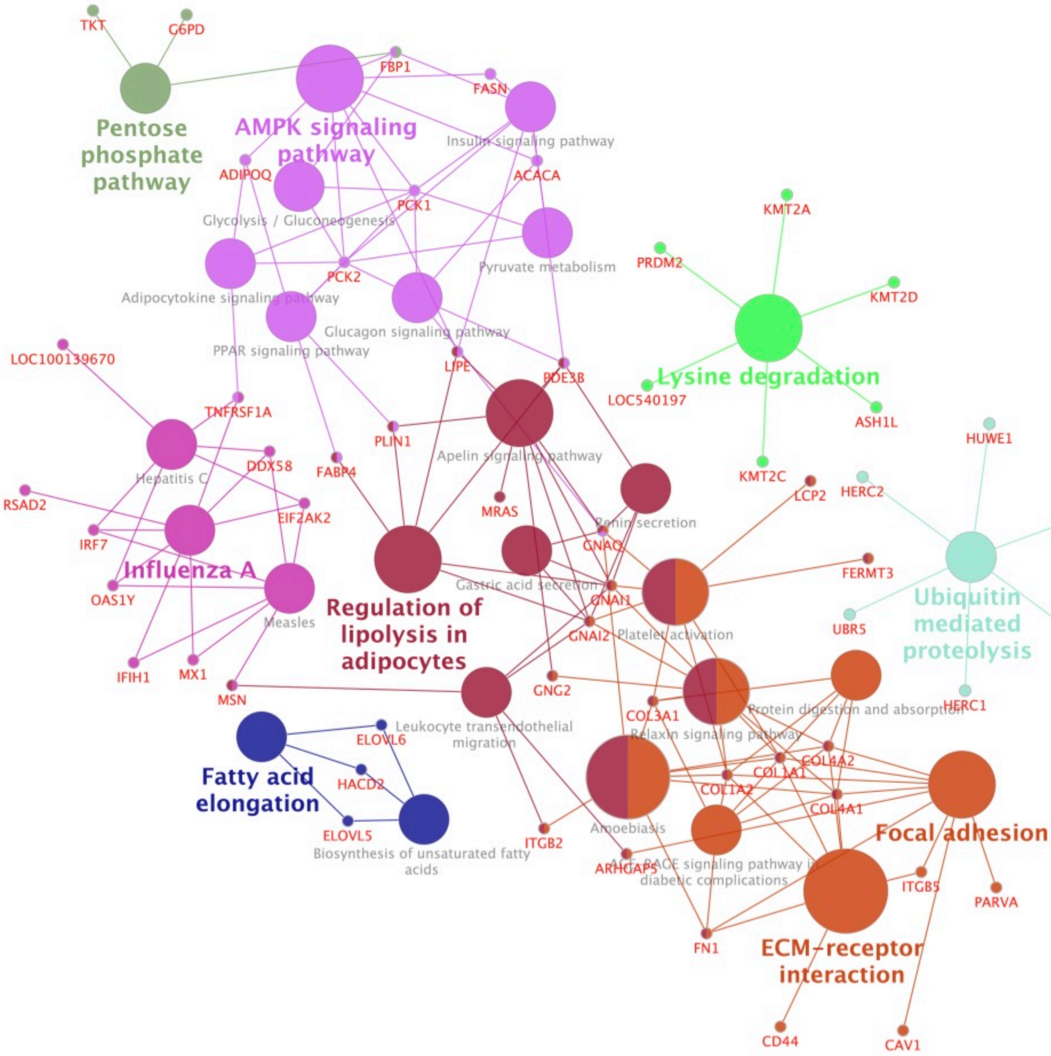

Functionally related groups partially overlap and are arbitrarily colored. The node size represents the pathway enrichment significance.

Table 2.1. Module characterization. The table shows hub genes and eQTL information for each module found to be significantly associated with two or more traits in Figure 2.3.

Module[a]	**eQTLs**[b]	**TGE**[c]	**Hub genes**[d]	**Enriched pathways**[e]
M1 (78)	13	8 (4)	(10) *RSAD2, LOC100139670, MX1, IFIH1, OAS1Y, DDX58, EIF2AK2, IRF7, LOC512486, IFI16*	• NOD-like receptor signaling pathway
M5 (88)	45	15 (3)	(9) *PTPRC, CTSS,* ***DOCK2***, ***IL10RA***, *FERMT3, ITGB2,* ***LCP2***, *CORO1A, PTPRJ*	• Phagosome • Cell adhesion molecules (CAMs)
M6 (190)	89	20 (6)	(20) *GNAI1, PLIN1, FABP4, PPP1R1B, PCK2, ADIPOQ,* ***PDE3B***, *TKT, MGST1, LIPE, ELOVL6, MRAS, ACACA, GNG2, HACD2,* ***FASN***, *FBP1,* ***ELOVL5***, *PCK1, G6PD*	• Adipocytokine signaling pathway • AMPK signaling pathway
M7 (704)	276	76 (2)	(11) *CAV1, COL4A2, GNAI2, SEPT9, TNFRSF1A, YWHAB, COL4A1, TMSB4X, SPTAN1, MSN, PARVA*	• Ras signaling pathway • Focal adhesion •
M8 (1,200)	414	129 (5)	(10) *COL1A2, DCN, FN1, COL1A1, FGFR1, COL3A1, CD44, ITGB5, DSE, CTSK*	• Glycosaminoglycan degradation • Steroid biosynthesis
M9 (69)	16	9 (2)	(1) *JUND*	• TGF-beta signaling pathway • Osteoclast differentiation
M17 (975)	126	66 (2)	(21) *ASH1L, BIRC6, MED13, HERC1, MED13L, KMT2A, HUWE1, KMT2C, ATM, HERC2, KMT2D, MED1, GNAQ, SMC1A, TPR, NSD1, UBR5, ARHGAP5, KAT6A, PRDM2, ITCH*	• Apoptosis • mTOR signaling pathway
Total - 3304	**979**[f]	**323 (24)**	**82**	

[a]Selected modules with the number of contained genes in parenthesis. [b]eQTLs - Number of eQTLs associated with genes in a module (Based on Cesar et al., 2018); [c]**TGE** - Number of module genes associated with eQTLs. In the parenthesis are the number of genes with a MM $\geq$ 0.8; [d]Selected hub genes based on pathway analysis and MM; Hub genes associated with eQTLs are in bold; [e]Pathways from module over-representation analysis taking all genes into the module (Supplementary Table 4) Group p-V $\leq$ 0.05; [f]760 unique eQTLs identified.

2.4. DISCUSSION

In this study, we analyzed genome-wide co-expression in skeletal muscle for association with mineral concentration and meat quality traits. Skeletal muscle metabolism is an integrated system dependent on the efficient coordination of gene expression, which are tightly regulated (SMITH; MEYER; LIEBER, 2013). We found several co-expression modules associated with two or more minerals, meat tenderness, and IMF, which indicates that common pathways influence these traits. From pathway analysis of module hub genes, we further found an over-representation for energy and protein metabolism (AMPK and mTOR). These pathways have been reported as the main drivers regulating energy balance in muscle (SMITH; MEYER; LIEBER, 2013). AMPK and mTOR are metabolically linked, nutritional and hormonal responsive, with an intricated relationship with insulin, thyroid hormone, and TGF-beta signaling pathways (XU; JI; YAN, 2012), which were reported here as well. In addition, these pathways have been associated with muscle development, fat deposition, and beef quality traits (DU et al., 2009). Pathways related with muscle structure such as extracellular matrix, and focal adhesion, identified here, have also been identified in cattle co-expression networks (REVERTER et al., 2006). The above-mentioned pathways are not the only ones acting on muscle metabolism. However, they showed an interaction with mineral concentration and meat quality in our study.

2.4.1. Phenotype Correlation and Co-expression Network Analysis

In agreement with previous reports, we found several minerals positively correlated with IMF, but negatively correlated with meat pH. For instance, Cu-supplemented Angus were found with reduced back fat and reduced serum cholesterol level (ENGLE et al., 2000). Pigs supplemented with Mn showed an increased marbling and decreased pH consistent with the correlation identified here (CONSTANTINO et al., 2014). Furthermore, Se supplementation improved pork meat quality traits by increasing muscle pH (CALVO et al., 2017). In addition, these studies reported a positive effect against lipid oxidation. On the other hand, reduced levels of IMF were associated with low Zn concentration in lambs (PANNIER et al., 2014).

Co-expression analysis resulted in 23 modules from which we considered seven modules for further analysis based on their association with at least two traits. The genes in modules like M5, M7, M8, and M9 were associated with IMF and several minerals suggesting a certain extent of co-regulation. It’s well known that minerals are essential in a wide range of biological processes. Here, we provide evidences that mineral content and meat quality traits are interrelated, as well as interplay with specific genes and pathways (as discussed below).

Variation in eQTL loci can explain a substantial fraction of variation observed on the gene expression level (WANG; MICHOEL, 2016). It has been observed that variation in eQTL loci is associated with concerted expression changes of many genes in co-expression clusters, thereby also impact the phenotype. Screening the detected co-expression modules, we found 323 genes affected by at least one eQTL. Despite 132 eQTLs targeting more than one module, most of the eQTLs were module-specific. However, no significant over-/under-representation (Fisher's exact test) was detectable in these modules, suggesting that other regulatory mechanisms are involved. Despite that, the expression level of six hub genes was found affected by trans-eQTLs. These genes are involved with lipid metabolism [fatty acid synthase (*FASN*), and ELOVL fatty acid elongase 5 (*ELOVL5*), phosphodiesterase 3B (*PDE3B*)], immune system [lymphocyte cytosolic protein 2 (*LCP2*), and interleukin 10 receptor subunit alpha (*IL10RA*)], and actin remodeling (dedicator of cytokinesis 2 - *DOCK2*).

2.4.2. Pathway Analysis

Over-representation pathway analysis in the selected modules (Table 2.1 and Supplementary Table 4) yielded glycosaminoglycan biosynthesis and degradation, lysosome, and steroid biosynthesis in the M8 module. Phagosome, cell adhesion molecular pathways, and NOD-like receptor signaling pathway were found enriched in M1 and M5. For the M17, enriched pathways included protein synthesis pathways such as mTOR, PI3K-Akt, thyroid hormone, and AMPK signaling. We also found protein degradation pathways enriched in the M17 module such as ubiquitin-mediated proteolysis. TGF-beta signaling and osteoclast differentiation were enriched in the M9 module. Energy metabolism pathways were found enriched in M6, including glycolysis, fatty acid biosynthesis, AMPK and insulin signaling. Ras, PI3K-Akt signaling pathways, and protein processing were found enriched in M7.

We also carried out cross-module enrichment analysis considering all hub genes, which indicated that the AMPK signaling pathway plays an important role for muscle mineral metabolism and meat quality traits. The genes of the AMPK pathway were also associated with IMF, Cr, and Fe. Furthermore, the AMPK pathway was also found enriched in genes of M17 (associated with WBSF7, Co, and Mg) and M6 (associated with Cr and Fe concentration).

2.4.3. Energy and Lipid Metabolism

AMPK signaling is a major regulator of the cellular energy status, protein metabolism, and muscle metabolism (JE et al., 2006; DU et al., 2009; MIHAYLOVA; SHAW, 2011). We found carbohydrate and fatty acid metabolism connected by the AMPK pathway (Figure 2.4). Hub gene *ACACA* was thereby involved in pyruvate metabolism, glucagon and insulin signaling pathways. Co-expressed in the M6 module, *ACACA* and *FASN* encode rate-limiting enzymes for long-chain fatty acid synthesis (MIHAYLOVA; SHAW, 2011; ROPKA-MOLIK et al., 2017). *ACACA* catalyzes malonyl-CoA from acetyl-CoA, which is a substrate for the *FASN* enzyme in *de novo* fatty acid synthesis (MENENDEZ; LUPU, 2007; DU et al., 2009). These genes, as well as fatty acid binding protein 4, adipocyte (*FABP4*), are regulated by the thyroid hormone responsive gene (*THRSP*) (GRAUGNARD et al., 2009; LOOR, 2010; OH et al., 2014).

The co-expression of these genes, as well as the negative association between Fe concentration and lipid metabolism, were reported in our previous RNA-Seq work where *FASN*, *THRSP,* and *FABP4* were shown to be downregulated in animals with low Fe concentration in muscle (DINIZ et al., 2016). Hay et al. (2016) reported a major role of Fe for lipid oxidative metabolism based on the downregulation of peroxisome proliferator-activating receptor gamma coactivator 1*α (PPARG1A)* measured by qRT-PCR*.* Thyroid hormone (TH) is also essential for energy metabolism regulation, and Fe deficiency was found to impair TH synthesis and its regulatory function (CUNNINGHAM et al., 1998). Adipogenic genes are responsive to *PPARG* and *TH* (GRAUGNARD et al., 2009). Thus, reduced adipogenesis has been associated with Fe deficiency (CUNNINGHAM et al., 1998; DINIZ et al., 2016; HAY et al., 2016).

In addition to factors that increase the intracellular cyclic AMP level (OMAR et al., 2009), Cr increases AMPK activity and positively affects the insulin sensitivity in skeletal muscle cells (HOFFMAN et al., 2015). As part of the insulin pathway, we found phosphoenolpyruvate carboxykinase 1 and 2 (*PCK1*, *PCK2*), fructose-bisphosphatase 1 (*FBP1*), and phosphodiesterase 3B (*PDE3B*), major regulators of glycolysis and gluconeogenesis (PILKIS; GRANNER, 1992). The *PDE3B* enzyme is stimulated by insulin and cAMP (DEGERMAN et al., 2011) and affects the activation of AMPK

(OMAR et al., 2009). AMPK activation inhibits fatty acid synthesis and gluconeogenesis via repression of *ACACA* and *PCK*, respectively (HARDIE, 2011). Unlike Fe, the concentration of Cr showed a positive correlation with M6. These minerals may have an antagonistic relationship (STANIEK; WÓJCIAK, 2018). However, the correlation between Fe and Cr concentration was not significant in this study most likely due to the limited sample size for Cr concentration.

Supplementing goats with Cr decreased the expression level of *ACACA*, *FASN*, and *FABP4* (SADEGHI et al., 2015) as measured by RT-PCR. Furthermore, increased *Longissimus* muscle area and reduced fat thickness was associated with a downregulation of *ACACA* expression in Cr-supplemented goats (NAJAFPANAH et al., 2014). It seems to follow that Cr supplementation can improve meat quality by altering the direction of energy accumulation from fat deposition towards muscle growth in goats (NAJAFPANAH et al., 2014; SADEGHI et al., 2015). Cr-supplemented Angus-cross steers were also found with increased *Longissimus* muscle area and decreased IMF without affecting growth performance (KNEESKERN et al., 2016). Similar results were reported for Cr-supplemented pigs which showed lower backfat thickness and fat percentage (PAMEI et al., 2014).

2.4.4. Muscle Development, Structure, and Proteolysis

As part of the TGF-beta signaling pathway, we identified the transforming growth factor beta 3 (*TGFB3*), which is involved in muscle proliferation, differentiation, and growth (NISHIMURA, 2015). However, muscle hypertrophy results from a balance of protein turnover in which AMPK signaling negatively affects the protein synthesis (DU et al., 2009). AMPK signaling also acts on cytoskeletal dynamics (MIHAYLOVA; SHAW, 2011). As pointed out in Figure 2.4, common genes act on focal adhesion and ECM-receptor interaction. For these pathways, we found members of the collagen gene family (*COL1A1, COL1A2, COL3A1, COL4A1,* and *COL4A2*), glycoproteins and proteoglycans such as fibronectin 1 (*FBN1*) and decorin (*DCN*), respectively. These molecules are structural components of the ECM and are thus critical for muscle development (MCCORMICK, 2009; NISHIMURA, 2015). These genes were also found associated with meat quality traits such as tenderness and IMF (PONSUKSILI et al., 2013; CESAR et al., 2015; NISHIMURA, 2015). Except for *COL4A1* and *COL4A2*, all collagen genes reported above and which we found co-expressed in M8 were associated with the concentration of Ca, Cr, Fe, K, Mg, Na, P, S, and IMF. Tajima et al. (1981) reported that hypocalcemic fibroblast cells showed an increased synthesis of collagen. Fe concentration has also been associated with collagen metabolism due to the iron-dependent enzymes involved in collagen synthesis (CAMMACK; WRIGGLESWORTH; BAUM, 1990).

We found ubiquitin-mediated proteolysis enriched across modules as well as for genes in the M17 (Supplementary Table 3), which was associated with WBSF7, Co, and Mn. Proteolytic enzymes are important for protein turnover and postmortem meat aging (KOOHMARAIE et al., 2002; GONÇALVES et al., 2018). Baculoviral IAP repeat containing 6 (*BIRC6*) is a caspase inhibitor and apoptotic suppressor protein (VERHAGEN; COULSON; VAUX, 2001). *BIRC6* is part of the ubiquitin-mediated proteolysis pathway and was positively associated with M17. By impairing proteolysis, the up-regulation of *BIRC6* likely increases shear force (LIU et al., 2016). Genes from the E3 ubiquitin-protein ligase family (*HERC1, HERC2, HUWE1, ITCH,* and *UBR5*) were also identified in agreement with a recent report that found ubiquitination and apoptosis to be potential regulators of meat tenderness in Nelore cattle (GONÇALVES et al., 2018).

2.5. CONCLUSIONS

We demonstrated transcriptional relationships among mineral concentration and meat quality traits in the skeletal muscle of Brazilian Nelore cattle. We identified 82 hub genes across seven co-expression modules which seem to be critical for this interplay. The AMPK and mTOR signaling pathways were hereby found to link mineral and muscle metabolism in Nelore cattle. Future studies investigating different levels of mineral supplementation, the mineral interaction, and their effect in the gene expression and meat quality traits could help us to elucidate the regulatory mechanisms by which the genes/pathways are affected.

DATA AVAILABILITY

All relevant data are within the paper and its Supporting Information files. All sequencing data is available in the European Nucleotide Archive (ENA) repository (EMBL-EBI), under accession PRJEB13188, PRJEB10898, and PRJEB19421 [https://www.ebi.ac.uk/ena/submit/sra/]. All additional datasets generated and analysed during this study may be available upon request from the corresponding author on reasonable request.

AUTHORS CONTRIBUTIONS

WJSD, PCT, LCAR, LLC, and HNK conceived the idea of this research. WJSD, GM, LG, FB, and ASMC, JA, PSNO, PCT carried out the bioinformatics and data analysis. WJSD, GM, PB, FB, HNK, JA, LLC, LCAR collaborated with the interpretation of results, discussion and review the manuscript. WJSD, PB, and GM drafted the manuscript. All authors have read and approved the final manuscript and agree to be accountable for the content of the work.

FUNDING

This study was conducted with funding from EMBRAPA (Macroprograma 1, 01/2005), FAPESP (grant# 2012/23638-8), and by the Coordenação de Aperfeiçoamento de Pessoal de Nível Superior - Brasil (CAPES) - Finance Code 001. LCAR and LLC were granted CNPq fellowships. WJSD was granted by São Paulo Research Foundation (FAPESP) grant# 2015/09158-1 and grant# 2017/20761-7 scholarships.

ACKNOWLEDGMENTS

We are thankful to Bruno G. N. Andrade for the server management and support; Dr. Ana Rita Araújo Nogueira and Dr. Caio F. Gromboni for the mineral data; and the Technical University of Denmark (DTU compute) for accepting the first author as a visiting scholar.

COMPETING FINANCIAL INTERESTS

The authors declare that the research was conducted in the absence of any commercial or financial relationships that could be construed as a potential conflict of interest.

2.6. REFERENCES

ABIEC. **Perfil da pecuária no Brazil**. [s.l: s.n.]. Disponível em: <http://abiec.siteoficial.ws/images/upload/sumario-pt-010217.pdf>.

AHLBERG, C. M. et al. Genome wide association study of cholesterol and poly- and monounsaturated fatty acids, protein, and mineral content of beef from crossbred cattle. **Meat Science**, v. 98, n. 4, p. 804–814, dez. 2014.

ANDERS, S.; HUBER, W. Differential expression analysis for sequence count data. **Genome Biology**, v. 11, n. 10, p. R106, 2010.

ANDREWS, S. **FastQC: a quality control tool for high throughput sequence data**. Disponível em: <https://www.bioinformatics.babraham.ac.uk/projects/fastqc/>.

BINDEA, G. et al. ClueGO: A Cytoscape plug-in to decipher functionally grouped gene ontology and pathway annotation networks. **Bioinformatics**, v. 25, n. 8, p. 1091–1093, 2009.

CALVO, L. et al. Effect of dietary selenium source (organic vs. mineral) and muscle pH on meat quality characteristics of pigs. **Food Science & Nutrition**, v. 5, n. 1, p. 94–102, jan. 2017.

CAMMACK, R.; WRIGGLESWORTH, J. M.; BAUM, H. Iron-dependent enzymes in mammalian systems. In: PONKA, P. et al. (Ed.). **Iron:transport and storage**. United States of America: CRC Press, 1990. p. 17–39.

CÁNOVAS, A. et al. Muscle transcriptomic profiles in pigs with divergent phenotypes for fatness traits. **BMC Genomics**, v. 11, p. 372, jan. 2010.

CESAR, A. S. M. et al. Genome-wide association study for intramuscular fat deposition and composition in Nellore cattle. **BMC genetics**, v. 15, n. 1, p. 39, 2014.

CESAR, A. S. M. et al. Putative Regulatory Factors Associated with Intramuscular Fat Content. **Plos One**, v. 10, n. 6, p. e0128350, 2015.

CESAR, A. S. M. et al. Identification of putative regulatory regions and transcription factors associated with intramuscular fat content traits. **BMC Genomics**, v. 19, p. 1–20, 2018.

CLUGSTON, G. A.; SMITH, T. E. Global nutrition problems and novel foods Global nutrition problems and novel foods S101. **Asia Pacific J Clin Nutr**, v. 11, n. S6, p. 100–111, 2002.

CONSTANTINO, C. et al. Performance, carcass and meat quality of ewes supplemented with magnesium oxide. **Revista Brasileira de Zootecnia**, v. 43, n. 1, p. 27–35, jan. 2014.

CUNNINGHAM, B. A. et al. “Spot 14” protein: a metabolic integrator in normal and neoplastic cells. **Thyroid**, v. 8, n. 9, p. 815–825, 1998.

DEGERMAN, E. et al. From PDE3B to the regulation of energy homeostasis. **Current Opinion in Pharmacology**, v. 11, n. 6, p. 676–682, dez. 2011.

DINIZ, W. J. da S. et al. Iron Content Affects Lipogenic Gene Expression in the Muscle of Nelore Beef Cattle. **PLOS ONE**, v. 11, n. 8, p. e0161160, 17 ago. 2016

DOBIN, A. et al. STAR: ultrafast universal RNA-seq aligner. **Bioinformatics**, v. 29, n. 1, p. 15–21, jan. 2013.

DU, M. et al. AMP-Activated Protein Kinase in Muscle Growth, Fat Deposition, and Meat Quality. In: DU, M.; MCCORMICK, R. J. (Ed.). **Applied Muscle Biology and Meat Science**. 1. ed. Boca Raton: CRC Press, 2009. p. 360.

ENGLE, T. E. et al. Effects of dietary copper source and concentration on carcass characteristics and lipid and cholesterol metabolism in growing and finishing steers. **Journal of Animal Science**, v. 78, n. 4, p. 1053, 2000.

EWELS, P. et al. MultiQC: summarize analysis results for multiple tools and samples in a single report. **Bioinformatics**, v. 32, n. 19, p. 3047–3048, 1 out. 2016.

GEISTLINGER, L. et al. Widespread modulation of gene expression by copy number variation in skeletal muscle. **Scientific Reports**, v. 8, n. 1, p. 1399, 23 dez. 2018.

GONÇALVES, T. M. et al. Gene Co-expression Analysis Indicates Potential Pathways and Regulators of Beef Tenderness in Nellore Cattle. **Frontiers in Genetics**, v. 9, p. 441, 5 out. 2018.

GRAUGNARD, D. E. et al. Adipogenic and energy metabolism gene networks in longissimus lumborum during rapid post-weaning growth in Angus and Angus x Simmental cattle fed high-starch or low-starch diets. **BMC Genomics**, v. 10, p. 142, 2009.

HARDIE, D. G. AMP-activated protein kinase--an energy sensor that regulates all aspects of cell function. **Genes & Development**, v. 25, n. 18, p. 1895–1908, 15 set. 2011.

HAY, S. M. et al. The effect of iron deficiency on the temporal changes in the expression of genes associated with fat metabolism in the pregnant rat. **Physiological reports**, v. 4, p. 1–9, 2016.

HOFFMAN, N. J. et al. Chromium Enhances Insulin Responsiveness via AMPK. **J Nutr Biochem.**, v. 25, n. 5, p. 565–572, 2015.

JE, W. et al. AMPK activation increases fatty acid oxidation in skeletal muscle by activating PPAR. v. 340, p. 291–295, 2006.

KNEESKERN, S. G. et al. Effects of chromium supplementation to feedlot steers on growth performance, insulin sensitivity, and carcass characteristics. **Journal of Animal Science**, v. 94, n. 1, p. 217–226, 2016.

KOOHMARAIE, M. et al. Meat tenderness and muscle growth: is there any relationship? **Meat Science**, v. 62, n. 3, p. 345–352, nov. 2002.

LANGFELDER, P.; HORVATH, S. Eigengene networks for studying the relationships between co-expression modules. **BMC Systems Biology**, v. 1, n. 1, p. 54, 2007.

LANGFELDER, P.; HORVATH, S. WGCNA: An R package for weighted correlation network analysis. **BMC Bioinformatics**, v. 9, 2008.

LANGFELDER, P.; ZHANG, B.; HORVATH, S. Defining clusters from a hierarchical cluster tree: The Dynamic Tree Cut package for R. **Bioinformatics**, v. 24, n. 5, p. 719–720, 2008.

LI, J. et al. Application of Weighted Gene Co-expression Network Analysis for Data from Paired Design. **Scientific Reports**, v. 8, n. 1, p. 1–8, 2018.

LIU, Y. et al. Role of the ubiquitin-proteasome pathway on proteolytic activity in postmortem proteolysis and tenderisation of sheep skeletal muscle. **International Journal of Food Science & Technology**, v. 51, n. 11, p. 2353–2359, nov. 2016.

LOOR, J. J. Transcriptomics of muscle and fat development in growing cattle. In: CROVETTO, G. M. (Ed.). **Energy and protein metabolism and nutrition**. 3. ed. Italy: Wageningen Academic Publishers, 2010. p. 59–68.

MATEESCU, R. It is possible to genetically change the nutrient profile of beef. (Beef Improvement Federation, Ed.) In: Beef improvement Federation Research Symposium & Annual Meeting, Lincoln, Nebraska. **Anais**... Lincoln, Nebraska: 2014. Disponível em: <http://www.bifconference.com/bif2014/newsroom.html>.

MATEESCU, R. G.; GARRICK, D. J.; REECY, J. M. Network analysis reveals putative genes affecting meat quality in Angus cattle. **Frontiers in Genetics**, v. 8, n. NOV, 2017.

MCCORMICK, R. J. Collagen. In: DU, M.; MCCORMICK, R. J. (Ed.). **Applied Muscle Biology and Meat Science**. 1. ed. Boca Raton: CRC Press, 2009. p. 360.

MENENDEZ, J. A.; LUPU, R. Fatty acid synthase and the lipogenic phenotype in cancer pathogenesis. **Nature reviews cancer**, v. 7, p. 763–777, 2007.

MIHAYLOVA, M. M.; SHAW, R. J. The AMPK signalling pathway coordinates cell growth, autophagy and metabolism. **Nature Cell Biology**, v. 13, n. 9, p. 1016–1023, 1 set. 2011.

NAJAFPANAH, M. J. et al. Chromium downregulates the expression of Acetyl CoA Carboxylase 1 gene in lipogenic tissues of domestic goats : a potential strategy for meat quality improvement. **Gene**, v. 543, n. 2, p. 253–258, 2014.

NCBI. **ARS-UCD1.2**. Disponível em: <https://www.ncbi.nlm.nih.gov/genome/annotation_euk/Bos_taurus/106/>.

NISHIMURA, T. Role of extracellular matrix in development of skeletal muscle and postmortem aging of meat. **Meat Science**, v. 109, p. 48–55, 2015.

OH, D. et al. Identification of exonic nucleotide variants of the thyroid hormone responsive protein gene associated with carcass traits and Fatty Acid composition in korean cattle. **Asian-Australasian Journal of Animal Sciences**, v. 27, n. 10, p. 1373–80, out. 2014.

OMAR, B. et al. Regulation of AMP-activated protein kinase by cAMP in adipocytes: Roles for phosphodiesterases, protein kinase B, protein kinase A, Epac and lipolysis. **Cellular Signalling**, v. 21, n. 5, p. 760–766, maio 2009.

PAMEI, G. et al. Influence of dietary supplementation of chromium on the carcass traits of crossbred pigs. **Journal of Advanced Veterinary and Animal Research**, v. 1, n. September, p. 1, 2014.

PANNIER, L. et al. Associations of genetic and non-genetic factors with concentrations of iron and zinc in the longissimus muscle of lamb. **Meat Science**, v. 96, n. 2, p. 1111–1119, 2014.

PIGHIN, D. et al. A Contribution of Beef to Human Health: A Review of the Role of the Animal Production Systems. **The Scientific World Journal**, v. 2016, 2016.

PILKIS, S. J.; GRANNER, D. K. Molecular Physiology of the Regulation of Hepatic Gluconeogenesis and Glycolysis. **Annual Review of Physiology**, v. 54, n. 1, p. 885–909, 1992.

PONSUKSILI, S. et al. Correlated mRNAs and miRNAs from co-expression and regulatory networks affect porcine muscle and finally meat properties. **BMC genomics**, v. 14, n. 1, p. 533, 2013.

REVERTER, A. et al. A gene coexpression network for bovine skeletal muscle inferred from microarray data. **Physiological genomics**, v. 28, p. 76–83, 2006.

RITCHIE, H.; ROSER, M. **Micronutrient Deficiency**. Disponível em: <https://ourworldindata.org/micronutrient-deficiency>. Acesso em: 22 ago. 2018.

RITCHIE, M. E. et al. limma powers differential expression analyses for RNA-sequencing and microarray studies. **Nucleic Acids Research**, v. 43, n. 7, p. e47–e47, 20 abr. 2015.

ROBINSON, M. D.; MCCARTHY, D. J.; SMYTH, G. K. edgeR: a Bioconductor package for differential expression analysis of digital gene expression data. **Bioinformatics**, v. 26, n. 1, p. 139–140, 1 jan. 2010.

ROPKA-MOLIK, K. et al. Nutritional modification of SCD, ACACA and LPL gene expressions in different ovine tissues. **Arch. Anim. Breed**, v. 60, p. 243–250, 2017.

SADEGHI, M. et al. Transcription analysis of genes involved in lipid metabolism reveals the role of chromium in reducing body fat in animal models. **Journal of Trace Elements in Medicine and Biology**, v. 32, p. 45–51, 2015.

SHANNON, P. et al. Cytoscape : A Software Environment for Integrated Models of Biomolecular Interaction Networks. n. Karp 2001, p. 2498–2504, 2003.

SILVA-VIGNATO, B. et al. Comparative muscle transcriptome associated with carcass traits of Nellore cattle. **BMC Genomics**, v. 18, n. 1, p. 506, 2017.

SILVA, V. H. da et al. Genome-Wide Detection of CNVs and Their Association with Meat Tenderness in Nelore Cattle. **Plos One**, v. 11, n. 6, p. e0157711, 2016.

SMITH, L. R.; MEYER, G.; LIEBER, R. L. Systems analysis of biological networks in skeletal muscle function. **Wiley Interdisciplinary Reviews: Systems Biology and Medicine**, v. 5, n. 1, p. 55–71, 1 jan. 2013.

STANIEK, H.; WÓJCIAK, R. W. The combined effect of supplementary Cr(III) propionate complex and iron deficiency on the chromium and iron status in female rats. **Journal of Trace Elements in Medicine and Biology**, v. 45, n. July 2017, p. 142–149, 2018.

SURAVAJHALA, P.; KOGELMAN, L. J. A.; KADARMIDEEN, H. N. Multi-omic data integration and analysis using systems genomics approaches: methods and applications in animal production, health and welfare. **Genetics Selection Evolution**, v. 48, n. 1, p. 38, 29 dez. 2016.

TAJIMA, T. et al. The influence of calcium ions on the synthesis of collagen and glycosaminoglycans in human diploid cells in culture. **Experimental pathology**, v. 19, n. 4, p. 219–25, 1981.

TARAZONA, S. et al. Data quality aware analysis of differential expression in RNA-seq with NOISeq R/Bioc package. **Nucleic Acids Research**, p. gkv711, 16 jul. 2015.

TIZIOTO, P. C. et al. Genome scan for meat quality traits in Nelore beef cattle. **Physiological Genomics**, v. 45, n. 21, p. 1012–1020, 1 nov. 2013.

TIZIOTO, P. C. et al. Calcium and potassium content in beef: influences on tenderness and associations with molecular markers in Nellore cattle. **Meat science**, v. 96, n. 1, p. 436–40, jan. 2014.

TIZIOTO, P. C. et al. Detection of quantitative trait loci for mineral content of Nelore longissimus dorsi muscle. **Genetics Selection Evolution**, v. 47, n. 1, p. 15, 2015.

VERHAGEN, A. M.; COULSON, E. J.; VAUX, D. L. Inhibitor of apoptosis proteins and their relatives: IAPs and other BIRPs. **Genome biology**, v. 2, n. 7, p. REVIEWS3009, 2001.

WANG, L.; MICHOEL, T. Detection of Regulator Genes and eQTLs in Gene Networks. In: KADARMIDEEN, H. N. (Ed.). **Systems Biology in Animal Production and Health, Vol. 1**. Cham: Springer International Publishing, 2016. p. 1–23.

XU, J.; JI, J.; YAN, X. Cross-Talk between AMPK and mTOR in Regulating Energy Balance. **Critical Reviews in Food Science and Nutrition**, v. 52, n. 5, p. 373–381, maio 2012.

ZHBANNIKOV, I. Y. et al. SeqyClean: A Pipeline for High-throughput Sequence Data Preprocessing. In: Proceedings of the 8th ACM International Conference on Bioinformatics, Computational Biology, and Health Informatics, New York, NY, USA. **Anais**... New York, NY, USA: ACM, 2017.

Chapter 3

Interplay among miR-29 family, mineral metabolism, and gene regulation in *Bos indicus* muscle[3]

ABSTRACT

An interplay between gene expression, mineral concentration, and beef quality traits in *Bos indicus* muscle has been reported previously under a network approach. However, growing evidence suggested that miRNAs not only modulate gene expression but are also involved with mineral homeostasis. To our knowledge, understanding of the miRNA-gene expression-mineral concentration relationship in mammals is still minimal. Therefore, we carried out a miRNA co-expression and multi-level miRNA-mRNA integration analyses to predict the putative drivers (miRNAs and genes) associated with muscle mineral concentration in Nelore steers. In this study, we identified calcium and iron to be the pivotal minerals associated with miRNAs and gene targets. We also identified the mir-29 family (miR-29a, -29b, -29c, -29d-3p, and -29e) as the putative key regulators modulating mineral homeostasis. The miR-29 family target genes were also found involved with AMPK, insulin, mTOR, and thyroid hormone signaling pathways. This is the first study reporting an interplay among miRNAs, mRNAs, and minerals acting cooperatively to maintain the cellular homeostasis in Nelore muscle. We provided some evidence to understand this complex relationship, opening up several possibilities for the potential development of predictive biomarkers for mineral concentration in meat, and improving animal nutrition.

Keywords: calcium, co-expression, iron, mineral homeostasis, regulatory network, systems biology.

---

[3] Diniz, WJS; Banerjee, P; Mazzoni, G.; Coutinho, LL; Cesar, ASM; Afonso, J; Gromboni, VF; Nogueira, ARA; Kadarmideen, HN; Regitano, LCA. **Under review on Molecular Genetics and Genomics Journal** (MGAG-D-19-00536).

3.1. INTRODUCTION

Advancements have been made to understand the mineral metabolism and its role in human health and animal production (SUTTLE, 2010; FLEET; REPLOGLE; SALT, 2011). However, mineral deficiencies, mainly iron and zinc, are the most common worldwide health hazards (RITCHIE; ROSER, 2018). Although required in small amounts in the diet, an adequate mineral supply is necessary for the body metabolism, which includes muscle performance and energy utilization (GARMYN et al., 2011; TIZIOTO et al., 2015). Macro and micro minerals have multiple roles. They are crucial for biological processes such as DNA synthesis, gene expression, cell growth and differentiation, and energy metabolism (FLEET; REPLOGLE; SALT, 2011; DAVIS et al., 2012b; BECKETT et al., 2014). Both deficiency or mineral overload are potentially deleterious (SUTTLE, 2010). Therefore, tight regulation is necessary to keep mineral levels within a narrow range. Besides the intake-output imbalance and environmental factors, several transcriptional and post-transcriptional mechanisms involved in mineral homeostasis were reported (SUTTLE, 2010).

Genome-wide association studies in cattle have suggested that muscle mineral content is under genetic control (TIZIOTO et al., 2015; MATEESCU; GARRICK; REECY, 2017). Tizioto et al. (2015) reported candidate genes with an additive effect on muscle mineral concentration in cattle. Also, several genes differentially expressed in Nelore steers genetically divergent for muscle mineral deposition, including calcium (Ca), copper (Cu), iron (Fe), selenium (Se), and zinc (Zn), underlie a complex network (AFONSO et al., 2019; DINIZ et al., 2019). Based on co-expression analysis, we reported that genes acting in pathways related to energy and protein metabolism were also associated with the mineral concentration in muscle. Moreover, studies have reported that minerals not only modulate gene translation but are also involved with miRNA biosynthesis, which in turn regulates mineral homeostasis (AZZOUZI et al., 2013; BECKETT et al., 2014; MAGENTA et al., 2016). MiRNAs have a role in a wide range of biological functions (BUDAK; ZHANG, 2017) underpinning traits like meat tenderness (KAPPELER et al., 2019) and intramuscular fat content (OLIVEIRA et al., 2018a, 2018b). Likewise, Ca, Fe, and Zn were also associated with these traits (GARMYN et al., 2011; AHLBERG et al., 2014; CASAS et al., 2014; TIZIOTO et al., 2014), and have been reported as modulating miRNA biosynthesis (BECKETT et al., 2014; MAGENTA et al., 2016; RIPA et al., 2017).

Mineral metabolism should be viewed as a system, both because of their interactions among themselves, as well as their role with the functional genome variation in different regulatory layers (FLEET; REPLOGLE; SALT, 2011). Supporting this holistic approach, a growing number of studies have shown the interaction between minerals and gene expression/translation (DAVIS et al., 2012a; XU; SHI; LI, 2013; BECKETT et al., 2014). In this scenario, a feedback loop has been suggested as the mechanism modulating miRNA-gene-mineral interaction (BECKETT et al., 2014). Integrative genomic approaches have proven to be a fruitful tool to study these interactions (SU; KLEINHANZ; SCHADT, 2014; BAO; GREENWOLD; SAWYER, 2017). However, to date, there is still a knowledge gap about the genetic architecture underlying mineral homeostasis in muscle, as well as the miRNA-gene-mineral interconnection.

Therefore, we carried out an exploratory miRNA co-expression and multi-level miRNA-mRNA integration analyses to uncover the pathways and regulatory networks underlying mineral concentration in Nelore cattle muscle. From a systems biology perspective, we identified miRNAs acting cooperatively to modulate co-expressed genes and signaling pathways, both involved with mineral and energy homeostasis. Understanding this complex relationship opens up several possibilities to potentially develop predictive biomarkers for mineral concentration in meat, to improve animal nutrition, and to develop functional food.

3.2. MATERIAL AND METHODS

3.2.1. Ethics statement

Experimental procedures involving the animals used in this study were carried out in accordance with the Institutional Animal Care and Use Committee Guidelines of the Empresa Brasileira de Pesquisa Agropecuária (EMBRAPA – Pecuária Sudeste) (approval code CEUA 01/2013).

3.2.2. Animals and phenotypes

The animal resources used in this research came from a population of 200 Nelore steers sired by 34 unrelated Nelore bulls (TIZIOTO et al., 2015). Steers were raised under similar production system, diet, and management (DINIZ et al., 2016), and were slaughtered with an average age of 25 months after 90 days of a feedlot trial, as detailed by Oliveira et al. (2014).

Muscle samples were harvested as a cross-section of the LT muscle (11th and 13th ribs) at slaughter for mineral measurement and RNA extraction. The samples for RNA analysis were immediately snap-frozen in liquid nitrogen after sampling and kept at -80 ºC until RNA extraction.

Macro and micro minerals, respectively, [calcium (Ca), magnesium (Mg), phosphorus (P), potassium (K), sodium (Na), and sulphur (S)], [copper (Cu), manganese (Mn), selenium (Se), iron (Fe), and zinc (Zn)] were measured using inductively coupled plasma-optical emission spectrometry (ICP OES; Vista Pro-CCD ICP OES1, radial view, Varian, Mulgrave, Australia), as previously reported by Tizioto et al. (2014, 2015).

3.2.3. RNA extraction, library preparation, and sequencing

Trizol® standard protocol (Life Technologies, Carlsbad, CA) was used to extract total RNA from 100 mg of frozen muscle tissue. The RNA quality and integrity were evaluated by Bioanalyzer 2100 (Agilent, Santa Clara, CA, USA) with the RNA 6000 Nano kit.

Libraries were prepared and sequenced in the Laboratory Multiuser ESALQ in Piracicaba-SP, Brazil, as reported elsewhere (OLIVEIRA et al., 2018b). Briefly, for library preparation 200 ng/µL of RNA from each sample was used following the TruSeq® smallRNA Sample Preparation kit (Illumina - San Diego, USA). Libraries were further quantified by quantitative PCR with the KAPA Library Quantification kit (KAPA Biosystems, Foster City, CA, USA).

The single-end sequencing of 42 bp was carried out on MiSeq sequencer (Illumina®), using MiSeq Reagent Kit v3 (150 cycles), generating around 1 million reads/sample.

3.2.4. Data quality control, miRNA identification, and expression normalization

Raw data quality control was carried out with FastQC version 0.11.2 (https://goo.gl/mcyE5Sn) (ANDREWS, 2010) and trimmed using FASTX - Toolkit software (https://goo.gl/MueTV5) (FASTX-TOOLKIT, 2009). Reads with quality Phred score lower than 28 and shorter than 18 nt were discarded.

The reads were mapped to the bovine reference genome *Bos taurus* ARS-UCD 1.2 by Bowtie version 1.2.1.1 (FRIEDLÄNDER et al., 2008). Mapped reads were further used to identify known and novel miRNAs for *B. taurus* using the miRDeep2.pl module (FRIEDLÄNDER et al., 2008). The mature miRNA sequences from bovine and humans, and the bovine hairpin structure were retrieved from the miRBase v. 22 (KOZOMARA; GRIFFITHS-JONES, 2014).

The raw counts generated by miRDeep2 were processed in order to filter out low or not expressed miRNAs applying the *cpm* function from edgeR version 3.24.0 (ROBINSON; MCCARTHY; SMYTH, 2010). MiRNA counts with less than 0.5 *cpm* in more than 70% of the samples were filtered out. The library normalization, as well as the data variance stabilization, were carried out by *VST* function implemented in DESeq2 (ANDERS; HUBER, 2010).

Principal Component Analysis (PCA) and hierarchical clustering on normalized data were performed with NOISeq version 2.26.0 (TARAZONA et al., 2015). *Limma* version 3.34.9 (RITCHIE et al., 2015) was adopted to fit a linear model to adjust the gene expression since a flow cell effect was identified.

3.2.5. MiRNA co-expression network analysis

A co-expression network analysis was carried out taking the expression profile of 343 miRNAs from 50 samples based on the general framework implemented in WGCNA R-package, version 1.66 (LANGFELDER; HORVATH, 2008). Briefly, an adjacency matrix was calculated by raising the absolute Pearson's correlation coefficient between the miRNAs to a power $\beta = 9$ (soft threshold) to reach the scale-free network topology index ($R^2 > 0.9$) (ZHAO et al., 2010).

Average linkage hierarchical clustering method was used to define the miRNA clusters using the Dynamic Tree algorithm (LANGFELDER; ZHANG; HORVATH, 2008). MiRNA modules were generated considering a branch cut-off of 0.99, deepSplit = 4, and minimum module size of 5 was chosen due to the small miRNA transcriptome (OLIVEIRA et al., 2018a, 2018b). Following this, modules were detected and labeled by color. From each module, the eigengene (module eigengene - ME) was the first principal component (LANGFELDER; HORVATH, 2007) and represented a measure of miRNA expression profiles in the module.

3.2.6. Module-trait association and hub miRNA selection

The module-trait relationship was estimated by fitting a linear model to analyze the association between the expression profiles of the modules (MEs) and the phenotypes (mean centered and scaled). The statistical model included the fixed effect of place of birth, and animal's age at slaughter as a covariate, according to the equation:

$$y_{ijk} = \mu + C_i + A_j + T_k + \varepsilon_{ijk}$$

Where:

y_{ijk}: is the expression level of the eigengene in each module (n =24);

μ: is the intercept of ME;

C_i: is the fixed effect for the place of birth (3 levels = CPPSE, IMA, NOHO);

A_j: is the covariate for the animal's age;

T_k:is the trait observation for each animal;

ε_{ijk}: is the random residual effect associated with each observation.

Putative relevant modules were taken for further analyses with $p \leq 0.05$. As reported by Su et al. (2011) miRNAs exist as highly connected hub nodes within a transcriptional network and drive changes in mRNA expression. Thus, from the associated modules the hub miRNAs were selected based on the module membership ≥ 0.7 (LANGFELDER; HORVATH, 2008).

3.2.7. MiRNA - mRNA regulatory network and miRNA target prediction

The samples used here are part of the previous work that was carried out to identify co-expressed genes associated with meat quality and mineral traits in a population with 194 animals (DINIZ et al., 2019). Because the miRNAs exert a pivotal role in gene expression, the miRNA - mRNA expression data were integrated to identify the putative regulatory link between them and their role in phenotypes. In that study, 15 modules were associated with at least one trait ($p \leq 0.05$), which were taken for the integrative analysis. Since multiple miRNAs can target the genes, a module approach was adopted to alleviate the multiple test problem (LANGFELDER; HORVATH, 2008). For this, 48 animals were identified with paired expression data, and the miRNA MEs (9 modules; from current study) were correlated with mRNAs MEs (15 modules; from the previous study). MiRNAs are expected to downregulate the expression level of targets (SU; KLEINHANZ; SCHADT, 2014), and thereby modules with negative correlation lower than - 0.3 and $p \leq 0.05$ were selected for functional analysis.

A computational prediction method was applied based on paired miRNA-mRNA profiling to identify the potential target mRNAs of the hub miRNAs. The significant negative correlated modules were intersected with miRNA-mRNA interactions predicted from TargetScan (AGARWAL et al., 2015) to point out only those putative acting pairs. To this end, hoardeR package version 0.9.2 (FISCHER; SIRONEN, 2016) was used to search for the putative mRNA targets on TargetScan bovine database, release 7.2. To better predict the putative targets, the genes retrieved from TargetScan were filtered by skeletal muscle expression data previously analyzed in the same samples (DINIZ et al., 2019). MicroRNA family information was obtained from miRbase v. 22 (KOZOMARA; GRIFFITHS-JONES, 2014).

3.2.8. Identification of key transcription factors

The compendium of bovine transcription factors (SOUZA et al., 2018) was employed to explore the gene regulatory network in the co-expressed modules, as well as the cross-talk between miRNAs, transcription factors, and their targets. To detect regulatory modules, the miRNA-mRNA pairs identified were screened out to reveal enriched transcription factors. The regulatory network was visualized in Cytoscape 3.7.0 (CLINE et al., 2007).

3.2.9. Functional and pathway enrichment analyses

Based on the *B. taurus* genome background, KEGG pathway analysis was carried out using Cytoscape plugins: ClueGO v. 2.5.3 and CluePedia v. 1.5.3 (BINDEA et al., 2009) to shed light on the biological functions over-represented in the associated module genes. KEGG pathways with pV $\leq$ 0.05 (group p-value corrected with Bonferroni step down) were considered significantly enriched. Redundant terms were grouped based on the kappa score = 0.4 (BINDEA et al., 2009). Interaction networks were constructed and visualized in Cytoscape (CLINE et al., 2007).

3.3. RESULTS

We established co-expression networks to shed light on the miRNA-trait relationship, as well as the regulatory mechanisms among miRNA, gene targets, and mineral concentration. We first identified co-expressed miRNA modules relying on WGCNA method, and then a linear association model was fitted to identify modules biologically associated with the phenotypes. Further, we integrated these miRNA modules to gene co-expression modules identified in our previous study (DINIZ et al., 2019), based on module eigengene (MEs) correlation. We also intersected the significant negatively correlated modules to miRNA-mRNA interactions predicted from TargetScan (AGARWAL et al., 2015). Next, we carried out a transcription factor prediction and enrichment analysis to, respectively, bring up putative regulators and biological pathways (Figure 3.1).

3.3.1. Phenotypic and sequencing data

The heritability for mineral concentration evaluated for this Nelore population ranged from 0.29 to 0.33, as previously published (TIZIOTO et al., 2015). These minerals were strongly and significantly correlated among themselves ranging from 0.45 to 0.99 (DINIZ et al., 2019).

MiRNA sequencing from 50 *Longissimus thoracis* (LT) samples yielded 1,4 million sequence reads per sample, on average. An average of 84.7% of the reads was mapped to *Bos taurus* ARS-UCD 1.2. After filtering out the lowly expressed miRNAs, we kept 343 known miRNAs used in the co-expression analysis.

Figure 3.1. Co-expression pipeline analysis.

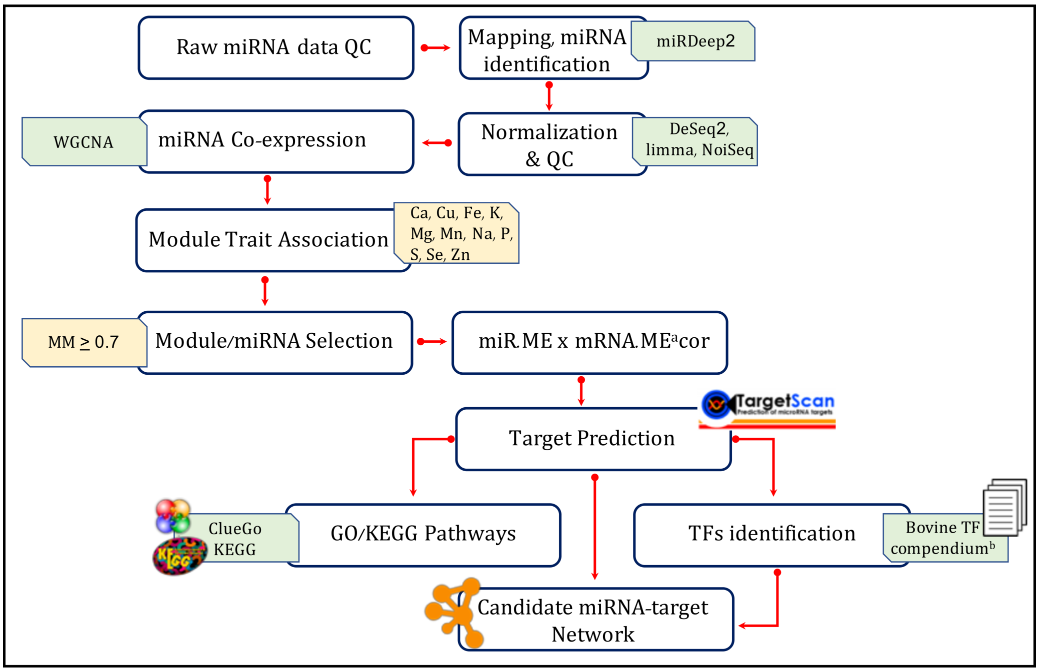

The main analyses steps to data processing and co-expression, and data integration are shown in white boxes. Tools applied in each analysis are shown in green boxes. Inputs and outputs are shown in lightyellow boxes. QC - quality control; MM – module membership; [a]mRNA modules from (Diniz 2019); [b]Based on the curated compendium of bovine transcription factors (TFs) from (SOUZA et al. 2018).

3.3.2. Co-expression analysis and module-trait association

To identify the miRNA co-expression network, we clustered 343 miRNAs adopting the WGCNA framework (LANGFELDER; HORVATH, 2008). We gathered 24 modules labeled by color names and module size, ranging from 5 (miR.MEdarkgreen, miR.MEdargrey, and miR.MEred) to 34 miRNAs (miR.MEturquoise) (Supplementary Table S1). We calculated the proportion of variance explained by the MEs, which ranged from 0.29 (miR.MEgreen) to 0.67 (miR.MEdarkgreen) (Supplementary Table S1).

We fitted a linear model to associate the MEs with mineral concentration, selected the significant ($p \leq 0.05$) modules, and investigated their biological relevance. Our approach identified nine miRNA modules, which were significantly ($p \leq 0.05$) associated with at least one mineral, as summarized in Table 3.1. The coefficient values from the linear model for the significant associations ranged from -0.058 to 0.071 (Supplementary Figure S1). A positive association means the trait increases with increasing “eigengene expression” or vice-versa. We found the highest number of significantly associated traits between miR.MEcyan (positively associated with ten minerals) and miR.MEgreen (negatively associated with six minerals). A positive association was identified among minerals and miR.MEbrown (Ca Na, S), miR.MEmidnightblue (Ca, Fe, S, Zn), and miR.MEgrey60 (Fe). Further, we also showed a negative relationship for the miR.MElightyellow (Ca, Mg, Na), miR.MEmagenta (Fe), miR.MEtan (Cu), and miR.MEred (Cu, Mn).

Next, we selected the miRNAs with a pivotal role in the network topology and biological pathways based on the module membership (MM) criteria (LANGFELDER; HORVATH, 2008). We identified 50 miRNAs with a MM $\geq$ 0.7 (Table 3.1), belonging to 23 families through the nine associated modules (Supplementary Table S2). The main miRNA families identified were let-7 and mir-29, with six members each, followed by mir-154 and mir-199, both with four miRNAs each.

Table 3.1. Module characterization and significant module-trait association in Nelore cattle.

miRNA modules	**Number of miRNAs (MM)**[a]	**Mes**[b]	**Associated traits**[c]
miR.MEbrown	25 (5)	0.35	Ca, Na, S
miR.MEcyan	10 (6)	0.47	Ca, Cu, Fe, K, Mg, Mn, P, Na, S, Zn
miR.MEgreen	23 (5)	0.29	Ca, K, Mg, P, Na, Zn
miR.MEgrey60	8 (5)	0.54	Fe
miR.MElightyellow	8 (5)	0.50	Ca, Mg, Na
miR.MEmagenta	17 (8)	0.41	Fe
miR.MEmidnightblue	9 (6)	0.49	Ca, Fe, S, Zn
miR.MEred	21 (5)	0.37	Cu, Mn
miR.MEtan	12 (5)	0.40	Cu
Total	133(**50**)		

[a]MiRNAs clustered into the module. Number of hub miRNAs with MM $\geq$ 0.7 in the parenthesis
[b]Module eigengene; [c]$p \leq 0.05$.

3.3.3. MiRNA - mRNA regulatory network and identification of key transcription factors

To have an overview of the miRNA-gene-trait interactions and to better understand their regulatory relationship, we integrated miRNAs and mRNAs modules. We selected 15 mRNA modules associated with mineral concentration and meat quality traits (intramuscular fat content - IMF, and tenderness-WBSF7) from our previous work (DINIZ et al., 2019) (Supplementary Table S3) and the nine miRNA modules reported here. We identified 48 animals with paired data (miRNA and mRNA), for which Pearson's correlation was calculated among the MEs. A total of 16 pairs of miRNAs and mRNAs MEs showed significant negative correlations, which ranged from r = -0.3 to r = -0.68 ($p \leq 0.05$) (Figure 3.2). We also identified strong, positive, and significant module correlations ranging from r = 0.3 to r = 0.61. Nonetheless, it is still unclear whether the positively correlated pairs are a direct (MAMDANI et al., 2015) or intermediate, such as feedback motifs, miRNA effect (RITCHIE et al., 2009; SU; KLEINHANZ; SCHADT, 2014). Thus, as the main direct effect of miRNAs is downregulating the mRNA abundance (SU; KLEINHANZ; SCHADT, 2014), we focused on negative correlations for further investigations.

We found the highest number of significant negative correlated modules between miR.MEcyan (MEgrey60, MEgreenyellow, and MEgreen), miR.MEtan (MEorange, MEsalmon, and MEyellow), and miR.MElightyellow (MElightyellow, MEsalmon, and MEyellow), followed by miR.MEmidnightblue (MEgreenyellow and MEgrey60) (Figure 3.2). The miR.MEbrown, miR.MEgreen, miR.MEred, and miR.MEmagenta were correlated, respectively, with MEgreenyellow, MEroyalblue, MEdarkturquoise, and MEroyalblue. No significant negative correlation was identified between miR.MEgrey60 and any mRNA MEs. The network among all the trait-correlated MEs, as well as the negatively correlated mRNA-miRNA, showed that Ca and Fe were the most associated minerals, with eight and nine interactions, respectively (from both miRNA and mRNA MEs) (Figure 3.3).

Figure 3.2. MiRNA-mRNA module correlation.

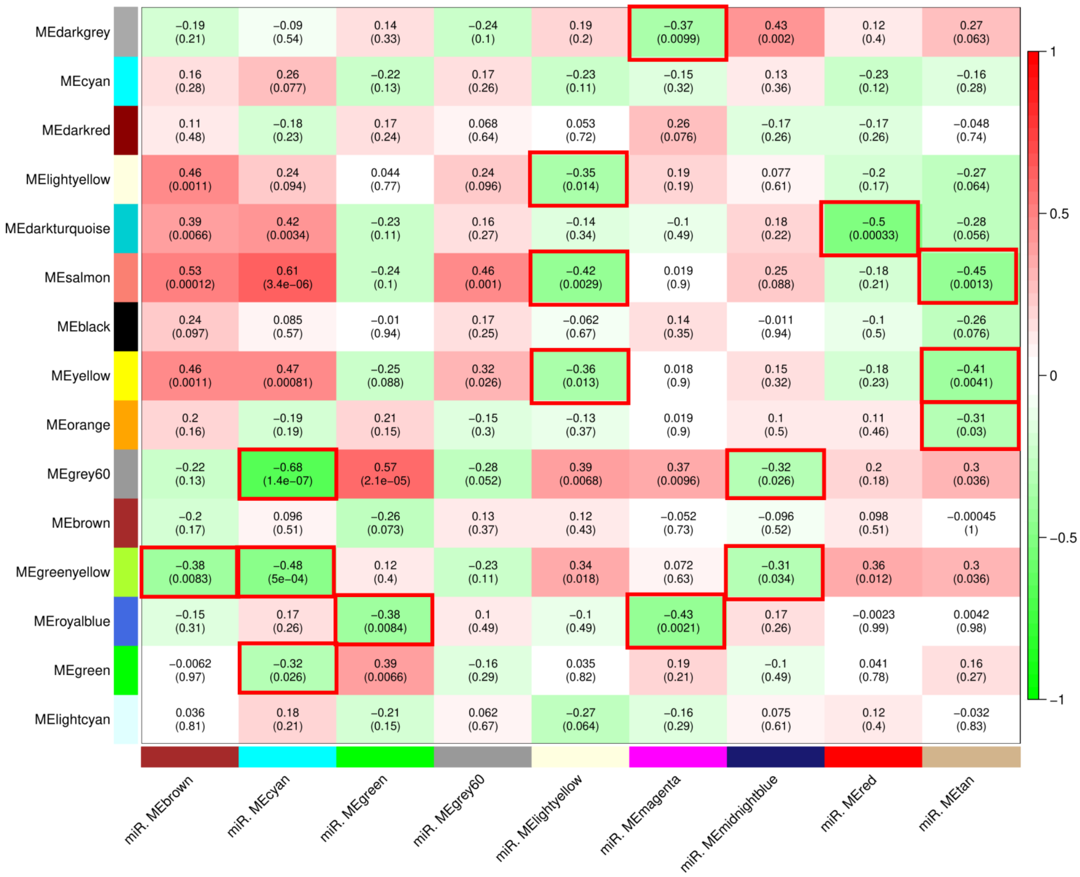

	miR. MEbrown	miR. MEcyan	miR. MEgreen	miR. MEgrey60	miR. MElightyellow	miR. MEmagenta	miR. MEmidnightblue	miR. MEred	miR. MEtan
MEdarkgrey	−0.19 (0.21)	−0.09 (0.54)	0.14 (0.33)	−0.24 (0.1)	0.19 (0.2)	−0.37 (0.0099)	0.43 (0.002)	0.12 (0.4)	0.27 (0.063)
MEcyan	0.16 (0.28)	0.26 (0.077)	−0.22 (0.13)	0.17 (0.26)	−0.23 (0.11)	−0.15 (0.32)	0.13 (0.36)	−0.23 (0.12)	−0.16 (0.28)
MEdarkred	0.11 (0.48)	−0.18 (0.23)	0.17 (0.24)	0.068 (0.64)	0.053 (0.72)	0.26 (0.076)	−0.17 (0.26)	−0.17 (0.26)	−0.048 (0.74)
MElightyellow	0.46 (0.0011)	0.24 (0.094)	0.044 (0.77)	0.24 (0.096)	−0.35 (0.014)	0.19 (0.19)	0.077 (0.61)	−0.2 (0.17)	−0.27 (0.064)
MEdarkturquoise	0.39 (0.0066)	0.42 (0.0034)	−0.23 (0.11)	0.16 (0.27)	−0.14 (0.34)	−0.1 (0.49)	0.18 (0.22)	−0.5 (0.00033)	−0.28 (0.056)
MEsalmon	0.53 (0.00012)	0.61 (3.4e−06)	−0.24 (0.1)	0.46 (0.001)	−0.42 (0.0029)	0.019 (0.9)	0.25 (0.088)	−0.18 (0.21)	−0.45 (0.0013)
MEblack	0.24 (0.097)	0.085 (0.57)	−0.01 (0.94)	0.17 (0.25)	−0.062 (0.67)	0.14 (0.35)	−0.011 (0.94)	−0.1 (0.5)	−0.26 (0.076)
MEyellow	0.46 (0.0011)	0.47 (0.00081)	−0.25 (0.088)	0.32 (0.026)	−0.36 (0.013)	0.018 (0.9)	0.15 (0.32)	−0.18 (0.23)	−0.41 (0.0041)
MEorange	0.2 (0.16)	−0.19 (0.19)	0.21 (0.15)	−0.15 (0.3)	−0.13 (0.37)	0.019 (0.9)	0.1 (0.5)	0.11 (0.46)	−0.31 (0.03)
MEgrey60	−0.22 (0.13)	−0.68 (1.4e−07)	0.57 (2.1e−05)	−0.28 (0.052)	0.39 (0.0068)	0.37 (0.0096)	−0.32 (0.026)	0.2 (0.18)	0.3 (0.036)
MEbrown	−0.2 (0.17)	0.096 (0.51)	−0.26 (0.073)	0.13 (0.37)	0.12 (0.43)	−0.052 (0.73)	−0.096 (0.52)	0.098 (0.51)	−0.00045 (1)
MEgreenyellow	−0.38 (0.0083)	−0.48 (5e−04)	0.12 (0.4)	−0.23 (0.11)	0.34 (0.018)	0.072 (0.63)	−0.31 (0.034)	0.36 (0.012)	0.3 (0.036)
MEroyalblue	−0.15 (0.31)	0.17 (0.26)	−0.38 (0.0084)	0.1 (0.49)	−0.1 (0.49)	−0.43 (0.0021)	0.17 (0.26)	−0.0023 (0.99)	0.0042 (0.98)
MEgreen	−0.0062 (0.97)	−0.32 (0.026)	0.39 (0.0066)	−0.16 (0.29)	0.035 (0.82)	0.19 (0.21)	−0.1 (0.49)	0.041 (0.78)	0.16 (0.27)
MElightcyan	0.036 (0.81)	0.18 (0.21)	−0.21 (0.15)	0.062 (0.67)	−0.27 (0.064)	−0.16 (0.29)	0.075 (0.61)	0.12 (0.4)	−0.032 (0.83)

MiRNA (*x*-axis) and mRNA (*y*-axis) modules are labeled by color. The matrix is color-coded based on Pearson's correlation (p-values in the parenthesis) according to the legend. Positive and negative correlations are showed, respectively, in red and green colors. Significant negative correlations ($p \leq 0.05$) are highlighted with a red rectangle

Next, we applied two complementary approaches to identify the miRNA-target pairs and shed light on their role in biological pathways related to mineral concentration. Firstly, for all the 50 miRNAs hubs, we used the hoardeR package (FISCHER; SIRONEN, 2016) to build a list of predicted targets of cattle miRNA hubs from

TargetScan. In total, we reported 8,123 unique putative targets (out of 24,698 targets) among all the modules (Table 3.2) expressed in the mRNA muscle transcriptome from the same animals (Supplementary Table S2). The miR.MEgrey60 (five hubs) was not considered for subsequent analysis as it was not correlated with any mRNA modules. Then, to establish the most likely miRNA-target pairs, we intersected the predicted interactions with the significant negatively correlated miRNA-mRNA MEs (Supplementary Table S4). Putative new interactions based only on the negative ME correlation are reported in Supplementary Table S4.

Figure 3.3. Network of negatively correlated miRNA-mRNA modules and associated phenotypes in Nelore cattle muscle.

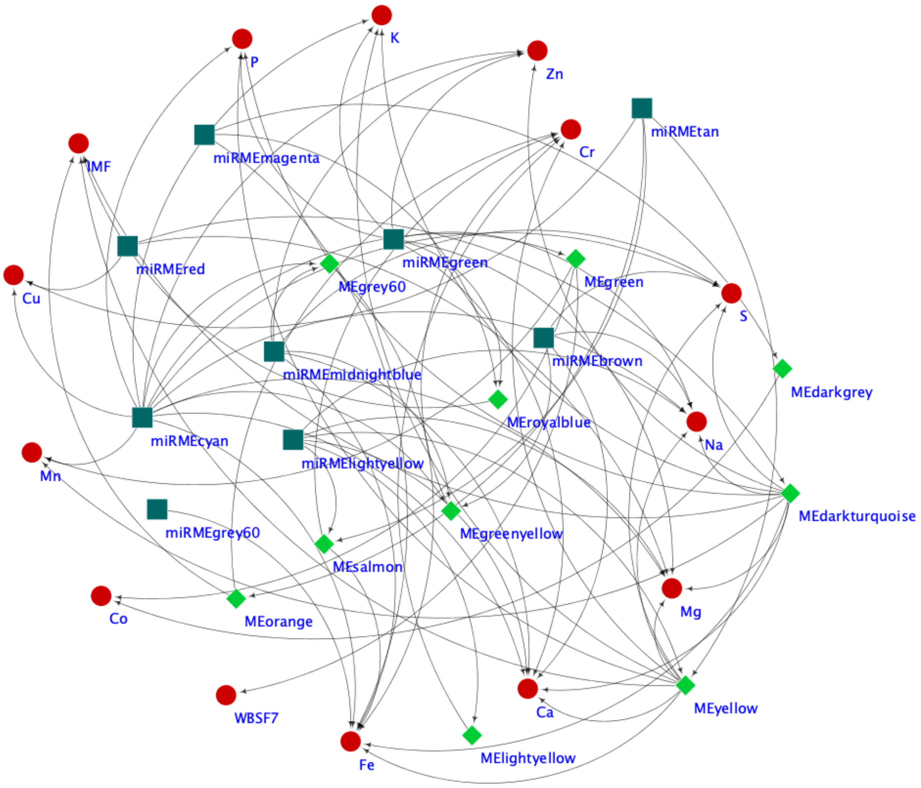

Square, diamond, and ellipse shapes show, respectively, miRNA, mRNA, and phenotypes. Each arrow indicates the direction of regulation. *Cr, Co, IMF, and WBSF7 were evaluated only in (Diniz 2019).

MiRNAs were targeting several genes. Figure 3.4 shows the miRNA-gene target interactions for the miRNAs clustered into the miR.MEtan and miR.MElightyellow. The whole network, with a total of 4,045 miRNA-target pair interactions among the ten mRNA modules, corresponding to 1,815 unique targets, is represented in Supplementary Figure S2 and Supplementary Table S4. On average, 41 out of 45 hub miRNAs targeted 98 genes with a maximum of 600 genes (Figure 3.5, Supplementary Table S4). However, we did not find targets for the bta-miRs- 410, -411a, and -487b for miR.MEred, as well as for the bta-let-7c (miR.MEtan). The mir-29 family (miR-29e, 29a, 29b, 29c, 29d-3p, in order of the number of targets) targeted the highest number of genes. At least two miRNAs targeted around 50% of the genes. We found that the genes *HLF* and *TRAF3* were targeted by ten miRNAs each, followed by *ATP2B2*, *DYNLL2*, and *YY1* with nine regulators.

Table 3.2. Summary of miRNA target prediction based on TargetScan and mRNA associated modules in Nelore cattle muscle.

miRNA Modules^{a}	**TargetScan^{b}**	**r^{d}**	**mRNA modules^{e}**	**Target^{f}**
miR.MEbrown (5)	1,591	-0.38	MEgreenyellow (2008)	198
		- 0.68	MEgrey60 (118)	66
miR.MEcyan (6)	3,811	- 0.48	MEgreenyellow (2008)	529
		- 0.32	MEgreen (975)	548
miR.MEgreen (5)	4,646	- 0.38	MEroyalblue (98)	32
miR.MEgrey60 (5)	2,461		-	-
		- 0.35	MElightyellow (714)	189
miR.MElightyellow (5)	1,788	- 0.42	MEsalmon (190)	33
		- 0.36	MEyellow (1200)	154
miR.MEmagenta (8)	5,492	- 0.43	MEroyalblue (98)	35
		- 0.37	MEdarkgrey (78)	21
miR.MEmidnightblue (6)	1,707	- 0.32	MEgrey60 (118)	25
		- 0.31	MEgreenyellow (2008)	194
miR.MEred (5)	2,372	- 0.50	MEdarkturquoise (88)	9
		- 0.45	MEsalmon (190)	12
miR.MEtan (5)	830	- 0.41	MEyellow (1200)	76
		- 0.31	MEorange (69)	6
Total: 9 modules (50)	24,698 (8,123)^{e}		2,127 (1,815)^{g}	

^{a}Between parenthesis is the number of hub miRNAs; ^{b}Total of predicted targets from TargetScan and expressed in muscle; ^{c}Total of unique targets identified from TargetScan; ^{d}Significant miRNA-mRNA module correlation values ($p \leq 0.05$); ^{e}Between parenthesis is the number of genes in the mRNA modules (DINIZ et al., 2019); ^{f}Total number of genes intersected between TargetScan and present in the correlated mRNA module; ^{g}Total of unique targets.

Figure 3.4. Regulatory network of negative miRNA-mRNA pairs from miR.MElightyellow and miR.MEtan in Nelore muscle.

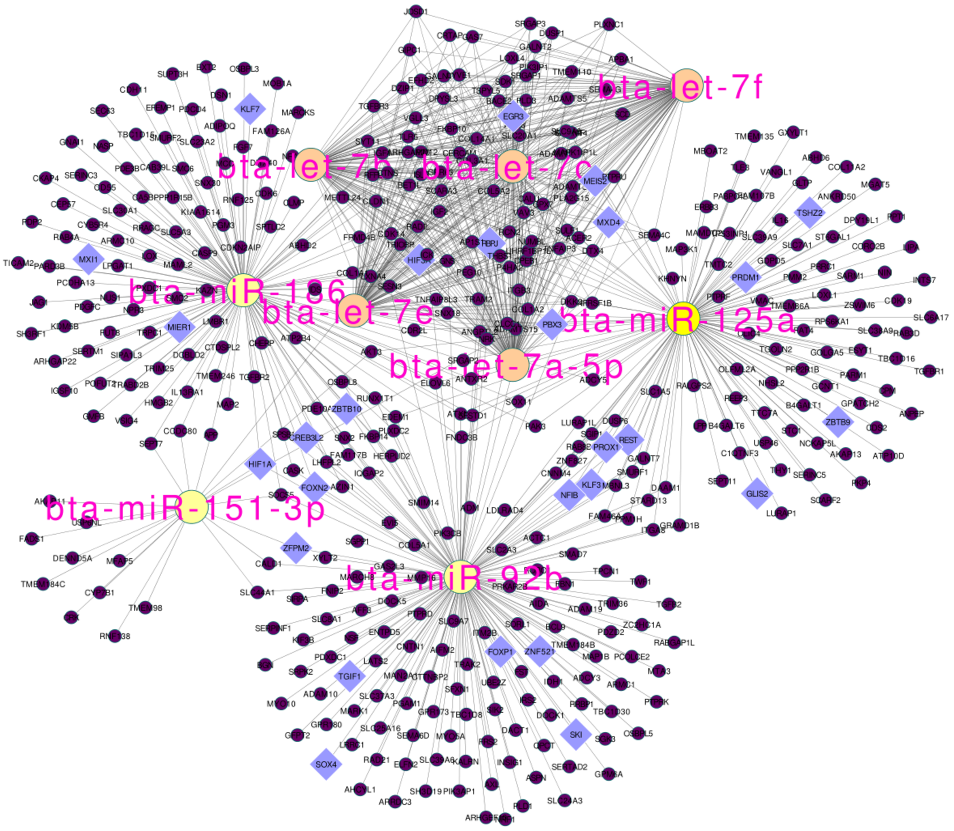

The edges are colored according to miRNA module and transcription factors are represented by light purple diamond shape.

To identify enriched transcription factors (TFs) targeted by miRNAs, we screened out the 1,815 reported genes to the compendium of bovine transcription factors (SOUZA et al., 2018). We found 131 TFs, of which at least two miRNAs targeted 58% (76/131) of the TFs (Supplementary Table S4). Among the TFs, *HLF*, *YY1,* and *THRA* were targeted by 10, 9, and 8 different miRNAs, respectively. We further evaluated the connectivity for these TFs considering their module membership (MM) from our previous work (DINIZ et al., 2019). We identified 30 TFs with a MM higher than 0.7, which highlight their importance for the network's topology architecture (Supplementary Table S4).

Figure 3.5. Number of targeted genes by miRNA co-expression network in Nelore muscle (ranked in descending order).

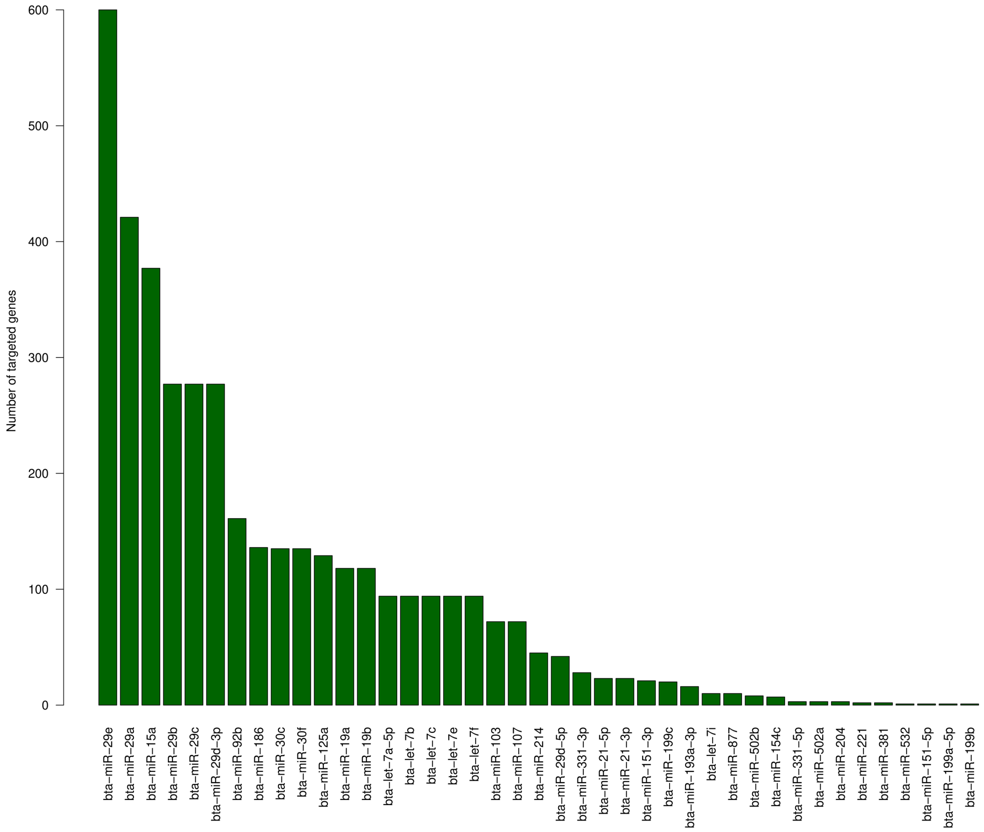

3.3.4. Pathway over-representation analysis

To reveal the biological pathways in which the miRNA targets are acting, we carried out a pathway enrichment analysis using Cluego (BINDEA et al., 2009). As we sought to point a biological relationship between miRNAs and mRNAs, we focused the analysis on those genes that were overlapped between TargetScan prediction and mRNA-miRNA associated modules (Supplementary Table S4). Based on that approach, we identified 37 significant enriched KEGG pathways (pV $\leq$ 0.05) (Figure 3.6) among the five modules (Supplementary Table S5). No results were retrieved from miR.MEgreen, miR.MEmagenta, and miR.MEred.

The miR.MEcyan showed the highest number of enriched pathways such as those related to protein (mTOR signaling pathway, protein processing, ubiquitin-mediated proteolysis) and energy metabolism (insulin and thyroid hormone signaling pathways). Among the pathways, we also identified ferroptosis (miR.MEbrown), TGF-beta signaling pathway, focal adhesion (miR.MElightyellow), and ECM-receptor interaction (miR.MEtan).

Figure 3.6. Over-represented signaling pathways of miRNA target genes in Nelore muscle co-expression network.

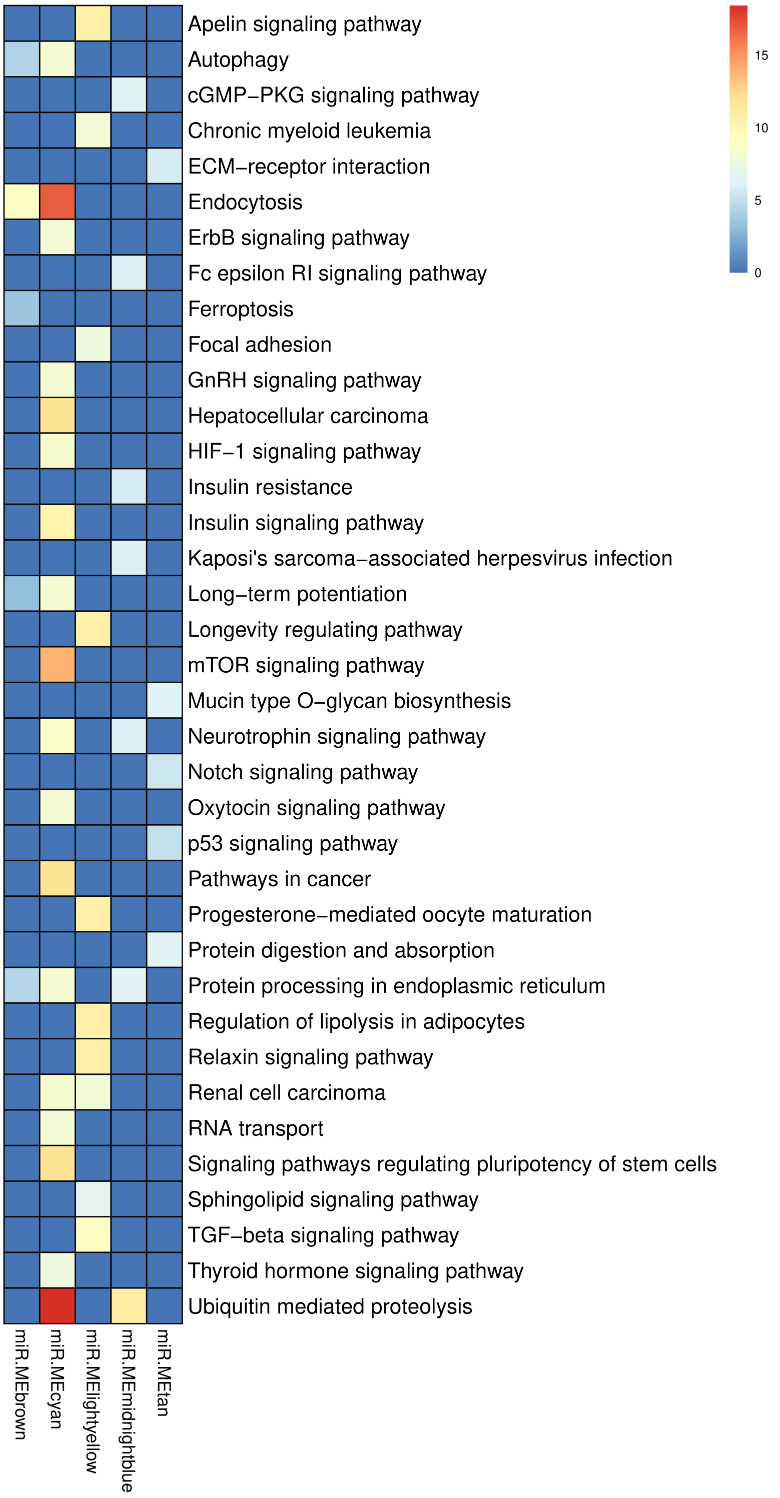

The matrix is color-coded based on -log10 (p-value adjusted) according to the legend.

3.4. DISCUSSION

Previously, we reported an interplay among gene expression, mineral concentration, and meat quality traits based on gene co-expression network (DINIZ et al., 2019). As part of this picture, in addition to the gene expression regulation role, growing evidence shows the cross talk between miRNA and mineral homeostasis (XU; SHI; LI, 2013; AN et al., 2014; BECKETT et al., 2014). However, our understanding of the miRNA-gene-mineral relationship is still minimal. Herein, we identified mineral-associated co-expressed miRNAs, along with multi-level miRNA-mRNA integration, shedding light upon regulatory networks contributing to mineral metabolism in Nelore muscle.

We found 50 hubs out of 343 miRNAs, among nine co-expressed modules, associated with at least one mineral ($p \leq 0.05$). By integrating the associated miRNA - mRNA MEs and intersecting with TargetScan prediction, we reduced the number of false-positive pairs when compared to predictions alone (MAMDANI et al., 2015), and pointed out putative mineral-mRNA-miRNA relationships. Further, by focusing the analysis on the MEs, one key advantage of our approach is that we alleviate the multiple testing problems inherent in RNA-Seq multi-level data integration (LANGFELDER; HORVATH, 2008). Our approach gathered 41 miRNAs and 1,815 target genes inversely correlated. MiRNA hubs play a pivotal role both in the network's topology (LANGFELDER; HORVATH, 2008) and gene expression coordination within the transcriptional network (SU; KLEINHANZ; SCHADT, 2014). We also found genes targeted by several miRNAs (over-targeted), as well as miRNAs with multiple targets. It's worth to highlight that transcription factors (TFs), such as *HLF, YY1,* and *THRA,* were among the over-targeted genes. Likewise, the miR-29 family, associated with the concentration of ten minerals, showed the highest number of putative targets. These results reinforce the general concept that the genes are redundantly regulated by multiple miRNA interactions (SU; KLEINHANZ; SCHADT, 2014), as well as by a putative combinatorial TFs co-regulation (SHALGI et al., 2007).

Because we have a lack of knowledge regarding the miRNA-mineral relationship in cattle so far, and most mammalian genes are conserved targets of miRNAs (FRIEDMAN et al., 2008), we will make cross talk between the results identified here and the current research in humans and animal models. Ca and Fe showed correlation values with other minerals ranging from moderate to strong (DINIZ et al., 2019) and were the main ones associated with miRNA MEs. Further, these minerals have been associated with gene expression and miRNA biogenesis in a bi-directional regulatory circuit (DAVIS; CLARKE, 2013; BECKETT et al., 2014; MAGENTA et al., 2016). Thus, our discussion will focus mainly on Ca and Fe and their relationship with miRNA and gene targets.

Cellular Ca and Fe play an essential role in both gene expression and miRNA biogenesis (DAVIS; CLARKE, 2013; MAGENTA et al., 2016). We identified the genes *PCBP1* and *PCBP2* (Poly (RC) Binding Protein) targeted by the miR-21-5p (miR.MEbrown), and four gene members of the Argonaute family (*AGO1*, *AGO2*, *AGO3*, and *AGO4*) mutually targeted by miR-29e (miR.MEcyan). Li et al. (2012) reported that cytosolic Fe could modulate the *PCBP2 - AGO1* relationship, leading to decreased mature miRNA production. Some of the hub miRNAs clustered into the miR.MEcyan and miR.MEbrown correlated both with minerals and gene modules, have also been associated to miRNA biosynthesis and mineral homeostasis in humans. The miR-29 family members (-a, -b, -c, -d-3p and -e), along with miR-15a targeted most of the genes identified, including those with a known involvement in Ca, Cu, Fe, and Zn metabolism (LI et al., 2012). For instance, the transcription factors coded by *YY1* and *SP1* genes*,* both targets of miR-29 family, bind the human transferrin (*TF*) gene and modulate its expression level (AMODIO et al., 2015). In addition, *YY1* was targeted by miR-19a, -19b (miR.MEbrown), -30c, and 30f (miR.MEmidnightblue). Still, concerning Fe metabolism, we also found the transferrin receptor gene (*TFRC*) targeted by four miRNAs (miR-103, -107, -15a, and 29e). The interplay between the *TF* protein and its receptor (*TFRC)* control the level of free Fe in the biological fluids, in addition to other mechanisms and post-transcriptional regulation (XU; SHI; LI, 2013).

The interaction between reactive oxygen species (ROS) and hypoxia has a crucial role in miRNA biogenesis (DENGLER; GALBRAITH; ESPINOSA, 2014; HE; JIANG, 2016; MAGENTA et al., 2016). Transition metals, such as Cu, Fe, and Zn catalyzes the production of ROS (PEÑA and KISELYOV, 2015) which were associated with hypoxia-induced miRNAs. Although Ca is not a transition metal, it has been associated with ROS and miRNA expression as well (MAGENTA et al., 2016). Through the MEs, we identified miRNAs hypoxia-induced, such as miR-15a, -29a (miR.MEcyan) (GAMBACCIANI et al., 2014; HAO et al., 2014), miR-204, -214, and -199 (miR.MEmagenta) (AZZOUZI et al., 2013; QIU; LI; LIU, 2018), and miR-30c (miR.MEmidnightblue) (GAMBACCIANI et al., 2014). We also identified between the miR.MEtan and miR.MEcyan targets, respectively, the TFs *TFEB* (transcription factor

EB), *HIF1A,* and *HIF3A* (hypoxia-inducible factor), which are metal-affected and miRNA regulated (LI et al., 2006; PEÑA and KISELYOV, 2015).

We carried out a pathway over-representation analysis to assign biological meaning to the associated miRNA-mRNA modules. Genes clustered into the module act cooperatively in the same pathway (LANGFELDER; HORVATH, 2007), which are also under the regulation of co-expressed miRNAs (SU; KLEINHANZ; SCHADT, 2014). We unveiled several pathways over-represented, including those reported on our gene-co-expression network (apelin, insulin, mTOR, relaxin, TGF-beta signaling pathways, ECM-receptor interaction, focal adhesion, protein digestion and absorption, and ubiquitin-mediated proteolysis) (DINIZ et al., 2019).

The miR.MEcyan showed over-represented KEGG signaling pathways that are central in cellular and organismal metabolism. These pathways include thyroid hormone (TH), mammalian target of rapamycin (mTOR), hypoxia-inducible factor-1 (HIF-1), and insulin. Furthermore, we identified the TGF-beta signaling pathway underlying the miR.MElightyellow. It is worth mentioning that these pathways have a pleiotropic action and are also interrelated with the AMPK pathway (5’-adenosine monophosphate-activated protein kinase) (XU; JI; YAN, 2012). Although not over-represented here, the AMPK pathway was the main one identified among the modules associated with the mineral concentration in our previous work (DINIZ et al., 2019). Afonso et al. (2019) also reported AMPK underlying differentially expressed genes from Nelore cattle genetically divergent for Cu concentration in muscle.

By integrating the information from the literature, the clustered genes, and KEGG database, we draw an overview of the relationship among the overmentioned pathways, miRNA, genes, and minerals (Figure 3.7). Genes from the families *PIK3*, *EIF4EBP*, and *RSK* were identified linking the miR.MEcyan pathways. MiR-15a, -29b, 29-c, 29d-3p, and 29e targeted *RPS6KA3* (members of RSK family), whereas miR-125a and -29a targeted *RPS6KA1* and *RPS6KB1,* respectively. Nutrient and growth factors are the main sensors modulating AMPK and mTOR pathways (CHEN; LONG, 2018). AMPK inhibits mTOR activity by modulating both *S6K* and *EIF4EBP*, which in turn inhibit the translation to maintain homeostasis (XU; JI; YAN, 2012). Both pathways are mineral responsive. Watson et al. (2016) reported a downregulation in mTORC1 signaling and decreased protein synthesis as a result of iron depletion. Calcium flux also modulates AMPK pathways via *CaMKK*, whereas mTOR modulates intracellular Ca^{2+} signaling machinery under nutrient deprivation (BRINI et al., 2013).

Figure 3.7. Schematic overview showing the relationship among over-represented metabolic signaling pathways, minerals and miRNA/genes in Nelore cattle.

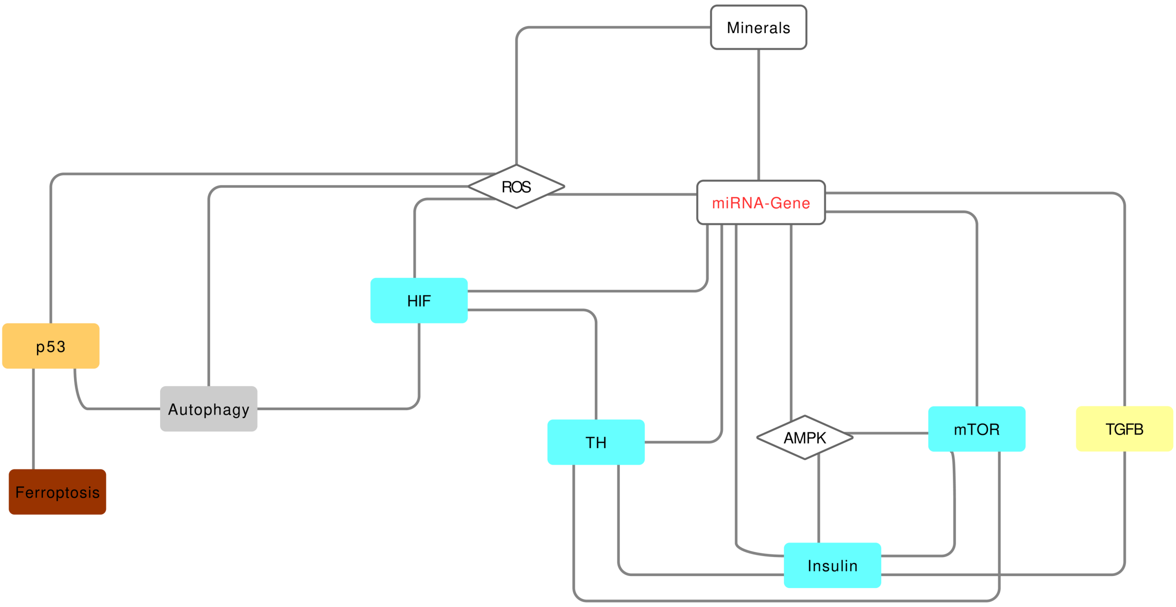

Signaling pathways are colored according to their miRNA module. Autophagy was over-represented in both miR.MEcyan and miR.MEbrown. ROS and AMPK pathways were added considering respectively, KEGG information and our previous work (Diniz 2019).

In this complex landscape, mTOR is also involved with autophagy regulation through *TFEB* gene expression (ROCZNIAK-FERGUSON et al., 2012). Autophagy pathway, over-represented in both miR.MEbrown and miR.MEcyan, is regulated in different ways, including TH, HIF, and p53 pathways (HE; JIANG, 2016). The HIF family controls the transcriptional mechanism as a response to hypoxia (DENGLER; GALBRAITH; ESPINOSA, 2014), which can be an outcome of ROS (MAGENTA et al., 2016). *HIF1A* and *HIF3A* genes are oxygen responsive and activate genes involved with iron metabolism, glucose, and glycolysis (LI et al., 2006; DENGLER; GALBRAITH; ESPINOSA, 2014). We also identified TFs related to HIFs, including *CREBP1* and *E2F4* regulated, respectively, by miR-29e and -29a, and nuclear receptor coactivator genes (*NCOA*) (DENGLER; GALBRAITH; ESPINOSA, 2014). *NCOA1* and *NCOA2* were both targeted by miR-29e, whereas *NCOA3* has been targeted by miR-29b, -29c, and -29d-3p. It is essential to highlight that HIF induced genes are also under TH regulation (OTTO; FANDREY, 2008). Otto and Fandrey (2008) showed that triiodothyronine (T3) increased *HIF1A* expression as an outcome of increased hepatic leukemia factor gene (*HLF*), which was the most targeted in our analysis (10 miRNAs). Previous works have described the association between HIF genes and miRNA biogenesis (AZZOUZI et al., 2013; MAGENTA et al., 2016), as well as the role of metals, such as Cu and Fe, in *HIF* and TH regulation (LI et al., 2006; KACZMAREK et al., 2009).

Iron is one of the most studied minerals due to its double role in cell metabolism. Both deficiency or overload are harmful, and iron/metal excess is closely related to ROS production (SPEER et al., 2013). Among the pathways identified in the miR.MEtan, p53 signaling pathway has a pro-oxidative activity and regulates ferroptosis (CAO; DIXON, 2016), which was enriched in miR.MEbrown. Shen et al. (2014) showed that Fe deprivation increased the p53 protein level avoiding ferroptosis. Besides p53, *TFRC,* and *IREB2* (encodes for IRP2 protein) genes are also essential for ferroptosis (CAO; DIXON, 2016). *IREB2*, a master regulator of Fe homeostasis (CAO; DIXON, 2016), was targeted by the miR-29 family. Ripa et al. (2017) showed that Fe loading induces miR-29 up-regulation, whereas its downregulation is followed by increased levels of *TFRC*, *IRP2*, Fe uptake, and oxidative stress.

Some of the miRNAs target genes associated with mineral homeostasis are also associated with energy metabolism. The miR-29 family mainly targeted TFs involved with insulin and glucose metabolism, including *CREB1*, *CRTC1,* and *FOXO3* (OH et al., 2013). In addition, *IGF1* and *IGF2* genes were targeted by the let7 family (let-7a-5p, -b, -c, and -e). Family members are thought to share the seed region exhibiting a functional collaborative relationship in mRNA targets (SU; KLEINHANZ; SCHADT, 2014; OLIVEIRA et al., 2018b). Massart et al. (2017) identified that miR-29a and -29c negatively regulate both glucose uptake and fatty acid oxidation. Likewise, overexpression of let-7 in mice was associated with impaired glucose tolerance, decreased fat mass, and body weight (FROST; OLSON, 2011). Altogether, the miRNAs are an additional layer of regulation in energy homeostasis, acting in the interrelated TH, insulin, AMPK, and mTOR signaling pathways.

We reported for the first time an interplay among miRNAs, mRNAs, and minerals in Nelore muscle. Although we have shown an exploratory *in silico* study, the results demonstrated a strong relationship among several biological pathways to maintain the cellular homeostasis (HE; JIANG, 2016). By screening the genes, we identified several known transcription factors as being miRNA targets, as well as miRNAs acting cooperatively to regulate their targets, as supported by TargetScan prediction and negative correlation analysis. Nonetheless, *in vitro* and *in vivo* analyses should be carried out to better understand the potential for dietary modulated miRNAs and their complex relationship with gene targets. Likewise, further validation of miRNA-gene target interactions and hub genes identified here in a larger cohort could support these findings. This would allow for establishing a framework for understanding the role of minerals in gene/miRNA expression and metabolism regulation.

3.5. CONCLUSION

MiRNAs showed a co-expression pattern where highly connected hubs drive the gene expression. To our knowledge, this is the first exploratory study of miRNA-mRNA integration in the context of minerals in cattle. The significant associations identified here among miRNAs with Ca and Fe, and their potential gene targets support the hypotheses of an intricate interplay among them. The mir-29 family plays a pivotal role in genes involved with major pathways like insulin, TH, AMPK, and mTOR, suggesting their importance in mineral metabolism, which can affect health and production. Future work should determine the functional implications of minerals for miRNA levels and their feedback regulation system.

ACKNOWLEDGMENTS

We are thankful to the EMBRAPA Multiuser Bioinformatics Laboratory (Laboratório Multiusuário de Bioinformática da Embrapa - LMB) for providing high-performance computational infrastructure; Dr. Bruno G. N. Andrade for the server management and support in the EMBRAPA Pecuária Sudeste; and the Technical University of Denmark (DTU) for accepting the first author as a visiting scholar.

AVAILABILITY OF DATA AND MATERIAL

All relevant data are within the paper and its Supporting Information files. All sequencing data is available in the European Nucleotide Archive (ENA) repository (EMBL-EBI), under accession PRJEB13188, PRJEB10898, and PRJEB19421 [https://www.ebi.ac.uk/ena/submit/sra/]. All additional datasets generated and analysed during this study are available from the corresponding author on reasonable request.

COMPETING FINANCIAL INTERESTS

The authors declare that the research was conducted in the absence of any commercial or financial relationships that could be construed as a potential conflict of interest.

AUTHORS CONTRIBUTIONS

WJSD, LCAR, LLC, and HNK conceived the idea of this research. ARAN and CFG carried out the mineral measurement; WJSD, PB, and GM carried out the bioinformatics and data analysis. ASMC carried out the miRNA data analysis (quality control, mapping, and counting). WJSD, PB, GM, ASMC, HNK, JA, LCAR collaborated with the interpretation of results, discussion and review the manuscript. WJSD and PB drafted the manuscript. All authors have reviewed, discussed, and approved the final version of the manuscript.

FUNDING

This study was conducted with funding from EMBRAPA (Macroprograma 1, 01/2005), São Paulo Research Foundation (FAPESP) (grant #2012/23638-8), and by the Coordenação de Aperfeiçoamento de Pessoal de Nível Superior - Brasil (CAPES) - Finance Code 001. ARAN, LCAR and LLC were granted CNPq fellowships. JA was granted CAPES fellowship. WJSD was granted FAPESP (grant #2015/09158-1 and #2017/20761-7) scholarship.

3.6. REFERENCES

AFONSO, J. et al. Muscle transcriptome analysis reveals genes and metabolic pathways related to mineral concentration in *Bos indicus*. **Scientific Reports**, v. 9, n. 1, p. 12715, 3 dez. 2019.

AGARWAL, V. et al. Predicting effective microRNA target sites in mammalian mRNAs. **eLife**, v. 4, n. AUGUST2015, p. 1–38, 2015.

AHLBERG, C. M. et al. Genome wide association study of cholesterol and poly- and monounsaturated fatty acids, protein, and mineral content of beef from crossbred cattle. **Meat Science**, v. 98, n. 4, p. 804–814, dez. 2014.

AMODIO, N. et al. miR-29s: a family of epi-miRNAs with therapeutic implications in hematologic malignancies. **Oncotarget**, v. 6, n. 15, p. 12837–12861, 30 maio 2015.

AN, J. H. et al. Changes of microRNA profile and microRNA-mRNA regulatory network in bones of ovariectomized mice. **Journal of Bone and Mineral Research**, v. 29, n. 3, p. 644–656, 2014.

ANDERS, S.; HUBER, W. Differential expression analysis for sequence count data. **Genome Biology**, v. 11, n. 10, p. R106, 2010.

ANDREWS, S. **FastQC: a quality control tool for high throughput sequence data**. Disponível em: <https://www.bioinformatics.babraham.ac.uk/projects/fastqc/>.

AZZOUZI, H. El et al. The Hypoxia-Inducible MicroRNA Cluster miR-199a~214 Targets Myocardial PPARδ and Impairs Mitochondrial Fatty Acid Oxidation. **Cell Metabolism**, v. 18, n. 3, p. 341–354, 3 set. 2013.

BAO, W.; GREENWOLD, M. J.; SAWYER, R. H. Using scale and feather traits for module construction provides a functional approach to chicken epidermal development. **Functional & Integrative Genomics**, v. 17, n. 6, p. 641–651, 5 nov. 2017.

BECKETT, E. L. et al. The role of vitamins and minerals in modulating the expression of microRNA. **Nutrition research reviews**, v. 27, p. 94–106, 2014.

BINDEA, G. et al. ClueGO: A Cytoscape plug-in to decipher functionally grouped gene ontology and pathway annotation networks. **Bioinformatics**, v. 25, n. 8, p. 1091–1093, 2009.

BRINI, M. et al. Calcium in Health and Disease. In: ASTRID SIGEL, HELMUT SIGEL, R. K. O. S. (Ed.). **Interrelations between essential metal ions and human diseases**. [s.l.] Springer Dordrecht Heidelberg, 2013. p. 81–137.

BUDAK, H.; ZHANG, B. MicroRNAs in model and complex organisms. **Functional & Integrative Genomics**, v. 17, n. 2–3, p. 121–124, 20 maio 2017.

CAO, J. Y.; DIXON, S. J. Mechanisms of ferroptosis. **Cellular and Molecular Life Sciences**, v. 73, n. 11–12, p. 2195–2209, 5 jun. 2016.

CASAS, E. et al. Polymorphisms in calpastatin and mu-calpain genes are associated with beef iron content. **Animal Genetics**, v. 45, n. 2, p. 283–284, abr. 2014.

CHEN, J.; LONG, F. mTOR signaling in skeletal development and disease. **Bone research**, v. 6, p. 1, 2018.

CLINE, M. S. et al. Integration of biological networks and gene expression data using Cytoscape. **Nature protocols**, v. 2, n. 10, p. 2366–2382, 2007.

DAVIS, M.; CLARKE, S. Influence of microRNA on the maintenance of human iron metabolism. **Nutrients**, v. 5, p. 2611–2628, 2013.

DAVIS, M. R. et al. Enhanced expression of lipogenic genes may contribute to hyperglycemia and alterations in plasma lipids in response to dietary iron deficiency. **Genes and Nutrition**, v. 7, n. 3, p. 415–425, 2012a.

DAVIS, M. R. et al. Comparisons of the iron deficient metabolic response in rats fed either an AIN-76 or AIN-93 based diet. **Nutrition & Metabolism**, v. 9, n. 1, p. 95, jan. 2012b.

DENGLER, V. L.; GALBRAITH, M.; ESPINOSA, J. M. Transcriptional regulation by hypoxia inducible factors. **Critical reviews in biochemistry and molecular biology**, v. 49, n. 1, p. 1–15, 2014.

DINIZ, W. J. da S. et al. Iron Content Affects Lipogenic Gene Expression in the Muscle of Nelore Beef Cattle. **PLOS ONE**, v. 11, n. 8, p. e0161160, 17 ago. 2016.

DINIZ, W. J. S. da S. et al. Detection of Co-expressed Pathway Modules Associated with Mineral Concentration and Meat Quality in Nelore Cattle. **Frontiers in Genetics**, v. 10, p. 210, 13 mar. 2019.

FASTX-TOOLKIT. **FASTX-Toolkit**. Disponível em: <http://hannonlab.cshl.edu/fastx_toolkit/>.

FISCHER, D.; SIRONEN, A. **An Introduction to hoardeR**. Disponível em: <https://cran.r-project.org/web/packages/hoardeR/vignettes/hoardeR-vignette.pdf>.

FLEET, J. C.; REPLOGLE, R.; SALT, D. E. Systems Genetics of Mineral Metabolism. **The Journal of Nutrition**, v. 141, p. 520–525, 2011.

FRIEDLÄNDER, M. R. et al. Discovering microRNAs from deep sequencing data using miRDeep. **Nature biotechnology**, v. 26, n. 4, p. 407–415, 2008.

FRIEDMAN, R. C. et al. Most mammalian mRNAs are conserved targets of microRNAs. **Genome Research**, v. 19, n. 1, p. 92–105, 29 out. 2008.

FROST, R. J. A.; OLSON, E. N. Control of glucose homeostasis and insulin sensitivity by the Let-7 family of microRNAs. **Proceedings of the National Academy of Sciences**, v. 108, n. 52, p. 21075–21080, 27 dez. 2011.

GAMBACCIANI, C. et al. miR-29a and miR-30c negatively regulate DNMT 3a in cardiac ischemic tissues: implications for cardiac remodelling. **microRNA Diagnostics and Therapeutics**, v. 1, n. 1, 2014.

GARMYN, A. J. et al. Estimation of relationships between mineral concentration and fatty acid composition of longissimus muscle and beef palatability traits. **Journal of Animal Science**, v. 89, p. 2849–2858, 2011.

HAO, R. et al. Hypoxia-Induced miR-15a Promotes Mesenchymal Ablation and Adaptation to Hypoxia during Lung Development in Chicken. **PLoS ONE**, v. 9, n. 6, p. e98868, 2 jun. 2014.

HE, J.; JIANG, B.-H. Interplay between Reactive oxygen Species and MicroRNAs in Cancer. **Current pharmacology reports**, v. 2, n. 2, p. 82–90, abr. 2016.

KACZMAREK, M. et al. Metal ions-stimulated iron oxidation in hydroxylases facilitates stabilization of HIF-1 alpha protein. **Toxicological sciences : an official journal of the Society of Toxicology**, v. 107, n. 2, p. 394–403, fev. 2009.

KAPPELER, B. I. G. et al. MiRNAs differentially expressed in skeletal muscle of animals with divergent estimated breeding values for beef tenderness. **BMC Molecular Biol**, v. 20, p. 1, 2019.

KOZOMARA, A.; GRIFFITHS-JONES, S. miRBase: annotating high confidence microRNAs using deep sequencing data. **Nucleic Acids Research**, v. 42, n. D1, p. D68–D73, 1 jan. 2014.

LANGFELDER, P.; HORVATH, S. Eigengene networks for studying the relationships between co-expression modules. **BMC Systems Biology**, v. 1, n. 1, p. 54, 2007.

LANGFELDER, P.; HORVATH, S. WGCNA: An R package for weighted correlation network analysis. **BMC Bioinformatics**, v. 9, 2008.

LANGFELDER, P.; ZHANG, B.; HORVATH, S. Defining clusters from a hierarchical cluster tree: The Dynamic Tree Cut package for R. **Bioinformatics**, v. 24, n. 5, p. 719–720, 2008.

LI, Q. et al. Effects of 12 metal ions on iron regulatory protein 1 (IRP-1) and hypoxia-inducible factor-1 alpha (HIF-1α) and HIF-regulated genes. **Toxicology and Applied Pharmacology**, v. 213, n. 3, p. 245–255, 15 jun. 2006.

LI, Y. et al. Iron Homeostasis Regulates the Activity of the MicroRNA Pathway through Poly(C)-Binding Protein 2. **Cell Metabolism**, v. 15, n. 6, p. 895–904, jun. 2012.

MAGENTA, A. et al. Oxidative stress, microRNAs and cytosolic calcium homeostasis. **Cell Calcium**, v. 60, n. 3, p. 207–217, 1 set. 2016.

MAMDANI, M. et al. Integrating mRNA and miRNA Weighted Gene Co-Expression Networks with eQTLs in the Nucleus Accumbens of Subjects with Alcohol Dependence. **PLOS ONE**, v. 10, n. 9, p. e0137671, 18 set. 2015.

MASSART, J. et al. Altered miR-29 Expression in Type 2 Diabetes Influences Glucose and Lipid Metabolism in Skeletal Muscle. **Diabetes**, v. 66, n. 7, p. 1807–1818, jul. 2017.

MATEESCU, R. G.; GARRICK, D. J.; REECY, J. M. Network analysis reveals putative genes affecting meat quality in Angus cattle. **Frontiers in Genetics**, v. 8, n. Nov, 2017.

OH, K.-J. et al. CREB and FoxO1: two transcription factors for the regulation of hepatic gluconeogenesis. **BMB Rep**, v. 46, n. 12, p. 567–574, 2013.

OLIVEIRA, P. S. N. de et al. Identification of genomic regions associated with feed efficiency in Nelore cattle. **BMC genetics**, v. 15, n. 1, p. 100, jan. 2014.

OLIVEIRA, P. S. N. de et al. An integrative transcriptome analysis indicates regulatory mRNA-miRNA networks for residual feed intake in Nelore cattle. **Scientific Reports**, v. 8, n. 1, p. 17072, 20 dez. 2018a.

OLIVEIRA, G. B. et al. Integrative analysis of microRNAs and mRNAs revealed regulation of composition and metabolism in Nelore cattle. **BMC Genomics**, v. 19, n. 1, p. 126, 7 dez. 2018b.

OTTO, T.; FANDREY, J. Thyroid Hormone Induces Hypoxia-Inducible Factor 1α Gene Expression through Thyroid Hormone Receptor β/Retinoid X Receptor α-Dependent Activation of Hepatic Leukemia Factor. **Endocrinology**, v. 149, n. 5, p. 2241–2250, 1 maio 2008.

PEÑA, K. A.; KISELYOV, K. Transition metals activate TFEB in overexpressing cells. **Biochemical Journal**, v. 470, n. 1, p. 65–76, 15 ago. 2015.

QIU, R.; LI, W.; LIU, Y. MicroRNA-204 protects H9C2 cells against hypoxia/reoxygenation-induced injury through regulating SIRT1-mediated autophagy. **Biomedicine & Pharmacotherapy**, v. 100, p. 15–19, 1 abr. 2018.

RIPA, R. et al. MicroRNA miR-29 controls a compensatory response to limit neuronal iron accumulation during adult life and aging. **BMC Biology**, v. 15, n. 1, p. 9, 13 dez. 2017.

RITCHIE, H.; ROSER, M. **Micronutrient Deficiency**. Disponível em: <https://ourworldindata.org/micronutrient-deficiency>. Acesso em: 22 ago. 2018.

RITCHIE, M. E. et al. limma powers differential expression analyses for RNA-sequencing and microarray studies. **Nucleic Acids Research**, v. 43, n. 7, p. e47–e47, 20 abr. 2015.

RITCHIE, W. et al. Conserved Expression Patterns Predict microRNA Targets. **PLoS Comput Biol**, v. 5, n. 9, p. 1000513, 2009.

ROBINSON, M. D.; MCCARTHY, D. J.; SMYTH, G. K. edgeR: a Bioconductor package for differential expression analysis of digital gene expression data. **Bioinformatics**, v. 26, n. 1, p. 139–140, 1 jan. 2010.

ROCZNIAK-FERGUSON, A. et al. The transcription factor TFEB links mTORC1 signaling to transcriptional control of lysosome homeostasis. **Science signaling**, v. 5, n. 228, p. ra42, 12 jun. 2012.

SHALGI, R. et al. Global and Local Architecture of the Mammalian microRNA–Transcription Factor Regulatory Network. **PLoS Computational Biology**, v. 3, n. 7, p. e131, 2007.

SHEN, J. et al. Iron Metabolism Regulates p53 Signaling through Direct Heme-p53 Interaction and Modulation of p53 Localization, Stability, and Function. **Cell Reports**, v. 7, n. 1, p. 180–193, abr. 2014.

SOUZA, M. M. de et al. A comprehensive manually-curated compendium of bovine transcription factors. **Scientific Reports**, v. 8, n. 1, p. 13747, 13 dez. 2018.

SPEER, R. E. et al. Hypoxia-inducible factor prolyl hydroxylases as targets for neuroprotection by “antioxidant” metal chelators: From ferroptosis to stroke. **Free Radical Biology and Medicine**, v. 62, p. 26–36, 1 set. 2013.

SU, W.-L.; KLEINHANZ, R. R.; SCHADT, E. E. Characterizing the role of miRNAs within gene regulatory networks using integrative genomics techniques. **Molecular Systems Biology**, v. 7, n. 1, p. 490–490, 16 abr. 2014.

SUTTLE, N. **Mineral nutrition of livestock**. 4ª ed. Wallingford: CABI, 2010.

TARAZONA, S. et al. Data quality aware analysis of differential expression in RNA-seq with NOISeq R/Bioc package. **Nucleic Acids Research**, p. gkv711, 16 jul. 2015.

TIZIOTO, P. C. et al. Calcium and potassium content in beef: influences on tenderness and associations with molecular markers in Nellore cattle. **Meat science**, v. 96, n. 1, p. 436–40, jan. 2014.

TIZIOTO, P. C. et al. Detection of quantitative trait loci for mineral content of Nelore longissimus dorsi muscle. **Genetics Selection Evolution**, v. 47, n. 1, p. 15, 2015.

WATSON, A. et al. Iron depletion suppresses mTORC1-directed signalling in intestinal Caco-2 cells via induction of REDD1. **Cellular Signalling**, v. 28, n. 5, p. 412–424, 1 maio 2016.

XU, J.; JI, J.; YAN, X. Cross-Talk between AMPK and mTOR in Regulating Energy Balance. **Critical Reviews in Food Science and Nutrition**, v. 52, n. 5, p. 373–381, maio 2012.

XU, Z.; SHI, Z.; LI, Y. The Crosstalk between Micro RNA and Iron Homeostasis. **International Journal of Genomic Medicine**, v. 01, n. 02, p. 1–8, 2013.

ZHAO, W. et al. Weighted gene coexpression network analysis: state of the art. **Journal of biopharmaceutical statistics**, v. 20, n. June 2013, p. 281–300, 2010.

4. FINAL REMARKS

Identifying the genetic architecture and molecular mechanisms underpinning polygenic phenotypes are a challenging task. Several technologies and analytical methods have been developed over time, and it has allowed us to understand better how complex phenotypes are regulated. However, biological systems are complex by nature, and there is still a lot of knowledge to add so that we can fully understand how it works. Although several studies have focused on the molecular basis of meat quality, the interest in meat mineral composition and its relationship with meat quality is recent, and it is still unclear.

This thesis was based on the hypothesis that gene-miRNA co-expression networks underly both mineral homeostasis and meat quality traits. By employing a multi-level data integration under a co-expression framework, we shed light on the role of minerals in meat quality traits and its relationship with gene and miRNA expression. Additionally, we reported biological processes and regulatory mechanisms underpinning these traits. For example, the AMPK pathway has been suggested as pivotal in *postmortem* muscle metabolism. Ca has been reported as an essential cofactor of several proteolytic enzymes. Additionally, Ca is needed for the activation of CaMMkβ, which triggers the AMPK pathway and regulates the glycolysis level. It's well known that postmortem glycogen metabolism is related to muscle pH decay due to the accumulation of lactic acid with a direct effect on meat quality traits.

Furthermore, we reported for the first time the relationship among minerals, genes, and miRNAs in Nelore cattle. MiRNAs, mainly from the miR-29 family, potentially are the leading drivers in Ca and Fe homeostasis, as well as modulating the target genes partaking in the AMPK, mTOR, and insulin signaling pathways, which are central for protein synthesis and energy metabolism processes. The following scheme shows an example of how minerals, genes, and minerals are interconnected to keep the Fe homeostasis. The interaction between the transferrin (*TF*) and its receptor (*TFRC*) is one of the mechanisms regulating the serum Fe levels. These genes, besides to be controlled by the transcription factors *YY1* and *SP1*, are also modulated by several miRNAs, as showed in the scheme. Some of the minerals can also catalyze reactive oxygen species (ROS), leading to activation of transcriptional regulators responsive to hypoxia such as *HIF1A* and *HIF3A*. This complex relationship by modulating gene expression/translation may affect the protein level, and consequently, mineral uptake and several underlying biological processes. Considering a complex landscape, some of these miRNAs are also modulating genes involved with energy and protein metabolism, which also has different regulatory sources. These findings highlight that multifactorial traits emerge from a combination of various genomic and environmental factors.

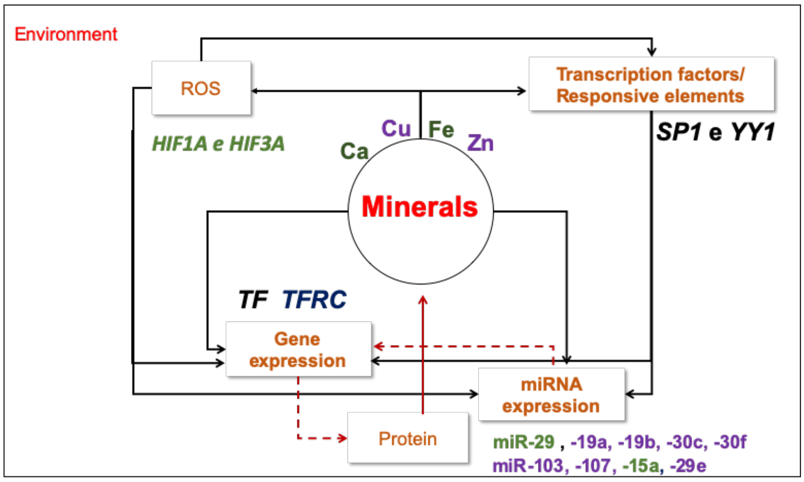

Adapated from Diniz et al. (2019, DOI: DOI: 10.1152/physiolgenomics.00072.2019).

Our approach provided potential regulatory mechanisms, candidate genes, and pathways involved with mineral composition and meat quality traits under a systems biology approach. However, it still not possible to point out the main driver modulating the studied phenotypes. Also, minerals interact among themselves, and they are acting together in the different processes identified, which highlights their importance. Due to our experimental design, we could not determine which are the best mineral combination to achieve beneficial effects. However, we are sure that mineral supplementation is the most essential, despite their small effect to determine meat quality traits. Thus, adding new layers of regulation based on omics approaches, like metabolomics and proteomics, can provide opportunities to clarify the genetic basis of the studied phenotypes.

Although we have improved our knowledge of how the genes and miRNAs interact to determine a trait, further studies are still needed to make this information useful for breeding selection programs. Likewise, it is crucial to investigate how different mineral supplementation levels can affect meat quality, and which is the best combination to achieve beneficial effects.

5. SUPPLEMENTARY MATERIAL

SUPPLEMENTARY MATERIAL

Detection of Co-expressed Pathway Modules Associated With Mineral Concentration and Meat Quality in Nelore Cattle

Wellison J. S. Diniz[1,2,3], Gianluca Mazzoni[4], Luiz L. Coutinho[5], Priyanka Banerjee[2], Ludwig Geistlinger[3,6], Aline S. M. Cesar[5], Francesca Bertolini[7], Juliana Afonso[1], Priscila S. N. de Oliveira[3], Polyana C. Tizioto[5], Haja N. Kadarmideen[2], Luciana C. A. Regitano[3*]

Can be accessed on:

Front. Genet., 13 March 2019 | https://doi.org/10.3389/fgene.2019.00210

Supplementary Figure 1. Correlation matrix of mineral concentration and meat quality traits in Nelore cattle. Each cell displays the correlation value when significant ($p \leq 0.05$). The matrix is color-coded by correlation according to the color legend.

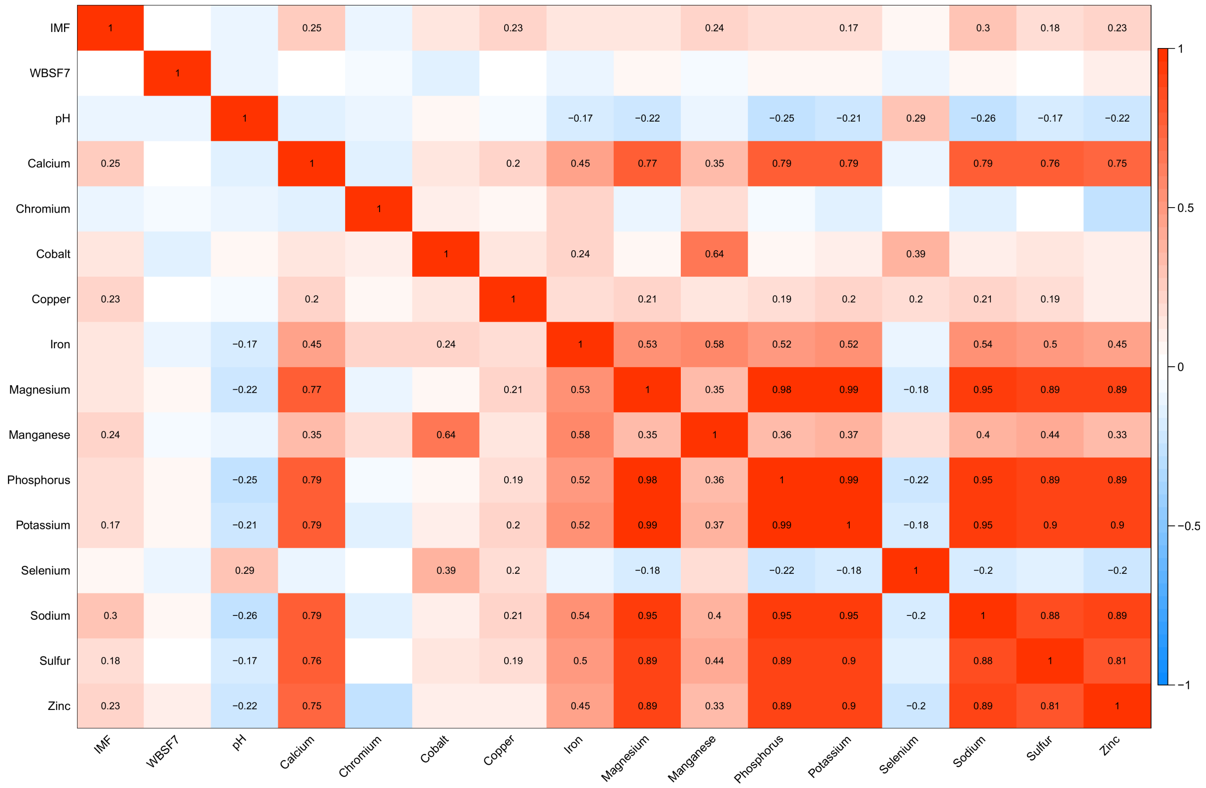

	IMF	WBSF7	pH	Calcium	Chromium	Cobalt	Copper	Iron	Magnesium	Manganese	Phosphorus	Potassium	Selenium	Sodium	Sulfur	Zinc
IMF	1			0.25			0.23			0.24		0.17		0.3	0.18	0.23
WBSF7		1														
pH			1					−0.17	−0.22		−0.25	−0.21	0.29	−0.26	−0.17	−0.22
Calcium	0.25			1			0.2	0.45	0.77	0.35	0.79	0.79		0.79	0.76	0.75
Chromium					1											
Cobalt						1		0.24		0.64			0.39			
Copper	0.23			0.2			1		0.21		0.19	0.2	0.2	0.21	0.19	
Iron			−0.17	0.45		0.24		1	0.53	0.58	0.52	0.52		0.54	0.5	0.45
Magnesium			−0.22	0.77			0.21	0.53	1	0.35	0.98	0.99	−0.18	0.95	0.89	0.89
Manganese	0.24			0.35		0.64		0.58	0.35	1	0.36	0.37		0.4	0.44	0.33
Phosphorus			−0.25	0.79			0.19	0.52	0.98	0.36	1	0.99	−0.22	0.95	0.89	0.89
Potassium	0.17		−0.21	0.79			0.2	0.52	0.99	0.37	0.99	1	−0.18	0.95	0.9	0.9
Selenium			0.29			0.39	0.2		−0.18		−0.22	−0.18	1	−0.2		−0.2
Sodium	0.3		−0.26	0.79			0.21	0.54	0.95	0.4	0.95	0.95	−0.2	1	0.88	0.89
Sulfur	0.18		−0.17	0.76			0.19	0.5	0.89	0.44	0.89	0.9		0.88	1	0.81
Zinc	0.23		−0.22	0.75				0.45	0.89	0.33	0.89	0.9	−0.2	0.89	0.81	1

Supplementary Table 1. Summary statistics of meat quality traits and mineral concentration in Nelore cattle.

Traits		Mean	Median	Minimum	Maximum	SD[b]	N[c]	CV[d]
Meat quality	IMF%	2.92	2.84	0.65	5.59	0.97	192	33.22
	WBSF7	5.26	5.22	1.95	9.56	1.61	188	30.61
	pH	5.6	5.56	5.33	5.95	0.14	194	2.5
Mineral concentration[a]								
Macro minerals	Calcium (Ca)	153.95	137.12	58.32	432.97	82.94	128	53.87
	Magnesium (Mg)	793.69	749.52	573.88	1.513.03	172.34	128	21.71
	Phosphorus (P)	7,687.84	7,102.01	5,422.77	15,587.43	1,940.13	128	25.24
	Potassium (K)	1,139.93	1,056.20	795.9	2,339.89	305.12	128	26.77
	Sodium (Na)	1,822.25	1,680.51	1,265.44	4,260.78	542.23	128	29.76
	Sulfur (S)	6,615.26	6,121.22	3,899.36	13,308.21	1,788.40	128	27.03
Micro minerals	Chromium (Cr)	0.29	0.15	0.02	3.19	0.52	57	179.31
	Cobalt (Co)	0.01	0.01	0.0001	0.02	0.004	96	40
	Copper (Cu)	1.64	1.41	0.99	12.06	1.07	128	65.24
	Selenium (Se)	0.2	0.2	0.06	0.4	0.007	128	3.5
	Manganese (Mn)	0.14	0.13	0.001	0.67	0.1	103	71.43
	Iron (Fe)	46.48	42.79	1.41	268.41	31.92	125	68.67
	Zinc (Zn)	83.92	77.8	46.67	217.46	29.49	128	35.14

[a] Mineral concentration unit as mg/kg; [b] Standard deviation (SD); [c] Number of animals (N); [d] Coefficient of variation (CV), Intramusculat Fat (IMF%); Warner-Bratzler shear force (WBSF7); Meat pH (pH).

Supplementary Table 2. The proportion of variance explained by the module eigengene (MEs).

Module	ME	Module	ME
M1	0.48	M13	0.25
M2	0.43	M14	0.23
M3	0.46	M15	0.36
M4	0.25	M16	0.29
M5	0.53	M17	0.36
M6	0.47	M18	0.29
M7	0.23	M19	0.26
M8	0.30	M20	0.18
M9	0.39	M21	0.28
M10	0.36	M22	0.41
M11	0.36	M23	0.41
M12	0.38		

Supplementary Table 3. Gene list and module membership (MM) for each selected module. Spreadsheet tabs are divided by module.

#M1

GS	MM	GS	MM	GS	MM	GS	MM
PARP14	0.92	*IFI16*	0.80	*LOC513659*	0.71	*TRIM21*	0.58
HERC6	0.92	*CMPK2*	0.80	*IRF9*	0.70	*LOC786352*	0.57
UBA7	0.91	*PARP9*	0.79	*PML*	0.70	*LOC508153*	0.56
RSAD2	0.9	*HERC5*	0.79	*SP140*	0.70	*CLEC2B*	0.56
IFI44L	0.89	*LOC511531*	0.78	*LOC112444847*	0.69	*CASP7*	0.55
LOC509283	0.88	*PARP10*	0.78	*IDO1*	0.69	*XRN2*	0.54
LOC100139670	0.88	*PARP12*	0.77	*TRIM56*	0.69	*RBM43*	0.54
MX1	0.87	*IFI27*	0.76	*GBP5*	0.67	*TAP2*	0.52
IFIH1	0.86	*GBP4*	0.76	*MOV10*	0.67	*LOC100336669*	0.50
OAS1Y	0.86	*SLFN11*	0.75	*SP110*	0.67	*LOC617565*	0.50
DDX58	0.86	*OAS1X*	0.75	*STXBP1*	0.65	*LOC618733*	0.49
EPSTI1	0.86	*DTX3L*	0.74	*NMI*	0.64	*LOC101903126*	0.45
EIF2AK2	0.85	*LGALS9*	0.74	*PLSCR2*	0.63	*LOC788334*	0.44
ZNFX1	0.85	*IRF1*	0.74	*LOC507055*	0.63	*LOC531557*	0.44
SAMD9	0.84	*ADAR*	0.74	*TNFSF10*	0.63	*GRAMD1C*	0.43
XAF1	0.83	*IFI6*	0.73	*NLRC5*	0.62	*LOC522540*	0.42
IRF7	0.83	*IFIT5*	0.73	*IFIT3*	0.62	*GNGT2*	0.40
RTP4	0.82	*WARS*	0.72	*MLKL*	0.60	*PLAC8*	0.40
LOC512486	0.81	*TAP1*	0.72	*LOC783920*	0.59	*IL15RA*	0.38
						SDS	0.33
						LOC518495	0.33

#M5

GS	MM	GS	MM	GS	MM	GS	MM
ARHGAP30	0.90	*CYTH4*	0.79	*SPI1*	0.74	*KIF21B*	0.66
LCP1	0.89	*UNC93B1*	0.79	*EVI2B*	0.73	*CD3E*	0.66
PTPRC	0.89	*ARHGAP45*	0.78	*AIF1*	0.73	*LYZ*	0.65
MPEG1	0.87	*ARHGAP4*	0.77	*IPCEF1*	0.72	*PIK3R5*	0.63
CD53	0.86	*INPP5D*	0.77	*FGD2*	0.72	*PIK3CD*	0.61
CTSS	0.86	*IKZF1*	0.77	*BOLA-DRB3*	0.72	*PTPRE*	0.61
LAPTM5	0.85	*THEMIS2*	0.77	*GMIP*	0.72	*CD52*	0.61
LOC100297676	0.84	*RASSF2*	0.77	*CD84*	0.72	*SELL*	0.61
DOCK2	0.83	*SYK*	0.77	*CCR1*	0.72	*WAS*	0.61
LY9	0.83	*LOC515418*	0.77	*CYBB*	0.72	*LAIR1*	0.61
IL10RA	0.83	*RAC2*	0.77	*CTSH*	0.72	*CMTM7*	0.61
NCKAP1L	0.82	*ITGAM*	0.77	*KCNA3*	0.71	*BOLA-DMB*	0.60
FERMT3	0.82	*BIN2*	0.77	*PSD4*	0.71	*ITGB7*	0.60

SHTN1	0.82	*PRKCB*	0.76	*PLD4*	0.71	*IL2RB*	0.59
WDFY4	0.81	*CSF2RB*	0.76	*CCR2*	0.70	*GIMAP8*	0.57
ITGB2	0.81	*DOCK8*	0.76	*PTAFR*	0.70	*NAAA*	0.57
LCP2	0.81	*PTPN6*	0.76	*GIMAP7*	0.70	*SAMHD1*	0.56
CORO1A	0.81	*BOLA-DRA*	0.76	*SPN*	0.69	*IL2RG*	0.54
PTPRJ	0.80	*GNA15*	0.75	*AKNA*	0.68	*ZAP70*	0.54
FNBP1	0.80	*TBC1D9*	0.75	*CYTIP*	0.68	*BOLA-DMA*	0.47
SRGN	0.80	*FCGR3A*	0.75	*CLEC12A*	0.68	*UBD*	0.46
VAV1	0.79	*IRF8*	0.74	*CD74*	0.67	*CIITA*	0.29

#M6

GS	MM	GS	MM	GS	MM	GS	MM
GNAI1	0.93	*SLC16A7*	0.81	*PTCH2*	0.68	*FZD1*	0.58
MCAM	0.93	*CRYBG1*	0.80	*APCDD1*	0.68	*LRRC75A*	0.58
CCDC3	0.93	*G6PD*	0.80	*ACER3*	0.67	*ORMDL3*	0.58
RBP4	0.92	*OAF*	0.80	*SLC24A3*	0.67	*SOD3*	0.58
TRARG1	0.92	*HSPA12A*	0.80	*IL17D*	0.67	*FGFRL1*	0.57
CIDEC	0.92	*SFRP5*	0.80	*MARC2*	0.67	*CABLES1*	0.56
PLIN1	0.92	*ADGRA2*	0.80	*ADM*	0.66	*AIFM2*	0.55
CLU	0.92	*COL18A1*	0.80	*CYP4V2*	0.66	*RAB11FIP1*	0.54
FABP4	0.91	*TMEM110*	0.79	*SLC38A10*	0.66	*TMEM254*	0.53
PPP1R1B	0.90	*CNTN1*	0.78	*B3GALNT1*	0.66	*PLIN4*	0.53
PCK2	0.90	*ESYT1*	0.78	*GPR63*	0.66	*SIK2*	0.52
ADIPOQ	0.90	*ALDH1L2*	0.78	*ID4*	0.65	*KAZN*	0.52
PDE3B	0.89	*IDH1*	0.78	*NET1*	0.65	*MAOB*	0.52
TKT	0.89	*NCS1*	0.78	*C2CD2*	0.65	*ACSS2*	0.52
MGST1	0.89	*PGD*	0.78	*STX12*	0.65	*NADK*	0.51
ADIRF	0.89	*SCRN1*	0.78	*PTK2B*	0.64	*DEPP1*	0.48
SMOC1	0.89	*IGFBP4*	0.78	*ACER2*	0.64	*SERTM1*	0.46
LIPE	0.89	*SQOR*	0.77	*ADAMTS16*	0.64	*TBC1D16*	0.46
ACSM1	0.87	*LOC784007*	0.77	*LOC107131134*	0.64	*ABHD11*	0.45
THRSP	0.87	*DOCK11*	0.77	*CDS2*	0.64	*VWF*	0.45
DGAT2	0.86	*RNF125*	0.76	*EPHX2*	0.63	*PPP2R5A*	0.45
MTURN	0.86	*NPC2*	0.76	*MEIS2*	0.63	*AGFG2*	0.43
RTN3	0.86	*EFNA5*	0.74	*SS18*	0.63	*ABHD6*	0.42
ELOVL6	0.86	*NTRK2*	0.74	*PGAM1*	0.63	*SPATA20*	0.42
EPHX1	0.85	*KDSR*	0.73	*ADCY5*	0.63	*DMRT2*	0.42
MRAS	0.85	*SCD*	0.73	*PLXNA4*	0.63	*AGPAT2*	0.41
CKB	0.85	*CTDSPL*	0.73	*SULT1A1*	0.63	*MTA3*	0.41
ACACA	0.85	*TRABD2B*	0.72	*HIF3A*	0.63	*LNP1*	0.41
SLC16A2	0.85	*GPM6B*	0.72	*TDRP*	0.62	*HERPUD2*	0.40
FGF2	0.85	*ACSS3*	0.72	*PON2*	0.62	*MCCC1*	0.39
GNG2	0.84	*NUPR1*	0.72	*LOC112446042*	0.62	*PC*	0.39

MBNL3	0.84	*FGL1*	0.71	*IGSF10*	0.62	*SLC16A13*	0.38
CYB5A	0.84	*RETSAT*	0.71	*NNAT*	0.62	*ASL*	0.38
ATF5	0.83	*COX6A1*	0.71	*ENPP2*	0.62	*PTGR1*	0.38
HACD2	0.83	*PDGFD*	0.71	*SLC1A5*	0.61	*THEM4*	0.36
DHRS7	0.83	*TBC1D2B*	0.71	*IMPDH1*	0.61	*ITPK1*	0.36
TMSB15B	0.82	*APOE*	0.71	*ENPP5*	0.61	*ME1*	0.36
PDP2	0.82	*ABCA10*	0.71	*TENM4*	0.61	*SIRPA*	0.35
FASN	0.82	*DHCR24*	0.70	*LGALS3BP*	0.61	*GGH*	0.35
FBP1	0.82	*FAH*	0.70	*LMO4*	0.61	*ECHDC1*	0.35
BNIP3L	0.82	*ICK*	0.70	*AOX1*	0.60	*ANKH*	0.33
SULF1	0.82	*ARL6IP1*	0.70	*SKAP1*	0.60	*CHP2*	0.32
CARD11	0.82	*VAV3*	0.69	*C1QTNF7*	0.60	*LOC100850659*	0.30
ELOVL5	0.81	*TALDO1*	0.68	*SAMD12*	0.60	*SORD*	0.29
MFNG	0.81	*CAMK1*	0.68	*SEMA3B*	0.60	*FAM83H*	0.28
PCK1	0.81	*PHLDA1*	0.68	*CIDEA*	0.60	*SCAP*	0.26
G0S2	0.81	*ZDHHC2*	0.68	*ADCYAP1R1*	0.60	*PLA2G15*	0.20
				WFS1	0.59	*LOC100299281*	0.19

#M7

GS	MM	GS	MM	GS	MM	GS	MM
CAP1	0.89	*CLEC3B*	0.58	*YIPF5*	0.43	*SRSF3*	0.31
CAV1	0.85	*POR*	0.58	*ARHGEF40*	0.43	*PTH1R*	0.31
EHD2	0.85	*SULF2*	0.58	*RPL22L1*	0.43	*KHDRBS3*	0.31
COL4A2	0.85	*BMP6*	0.58	*LRRC8B*	0.43	*PNPLA2*	0.31
GNAI2	0.85	*PNP*	0.58	*ARHGAP27*	0.43	*PRPS2*	0.31
SEPT9	0.84	*NR2F2*	0.58	*DTD1*	0.43	*PDCD6*	0.31
TNFRSF1A	0.84	*ACTA2*	0.57	*CSRP2*	0.43	*ENAH*	0.30
YWHAB	0.83	*RIPK1*	0.57	*FOXC1*	0.43	*PPM1D*	0.30
STOM	0.83	*HNRNPA0*	0.57	*LIMS2*	0.43	*CCL1*	0.30
MYADM	0.83	*AIF1L*	0.57	*ADAMTS7*	0.43	*STK24*	0.30
COL4A1	0.82	*IFITM3*	0.57	*VWA1*	0.43	*B3GNT3*	0.30
FAM129B	0.81	*MYL9*	0.57	*SQLE*	0.43	*LOC515697*	0.30
IL27RA	0.81	*CDR2*	0.57	*TSPAN12*	0.43	*H2AFX*	0.30
TMSB4X	0.81	*FRMD8*	0.57	*SLC16A11*	0.43	*ILVBL*	0.30
PYGL	0.81	*DNAJB11*	0.57	*KLF16*	0.43	*FAIM*	0.30
TMSB10	0.81	*SLC1A4*	0.57	*ANGPT2*	0.42	*RAB11FIP5*	0.30
SPTAN1	0.81	*COX7A2*	0.57	*HPCAL1*	0.42	*SPSB4*	0.30
MSN	0.80	*HIC1*	0.57	*ADGRE5*	0.42	*BZW1*	0.30
TAX1BP3	0.80	*ARF3*	0.56	*PIGW*	0.42	*GBE1*	0.29
PARVA	0.80	*OGFR*	0.56	*WDR1*	0.42	*STAP2*	0.29
PTPN9	0.80	*ZFP36L2*	0.56	*CAMK2N1*	0.42	*KCNMB1*	0.29
SELENON	0.80	*RBM15B*	0.56	*RAB35*	0.42	*RGS2*	0.29
TPM4	0.80	*XPO6*	0.56	*ADAM15*	0.42	*CASP6*	0.29

DPYSL2	0.80	*LRPAP1*	0.56	*CRELD2*	0.42	*PTPRCAP*	0.29
GNB1	0.79	*EFNB1*	0.56	*HS1BP3*	0.42	*RPH3AL*	0.29
CMTM6	0.79	*TSHZ3*	0.55	*ERP44*	0.42	*PITPNM1*	0.29
SERPINE2	0.79	*NOL4L*	0.55	*DRAM1*	0.42	*ADAMTSL2*	0.29
ACTB	0.78	*TRIB2*	0.55	*TMEM97*	0.42	*GNA12*	0.29
PPP1R18	0.78	*MYH10*	0.55	*FAM20A*	0.42	*PRR13*	0.28
ITGA5	0.78	*GOLM1*	0.55	*STK17A*	0.42	*VPS37B*	0.28
RAP1B	0.78	*GDI1*	0.55	*MOGS*	0.42	*CACNB3*	0.28
PDIA3	0.78	*HSD3B7*	0.55	*HAUS7*	0.42	*LOC101905956*	0.28
YWHAZ	0.77	*AMIGO2*	0.55	*INPP1*	0.42	*ATP6AP1*	0.28
CAVIN3	0.77	*ACTR3*	0.55	*TMEM127*	0.42	*DCXR*	0.28
CRIP2	0.77	*C15H11orf96*	0.55	*PIGT*	0.42	*ALG14*	0.28
CAVIN1	0.77	*PPP1R9B*	0.55	*PTK7*	0.41	*C1GALT1C1*	0.28
PGRMC1	0.77	*CRIM1*	0.55	*MTA2*	0.41	*NEK6*	0.28
ELMO1	0.76	*ERRFI1*	0.55	*ABR*	0.41	*PRKRA*	0.28
IGFBP7	0.76	*FAR2*	0.55	*PSMB8*	0.41	*TMEM237*	0.27
LOC534742	0.76	*C21H15orf39*	0.55	*NPC1*	0.41	*TXNDC11*	0.27
RAMP2	0.76	*RGS16*	0.54	*CORO1B*	0.41	*BANP*	0.27
ACTN1	0.76	*MARCKSL1*	0.54	*CPXM1*	0.41	*TMCC3*	0.27
TGFB1	0.75	*F2R*	0.54	*DIXDC1*	0.41	*ST3GAL5*	0.27
PTPRA	0.75	*MRGPRF*	0.54	*CCDC102A*	0.41	*LOC540014*	0.27
SEC61A1	0.75	*CARHSP1*	0.54	*ACTG2*	0.41	*PPP1R13L*	0.27
ACVRL1	0.75	*FAM241A*	0.54	*ADIPOR2*	0.41	*RELL1*	0.27
STMN1	0.75	*CD46*	0.54	*HYAL2*	0.41	*ECE2*	0.26
PLEKHO1	0.75	*MANF*	0.54	*SMAGP*	0.40	*ZNF783*	0.26
PPIA	0.75	*S1PR1*	0.54	*FAM212B*	0.40	*PNMA1*	0.26
TGFB1I1	0.75	*DSTN*	0.54	*ABI3*	0.40	*RND1*	0.26
PALM	0.75	*TUBB2B*	0.53	*RAB11A*	0.40	*MIS12*	0.26
DEGS1	0.75	*FUT4*	0.53	*SPNS2*	0.40	*C7H19orf25*	0.26
S1PR2	0.75	*LCAT*	0.53	*BAX*	0.40	*CAPZA1*	0.26
STAT6	0.75	*GAS6*	0.53	*PPP4R1*	0.40	*FAM101A*	0.26
ADAM17	0.74	*ENTPD1*	0.53	*DHH*	0.40	*DUSP10*	0.26
RGL1	0.74	*CRISPLD2*	0.53	*MMP28*	0.40	*HMOX1*	0.26
FSTL3	0.74	*ST3GAL4*	0.53	*GADD45B*	0.40	*PDK3*	0.26
KCTD10	0.74	*HMGCR*	0.53	*TMEM132A*	0.40	*LOC101908206*	0.26
RHOC	0.73	*RNF145*	0.53	*NOVA2*	0.40	*CAT*	0.25
ARHGDIA	0.73	*CHST11*	0.53	*IL1RAP*	0.40	*HES2*	0.25
GNAI3	0.73	*ARF6*	0.53	*NFKBIE*	0.40	*PRCP*	0.25
EMP1	0.72	*SGPL1*	0.52	*CHRNA3*	0.40	*NDRG4*	0.25
PLEKHO2	0.72	*CCND3*	0.52	*HMG20B*	0.40	*GGPS1*	0.25
CALR	0.72	*MYL6*	0.52	*GJA5*	0.39	*HEBP2*	0.25
SWAP70	0.72	*NXPE3*	0.52	*CD320*	0.39	*CPNE2*	0.25
KIAA0040	0.72	*ARHGEF18*	0.52	*GINS3*	0.39	*CYB5D1*	0.25

MYO1D	0.72	*JAM3*	0.52	*SMIM3*	0.39	*ZNF329*	0.25
RBPMS	0.72	*IER5L*	0.52	*S100B*	0.39	*ADRA1D*	0.25
CDC42SE1	0.72	*PLOD1*	0.52	*RARA*	0.39	*NREP*	0.25
RPL3	0.71	*GPAT3*	0.52	*LOC509006*	0.39	*DNAJC14*	0.25
COLGALT1	0.71	*PRRX1*	0.51	*HRCT1*	0.39	*SEMA3F*	0.25
RHOA	0.70	*KCNJ8*	0.51	*ACSS1*	0.39	*OTUD5*	0.24
MTAP	0.70	*ACSF2*	0.51	*LAYN*	0.39	*CCDC134*	0.24
CTNNA1	0.70	*CREB3L1*	0.51	*SLC25A33*	0.39	*SIRT6*	0.24
FADS3	0.70	*LPL*	0.51	*ELOVL7*	0.38	*WDR4*	0.24
ACTG1	0.70	*ABHD3*	0.51	*UAP1L1*	0.38	*TP53*	0.24
VASP	0.69	*BTG3*	0.51	*BMP2K*	0.38	*F2RL2*	0.24
ZYX	0.69	*CERS2*	0.51	*LOC101905365*	0.38	*IRF2BP2*	0.24
ECE1	0.69	*GNB5*	0.51	*MEAF6*	0.38	*AMACR*	0.24
APLP2	0.69	*TRAF3IP2*	0.51	*SRXN1*	0.38	*ZSCAN2*	0.24
CLIC2	0.69	*EDN1*	0.51	*TGIF2*	0.38	*VEGFC*	0.24
SYDE1	0.68	*PRKD1*	0.51	*STX5*	0.38	*GRAMD1A*	0.24
LITAF	0.68	*THSD1*	0.51	*LBH*	0.38	*LOC100847345*	0.23
ARPC3	0.68	*WDR45B*	0.51	*BoLA*	0.38	*MDK*	0.23
KDELR2	0.68	*CTSV*	0.50	*CNKSR3*	0.38	*LOC112444531*	0.23
TINAGL1	0.68	*PPP1R14A*	0.50	*SAR1A*	0.38	*AFAP1L1*	0.23
SLC29A1	0.68	*FES*	0.50	*ARMC5*	0.38	*C2CD2L*	0.23
MFGE8	0.68	*RELA*	0.50	*CREBL2*	0.38	*NCAPH*	0.23
SEC61B	0.68	*FITM2*	0.50	*KLHL36*	0.37	*HSD11B1*	0.23
EXT1	0.67	*LOC112448454*	0.50	*NFATC4*	0.37	*CMPK1*	0.23
CXCL16	0.67	*EPHA2*	0.50	*B4GALNT1*	0.37	*B2M*	0.23
PRELID1	0.67	*TXNRD1*	0.50	*ARHGAP25*	0.37	*TMEM14A*	0.23
SLC12A4	0.67	*PALD1*	0.49	*RAMP3*	0.37	*KCNAB1*	0.23
MANSC1	0.67	*RNF41*	0.49	*CSK*	0.37	*BCAT2*	0.23
RAB1A	0.67	*APBB1*	0.49	*RFX2*	0.37	*TTC38*	0.23
PDIA5	0.67	*PHC2*	0.49	*MPDU1*	0.37	*TMEM200B*	0.23
RARRES2	0.67	*FAM107A*	0.49	*FAM177A1*	0.37	*MEN1*	0.22
ENG	0.66	*RAB5C*	0.49	*SERPINB1*	0.37	*BREH1*	0.22
EIF4A1	0.66	*MGAT1*	0.49	*TCEA1*	0.37	*CCL2*	0.22
FSCN1	0.66	*RAB7B*	0.49	*ABCA3*	0.37	*ZBTB42*	0.21
C1QTNF5	0.66	*MOB3A*	0.49	*SEC62*	0.37	*MMD*	0.21
PYGB	0.66	*SPG21*	0.49	*TNFSF12*	0.37	*SNX9*	0.21
RHOB	0.66	*CD36*	0.49	*SNW1*	0.37	*SMIM15*	0.21
LYN	0.66	*SELP*	0.49	*OSTM1*	0.37	*WDR62*	0.21
TRAM1	0.66	*SEC23B*	0.49	*DOK4*	0.36	*TMEM252*	0.21
RAB27A	0.66	*CD151*	0.49	*CD247*	0.36	*LOC112445780*	0.21
LPIN2	0.66	*TUBB2A*	0.49	*HOXB2*	0.36	*EIF1AD*	0.21
TLNRD1	0.65	*RNF114*	0.48	*DTX1*	0.36	*FAM162B*	0.21
SERPINH1	0.65	*SOCS3*	0.48	*CYYR1*	0.36	*MAD2L1BP*	0.21

GEM	0.65	*GCHFR*	0.48	*NRROS*	0.36	*SYVN1*	0.21
RAB43	0.65	*BMP2*	0.48	*BCL3*	0.36	*LOC112447362*	0.20
KIFC3	0.65	*LDLR*	0.48	*SPATS2*	0.36	*DOPEY2*	0.20
CDKN1C	0.65	*RBPMS2*	0.48	*PDCD10*	0.36	*RBM22*	0.20
HSPA5	0.65	*CYTH2*	0.48	*SSR3*	0.35	*PALMD*	0.20
MYH9	0.65	*OSTF1*	0.48	*SERPINA5*	0.35	*GIPC2*	0.20
CNN2	0.65	*ELOVL1*	0.48	*DUSP11*	0.35	*CCDC85C*	0.20
PMEPA1	0.65	*HCLS1*	0.48	*TMEM214*	0.35	*RASL11A*	0.20
GAS2L1	0.65	*HAPLN3*	0.48	*CHP1*	0.35	*FARP1*	0.20
ACTR2	0.65	*APLN*	0.48	*PSEN2*	0.35	*DPH2*	0.20
JUP	0.64	*IFNGR1*	0.47	*TMEM165*	0.35	*LOC509972*	0.20
PLOD3	0.64	*TM9SF3*	0.47	*TMEM178A*	0.35	*ST3GAL2*	0.20
MYO1C	0.64	*FHL2*	0.47	*CYGB*	0.35	*PLA2G7*	0.20
MYDGF	0.64	*PRKAR1B*	0.47	*CANX*	0.35	*INAFM2*	0.20
XBP1	0.64	*SH3BGRL2*	0.47	*TMEM115*	0.35	*SNAPC1*	0.19
LTBR	0.64	*CDC42EP4*	0.47	*PIM1*	0.35	*ANGPTL4*	0.19
TSPAN9	0.63	*NRM*	0.47	*CCL14*	0.35	*SOCS2*	0.19
TP53I11	0.63	*TBC1D10A*	0.47	*RAB15*	0.35	*NTRK3*	0.19
TUBB6	0.63	*HYOU1*	0.47	*PPM1F*	0.35	*LOC520336*	0.19
ANO10	0.63	*REM1*	0.47	*TSPAN15*	0.35	*BFAR*	0.19
CHST7	0.63	*RCC2*	0.47	*ASPHD2*	0.34	*HDAC1*	0.19
EVA1B	0.63	*SMAD6*	0.46	*KLHL6*	0.34	*TNIP2*	0.18
HSP90B1	0.62	*SPRY1*	0.46	*REEP4*	0.34	*UFM1*	0.18
LFNG	0.62	*LOC101907813*	0.46	*DDX10*	0.34	*TMED7*	0.18
PDIA6	0.62	*LMO2*	0.46	*CCDC112*	0.34	*SNIP1*	0.18
EZR	0.62	*CAPN2*	0.46	*GSPT2*	0.34	*BMP5*	0.18
WTIP	0.62	*FAM84B*	0.46	*PSMB9*	0.34	*ERICH1*	0.18
ZDHHC9	0.62	*CNN1*	0.46	*TM9SF1*	0.34	*ACTL6A*	0.17
SDCBP	0.62	*SLC25A35*	0.46	*PI4K2A*	0.34	*SLC44A2*	0.17
PELI1	0.62	*ARF4*	0.46	*TRAFD1*	0.33	*IL4R*	0.17
H3F3B	0.61	*GRAP*	0.46	*MYH11*	0.33	*ARMC7*	0.17
SLC25A5	0.61	*SREBF2*	0.46	*RAVER1*	0.33	*SEMA7A*	0.17
MYLK	0.61	*RASL12*	0.46	*PGLS*	0.33	*LOC101902346*	0.16
ATP1B3	0.61	*GLCE*	0.46	*LZTS2*	0.33	*SUV39H1*	0.16
KDELC1	0.61	*FAM43A*	0.46	*BOK*	0.33	*ZNF408*	0.16
TAGLN	0.61	*CD37*	0.46	*ILDR2*	0.33	*CHIC2*	0.16
FLNA	0.61	*NACAD*	0.46	*FAM20C*	0.33	*LOC513767*	0.16
MFHAS1	0.61	*CLPTM1L*	0.45	*SCD5*	0.33	*ZNF513*	0.16
RALA	0.61	*RSL1D1*	0.45	*BCL10*	0.33	*RNF135*	0.15
ARHGEF2	0.60	*MTMR2*	0.45	*IFT57*	0.33	*TRNP1*	0.15
PQLC3	0.60	*GFOD2*	0.45	*CHTF8*	0.33	*GSS*	0.15
ICA1	0.60	*PSEN1*	0.45	*TRIM27*	0.33	*B4GALT3*	0.15
TMED9	0.60	*SLCO2A1*	0.45	*UMPS*	0.33	*ZBTB43*	0.14

WWTR1	0.60	*ATOH8*	0.45	*FAM46B*	0.33	*ARHGEF7*	0.14
ZCCHC3	0.60	*BCAR1*	0.45	*RAP1GAP2*	0.32	*SEMA5B*	0.14
TFPI2	0.60	*TMEM176A*	0.45	*LOC783680*	0.32	*ZBTB5*	0.14
CDH13	0.60	*C7H19orf66*	0.45	*STX7*	0.32	*CBX3*	0.14
HK1	0.60	*DYRK3*	0.45	*SLC35A2*	0.32	*GPN2*	0.14
CSRP1	0.60	*TMED10*	0.45	*TPST2*	0.32	*BIVM*	0.13
RAB8A	0.59	*POLDIP3*	0.45	*B3GALT2*	0.32	*GPR27*	0.13
ZFP36L1	0.59	*SYBU*	0.45	*ARHGAP23*	0.32	*ARL1*	0.13
MGAT2	0.59	*RILPL2*	0.44	*SUSD2*	0.32	*LYSMD2*	0.12
LMNA	0.59	*SERINC1*	0.44	*ATP13A1*	0.32	*LIMS1*	0.12
MTFR1	0.59	*CADPS2*	0.44	*TNFAIP1*	0.32	*PIGU*	0.11
FGR	0.59	*PGM5*	0.44	*TMEM268*	0.32	*BOLA*	0.11
RTL5	0.59	*PGF*	0.44	*TRIB1*	0.32	*GSR*	0.11
PXDN	0.59	*HHEX*	0.44	*DYNC1I2*	0.32	*C7*	0.11
TMEM50A	0.59	*TFE3*	0.44	*TGM2*	0.31	*AQP3*	0.11
SNPH	0.59	*HIGD1B*	0.44	*SIPA1*	0.31	*DCAF12*	0.10
SHC1	0.59	*LOC101908535*	0.44	*SRSF9*	0.31	*LRRC3B*	0.10
PACSIN2	0.58	*FBXO8*	0.44	*MEX3D*	0.31	*LOC534630*	0.10
EMILIN1	0.58	*ICOSLG*	0.44	*MYL12B*	0.31	*GPR146*	0.09
HDGFL3	0.58	*MEOX1*	0.44	*FAM214B*	0.31	*TIGD7*	0.07
TLN1	0.58	*TRIM62*	0.44	*S1PR3*	0.31	*KNOP1*	0.07
MOCOS	0.58	*C5AR2*	0.44	*NXT2*	0.31	*MMP15*	0.06
NME1	0.58	*RUNX1*	0.44	*MAPRE1*	0.31	*LOC505918*	0.06
IP6K1	0.58	*HEBP1*	0.44	*RDH11*	0.31	*GIPC3*	0.05

#M8

GS	MM	GS	MM	GS	MM	GS	MM
FSTL1	0.92	*KDELC2*	0.68	*LDAH*	0.52	*CHI3L1*	0.35
S100A10	0.92	*BICC1*	0.68	*MKI67*	0.52	*TTYH2*	0.35
VIM	0.91	*DAPK1*	0.68	*VKORC1*	0.52	*ADAMTS15*	0.35
COL5A2	0.89	*LOC112444473*	0.68	*CSTB*	0.52	*STX2*	0.35
ANXA1	0.89	*AMOTL2*	0.68	*PPIC*	0.52	*ELFN2*	0.35
COL1A2	0.88	*PAPSS1*	0.67	*SRBD1*	0.52	*IL17RC*	0.35
MMP14	0.87	*TRAM2*	0.67	*TMEM86A*	0.52	*SLC40A1*	0.35
DCN	0.87	*CFH*	0.67	*ERGIC3*	0.52	*FLT3LG*	0.35
DAB2	0.87	*CRTAP*	0.67	*RIC8A*	0.52	*COMMD2*	0.34
SERPINF1	0.87	*CTSB*	0.67	*VWA5A*	0.52	*SELENBP1*	0.34
QSOX1	0.87	*LOC504773*	0.67	*MXD4*	0.52	*TPCN1*	0.34
SEPT2	0.87	*COTL1*	0.67	*CFP*	0.52	*TRIL*	0.34
ANTXR2	0.87	*CR2*	0.67	*SYT11*	0.52	*FAM92A*	0.34
FN1	0.87	*ATP6AP2*	0.67	*QPCTL*	0.52	*FAM149A*	0.34
COL5A1	0.87	*RSU1*	0.67	*TRIP6*	0.51	*NLGN2*	0.34
COL14A1	0.86	*NT5E*	0.67	*ERLIN1*	0.51	*FST*	0.34

THY1	0.86	*MAN2B1*	0.67	*OLFML2A*	0.51	*MSMO1*	0.34
COL1A1	0.86	*PTMS*	0.67	*ATRNL1*	0.51	*MINDY4*	0.34
FGFR1	0.86	*LRRC17*	0.67	*AMPD2*	0.51	*PLAT*	0.34
ANXA5	0.86	*CAPG*	0.67	*KIAA1614*	0.51	*ETV5*	0.34
ADAMTS2	0.85	*ALDH1A3*	0.66	*PLPP5*	0.51	*LURAP1*	0.34
AXL	0.85	*LTBP1*	0.66	*MLLT11*	0.51	*DBNL*	0.33
FAM46A	0.85	*OS9*	0.66	*FCGR2B*	0.51	*GLTP*	0.33
ECM2	0.84	*MORC4*	0.66	*NUCB1*	0.51	*CHODL*	0.33
COL3A1	0.84	*GLIS2*	0.66	*TMEM181*	0.51	*ABHD12*	0.33
MARVELD1	0.84	*TRIM47*	0.66	*KCND1*	0.51	*LRP10*	0.33
EMILIN2	0.84	*IFI30*	0.66	*CTSA*	0.51	*SPRYD3*	0.33
TXNDC5	0.84	*IKBIP*	0.66	*LURAP1L*	0.51	*TLR5*	0.33
LHFPL2	0.84	*PI15*	0.66	*BCHE*	0.51	*LOC781977*	0.33
APP	0.83	*LTBP2*	0.66	*PCDHA13*	0.51	*PEG10*	0.33
MFAP5	0.83	*BMP1*	0.66	*QPCT*	0.51	*VPS26C*	0.33
ANXA2	0.83	*P3H2*	0.66	*THBS2*	0.51	*PDCD4*	0.33
CD44	0.83	*FMOD*	0.66	*LOC782776*	0.51	*SERP1*	0.33
IQGAP2	0.83	*MARCKS*	0.66	*SLC46A1*	0.51	*SBSPON*	0.33
MXRA7	0.83	*MBTPS1*	0.66	*COL21A1*	0.51	*SNX2*	0.33
GSN	0.83	*CASP4*	0.66	*PSAT1*	0.51	*SEMA4G*	0.33
ITGB5	0.83	*THBS1*	0.66	*APBA1*	0.51	*LOC101906676*	0.33
MAN1A1	0.83	*MDFIC*	0.66	*PRRG1*	0.51	*OGFOD3*	0.33
COL6A1	0.83	*ARAP1*	0.66	*CCDC82*	0.51	*GPX3*	0.33
RCN3	0.83	*COPZ2*	0.66	*SIGLEC1*	0.51	*C3*	0.33
TGFBI	0.83	*GPSM1*	0.66	*TNFRSF21*	0.51	*P3H4*	0.32
DSE	0.83	*ACSL5*	0.66	*SGMS2*	0.51	*DNAJC25*	0.32
TIMP2	0.82	*SDK1*	0.66	*NAB2*	0.50	*XRCC4*	0.32
BGN	0.82	*SRC*	0.65	*GPR173*	0.50	*CPNE8*	0.32
GALNT16	0.82	*CCL24*	0.65	*SH3BP1*	0.50	*LDLRAD4*	0.32
MRC2	0.82	*SGSH*	0.65	*RP2*	0.50	*RNF13*	0.32
GLIPR2	0.82	*PRKCSH*	0.65	*LLGL1*	0.50	*VMAC*	0.32
DAP	0.82	*EDEM2*	0.65	*SESN3*	0.50	*TMEM68*	0.32
PTTG1IP	0.82	*SLC9A9*	0.65	*VIPR2*	0.50	*BET1*	0.32
CDON	0.82	*SRPX2*	0.65	*PTPN18*	0.50	*UCP2*	0.32
TIMP1	0.82	*GBA*	0.65	*HSD17B12*	0.50	*ARRB2*	0.31
F13A1	0.82	*CPQ*	0.65	*CRISPLD1*	0.50	*NCSTN*	0.31
ANGPTL1	0.82	*FUCA2*	0.65	*SERPINB8*	0.50	*RASSF4*	0.31
RNASE6	0.82	*MPZL1*	0.65	*MANBA*	0.50	*LVRN*	0.31
PAM	0.82	*CERCAM*	0.65	*TPSB2*	0.50	*GLT8D1*	0.31
CD248	0.82	*HRH1*	0.65	*IGFBP3*	0.50	*CCL21*	0.31
COL6A2	0.82	*PTGS1*	0.65	*CNPY4*	0.50	*SLC2A3*	0.31
ISLR	0.82	*CD163*	0.65	*FADS2*	0.50	*PTI*	0.31
EMP3	0.82	*PRELP*	0.65	*HSPA2*	0.50	*DPY19L1*	0.31

CTSK	0.82	*CD14*	0.65	*NSDHL*	0.50	*TSPAN6*	0.31
YWHAQ	0.81	*GPR137B*	0.65	*CSGALNACT1*	0.50	*OCIAD2*	0.31
SPARC	0.81	*PLBD2*	0.65	*CDC25B*	0.50	*RASD1*	0.31
AEBP1	0.81	*DNM1*	0.65	*MAP3K12*	0.50	*B4GALT6*	0.31
LHFPL6	0.81	*C1S*	0.65	*CXCL14*	0.49	*WNT11*	0.31
KDELR3	0.81	*HSD17B11*	0.65	*ANKRD13A*	0.49	*GXYLT2*	0.31
FGL2	0.81	*PFKL*	0.65	*TCTN2*	0.49	*KHNYN*	0.30
PFKP	0.81	*WNT5A*	0.65	*PACS1*	0.49	*SHKBP1*	0.30
FKBP10	0.81	*TSPO*	0.65	*ID2*	0.49	*P2RY14*	0.30
LTBP3	0.81	*PLXDC1*	0.65	*CAB39L*	0.49	*SCUBE2*	0.30
TMED3	0.81	*EFHD1*	0.64	*VEGFD*	0.49	*GLB1*	0.30
IGFBP6	0.81	*FZD8*	0.64	*C19H17orf58*	0.49	*CHD5*	0.30
MXRA8	0.81	*XG*	0.64	*ACO1*	0.49	*PEF1*	0.30
LOC515150	0.81	*LXN*	0.64	*MCM6*	0.49	*CTSC*	0.30
PDGFRA	0.80	*HEXB*	0.64	*LAT2*	0.49	*MBLAC1*	0.30
CLMP	0.80	*SLC39A1*	0.64	*ENTPD2*	0.49	*LGMN*	0.30
ARPC5	0.80	*FMO5*	0.64	*LOC786948*	0.49	*APOD*	0.30
S100A11	0.80	*VGLL3*	0.64	*ZBED8*	0.49	*VASN*	0.30
RARRES1	0.80	*STAB1*	0.64	*SLC25A6*	0.49	*GPX8*	0.30
DBN1	0.80	*TUSC3*	0.64	*ADPGK*	0.48	*CAPRIN2*	0.30
CSF1	0.80	*CDK14*	0.64	*SINHCAF*	0.48	*TAGAP*	0.29
FBLN5	0.80	*PTPRF*	0.64	*SEMA4C*	0.48	*SMIM7*	0.29
COL16A1	0.80	*SRI*	0.64	*PLPP3*	0.48	*ZFYVE21*	0.29
LPAR1	0.80	*ANG*	0.64	*ITGB4*	0.48	*CHMP4A*	0.29
CD9	0.80	*PAPSS2*	0.64	*MTHFD1L*	0.48	*POLA2*	0.29
VAT1	0.80	*MEDAG*	0.64	*KIT*	0.48	*ARMC9*	0.29
FAP	0.80	*RFTN2*	0.64	*OLFML3*	0.48	*ZKSCAN4*	0.29
MMP16	0.80	*RASGRP4*	0.64	*RAB2B*	0.48	*TRIOBP*	0.29
S100A4	0.80	*PPL*	0.64	*PPM1M*	0.48	*VGLL4*	0.29
COL6A3	0.79	*CD68*	0.64	*LAMB2*	0.48	*TMEM192*	0.29
DCLK1	0.79	*PHF19*	0.64	*LDB2*	0.48	*BTBD19*	0.29
PLOD2	0.79	*CYBA*	0.64	*NT5DC2*	0.48	*REXO5*	0.29
RNASE4	0.79	*CYS1*	0.64	*NCAM1*	0.48	*CBX6*	0.29
PPIB	0.79	*CDR2L*	0.63	*GUSB*	0.48	*GRK6*	0.29
BRB	0.79	*B3GNT9*	0.63	*RAP1GDS1*	0.48	*MAGEH1*	0.29
PCOLCE	0.79	*TGIF1*	0.63	*MVP*	0.48	*FAM180A*	0.29
GLT8D2	0.79	*RBPJ*	0.63	*SNX7*	0.47	*PXYLP1*	0.28
LRP1	0.79	*A2M*	0.63	*CYB561*	0.47	*FEZ2*	0.28
SGCE	0.79	*THBS4*	0.63	*CFD*	0.47	*FAM117A*	0.28
PCDH18	0.79	*NHSL1*	0.63	*CPE*	0.47	*YPEL1*	0.28
LAMA4	0.79	*TNFAIP8L3*	0.63	*CPA3*	0.47	*NASP*	0.28
MFAP2	0.78	*PIEZO2*	0.63	*RAP2B*	0.47	*ARSA*	0.28
RRBP1	0.78	*IGF2*	0.63	*ADORA2B*	0.47	*CYP2D14*	0.28

FBN1	0.78	*PYCR1*	0.63	*HEPH*	0.47	*ATG4C*	0.28
MATN2	0.78	*FAM3C*	0.63	*CA5B*	0.47	*MAGEF1*	0.28
LOXL2	0.78	*KCTD12*	0.63	*NIPAL2*	0.47	*MAL*	0.28
GOLIM4	0.78	*PLAGL1*	0.63	*GALNT4*	0.47	*PTPRU*	0.28
LOC511937	0.78	*FKBP11*	0.62	*C29H11orf95*	0.47	*SPOCK1*	0.28
C1QA	0.78	*LYVE1*	0.62	*GALNT15*	0.46	*TUFT1*	0.28
ECM1	0.78	*DYNLT3*	0.62	*NUCB2*	0.46	*SNX10*	0.27
DDAH2	0.78	*ADGRD1*	0.62	*PLEKHA4*	0.46	*PSPH*	0.27
FOLR2	0.78	*C5AR1*	0.62	*GALNS*	0.46	*MBOAT7*	0.27
CYBRD1	0.78	*MMP19*	0.62	*C1QTNF2*	0.46	*LOC101907523*	0.27
EPB41L3	0.78	*PTGIS*	0.62	*MAN1C1*	0.46	*DMPK*	0.27
RIN2	0.78	*VAV2*	0.62	*PIK3CG*	0.46	*ARPIN*	0.27
MMP2	0.78	*GAS1*	0.62	*ARHGAP20*	0.46	*CIB1*	0.27
DKK3	0.78	*ETV1*	0.62	*ITPRIPL2*	0.46	*ASPA*	0.27
GJA1	0.77	*PEA15*	0.62	*C4A*	0.46	*EPHX3*	0.27
MXRA5	0.77	*MYD88*	0.61	*PIK3IP1*	0.46	*FAM102A*	0.27
FBLN1	0.77	*IGF1*	0.61	*P4HA1*	0.46	*GALT*	0.27
NOTCH2	0.77	*SELPLG*	0.61	*LOC107131209*	0.46	*VHL*	0.27
FYN	0.77	*FAM117B*	0.61	*ATP2A3*	0.45	*ARHGAP22*	0.26
OTULINL	0.77	*FKBP14*	0.61	*PRG4*	0.45	*ADH5*	0.26
EFS	0.77	*VCAN*	0.61	*RGS19*	0.45	*ALG11*	0.26
PI16	0.77	*RASSF5*	0.61	*CERK*	0.45	*BCAS1*	0.26
FAM114A1	0.77	*ADCY7*	0.61	*PMM2*	0.45	*ACTC1*	0.26
CCDC80	0.77	*SLIT3*	0.61	*SHB*	0.45	*LSS*	0.26
SH3BGRL3	0.77	*FGF7*	0.61	*GNS*	0.45	*JPT2*	0.26
PRRX2	0.77	*NAGA*	0.61	*CKAP2*	0.45	*ADD1*	0.26
SH3BGRL	0.76	*CPXM2*	0.61	*SLC39A11*	0.45	*SMAD9*	0.26
MEOX2	0.76	*SEMA4F*	0.61	*SPSB1*	0.45	*ZNF202*	0.26
PLEKHA2	0.76	*LIPA*	0.61	*ADAMTS5*	0.45	*TSEN34*	0.26
C3AR1	0.76	*TOP2A*	0.61	*AFAP1L2*	0.45	*RBKS*	0.26
IL13RA1	0.76	*NAALADL2*	0.61	*CX3CL1*	0.45	*AK5*	0.26
FAM129A	0.76	*LOC507581*	0.61	*SGPP1*	0.45	*SIGMAR1*	0.25
OLFML1	0.76	*GMFG*	0.61	*PCSK6*	0.44	*SLC35F6*	0.25
C1QB	0.76	*THBD*	0.61	*ANXA8L1*	0.44	*VNN2*	0.25
CRIP1	0.76	*LRRC8D*	0.61	*SOX4*	0.44	*PRMT2*	0.25
MAGED1	0.76	*MEST*	0.61	*DDX31*	0.44	*BMPER*	0.25
PLTP	0.76	*TSKU*	0.61	*NAGK*	0.44	*TMEM53*	0.25
NOV	0.76	*CYP27A1*	0.60	*TMEM100*	0.44	*FNDC4*	0.25
EFEMP2	0.76	*MYOC*	0.60	*ALDH3A2*	0.44	*RARG*	0.25
ADD3	0.76	*LAPTM4A*	0.60	*PRAF2*	0.44	*DKK2*	0.25
DUSP6	0.76	*PCOLCE2*	0.60	*RFFL*	0.44	*VPS41*	0.25
PROS1	0.76	*TENM3*	0.60	*ICAM3*	0.44	*IFT122*	0.25
EBF1	0.76	*SUMF1*	0.60	*GPRC5B*	0.44	*VPS26A*	0.24

TUBA1A	0.76	*PKIB*	0.60	*TNFAIP3*	0.44	*SC5D*	0.24
SFXN3	0.75	*CHSY1*	0.60	*ACP5*	0.44	*BLA.DQB*	0.24
APBB1IP	0.75	*ORAI3*	0.60	*AP3S1*	0.44	*PARP16*	0.24
FBLN2	0.75	*NONO*	0.60	*OSR1*	0.44	*ZNF217*	0.24
PEPD	0.75	*EXT2*	0.60	*TMEM184B*	0.44	*ALG8*	0.24
TNC	0.75	*ZFPM2*	0.60	*SLC35B3*	0.44	*NOD1*	0.24
C1QC	0.75	*KERA*	0.60	*ALDH9A1*	0.44	*CDH3*	0.24
GPX7	0.75	*NPTXR*	0.60	*TPPP3*	0.44	*LOC112448373*	0.23
GPR153	0.75	*SCIN*	0.60	*RCL1*	0.44	*RGMB*	0.23
ABI3BP	0.75	*PTN*	0.60	*AMPH*	0.43	*SUPT3H*	0.23
C1QTNF6	0.75	*CCDC50*	0.60	*ITGA10*	0.43	*TMCO4*	0.23
CNN3	0.75	*ANXA4*	0.60	*LMNB1*	0.43	*ENOPH1*	0.23
CDH11	0.75	*LPCAT1*	0.60	*CDC7*	0.43	*RCN2*	0.23
THBS3	0.75	*IL16*	0.60	*SIX5*	0.43	*LOC104975663*	0.23
PDIA4	0.75	*MFAP4*	0.60	*SFXN1*	0.43	*RACGAP1*	0.23
LASP1	0.75	*TNS3*	0.60	*PLD3*	0.43	*SIX2*	0.23
TGFBR3	0.75	*WDSUB1*	0.60	*KIAA1191*	0.43	*RPGRIP1*	0.23
CSF1R	0.75	*CD55*	0.59	*MAPK7*	0.43	*SNX18*	0.23
CLIP2	0.75	*PRDM8*	0.59	*AKR1A1*	0.43	*TMEM17*	0.22
CD109	0.75	*TMEM35A*	0.59	*KBTBD11*	0.43	*KLF5*	0.22
LGALS3	0.74	*CC2D2A*	0.59	*LOC534578*	0.43	*HAUS2*	0.22
SPON2	0.74	*SMO*	0.59	*P2RX4*	0.43	*UCHL1*	0.22
FRMD4B	0.74	*ARRB1*	0.59	*HMGB2*	0.43	*ABHD14A*	0.22
DPT	0.74	*TNFRSF1B*	0.59	*CARMIL1*	0.43	*PRSS23*	0.22
ITM2C	0.74	*TTC7A*	0.59	*UBTD2*	0.43	*CBR3*	0.22
SCARA5	0.74	*CLTRN*	0.59	*IL34*	0.43	*CLDN1*	0.22
MRC1	0.74	*SCARF2*	0.59	*TCEAL8*	0.43	*BBS9*	0.22
ITGB3	0.74	*GPR108*	0.59	*CXCL12*	0.43	*MAP1A*	0.22
LUM	0.74	*TWSG1*	0.59	*GINS1*	0.42	*FBXW8*	0.22
CMTM3	0.74	*PABPC1*	0.59	*AIG1*	0.42	*CAPN5*	0.22
LRRN4CL	0.74	*DOK1*	0.59	*SLC29A3*	0.42	*GALK1*	0.22
PPT1	0.74	*SHOX2*	0.59	*NRK*	0.42	*IFT27*	0.22
CHPF	0.74	*LEPROT*	0.59	*CTTN*	0.42	*ANGPT4*	0.22
SCARA3	0.74	*BEX3*	0.59	*DLK1*	0.42	*BOLA.DQB*	0.22
ITGA11	0.74	*SH3GL1*	0.59	*NIPSNAP3A*	0.42	*ZNHIT6*	0.21
SLC22A17	0.74	*P3H1*	0.59	*CBX4*	0.42	*CPLANE2*	0.21
SERPING1	0.74	*ARMCX2*	0.59	*ARMCX6*	0.42	*H19*	0.21
PKD2	0.74	*AQP1*	0.59	*ORMDL2*	0.42	*MAGOHB*	0.21
EVC	0.74	*TMEM173*	0.58	*WDR17*	0.42	*RADIL*	0.21
CD276	0.74	*MAGED2*	0.58	*CTSF*	0.42	*LOC100140586*	0.21
SCPEP1	0.74	*PXDC1*	0.58	*NIPAL3*	0.42	*METTL14*	0.21
GAS7	0.74	*ANPEP*	0.58	*PIP4K2A*	0.42	*ZNF423*	0.21
PLXDC2	0.74	*HHIPL1*	0.58	*CGREF1*	0.42	*ARSK*	0.20

ALDH3B1	0.74	*RAB32*	0.58	*METRNL*	0.42	*CEP170B*	0.20
COL8A1	0.73	*TIAM1*	0.58	*CYP51A1*	0.42	*AASDHPPT*	0.20
CALU	0.73	*PODN*	0.58	*ST5*	0.42	*TXNDC12*	0.20
WIPF1	0.73	*SPP2*	0.58	*PCDH7*	0.42	*CENPO*	0.20
CKAP4	0.73	*TPPP*	0.58	*EYA2*	0.41	*ERBB3*	0.20
IL1R1	0.73	*TM9SF2*	0.58	*CPEB1*	0.41	*TMEM184C*	0.20
PLAC9	0.73	*DDAH1*	0.58	*CCDC167*	0.41	*PM20D1*	0.20
TGFBR2	0.73	*FRMD6*	0.58	*GPM6A*	0.41	*YAP1*	0.20
ARPC1B	0.73	*AGTR1*	0.58	*FUT10*	0.41	*GDPD5*	0.20
OGFRL1	0.73	*GAREM1*	0.58	*HGSNAT*	0.41	*CEP78*	0.20
LOC112446388	0.73	*JDP2*	0.58	*NES*	0.41	*SMPD1*	0.19
C1QTNF1	0.73	*PPM1H*	0.58	*CNDP2*	0.41	*GOLGA5*	0.19
LOX	0.73	*PHGDH*	0.58	*ZNF521*	0.41	*MCM3*	0.19
DZIP1	0.73	*POLE4*	0.58	*TGFB2*	0.41	*ATP6V1H*	0.19
PHETA2	0.73	*MID1*	0.58	*SOX8*	0.41	*CEP57*	0.19
MSR1	0.73	*IDUA*	0.58	*P4HA2*	0.41	*TTC27*	0.19
CADM3	0.73	*AGMO*	0.57	*ARSB*	0.41	*HSDL1*	0.19
SEPT6	0.73	*SEPT5*	0.57	*FGD1*	0.41	*SHISA3*	0.19
MAN2A1	0.73	*HVCN1*	0.57	*GREM1*	0.41	*TASP1*	0.19
HACD4	0.73	*PLA2G4A*	0.57	*WEE1*	0.41	*PIGX*	0.19
VSIG4	0.73	*RPN2*	0.57	*LOC112442619*	0.41	*C23H6orf62*	0.19
TAGLN2	0.73	*GLMP*	0.57	*RUBCNL*	0.41	*GMNN*	0.18
CD209	0.72	*NID1*	0.57	*SMARCA1*	0.41	*MYF5*	0.18
LOC510860	0.72	*GPR1*	0.57	*PMP22*	0.41	*IRF2*	0.18
TLR4	0.72	*TPST1*	0.57	*TCF7L2*	0.41	*APOL3*	0.18
OGN	0.72	*ARHGAP1*	0.57	*ARMC10*	0.41	*ZNF852*	0.18
CTSZ	0.72	*GALNT2*	0.57	*CFB*	0.40	*SHMT1*	0.18
RAB34	0.72	*LOXL4*	0.57	*PIGS*	0.40	*LOC107131874*	0.18
ITGBL1	0.72	*LARP6*	0.57	*LRRC1*	0.40	*CBS*	0.18
DDR2	0.72	*HTRA3*	0.57	*DDR1*	0.40	*RHBDD2*	0.17
POSTN	0.72	*AFF3*	0.57	*RALGDS*	0.40	*CAAP1*	0.17
FCER1G	0.72	*OSBPL5*	0.57	*FADS1*	0.40	*XRCC6*	0.17
POFUT1	0.72	*BCL7C*	0.56	*SERTAD2*	0.40	*CTNS*	0.17
KANK2	0.72	*AHNAK2*	0.56	*SND1*	0.40	*NCAPG*	0.17
FXYD5	0.72	*CTTNBP2*	0.56	*PLA2R1*	0.40	*SGK3*	0.17
ICAM1	0.72	*AACS*	0.56	*SPTLC1*	0.40	*HACD3*	0.17
CFL1	0.72	*FUCA1*	0.56	*A4GALT*	0.40	*MCM4*	0.17
MGP	0.72	*VCAM1*	0.56	*SEMA3C*	0.40	*GNPNAT1*	0.17
LTBP4	0.72	*TMEM59*	0.56	*CNRIP1*	0.40	*MON1B*	0.16
JAZF1	0.71	*MICAL1*	0.56	*CCL16*	0.40	*ACCS*	0.16
ASPN	0.71	*TRERF1*	0.56	*ARFIP1*	0.40	*ARL10*	0.16
CALHM2	0.71	*NDE1*	0.56	*CILP*	0.40	*CTNNAL1*	0.16
NDRG1	0.71	*LOC101905041*	0.56	*LOC100336368*	0.40	*RXFP2*	0.16

LAMB1	0.71	*PROCR*	0.56	*PJA1*	0.40	*CREG1*	0.16
FNDC1	0.71	*VIT*	0.56	*NFATC2*	0.39	*ORC5*	0.16
EFEMP1	0.71	*DACT1*	0.56	*STARD3NL*	0.39	*AZIN1*	0.16
LOXL1	0.71	*GLI2*	0.56	*LOC100847951*	0.39	*ZNF438*	0.16
ADAMTSL3	0.71	*SERPINE1*	0.56	*PAQR6*	0.39	*TMEM98*	0.16
PBX3	0.71	*DPYSL3*	0.56	*HSD17B4*	0.39	*OGG1*	0.15
SMIM14	0.71	*GPC3*	0.56	*STK38*	0.39	*ZMPSTE24*	0.15
SLC39A7	0.71	*NTN1*	0.55	*CEP112*	0.39	*RPGR*	0.15
LIMA1	0.71	*AP1S1*	0.55	*PLXNC1*	0.39	*TUBG2*	0.15
ACLY	0.71	*BACE2*	0.55	*ENDOD1*	0.39	*MXI1*	0.15
RBMS3	0.71	*EDA*	0.55	*WRB*	0.39	*MAD2L1*	0.15
SSC5D	0.71	*RNASET2*	0.55	*CASP9*	0.39	*SOX11*	0.15
CD86	0.71	*ZNF512*	0.55	*RTKN*	0.39	*TSPYL2*	0.15
PTGFRN	0.71	*SVBP*	0.55	*MARCH8*	0.39	*LOC508916*	0.15
CAMK1D	0.71	*EEF1A1*	0.55	*SLC25A16*	0.39	*CYB5RL*	0.14
AOC1	0.70	*FMNL1*	0.55	*C10H14orf119*	0.39	*SETD4*	0.14
ACKR3	0.70	*FOLH1B*	0.55	*UNC119*	0.39	*DTX4*	0.14
CD99	0.70	*STT3A*	0.55	*GIPC1*	0.39	*BCO2*	0.14
MAMDC2	0.70	*CXCR4*	0.55	*MUSK*	0.38	*RPS6KA1*	0.14
B4GALT4	0.70	*NAGLU*	0.55	*ISM1*	0.38	*DSN1*	0.14
LDLRAD3	0.70	*F3*	0.55	*LOC107132475*	0.38	*TMEM167B*	0.14
FKBP7	0.70	*ACAT2*	0.55	*HFE*	0.38	*PLP1*	0.14
ATP10A	0.70	*SLC44A1*	0.55	*SLC38A6*	0.38	*RNFT2*	0.14
SRPX	0.70	*GM2A*	0.55	*ABCG2*	0.38	*C8H9orf64*	0.14
RAB3IL1	0.70	*BASP1*	0.55	*FAM122B*	0.38	*MYH3*	0.14
UGDH	0.70	*IL17RD*	0.55	*SLC41A2*	0.38	*WWOX*	0.14
EFHD2	0.70	*SYT9*	0.55	*TSPYL5*	0.38	*CYP4B1*	0.14
C2	0.70	*GDA*	0.55	*LOC100847759*	0.38	*ZBTB9*	0.14
TMEM43	0.70	*GRN*	0.55	*INSIG1*	0.38	*SLC35E3*	0.14
SFRP4	0.70	*LOC530102*	0.55	*IQSEC2*	0.37	*TMEM209*	0.14
ITIH5	0.70	*PLVAP*	0.54	*DACT2*	0.37	*APLF*	0.13
GLI3	0.70	*SRGAP3*	0.54	*NR2F1*	0.37	*CHPF2*	0.13
ANGPTL2	0.70	*C1H3orf58*	0.54	*ASNS*	0.37	*NPAS2*	0.13
RECK	0.70	*ARHGEF26*	0.54	*SLC36A4*	0.37	*TCEAL4*	0.13
GPR34	0.70	*ADCY3*	0.54	*LOC515828*	0.37	*LOC100299025*	0.13
AKAP12	0.69	*ALOX5*	0.54	*PARD6G*	0.37	*COPB2*	0.13
FAM171A1	0.69	*HOPX*	0.54	*SELENOP*	0.37	*TMEM231*	0.13
ITM2B	0.69	*TLR2*	0.54	*LOC104969299*	0.37	*NANP*	0.12
PDGFRL	0.69	*ENC1*	0.54	*ACOT9*	0.37	*LRRC57*	0.12
COL12A1	0.69	*LOXL3*	0.54	*RGS1*	0.37	*CEPT1*	0.12
PDGFC	0.69	*ADAMTS17*	0.54	*TMX1*	0.37	*XYLT2*	0.12
RCN1	0.69	*SPP1*	0.54	*PDLIM4*	0.37	*LOC100848815*	0.10
PTMA	0.69	*CD5L*	0.54	*HNMT*	0.37	*GRID1*	0.10

SRGAP1	0.69	*CST3*	0.54	*ARFIP2*	0.36	*LOC510362*	0.10
TNFAIP8	0.69	*C1QTNF3*	0.53	*CHN2*	0.36	*C11H2orf42*	0.10
PDE1A	0.69	*HPGD*	0.53	*DHDDS*	0.36	*ARHGAP18*	0.10
BOC	0.69	*TRPV2*	0.53	*VMP1*	0.36	*MED16*	0.10
TNFAIP6	0.69	*CDO1*	0.53	*SMOC2*	0.36	*IFT140*	0.10
UST	0.69	*CYB5R3*	0.53	*FIBIN*	0.36	*POMK*	0.09
OLFML2B	0.69	*FAM171B*	0.53	*ZDHHC24*	0.36	*LOC614091*	0.09
CLIC1	0.69	*GFPT2*	0.53	*STX11*	0.36	*NCR3LG1*	0.09
PID1	0.69	*GANAB*	0.53	*CYP20A1*	0.36	*CYB5R4*	0.08
LUZP6	0.69	*ARMCX1*	0.53	*SDK2*	0.36	*UHRF1*	0.08
ELN	0.69	*PLAU*	0.53	*RBP1*	0.36	*DENND2A*	0.08
MBOAT1	0.69	*IRF5*	0.53	*FRRS1L*	0.36	*MPZ*	0.08
COL5A3	0.69	*FUT8*	0.53	*RHOU*	0.36	*ARHGAP24*	0.08
C1R	0.69	*CITED2*	0.53	*KIAA1755*	0.36	*LOC104970105*	0.07
NCALD	0.69	*POFUT2*	0.53	*CYBC1*	0.36	*VRK1*	0.07
GPNMB	0.68	*DGKA*	0.53	*SRD5A3*	0.36	*PKMYT1*	0.07
ARFGAP3	0.68	*NUMBL*	0.53	*RALGPS2*	0.36	*DTNB*	0.07
TNXB	0.68	*CTSO*	0.53	*IP6K2*	0.35	*CSTF1*	0.06
COLEC12	0.68	*PREX1*	0.53	*PTGDS*	0.35	*PRX*	0.05
LOC508666	0.68	*LOC533597*	0.53	*BET1L*	0.35	*PAQR4*	0.05
PSTPIP1	0.68	*DNASE2*	0.53	*SLC2A1*	0.35	*GDPGP1*	0.04
PLEKHA5	0.68	*CHST14*	0.53	*IL33*	0.35	*PLEKHB1*	0.04
ARHGEF10	0.68	*SLC6A6*	0.52	*EFCC1*	0.35	*ETV4*	0.03
TMEM45A	0.68	*SELENOM*	0.52	*MYMX*	0.35	*SFRP1*	0.01
PLCD1	0.68	*ERMP1*	0.52	*NCKAP5L*	0.35	*MAP2K1*	-0.02
PRKCD	0.68	*ST6GAL1*	0.52	*ASAH1*	0.35	*DRP2*	-0.02

#M9

GS	MM	GS	MM	GS	MM	GS	MM
CSRNP1	0.90	*ZC3H12A*	0.70	*JUN*	0.64	*FAM166B*	0.52
ATF3	0.85	*ERF*	0.69	*SNAI2*	0.62	*APOLD1*	0.52
MCL1	0.83	*ARID5A*	0.69	*RND3*	0.62	*KLF2*	0.50
JUND	0.80	*MIDN*	0.69	*PPP1R10*	0.60	*PPP1R15A*	0.50
BTG2	0.78	*IQCN*	0.68	*EGR1*	0.60	*EGR3*	0.49
IER5	0.77	*MYC*	0.68	*ATG101*	0.60	*RGCC*	0.48
KLF4	0.77	*NR4A1*	0.68	*GRASP*	0.60	*SDE2*	0.47
PLK3	0.77	*ZBTB21*	0.68	*RYBP*	0.60	*CYR61*	0.45
NR4A2	0.76	*TIPARP*	0.67	*ZFP36*	0.59	*NFE2L2*	0.43
NR4A3	0.75	*TGFB3*	0.67	*JOSD1*	0.59	*ID1*	0.42
FOS	0.75	*FOSB*	0.67	*DDIT3*	0.59	*IER2*	0.42
SIK1	0.74	*SLC20A1*	0.66	*JUNB*	0.58	*ZBTB48*	0.40
KLF6	0.74	*SPRY2*	0.65	*CSRNP2*	0.58	*TCIM*	0.37
COQ10B	0.73	*ADAMTS4*	0.65	*MAPK1IP1L*	0.57	*DUSP1*	0.35

OTUD1	0.72	*TRA2B*	0.65	*SGK1*	0.56	*SOX17*	0.26
ADAMTS1	0.71	*PTGS2*	0.64	*CREB5*	0.56	*EGFL7*	0.25
IFRD1	0.70	*FOSL2*	0.64	*CTGF*	0.55	*ID3*	0.23
RASGEF1B	0.70						

#M17

GS	MM	GS	MM	GS	MM	GS	MM
ASH1L	0.94	*MED23*	0.70	*NCK1*	0.58	*SNRNP200*	0.48
BIRC6	0.93	*VIRMA*	0.70	*DLG1*	0.58	*FRMD4A*	0.48
CEP350	0.93	*RAD54L2*	0.70	*ATP6V0A2*	0.58	*CASZ1*	0.48
VPS13D	0.91	*ZKSCAN1*	0.70	*SOCS4*	0.58	*TET2*	0.48
MED13	0.91	*KAT6B*	0.70	*GIT2*	0.58	*KMT2B*	0.48
DMXL1	0.91	*AP1G1*	0.69	*NEMF*	0.58	*TNKS2*	0.48
BPTF	0.91	*LRRK2*	0.69	*STX17*	0.58	*TECPR2*	0.48
ANKHD1	0.90	*ZBTB41*	0.69	*ARL5B*	0.58	*RYR3*	0.48
HERC1	0.90	*LNPEP*	0.69	*RAB22A*	0.58	*STAG1*	0.48
ATRX	0.90	*YLPM1*	0.69	*MAP3K7*	0.58	*SEC16A*	0.48
TNRC6B	0.90	*CEP97*	0.69	*ZBTB38*	0.58	*POGLUT1*	0.48
PRRC2C	0.89	*WNK1*	0.69	*KDM3A*	0.58	*NUP160*	0.47
MED13L	0.89	*RORA*	0.69	*CPEB4*	0.58	*USP42*	0.47
KMT2A	0.88	*RNF214*	0.69	*TRIP12*	0.58	*OGA*	0.47
HUWE1	0.88	*ZC3H13*	0.69	*FAM120C*	0.58	*SMARCC1*	0.47
KMT2C	0.88	*ARNT*	0.69	*DCAF10*	0.58	*MAP1S*	0.47
NIPBL	0.88	*PEAK1*	0.69	*MTMR10*	0.58	*TMED5*	0.47
MYCBP2	0.88	*CLPB*	0.69	*NR3C1*	0.58	*SUZ12*	0.47
PHC3	0.88	*ZNF451*	0.69	*ATF7*	0.58	*PLEC*	0.47
ATM	0.88	*TAOK1*	0.69	*GTF2A1*	0.58	*SPRTN*	0.47
KIAA1109	0.87	*GBF1*	0.69	*FNIP1*	0.58	*FAM120A*	0.47
KDM7A	0.87	*KIAA1958*	0.69	*FAM135A*	0.57	*MAGI3*	0.47
KDM5A	0.87	*PGM2*	0.69	*KLHL31*	0.57	*KIN*	0.47
HERC2	0.86	*SUFU*	0.69	*HS2ST1*	0.57	*NACA*	0.47
KMT2D	0.86	*ABCC9*	0.69	*C1GALT1*	0.57	*TANC2*	0.47
HELZ	0.86	*WDR26*	0.69	*KIF13A*	0.57	*GCN1*	0.47
CHD9	0.86	*GSK3B*	0.68	*DCP1A*	0.57	*ERN1*	0.47
MED1	0.85	*FBXO28*	0.68	*LOC101906226*	0.57	*COG5*	0.47
AAK1	0.85	*IMPAD1*	0.68	*ERCC4*	0.57	*PDZD8*	0.47
NF1	0.85	*PRRC2B*	0.68	*DDX46*	0.57	*NAPEPLD*	0.47
HOOK3	0.85	*PRR14L*	0.68	*AMOTL1*	0.57	*ADAMTS20*	0.47
LCOR	0.85	*ANKRD12*	0.68	*NBR1*	0.57	*UVRAG*	0.47
HMBOX1	0.85	*SNX13*	0.68	*DHX36*	0.57	*LOC100848077*	0.47
FAM199X	0.85	*SP1*	0.68	*TP53BP1*	0.57	*SNX33*	0.46
HCFC2	0.85	*PHF3*	0.68	*NR3C2*	0.57	*ZNF793*	0.46
SCAF11	0.84	*PRKDC*	0.68	*FUBP1*	0.57	*BCORL1*	0.46

AFF4	0.84	*SACS*	0.68	*DENND4A*	0.57	*LOC512869*	0.46
USP34	0.84	*EARS2*	0.68	*UBAP2L*	0.57	*NUP58*	0.46
VPS13B	0.84	*TNPO1*	0.68	*ZEB1*	0.57	*RFX5*	0.46
UBR1	0.84	*USP24*	0.68	*KLF9*	0.56	*TMEM168*	0.46
GNAQ	0.84	*CHD6*	0.68	*BCLAF1*	0.56	*ZC3H7B*	0.46
PHIP	0.84	*FCHO2*	0.68	*PHF6*	0.56	*KIAA1328*	0.46
ZFHX4	0.84	*STXBP4*	0.68	*TOGARAM1*	0.56	*SMCR8*	0.46
ASXL2	0.84	*FILIP1*	0.68	*MTRR*	0.56	*BROX*	0.46
FAM208A	0.83	*ABL2*	0.68	*TRIM33*	0.56	*GNAT2*	0.46
MDN1	0.83	*RPRD2*	0.68	*FOXK1*	0.56	*RCOR1*	0.46
SMC1A	0.83	*LOC112443216*	0.68	*GOLGA4*	0.56	*NRIP1*	0.46
RALGAPA1	0.83	*RICTOR*	0.68	*SKIL*	0.56	*GPR161*	0.46
NFAT5	0.83	*KIF3A*	0.68	*EXOC5*	0.56	*GHR*	0.46
KIAA2026	0.83	*CCDC186*	0.68	*CEP120*	0.56	*ERCC6L*	0.46
AFF1	0.83	*TTC28*	0.67	*WDR47*	0.56	*ZNF317*	0.46
TPR	0.83	*NUP153*	0.67	*IARS*	0.56	*ZNF354C*	0.46
SHPRH	0.83	*ZNF638*	0.67	*ZEB2*	0.56	*WASL*	0.46
NSD1	0.82	*TSC1*	0.67	*HCFC1*	0.56	*SELENOI*	0.46
TTBK2	0.82	*RRP8*	0.67	*ETV3*	0.56	*DNAL1*	0.46
INO80D	0.82	*PCNX1*	0.67	*TCF20*	0.56	*C1H3orf38*	0.46
BRWD3	0.82	*XRN1*	0.67	*NAA16*	0.56	*PDCD6IP*	0.46
BDP1	0.82	*RNF111*	0.67	*SSH2*	0.56	*POLR3B*	0.45
UBR5	0.82	*RABGAP1*	0.67	*PCM1*	0.56	*LOC100848895*	0.45
RANBP2	0.82	*SEC24A*	0.67	*APAF1*	0.56	*GOSR1*	0.45
AHCTF1	0.82	*SETBP1*	0.67	*MAP3K2*	0.56	*CACUL1*	0.45
RC3H2	0.82	*UTP20*	0.67	*PARG*	0.56	*BAZ1A*	0.45
UHMK1	0.82	*TXLNG*	0.67	*RDX*	0.56	*RABGEF1*	0.45
SBNO1	0.81	*FAM8A1*	0.67	*HIVEP2*	0.56	*SHOC2*	0.45
SETX	0.81	*THUMPD1*	0.67	*GATAD2B*	0.55	*RPTOR*	0.45
BNIP2	0.81	*CLASP1*	0.67	*PAPOLG*	0.55	*CGGBP1*	0.45
ARHGAP5	0.81	*YEATS2*	0.67	*ANKRD52*	0.55	*YIPF6*	0.45
SON	0.81	*CLOCK*	0.67	*HOXA6*	0.55	*NDST1*	0.45
KAT6A	0.81	*MTR*	0.67	*MTO1*	0.55	*LOC107131289*	0.44
TTN	0.81	*LRP6*	0.67	*ANKIB1*	0.55	*TRIM2*	0.44
USF3	0.81	*DYNC1H1*	0.67	*YTHDC2*	0.55	*ZNF154*	0.44
SPEN	0.81	*TMTC3*	0.66	*RREB1*	0.55	*AMOT*	0.44
EP300	0.81	*C24H18orf25*	0.66	*MAP4*	0.55	*JADE1*	0.44
ZCCHC6	0.81	*ZZZ3*	0.66	*SETD1B*	0.55	*STXBP5*	0.44
SLF2	0.81	*ARMC8*	0.66	*UFL1*	0.55	*ZNF565*	0.44
BTAF1	0.81	*THOC2*	0.66	*TMEM19*	0.55	*TACO1*	0.44
FAM208B	0.80	*DHX33*	0.66	*LOC104975635*	0.55	*USP49*	0.44
UBN2	0.80	*ARCN1*	0.66	*XPR1*	0.55	*UBE2W*	0.44
PRDM2	0.80	*SPOPL*	0.66	*PTPN14*	0.55	*LOC112443503*	0.44

ITCH	0.80	*NHLRC2*	0.66	*SLC39A10*	0.55	*TRIM24*	0.44
SETD5	0.80	*DGKH*	0.66	*LMO7*	0.55	*ZBTB40*	0.44
QSER1	0.80	*LOC101903400*	0.66	*MIA3*	0.55	*ST8SIA5*	0.44
AQR	0.80	*APPL1*	0.66	*SPTY2D1*	0.55	*IPMK*	0.44
RSF1	0.80	*C2CD3*	0.66	*KIF2A*	0.55	*SAMD4A*	0.44
DST	0.80	*PJA2*	0.66	*HEATR5B*	0.55	*PANX1*	0.43
GPR107	0.80	*BICRAL*	0.66	*SPIRE1*	0.55	*LOC112443783*	0.43
NEB	0.79	*MARF1*	0.66	*NAB1*	0.55	*ABHD13*	0.43
ELK4	0.79	*PIK3C2A*	0.66	*INPP4B*	0.55	*CDC5L*	0.43
NCOA3	0.79	*POGZ*	0.66	*PYGO1*	0.55	*FOCAD*	0.43
UGGT1	0.79	*OTUD7B*	0.66	*MAP3K20*	0.55	*NUPL2*	0.43
ANKRD17	0.79	*BTBD7*	0.66	*ITGAV*	0.55	*DSTYK*	0.43
EP400	0.79	*CDK13*	0.66	*KIAA1551*	0.55	*SRFBP1*	0.43
ATXN7	0.79	*CPSF7*	0.66	*APPBP2*	0.55	*SCAF4*	0.43
HIPK1	0.79	*JMJD1C*	0.66	*LOC112442296*	0.54	*PLEKHA8*	0.43
KIAA0754	0.79	*LOC101907653*	0.65	*PRKD3*	0.54	*CENPI*	0.43
NSD3	0.78	*CEP85L*	0.65	*FBXO38*	0.54	*DIS3*	0.43
PANK3	0.78	*DPH5*	0.65	*EAF1*	0.54	*ZHX3*	0.43
ALMS1	0.78	*VPS13C*	0.65	*TMEM106B*	0.54	*TRNAE.UUC*	0.43
BOD1L1	0.78	*UTRN*	0.65	*PCYOX1*	0.54	*SP3*	0.43
LATS1	0.78	*ANKRD11*	0.65	*XIAP*	0.54	*GPALPP1*	0.43
AKAP9	0.78	*KDM3B*	0.65	*DPY19L4*	0.54	*ZNF592*	0.43
TRIP11	0.78	*ZHX1*	0.65	*LOC112449346*	0.54	*SEC23A*	0.43
CHD1	0.78	*TEAD1*	0.65	*LRBA*	0.54	*NUDT21*	0.43
BRAF	0.78	*TRAPPC10*	0.65	*ZBTB6*	0.54	*WDR44*	0.43
DNAJC13	0.78	*FEM1B*	0.65	*LOC100847604*	0.54	*Aug-04*	0.43
ZFX	0.78	*MKL2*	0.65	*SAMD8*	0.54	*ZNF432*	0.42
DICER1	0.78	*ITPR1*	0.65	*PDE3A*	0.54	*KDM6B*	0.42
LTN1	0.78	*LOC100848941*	0.65	*LOC104968522*	0.54	*STON2*	0.42
SENP5	0.78	*AHNAK*	0.65	*MPHOSPH9*	0.54	*CSGALNACT2*	0.42
GAN	0.77	*FRY*	0.65	*RIC8B*	0.54	*CEP128*	0.42
LMBRD2	0.77	*KIAA1217*	0.65	*LOC100848246*	0.54	*INTS9*	0.42
FAM160B1	0.77	*MON2*	0.64	*HIPK2*	0.54	*HMCN2*	0.42
USP9X	0.77	*MAP4K3*	0.64	*CHML*	0.54	*ZNF407*	0.42
CHD8	0.77	*TAB3*	0.64	*PPTC7*	0.54	*RAB3GAP1*	0.42
SMAD5	0.77	*CCDC13*	0.64	*NFRKB*	0.53	*NUP205*	0.42
EEA1	0.77	*MYO9A*	0.64	*PLEKHA1*	0.53	*SLC35E2*	0.42
SECISBP2L	0.77	*DOPEY1*	0.64	*SP4*	0.53	*SAP130*	0.42
ARHGEF12	0.77	*FANCM*	0.64	*MAP4K5*	0.53	*ZBTB16*	0.41
ATG2B	0.77	*AR*	0.64	*EPC1*	0.53	*ZMYND8*	0.41
ATP7A	0.77	*DHX9*	0.64	*TBC1D23*	0.53	*GABPA*	0.41
PBRM1	0.77	*CEP192*	0.64	*THADA*	0.53	*RPS6KA3*	0.41
NBEAL1	0.77	*ZNF507*	0.64	*PHLPP2*	0.53	*BCL2*	0.41

TAF1	0.77	*G3BP1*	0.64	*RBM12*	0.53	*RFX3*	0.41
MIB1	0.76	*GCC2*	0.64	*CACNA2D1*	0.53	*KATNBL1*	0.41
ARFGEF2	0.76	*EMSY*	0.64	*IGF1R*	0.53	*LOC789960*	0.41
TNKS	0.76	*CREBRF*	0.64	*PCGF5*	0.53	*INSR*	0.41
VPS13A	0.76	*MDM4*	0.64	*RSBN1*	0.53	*SAAL1*	0.40
LOC101904377	0.76	*TMF1*	0.64	*NUP98*	0.53	*PTK2*	0.40
HECTD4	0.76	*TULP4*	0.64	*ATP6V0A1*	0.53	*ZSCAN20*	0.40
UBR4	0.76	*ATXN1L*	0.64	*MPP5*	0.53	*ZC3H4*	0.40
ZNF644	0.76	*DYNC1LI2*	0.64	*KDM2A*	0.53	*XPOT*	0.40
ZNF292	0.76	*KLF12*	0.64	*CCDC93*	0.53	*JAK2*	0.40
NAA25	0.76	*CCSER2*	0.64	*PLEKHM3*	0.53	*SLC35B4*	0.40
CNOT1	0.76	*TROVE2*	0.64	*RASAL2*	0.53	*PTPRM*	0.39
SMCHD1	0.76	*IRAK3*	0.64	*ZFR*	0.53	*LOC107131779*	0.39
RBM26	0.76	*FAR1*	0.64	*ZNF304*	0.53	*NFIA*	0.39
GTF3C4	0.76	*ZC3H11A*	0.63	*HERC4*	0.53	*CLCN5*	0.39
MAN1A2	0.76	*BMPR2*	0.63	*MMS22L*	0.53	*LOC101905648*	0.39
RAB11FIP2	0.76	*TMEM30A*	0.63	*ACP2*	0.53	*ZNF281*	0.39
EPG5	0.76	*KDM6A*	0.63	*ASB1*	0.53	*RNF38*	0.39
MTF1	0.76	*GIGYF2*	0.63	*LARP4B*	0.53	*GTPBP8*	0.39
POU2F1	0.75	*REV3L*	0.63	*PIAS1*	0.52	*SMARCA2*	0.39
LOC787554	0.75	*TOP2B*	0.63	*FAM214A*	0.52	*TTLL4*	0.38
PUM1	0.75	*CBX5*	0.63	*RTTN*	0.52	*AFG1L*	0.38
BRWD1	0.75	*DDX6*	0.63	*STAM*	0.52	*POLH*	0.38
APC	0.75	*TNRC6C*	0.63	*ZNF207*	0.52	*NKAP*	0.38
MGA	0.75	*PURA*	0.63	*KIAA1549*	0.52	*SLC11A2*	0.38
BBX	0.75	*EDEM3*	0.63	*ANKFY1*	0.52	*WDR82*	0.38
MTREX	0.75	*IPO8*	0.63	*MBD5*	0.52	*PRKCE*	0.38
HEATR5A	0.75	*LOC101905588*	0.63	*OFD1*	0.52	*EYA3*	0.37
LMAN1	0.75	*WASHC4*	0.63	*TLK1*	0.52	*SMAD2*	0.37
KMT2E	0.75	*USP31*	0.63	*DCLRE1C*	0.52	*MGAT4A*	0.37
USP37	0.75	*KANSL1L*	0.63	*CHM*	0.52	*PRRC2A*	0.37
BAZ2A	0.75	*PREPL*	0.62	*NBEA*	0.52	*RANBP6*	0.37
ATXN1	0.75	*NCOA1*	0.62	*GOLGA1*	0.52	*GTF2E1*	0.37
SIKE1	0.75	*RLF*	0.62	*PCYT1A*	0.52	*SPATA5*	0.37
ATF7IP	0.75	*SFT2D2*	0.62	*ZNF318*	0.52	*MTF2*	0.36
PREX2	0.75	*CHD4*	0.62	*CEP76*	0.52	*ZNF335*	0.36
ARID2	0.75	*TTLL7*	0.62	*TMEM131*	0.52	*PHF12*	0.36
PKN2	0.74	*PPP6R3*	0.62	*UHRF1BP1*	0.52	*NR1D2*	0.36
DNTTIP2	0.74	*LARP4*	0.62	*ICE1*	0.52	*ZNF570*	0.36
RAB3GAP2	0.74	*AP4E1*	0.62	*AGPS*	0.52	*ATP2C1*	0.36
RBM15	0.74	*LOC101904642*	0.62	*EIF4G3*	0.52	*RNGTT*	0.36
LYST	0.74	*IL6ST*	0.62	*RALGAPA2*	0.51	*RNF169*	0.36
ZNF609	0.74	*NPAT*	0.62	*RBM27*	0.51	*EPC2*	0.36

CDC42BPA	0.74	*TRRAP*	0.62	*JMY*	0.51	*SCRN3*	0.36
NCOA2	0.74	*LIN54*	0.61	*GON4L*	0.51	*LCLAT1*	0.36
ZFHX3	0.74	*ZNF280D*	0.61	*NUP214*	0.51	*WASHC5*	0.35
CAND1	0.74	*SRPK1*	0.61	*POLR2A*	0.51	*USP12*	0.35
PTAR1	0.74	*ZNF75A*	0.61	*WIPF2*	0.51	*NARS*	0.35
OTUD4	0.74	*MIER3*	0.61	*POLR1A*	0.51	*LOC112445988*	0.35
FRYL	0.74	*RIC1*	0.61	*LOC112448582*	0.51	*NBAS*	0.35
ARID1A	0.74	*ZNF445*	0.61	*QKI*	0.51	*ZNF184*	0.35
SPAG9	0.74	*ASCC3*	0.61	*AVL9*	0.51	*WDR20*	0.35
ZMYM2	0.74	*ZBTB11*	0.61	*KANSL1*	0.51	*AEBP2*	0.34
RNMT	0.74	*PTPN11*	0.61	*PPARGC1B*	0.51	*CWC22*	0.34
CBL	0.74	*LOC523461*	0.61	*TTC3*	0.51	*PLAGL2*	0.34
CDK12	0.73	*SCAF8*	0.61	*DTWD2*	0.51	*KCTD20*	0.33
CLTC	0.73	*UBE4A*	0.61	*FBXO11*	0.51	*HIVEP3*	0.33
C7H5orf24	0.73	*ZCCHC14*	0.61	*PPFIBP1*	0.51	*MEF2C*	0.33
ZFYVE16	0.73	*LOC112444585*	0.61	*PPP4R3B*	0.51	*BMS1*	0.33
PHF20L1	0.73	*EAPP*	0.61	*DENND5B*	0.51	*OSBPL11*	0.33
ZZEF1	0.73	*ARHGAP21*	0.61	*DCAF7*	0.51	*EXOC6B*	0.33
AUG3	0.73	*CELF2*	0.61	*AREL1*	0.51	*ZFHX2*	0.33
NCOR1	0.73	*ERBIN*	0.61	*PHF20*	0.51	*KIAA1468*	0.33
GOLGA3	0.73	*ZMYM4*	0.61	*COPA*	0.50	*LOC786095*	0.33
DENND4C	0.73	*ZNF606*	0.61	*LOC107132636*	0.50	*SENP6*	0.32
RPS6KB1	0.73	*IWS1*	0.60	*ZNF248*	0.50	*KLHL20*	0.32
SETD2	0.73	*PAFAH1B2*	0.60	*ANK2*	0.50	*VPS53*	0.32
RC3H1	0.73	*KCNN3*	0.60	*IBTK*	0.50	*LOC518768*	0.32
ZNF24	0.73	*ATF6*	0.60	*MYNN*	0.50	*ELMSAN1*	0.31
KIAA0100	0.73	*PDE4DIP*	0.60	*SIX4*	0.50	*UBE2H*	0.31
TAF2	0.73	*EXOC8*	0.60	*MAML1*	0.50	*SELENOT*	0.31
BAZ1B	0.73	*RB1*	0.60	*SUPT6H*	0.50	*TPP1*	0.31
SNTB2	0.72	*AGGF1*	0.60	*ALS2*	0.50	*GSTCD*	0.31
PDS5B	0.72	*RFX7*	0.60	*TAF8*	0.50	*ME2*	0.30
PIK3CA	0.72	*TOR1AIP1*	0.60	*SYNRG*	0.50	*LOC101906230*	0.30
DMD	0.72	*RBM41*	0.60	*ATP9A*	0.50	*PARP11*	0.30
LARP1	0.72	*ATP11B*	0.60	*SYNJ1*	0.50	*SIN3A*	0.30
RALGAPB	0.72	*DNAJB14*	0.60	*MARCH7*	0.50	*GTF2I*	0.30
IREB2	0.72	*PPP1R9A*	0.60	*ETNK1*	0.50	*SLX4IP*	0.30
PDS5A	0.72	*AP5M1*	0.60	*FBXO30*	0.50	*FAM20B*	0.29
PGAP1	0.72	*USP53*	0.60	*TMEM123*	0.50	*KRIT1*	0.29
GOLGB1	0.72	*AKAP10*	0.60	*ZFYVE26*	0.49	*CSTF2*	0.29
ZNF462	0.72	*PUM2*	0.60	*EML4*	0.49	*FBXW2*	0.29
CASP8AP2	0.72	*RPP14*	0.60	*USPL1*	0.49	*ZNF496*	0.29
CCNT1	0.72	*LOC107132175*	0.60	*RSBN1L*	0.49	*LOC112445511*	0.28
TRPM7	0.72	*LOC100335642*	0.59	*PM20D2*	0.49	*ZCCHC10*	0.28

MTOR	0.72	*TRPS1*	0.59	*IKZF2*	0.49	*ABCC1*	0.27
WDFY3	0.72	*TMEM245*	0.59	*PAK2*	0.49	*C2H2orf69*	0.27
UBXN7	0.72	*RLIM*	0.59	*INO80*	0.49	*ACACB*	0.27
EIF4EBP2	0.72	*LOC101902991*	0.59	*USP1*	0.49	*MAP3K9*	0.27
STRN	0.71	*KIDINS220*	0.59	*CKAP5*	0.49	*OXCT1*	0.27
NCKAP1	0.71	*SLC35D1*	0.59	*KLHL24*	0.49	*SOBP*	0.26
CREBBP	0.71	*ITSN1*	0.59	*PIAS2*	0.49	*ASTE1*	0.26
GAPVD1	0.71	*PATJ*	0.59	*CHD7*	0.49	*ACAD11*	0.26
STAG2	0.71	*SEL1L*	0.59	*FKTN*	0.49	*ZNF879*	0.26
SYNE1	0.71	*SLK*	0.59	*TNRC18*	0.49	*CWC25*	0.25
NIP7	0.71	*RBBP6*	0.59	*FYTTD1*	0.49	*SART3*	0.25
KLHL28	0.71	*ABCA5*	0.59	*LIMCH1*	0.48	*PIK3C3*	0.24
ACAP2	0.71	*LCORL*	0.59	*UBA2*	0.48	*TFIP11*	0.24
DCAF1	0.71	*TTC17*	0.59	*KCTD3*	0.48	*SGMS1*	0.24
NCOA6	0.71	*KRAS*	0.59	*ERC1*	0.48	*TMED6*	0.24
CREB1	0.71	*PPP1R12A*	0.59	*TBL1XR1*	0.48	*OPA3*	0.24
LIMD1	0.71	*ZDHHC17*	0.59	*FAM168A*	0.48	*GTPBP1*	0.24
MKLN1	0.71	*GTF3C3*	0.59	*SRP72*	0.48	*TP53BP2*	0.24
TRIO	0.71	*FBXO42*	0.59	*USP8*	0.48	*LOC515570*	0.24
ARID4A	0.71	*ATXN2*	0.59	*DNAH12*	0.48	*THAP2*	0.24
SMG1	0.71	*CDC27*	0.59	*GPATCH2L*	0.48	*LOC100848282*	0.23
ATAD2B	0.71	*MORC3*	0.59	*LOC515333*	0.48	*CDYL2*	0.23
DIP2B	0.71	*TANC1*	0.59	*SYDE2*	0.48	*PLCB1*	0.23
ZNF148	0.71	*SENP7*	0.59	*PSD3*	0.48	*FAM234B*	0.23
MAST4	0.71	*RPE*	0.58	*NOL11*	0.48	*MSANTD4*	0.22
ZNF654	0.71	*ARHGAP17*	0.58	*COL4A3BP*	0.48	*FBXO34*	0.22
MAVS	0.71	*AUG1*	0.58	*CENPC*	0.48	*HMGCS1*	0.22
TNRC6A	0.71	*KMT5B*	0.58	*MCM3AP*	0.48	*LOC100124497*	0.22
TRAPPC8	0.70	*LOC112443502*	0.58	*MBTPS2*	0.48	*TCP11L2*	0.19
LIFR	0.70	*RBL2*	0.58	*SPPL2A*	0.48	*ZNF623*	0.18
LRRC58	0.70	*PARP4*	0.58	*ULK2*	0.48	*PDK1*	0.17
TMEM170B	0.70	*SSFA2*	0.58	*SMAD3*	0.48	*ULBP13*	0.16
ATRN	0.70	*USP54*	0.58	*SUDS3*	0.48	*ZBTB24*	0.12
PIKFYVE	0.70	*SP140L*	0.58	*ACVR2A*	0.48	*LOC112441490*	0.09
NR2C2	0.70	*TCF12*	0.58	*PURB*	0.48	*LOC783508*	0.01
BAZ2B	0.70	*TXLNA*	0.58	*LOC512672*	0.48		

Supplementary Table 4. Summary of pathway analysis from ClueGo for genes clustered into the selected modules. Spreadsheet tabs are divided by module.

#M1

GOTerm	Group PValue	Nr. Genes	Associated Genes Found
NOD-like receptor signaling pathway	0.00	11	[GBP4, GBP5, IFI16, IRF7, IRF9, LOC100336669, LOC507055, LOC511531, LOC512486, OAS1X, OAS1Y]
Hepatitis C	0.00	8	EIF2AK2, IRF1, IRF7, IRF9, LOC100139670, OAS1X, OAS1Y]
Measles	0.00	10	[ADAR, DDX58, EIF2AK2, IFIH1, IRF7, IRF9, MX1, OAS1X, OAS1Y, TNFSF10]
Influenza A	0.00	12	[ADAR, DDX58, EIF2AK2, IFIH1, IRF7, IRF9, MX1, OAS1X, OAS1Y, PML, RSAD2, TNFSF10]
Herpes simplex infection	0.00	12	[DDX58, EIF2AK2, IFIH1, IRF7, IRF9, LOC100139670, LOC618733, OAS1X, OAS1Y, PML, TAP1, TAP2]

#M5

GOTerm	Group PValue	Nr. Genes	Associated Genes Found
Phagosome	6,19E-16	10	[BOLA-DMA, BOLA-DMB, BOLA-DRA, BOLA-DRB3, CORO1A, CTSS, CYBB, FCGR3A, ITGAM, ITGB2]
Cell adhesion molecules (CAMs)	6,19E-16	10	[BOLA-DMA, BOLA-DMB, BOLA-DRA, BOLA-DRB3, ITGAM, ITGB2, ITGB7, PTPRC, SELL, SPN]
Antigen processing and presentation	6,19E-16	7	[BOLA-DMA, BOLA-DMB, BOLA-DRA, BOLA-DRB3, CD74, CIITA, CTSS]
Hematopoietic cell lineage	6,19E-16	7	[BOLA-DMA, BOLA-DMB, BOLA-DRA, BOLA-DRB3, CD3E, ITGAM, LOC515418]
Th1 and Th2 cell differentiation	6,19E-16	8	[BOLA-DMA, BOLA-DMB, BOLA-DRA, BOLA-DRB3, CD3E, IL2RB, IL2RG, ZAP70]
Th17 cell differentiation	6,19E-16	8	[BOLA-DMA, BOLA-DMB, BOLA-DRA, BOLA-DRB3, CD3E, IL2RB, IL2RG, ZAP70]
Intestinal immune network for IgA production	6,19E-16	5	[BOLA-DMA, BOLA-DMB, BOLA-DRA, BOLA-DRB3, ITGB7]
Type I diabetes mellitus	6,19E-16	4	[BOLA-DMA, BOLA-DMB, BOLA-DRA, BOLA-DRB3]
Leishmaniasis	6,19E-16	10	[BOLA-DMA, BOLA-DMB, BOLA-DRA, BOLA-DRB3, CYBB, FCGR3A, ITGAM, ITGB2, PRKCB, PTPN6]
Toxoplasmosis	6,19E-16	7	[BOLA-DMA, BOLA-DMB, BOLA-DRA, BOLA-DRB3, CIITA, IL10RA, PIK3R5]
Staphylococcus aureus infection	6,19E-16	8	[BOLA-DMA, BOLA-DMB, BOLA-DRA, BOLA-DRB3, FCGR3A, ITGAM, ITGB2, PTAFR]
Tuberculosis	6,19E-16	13	[BOLA-DMA, BOLA-DMB, BOLA-DRA, BOLA-DRB3, CD74, CIITA, CORO1A, CTSS, FCGR3A, IL10RA, ITGAM, ITGB2, SYK]
Asthma	6,19E-16	4	[BOLA-DMA, BOLA-DMB, BOLA-DRA, BOLA-DRB3]
Autoimmune thyroid disease	6,19E-16	4	[BOLA-DMA, BOLA-DMB, BOLA-DRA, BOLA-DRB3]
Inflammatory bowel disease (IBD)	6,19E-16	5	[BOLA-DMA, BOLA-DMB, BOLA-DRA, BOLA-DRB3, IL2RG]
Rheumatoid arthritis	6,19E-16	5	[BOLA-DMA, BOLA-DMB, BOLA-DRA, BOLA-DRB3, ITGB2]
Allograft rejection	6,19E-16	4	[BOLA-DMA, BOLA-DMB, BOLA-DRA, BOLA-DRB3]
Graft-versus-host disease	6,19E-16	4	[BOLA-DMA, BOLA-DMB, BOLA-DRA, BOLA-DRB3]
Viral myocarditis	6,19E-16	6	[BOLA-DMA, BOLA-DMB, BOLA-DRA, BOLA-DRB3, ITGB2, RAC2]

#M6

GOTerm	Group Pvalue	Nr. Genes	Associated Genes Found
Adipocytokine signaling pathway	0.00	3	[ADIPOQ, PCK1, PCK2]
Amphetamine addiction	0.01	3	[ADCY5, MAOB, PPP1R1B]
AMPK signaling pathway	0.00	9	[ACACA, ADIPOQ, FASN, FBP1, LIPE, PCK1, PCK2, PPP2R5A, SCD]
Apelin signaling pathway	0.01	7	[ADCY5, GNAI1, GNG2, LIPE, MRAS, PDE3B, PLIN1]
Biosynthesis of unsaturated fatty acids	0.01	4	[ELOVL5, ELOVL6, HACD2, SCD]
Central carbon metabolism in cancer	0.04	3	[G6PD, PGAM1, SLC1A5]
Circadian entrainment	0.01	4	[ADCY5, ADCYAP1R1, GNAI1, GNG2]
Citrate cycle (TCA cycle)	0.00	4	[IDH1, PC, PCK1, PCK2]
Cocaine addiction	0.01	4	[ADCY5, GNAI1, MAOB, PPP1R1B]
Dopaminergic synapse	0.01	6	[ADCY5, GNAI1, GNG2, MAOB, PPP1R1B, PPP2R5A]
Drug metabolism	0.04	3	[AOX1, MAOB, MGST1]
Fatty acid elongation	0.01	3	[ELOVL5, ELOVL6, HACD2]
Glucagon signaling pathway	0.00	6	[ACACA, PCK1, PCK2, PDE3B, PGAM1, SIK2]
Glutathione metabolism	0.02	4	[G6PD, IDH1, MGST1, PGD]
Glycolysis / Gluconeogenesis	0.00	5	[ACSS2, FBP1, PCK1, PCK2, PGAM1]
Insulin signaling pathway	0.00	7	[ACACA, FASN, FBP1, LIPE, PCK1, PCK2, PDE3B]
Morphine addiction	0.01	4	[ADCY5, GNAI1, GNG2, PDE3B]
Pentose phosphate pathway	0.00	5	[FBP1, G6PD, PGD, TALDO1, TKT]
PPAR signaling pathway	0.00	7	[ADIPOQ, FABP4, LOC510990, PCK1, PCK2, PLIN1, SCD]
Propanoate metabolism	0.00	4	[ACACA, ACSS2, ACSS3, ECHDC1]
Pyruvate metabolism	0.00	6	[ACACA, ACSS2, ME1, PC, PCK1, PCK2]
Regulation of lipolysis in adipocytes	0.01	6	[ADCY5, FABP4, GNAI1, LIPE, PDE3B, PLIN1]
Renin secretion	0.01	4	[ADCY5, ADCYAP1R1, GNAI1, PDE3B]
Sphingolipid metabolism	0.06	3	[ACER2, ACER3, KDSR]
Tyrosine metabolism	0.04	3	[AOX1, FAH, MAOB]

#M7

GOTerm	Group Pvalue	Nr. Genes	Associated Genes Found
Ras signaling pathway	0.00	14	[ANGPT2, ARF6, EPHA2, GNB1, GNB5, PGF, RAB5C, RALA, RAP1B, RELA, RGL1, RHOA, SHC1, VEGFC]
Rap1 signaling pathway	0.00	17	[ACTB, ACTG1, ANGPT2, BCAR1, EPHA2, F2R, GNAI2, GNAI3, PGF, PRKD1, RALA, RAP1B, RHOA, SIPA1, TLN1, VASP, VEGFC]
cGMP-PKG signaling pathway	0.00	15	[ADRA1D, ATP1B3, CREB3L1, GNA12, GNAI2, GNAI3, KCNJ8, KCNMB1, MYL9, MYLK, NFATC4, RGS2, RHOA, SLC25A5, VASP]
cAMP signaling pathway	0.00	9	[ATP1B3, CREB3L1, F2R, GNAI2, GNAI3, MYL9, RAP1B, RELA, RHOA]
Focal adhesion	0.00	23	[ACTB, ACTG1, ACTN1, BCAR1, CAPN2, CAV1, CCND3, COL4A1, COL4A2, FLNA, ITGA5, MYL12B, MYL9, MYLK, PARVA, PGF, RAP1B, RHOA, SHC1, TLN1, VASP, VEGFC, ZYX]
Adherens junction	0.00	5	[ACTB, ACTG1, ACTN1, CTNNA1, RHOA]
Tight junction	0.00	21	[ACTB, ACTG1, ACTN1, ACTR2, ACTR3, ARHGEF18, ARHGEF2, EZR, HCLS1, JAM3, MSN, MYH10, MYH11, MYH9, MYL12B, MYL6, MYL9, RAB8A, RHOA, RUNX1, VASP]
Platelet activation	0.00	12	[ACTB, ACTG1, F2R, GNAI2, GNAI3, LYN, MYL12B, MYLK, RAP1B, RHOA, TLN1, VASP]
Leukocyte transendothelial migration	0.00	16	[ACTB, ACTG1, ACTN1, BCAR1, CTNNA1, EZR, GNAI2, GNAI3, JAM3, MSN, MYL12B, MYL9, RAP1B, RHOA, SIPA1, VASP]
Regulation of actin cytoskeleton	0.00	17	[ACTB, ACTG1, ACTN1, ARHGEF7, ARPC3, BCAR1, ENAH, EZR, F2R, GNA12, ITGA5, MSN, MYL12B, MYL9, MYLK, RHOA, TMSB4X]
Oxytocin signaling pathway	0.00	11	[ACTB, ACTG1, CACNB3, GNAI2, GNAI3, MYL6, MYL9, MYLK, NFATC4, RGS2, RHOA]
Protein processing in endoplasmic reticulum	0.00	20	[BAX, CALR, CANX, CAPN2, DNAJB11, HSP90B1, HSPA5, HYOU1, MOGS, PDIA3, PDIA6, SAR1A, SEC23B, SEC61A1, SEC61B, SEC62, SSR3, SYVN1, TRAM1, XBP1]
Phagosome	0.00	20	[ACTB, ACTG1, ATP6AP1, BOLA, BoLA, CALR, CANX, CD36, CTSV, DYNC1I2, ITGA5, LOC509006, RAB5C, RAB7B, SEC61A1, SEC61B, STX7, TUBB2A, TUBB2B, TUBB6]
Glycosphingolipid biosynthesis	0.02	6	[B3GALT2, B3GNT3, B4GALT3, FUT4, LOC520336, ST3GAL4]
Apoptosis	0.04	13	[ACTB, ACTG1, BAX, CAPN2, CASP6, CTSV, GADD45B, LMNA, RELA, RIPK1, SPTAN1, TNFRSF1A, TP53]
Adherens junction	0.04	5	[ACTB, ACTG1, ACTN1, CTNNA1, RHOA]
Leukocyte transendothelial migration	0.04	16	[ACTB, ACTG1, ACTN1, BCAR1, CTNNA1, EZR, GNAI2, GNAI3, JAM3, MSN, MYL12B, MYL9, RAP1B, RHOA, SIPA1, VASP]
Bacterial invasion of epithelial cells	0.04	12	[ACTB, ACTG1, ARPC3, BCAR1, CAV1, CTNNA1, ELMO1, HCLS1, ITGA5, RHOA, SEPT9, SHC1]
Influenza A	0.04	8	[ACTB, ACTG1, CCL2, IFNGR1, NXT2, RELA, SOCS3, TNFRSF1A]

Proteoglycans in cancer	0.04	12	[ACTB, ACTG1, CAV1, CTSV, EZR, FLNA, HCLS1, ITGA5, MSN, RHOA, TGFB1, TP53]
Hypertrophic cardiomyopathy (HCM)	0.04	7	[ACTB, ACTG1, CACNB3, ITGA5, LMNA, TGFB1, TPM4]
Arrhythmogenic right ventricular cardiomyopathy (ARVC)	0.04	7	[ACTB, ACTG1, CACNB3, CTNNA1, ITGA5, JUP, LMNA]
Dilated cardiomyopathy (DCM)	0.04	7	[ACTB, ACTG1, CACNB3, ITGA5, LMNA, TGFB1, TPM4]
Fluid shear stress and atherosclerosis	0.04	13	[ACTB, ACTG1, ARHGEF2, CAV1, CCL2, CTSV, EDN1, HMOX1, HSP90B1, RELA, RHOA, TNFRSF1A, TP53]
cGMP-PKG signaling pathway	0.05	15	[ADRA1D, ATP1B3, CREB3L1, GNA12, GNAI2, GNAI3, KCNJ8, KCNMB1, MYL9, MYLK, NFATC4, RGS2, RHOA, SLC25A5, VASP]
cAMP signaling pathway	0.05	9	[ATP1B3, CREB3L1, F2R, GNAI2, GNAI3, MYL9, RAP1B, RELA, RHOA]
PI3K-Akt signaling pathway	0.05	18	[ANGPT2, CCND3, COL4A1, COL4A2, CREB3L1, EPHA2, F2R, GNB1, GNB5, HSP90B1, IL4R, ITGA5, PGF, RELA, TP53, VEGFC, YWHAB, YWHAZ]
Adrenergic signaling in cardiomyocytes	0.05	7	[ADRA1D, ATP1B3, CACNB3, CREB3L1, GNAI2, GNAI3, TPM4]
Vascular smooth muscle contraction	0.05	12	[ACTA2, ACTG2, ADRA1D, GNA12, KCNMB1, MYL6, MYL9, MYLK, PPP1R14A, RAMP2, RAMP3, RHOA]
Apelin signaling pathway	0.05	7	[ACTA2, APLN, GNAI2, GNAI3, GNB1, GNB5, MYLK]
Platelet activation	0.05	12	[ACTB, ACTG1, F2R, GNAI2, GNAI3, LYN, MYL12B, MYLK, RAP1B, RHOA, TLN1, VASP]
Cholinergic synapse	0.05	6	[CHRNA3, CREB3L1, GNAI2, GNAI3, GNB1, GNB5]
Estrogen signaling pathway	0.05	5	[CREB3L1, GNAI2, GNAI3, HSP90B1, SHC1]
Oxytocin signaling pathway	0.05	11	[ACTB, ACTG1, CACNB3, GNAI2, GNAI3, MYL6, MYL9, MYLK, NFATC4, RGS2, RHOA]
Relaxin signaling pathway	0.05	13	[ACTA2, COL4A1, COL4A2, CREB3L1, EDN1, GNAI2, GNAI3, GNB1, GNB5, RELA, SHC1, TGFB1, VEGFC]
AGE-RAGE signaling pathway in diabetic complications	0.05	9	[BAX, CCL2, COL4A1, COL4A2, EDN1, PIM1, RELA, TGFB1, VEGFC]
Gastric acid secretion	0.05	5	[ATP1B3, EZR, GNAI2, GNAI3, MYLK]
Pancreatic secretion	0.05	5	[ATP1B3, RAB11A, RAB8A, RAP1B, RHOA]
Pertussis	0.05	5	[GNAI2, GNAI3, ITGA5, RELA, RHOA]

#M8

GOTerm	Group Pvalue	Nr. Genes	Associated Genes Found
Glycosaminoglycan degradation	0.00	10	[ARSB, GALNS, GLB1, GNS, GUSB, HEXB, HGSNAT, IDUA, NAGLU, SGSH]
Lysosome	0.00	37	[ACP5, AP1S1, AP3S1, ARSA, ARSB, ASAH1, ATP6V1H, CD68, CTNS, CTSA, CTSB, CTSC, CTSF, CTSK, CTSO, CTSZ, DNASE2, GALNS, GBA, GLB1, GM2A, GNS, GUSB, HEXB, HGSNAT, IDUA, LAPTM4A, LGMN, LIPA, MAN2B1, MANBA, NAGA, NAGLU, PPT1, SGSH, SMPD1, SUMF1]
Glycosaminoglycan biosynthesis	0.00	8	[CHPF, CHPF2, CHST14, CHSY1, CSGALNACT1, DSE, UST, XYLT2]
Amino sugar and nucleotide sugar metabolism	0.00	12	[CYB5R3, CYB5R4, CYB5RL, GALK1, GALT, GFPT2, GNPNAT1, HEXB, NAGK, NANP, PMM2, UGDH]
AGE-RAGE signaling pathway in diabetic complications	0.01	17	[AGTR1, COL1A1, COL1A2, COL3A1, F3, FN1, ICAM1, LOC534578, MMP2, PLCD1, PRKCD, SERPINE1, TGFB2, TGFBR2, THBD, VCAM1, VEGFD]
Proteoglycans in cancer	0.01	26	[CD44, CTTN, DCN, ERBB3, FGFR1, FN1, FZD8, GPC3, IGF1, IGF2, ITGB3, ITGB5, LUM, MAP2K1, MMP2, PDCD4, PLAU, SMO, SRC, TGFB2, THBS1, TIAM1, TLR2, TLR4, WNT11, WNT5A]
Other glycan degradation	0.02	7	[FUCA1, FUCA2, GBA, GLB1, HEXB, MAN2B1, MANBA]
Steroid biosynthesis	0.04	6	[CYP51A1, LIPA, LSS, MSMO1, NSDHL, SC5D]

#M9

GOTerm	Group PValue	Nr. Genes	Associated Genes Found
TGF-beta signaling pathway	0.00	4	[ID1, ID3, MYC, TGFB3]
Osteoclast differentiation	0.00	6	[FOS, FOSB, FOSL2, JUN, JUNB, JUND]
IL-17 signaling pathway	0.00	5	[FOS, FOSB, JUN, JUND, PTGS2]
TNF signaling pathway	0.00	5	[CREB5, FOS, JUN, JUNB, PTGS2]
Amphetamine addiction	0.00	4	[CREB5, FOS, FOSB, JUN]
Leishmaniasis	0.00	4	[FOS, JUN, PTGS2, TGFB3]
Colorectal cancer	0.00	4	[FOS, JUN, MYC, TGFB3]

#M17

GOTerm	Group PValue	Nr. Genes	Associated Genes Found
ErbB signaling pathway	0.00	11	[ABL2, BRAF, CBL, GSK3B, KRAS, MTOR, NCK1, PAK2, PIK3CA, PTK2, RPS6KB1]
Rap1 signaling pathway	0.00	10	[BRAF, GNAQ, IGF1R, INSR, KRAS, KRIT1, MAGI3, PIK3CA, PLCB1, PRKD3]
cGMP-PKG signaling pathway	0.00	10	[CREB1, GNAQ, GTF2I, INSR, ITPR1, MEF2C, PDE3A, PLCB1, PPP1R12A, PRKCE]
Chemokine signaling pathway	0.00	8	[BRAF, GSK3B, JAK2, KRAS, PIK3CA, PLCB1, PTK2, WASL]
HIF-1 signaling pathway	0.00	9	[ARNT, BCL2, CREBBP, IGF1R, INSR, MTOR, PDK1, PIK3CA, RPS6KB1]
FoxO signaling pathway	0.00	10	[ATM, BRAF, CREBBP, IGF1R, INSR, KRAS, PIK3CA, RBL2, SMAD2, SMAD3]
Sphingolipid signaling pathway	0.00	8	[ABCC1, BCL2, GNAQ, KRAS, PIK3CA, PLCB1, PRKCE, SGMS1]
Phospholipase D signaling pathway	0.00	8	[DGKH, INSR, KRAS, MTOR, PIK3CA, PLCB1, PTPN11, TSC1]
Cell cycle	0.00	12	[ATM, CDC27, CREBBP, GSK3B, PRKDC, RB1, RBL2, SMAD2, SMAD3, SMC1A, STAG1, STAG2]
Oocyte meiosis	0.00	8	[AR, CDC27, CPEB4, IGF1R, ITPR1, RPS6KA3, SLK, SMC1A]
Autophagy	0.00	5	[ATG2B, MTOR, PIK3C3, RPTOR, ULK2]
Autophagy	0.00	16	[ATG2B, BCL2, IGF1R, ITPR1, KRAS, LOC524719, MAP3K7, MTOR, PIK3C3, PIK3CA, RPS6KB1, RPTOR, STX17, TSC1, ULK2, UVRAG]
mTOR signaling pathway	0.00	15	[BRAF, FNIP1, GSK3B, IGF1R, INSR, KRAS, LRP6, MTOR, PIK3CA, RICTOR, RPS6KA3, RPS6KB1, RPTOR, TSC1, ULK2]
PI3K-Akt signaling pathway	0.00	18	[BCL2, CREB1, GHR, GSK3B, IGF1R, INSR, ITGAV, JAK2, KRAS, MTOR, PHLPP2, PIK3CA, PKN2, PTK2, RBL2, RPS6KB1, RPTOR, TSC1]
AMPK signaling pathway	0.00	10	[ACACB, CREB1, IGF1R, INSR, MAP3K7, MTOR, PIK3CA, RPS6KB1, RPTOR, TSC1]
Apoptosis	0.00	9	[APAF1, ATM, BCL2, ITPR1, KRAS, LOC524719, PARP4, PIK3CA, XIAP]
Longevity regulating pathway	0.00	10	[APPL1, CREB1, IGF1R, INSR, KRAS, MTOR, PIK3CA, RPS6KB1, RPTOR, TSC1]
Longevity regulating pathway	0.00	9	[CLPB, EIF4EBP2, IGF1R, INSR, KRAS, MTOR, PIK3CA, RPS6KB1, RPTOR]
Cellular senescence	0.00	15	[ATM, HIPK1, HIPK2, ITPR1, KRAS, LIN54, LOC512672, MTOR, PIK3CA, RB1, RBL2, SMAD2, SMAD3, TRPM7, TSC1]
Vascular smooth muscle contraction	0.00	7	[ARHGEF12, BRAF, GNAQ, ITPR1, PLCB1, PPP1R12A, PRKCE]
Wnt signaling pathway	0.00	8	[APC, CHD8, CREBBP, GSK3B, LRP6, MAP3K7, PLCB1, TBL1XR1]
Axon guidance	0.00	11	[ARHGEF12, BMPR2, GSK3B, KRAS, NCK1, PAK2, PDK1, PIK3CA, PTK2, PTPN11, SSH2]

Apelin signaling pathway	0.00	12	[GNAQ, ITPR1, KRAS, MEF2C, MTOR, PIK3C3, PLCB1, PRKCE, RPS6KB1, RYR3, SMAD2, SMAD3]
Focal adhesion	0.00	11	[ARHGAP5, BCL2, BRAF, GSK3B, IGF1R, ITGAV, PAK2, PIK3CA, PPP1R12A, PTK2, XIAP]
Adherens junction	0.00	9	[CREBBP, IGF1R, INSR, LMO7, MAP3K7, PTPRM, SMAD2, SMAD3, WASL]
Gap junction	0.00	5	[GNAQ, ITPR1, KRAS, MAP3K2, PLCB1]
Signaling pathways regulating pluripotency of stem cells	0.00	17	[ACVR2A, APC, BMPR2, GSK3B, IGF1R, IL6ST, JAK2, KAT6A, KRAS, LIFR, PCGF5, PIK3CA, SKIL, SMAD2, SMAD3, SMAD5, ZFHX3]
Platelet activation	0.00	6	[ARHGEF12, GNAQ, ITPR1, PIK3CA, PLCB1, PPP1R12A]
Natural killer cell mediated cytotoxicity	0.00	8	[BRAF, KRAS, LOC100848282, LOC783508, LOC786095, PIK3CA, PTPN11, ULBP13]
Th17 cell differentiation	0.00	6	[IL6ST, JAK2, MTOR, RORA, SMAD2, SMAD3]
T cell receptor signaling pathway	0.00	8	[CBL, DLG1, GSK3B, KRAS, MAP3K7, NCK1, PAK2, PIK3CA]
Circadian entrainment	0.00	5	[CREB1, GNAQ, ITPR1, PLCB1, RYR3]
Long-term potentiation	0.00	7	[BRAF, CREBBP, GNAQ, ITPR1, KRAS, PLCB1, RPS6KA3]
Neurotrophin signaling pathway	0.00	9	[BCL2, BRAF, GSK3B, IRAK3, KIDINS220, KRAS, PIK3CA, PTPN11, RPS6KA3]
Cholinergic synapse	0.00	8	[BCL2, CREB1, GNAQ, ITPR1, JAK2, KRAS, PIK3CA, PLCB1]
Serotonergic synapse	0.00	5	[BRAF, GNAQ, ITPR1, KRAS, PLCB1]
Dopaminergic synapse	0.00	6	[CLOCK, CREB1, GNAQ, GSK3B, ITPR1, PLCB1]
Long-term depression	0.00	6	[BRAF, GNAQ, IGF1R, ITPR1, KRAS, PLCB1]
Inflammatory mediator regulation of TRP channels	0.00	5	[GNAQ, ITPR1, PIK3CA, PLCB1, PRKCE]
Regulation of actin cytoskeleton	0.00	14	[APC, ARHGEF12, BRAF, ITGAV, KRAS, NCKAP1, PAK2, PIK3CA, PIKFYVE, PPP1R12A, PTK2, RDX, SSH2, WASL]
Insulin signaling pathway	0.00	12	[ACACB, BRAF, CBL, GSK3B, INSR, KRAS, MTOR, PIK3CA, RPS6KB1, RPTOR, SOCS4, TSC1]
GnRH signaling pathway	0.00	5	[GNAQ, ITPR1, KRAS, MAP3K2, PLCB1]
Progesterone-mediated oocyte maturation	0.00	7	[BRAF, CDC27, CPEB4, IGF1R, KRAS, PIK3CA, RPS6KA3]
Estrogen signaling pathway	0.00	7	[CREB1, GNAQ, ITPR1, KRAS, PIK3CA, PLCB1, SP1]
Melanogenesis	0.00	6	[CREB1, CREBBP, GNAQ, GSK3B, KRAS, PLCB1]
Prolactin signaling pathway	0.00	5	[GSK3B, JAK2, KRAS, PIK3CA, SOCS4]

Oxytocin signaling pathway	0.00	8	[CACNA2D1, GNAQ, ITPR1, KRAS, MEF2C, PLCB1, PPP1R12A, RYR3]
Glucagon signaling pathway	0.00	7	[ACACB, CREB1, CREBBP, GNAQ, ITPR1, PLCB1, PPP4R3B]
Renin secretion	0.00	5	[CREB1, GNAQ, ITPR1, PDE3A, PLCB1]
Aldosterone synthesis and secretion	0.00	6	[CREB1, GNAQ, ITPR1, PLCB1, PRKCE, PRKD3]
Relaxin signaling pathway	0.00	6	[CREB1, KRAS, PIK3CA, PLCB1, SMAD2, SMAD3]
Type II diabetes mellitus	0.00	5	[INSR, MTOR, PIK3CA, PRKCE, SOCS4]
Insulin resistance	0.00	11	[ACACB, CREB1, GSK3B, INSR, MTOR, PIK3CA, PPARGC1B, PRKCE, PTPN11, RPS6KA3, RPS6KB1]
AGE-RAGE signaling pathway in diabetic complications	0.00	8	[BCL2, JAK2, KRAS, PIK3CA, PLCB1, PRKCE, SMAD2, SMAD3]
Alzheimer's disease	0.00	8	[APAF1, ATF6, GNAQ, GSK3B, ITPR1, LOC524719, PLCB1, RYR3]
Huntington's disease	0.00	13	[APAF1, CLTC, CREB1, CREBBP, DNAH12, DNAL1, GNAQ, ITPR1, PLCB1, POLR2A, RCOR1, SIN3A, SP1]
Bacterial invasion of epithelial cells	0.00	5	[CBL, CLTC, PIK3CA, PTK2, WASL]
Chagas disease (American trypanosomiasis)	0.00	5	[GNAQ, PIK3CA, PLCB1, SMAD2, SMAD3]
Hepatitis C	0.00	6	[BRAF, GSK3B, KRAS, MAVS, PIAS1, PIK3CA]
Hepatitis B	0.00	8	[APAF1, BCL2, CREB1, CREBBP, KRAS, MAVS, PIK3CA, RB1]
Human papillomavirus infection	0.00	23	[APC, ATM, ATP6V0A1, ATP6V0A2, CHD4, CREB1, CREBBP, DLG1, GSK3B, ITGAV, KRAS, LOC512672, MAML1, MPP5, MTOR, PATJ, PIK3CA, PTK2, RB1, RBL2, RPS6KB1, TSC1, UBR4]
HTLV-I infection	0.00	16	[APC, ATM, CDC27, CREB1, CREBBP, DLG1, ELK4, GSK3B, KRAS, LOC512672, PIK3CA, RB1, SMAD2, SMAD3, TRRAP, XIAP]
Kaposi's sarcoma-associated herpesvirus infection	0.00	12	[CREB1, CREBBP, GSK3B, IL6ST, ITPR1, JAK2, KRAS, LOC512672, MTOR, PIK3C3, PIK3CA, RB1]
Epstein-Barr virus infection	0.00	11	[BCL2, CREBBP, GSK3B, GTF2E1, LOC512672, MAP3K7, NUP214, PIK3CA, POLR2A, POLR3B, RB1]
Pathways in cancer	0.00	34	[APAF1, APC, APPL1, AR, ARHGEF12, ARNT, BCL2, BRAF, CBL, CREBBP, EML4, GNAQ, GSK3B, IGF1R, IL6ST, ITGAV, JAK2, KRAS, LRP6, MTOR, NCOA1, NCOA3, PIK3CA, PLCB1, PTK2, RB1, RPS6KB1, SMAD2, SMAD3, SP1, SUFU, TPR, XIAP, ZBTB16]
Proteoglycans in cancer	0.00	15	[ARHGEF12, BRAF, CBL, IGF1R, ITGAV, ITPR1, KRAS, LOC539238, MTOR, PIK3CA, PPP1R12A, PTK2, PTPN11, RDX, RPS6KB1]
Colorectal cancer	0.00	9	[APC, APPL1, BCL2, BRAF, GSK3B, KRAS, PIK3CA, SMAD2, SMAD3]
Renal cell carcinoma	0.00	7	[ARNT, BRAF, CREBBP, KRAS, PAK2, PIK3CA, PTPN11]

Pancreatic cancer	0.00	8	[BRAF, KRAS, MTOR, PIK3CA, RB1, RPS6KB1, SMAD2, SMAD3]
Endometrial cancer	0.00	5	[APC, BRAF, GSK3B, KRAS, PIK3CA]
Glioma	0.00	6	[BRAF, IGF1R, KRAS, MTOR, PIK3CA, RB1]
Prostate cancer	0.00	11	[AR, BCL2, BRAF, CREB1, CREBBP, GSK3B, IGF1R, KRAS, MTOR, PIK3CA, RB1]
Melanoma	0.00	5	[BRAF, IGF1R, KRAS, PIK3CA, RB1]
Chronic myeloid leukemia	0.00	6	[BRAF, CBL, KRAS, PIK3CA, PTPN11, RB1]
Acute myeloid leukemia	0.00	6	[BRAF, KRAS, MTOR, PIK3CA, RPS6KB1, ZBTB16]
Non-small cell lung cancer	0.00	5	[BRAF, EML4, KRAS, PIK3CA, RB1]
Breast cancer	0.00	13	[APC, BRAF, GSK3B, IGF1R, KRAS, LRP6, MTOR, NCOA1, NCOA3, PIK3CA, RB1, RPS6KB1, SP1]
Hepatocellular carcinoma	0.00	17	[APC, ARID1A, ARID2, BRAF, GSK3B, IGF1R, KRAS, LRP6, MTOR, PBRM1, PIK3CA, RB1, RPS6KB1, SMAD2, SMAD3, SMARCA2, SMARCC1]
Gastric cancer	0.00	12	[APC, BCL2, BRAF, GSK3B, KRAS, LRP6, MTOR, PIK3CA, RB1, RPS6KB1, SMAD2, SMAD3]
Choline metabolism in cancer	0.00	9	[DGKH, KRAS, MTOR, PCYT1A, PIK3CA, RPS6KB1, SP1, TSC1, WASL]

Supplementary Table 5. Genes targeted by eQTLs for each selected module. Genes with MM ≥ 0.8 are highlighted in bold. Spreadsheet tabs are divided by module.

#M1

GS	SNP ID	Number of eQTLs	MM
PARP14	rs111027859	1	0.92
HERC6	rs111027859	1	0.92
UBA7	rs135770163, rs41584849, rs42368640, rs43444149	4	0.91
EPSTI1	rs109337245	1	0.86
GBP4	rs111027859, rs135770163, rs42368640, rs133367268, rs134847248, rs135621295, rs135894931, rs137451109	8	0.76
WARS	rs41584849	1	0.72
TAP1	rs41722255	1	0.72
PML	rs137522194	1	0.70

#M5

GS	SNP ID	Number of eQTLs	MM
DOCK2	rs109984248, rs132703816, rs136800085, rs110639278, rs133917922	5	0.83
IL10RA	rs110237175	1	0.83
LCP2	rs41958687, rs110230607	2	0.81
SRGN	rs109000740, rs109896392	2	0.80
THEMIS2	rs43230751, rs43231337, rs135914685, rs109984248, rs132703816, rs136800085, rs110639278, rs133917922, rs108988328, rs133734177, rs134095631, rs42120466, rs137740028	13	0.77
EVI2B	rs41958687, rs110230607	2	0.73
CCR2	rs41958687, rs41958646, rs110230607, rs110946918, rs41957944, rs41957950, rs109886314	7	0.70
GIMAP7	rs42367495	1	0.70
AKNA	rs134095631	1	0.68
PIK3R5	rs134222862, rs41958687, rs110230607	3	0.63
SELL	rs43439302, rs137655201, rs135546810, rs136385712	4	0.61
CMTM7	rs43726953	1	0.61
ITGB7	rs135914685, rs109940676, rs110545035, rs135514086, rs133094747, rs41814665, rs109440367, rs134155084, rs135311765, rs133666409, rs134993302, rs109486557, rs134309048, rs137552295, rs137740028	15	0.60
NAAA	rs134794466, rs136202090	2	0.57

#M6

GS	SNP ID	Number of eQTLs	MM
PDE3B	rs137766044, rs109873557	2	0.89
THRSP	rs133473528, rs134780857	2	0.87
DGAT2	rs29013933	1	0.86
FASN	rs133473528	1	0.82
ELOVL5	rs133473528	1	0.81
SLC16A7	rs132879289, rs41581191	2	0.81
NCS1	rs136921969, rs110599639	2	0.78
DOCK11	rs137766044, rs109873557	2	0.77
RNF125	rs137766044, rs109873557	2	0.76
ACER3	rs110557491, rs109984248, rs132703816, rs136800085, rs110639278, rs133917922, rs110242967, rs134225791, rs110196671, rs136610099, rs136609253	11	0.67
ADM	rs42092779	1	0.66
STX12	rs133097787, rs109504875, rs110686431, rs110225456, rs110170388, rs110672259, rs132745513	7	0.65
ACER2	rs109579679	1	0.64
EPHX2	rs109811851, rs43229085	2	0.63
NNAT	rs135426758, rs110796345, rs134321661, rs109170602, rs43592223, rs43592218, rs43592201	7	0.62
LMO4	rs41931412, rs41572967	2	0.61
MAOB	rs43674778	1	0.52
MCCC1	rs43255057, rs42558288, rs42558326, rs136567853, rs137073255, rs43244621, rs134014064, rs136804068	8	0.39
SLC16A13	rs135914685, rs109940676, rs109984248, rs132703816, rs136800085, rs110639278, rs133917922, rs136610099	8	0.38
PTGR1	rs110622683, rs137549105, rs133543790, rs137315017, rs135602101, rs133064181, rs134823405, rs135985166, rs133817642, rs134646048, rs137720711, rs110697355, rs109714935, rs132781443, rs133822065, rs135980418, rs133122369, rs134750316, rs136548749, rs109335402, rs133224283, rs134624922, rs135385868, rs109566502, rs133510827, rs137317436, rs134840253, rs136486632, rs110565390, rs110753923, rs137451099, rs132781887, rs110937553, rs137054293, rs134304284, rs109693694, rs43577429, rs137621740	38	0.38

#M7

GS	SNP ID	Number of eQTLs	MM
FAM129B	rs110672259, rs132745513	2	0.81
TAX1BP3	rs41597279	1	0.80
ACTB	rs41582485	1	0.78
ARPC3	rs110332666	1	0.68
PDIA5	rs133097787, rs109504875, rs110686431, rs110225456, rs110170388, rs109777675, rs110672259, rs137435140, rs132745513, rs109435978	10	0.67
C1QTNF5	rs133097787, rs109504875, rs110686431, rs110225456, rs110170388, rs110672259, rs132745513	7	0.66
TSPAN9	rs109440794	1	0.63
TAGLN	rs135017776, rs41890252	2	0.61
FLNA	rs135017776	1	0.61
MFHAS1	rs135739001	1	0.61
PQLC3	rs109984248, rs132703816, rs136800085, rs110242967, rs134225791, rs110196671, rs110672259, rs132745513	8	0.60
FGR	rs135914685, rs109940676, rs109984248, rs110639278, rs133917922, rs108988328, rs110242967, rs134225791, rs110196671, rs41814665, rs109440367, rs110162928, rs137552295, rs137415979, rs43726953, rs43726967, rs41646812, rs137740028	18	0.59
PACSIN2	rs42778229	1	0.58
IFITM3	rs133944574, rs137400211	2	0.57
ENTPD1	rs136318998, rs133411436, rs137357399	3	0.53
ACSF2	rs133802660	1	0.51
ABHD3	rs134960961	1	0.51
TRAF3IP2	rs43726953	1	0.51
EDN1	rs43630160	1	0.51
EPHA2	rs132945184	1	0.50
MGAT1	rs42582790	1	0.49
RAB7B	rs132989618, rs29025402	2	0.49
CD36	rs109443524	1	0.49
BMP2	rs136926844, rs42326694, rs42326710, rs42326713, rs42326715, rs109179738, rs110470716, rs133780131, rs109664962, rs132961498, rs42327464, rs108944178, rs42364557, rs110356574	14	0.48
HAPLN3	rs41975019, rs136676186	2	0.48
CDC42EP4	rs133065280, rs135233135	2	0.47
SMAD6	rs42746549	1	0.46
BCAR1	rs109940676, rs41639637, rs109440367, rs137740028	4	0.45
CADPS2	rs136849238	1	0.44
ARHGAP27	rs109984248, rs132703816, rs136800085, rs110639278, rs133917922, rs110242967, rs134225791, rs110196671	8	0.43
HS1BP3	rs134590244, rs41751194, rs135914685, rs109940676, rs109984248, rs132703816, rs136800085, rs110639278, rs133917922, rs43163609, rs43469885, rs110396768, rs110801095, rs110076686, rs110175417, rs110598252,	50	0.42

	rs109896046, rs137732541, rs109084991, rs110242967, rs134225791, rs110196671, rs110077164, rs110561011, rs135061608, rs135520464, rs134767414, rs136478269, rs134279379, rs41814665, rs108974354, rs109440367, rs110685681, rs110481483, rs110162928, rs134155084, rs135311765, rs133666409, rs134993302, rs109486557, rs134309048, rs133528596, rs136160933, rs133525912, rs133731074, rs137552295, rs134388814, rs135393467, rs110063718, rs137740028		
FAM20A	rs137525867	1	0.42
DIXDC1	rs110988763, rs43493386, rs133942318, rs137767832, rs133857779, rs133582460, rs136613449, rs136319392, rs133619698, rs134382634, rs136294542, rs134620797, rs110312759, rs109499220, rs121918991	15	0.41
CCDC102A	rs109630523, rs135197631, rs137602930, rs133097787, rs109504875, rs110686431, rs110225456, rs110170388, rs109777675, rs110672259, rs137435140, rs132745513	12	0.41
SMAGP	rs134483943	1	0.40
BAX	rs135914685, rs41814665, rs108974354, rs109440367	4	0.40
GJA5	rs109936249	1	0.39
CD320	rs110639278, rs133917922	2	0.39
ACSS1	rs133356249, rs134658119, rs110988763, rs133739851, rs43493386, rs133942318, rs133769707, rs136613449, rs137726565, rs41605657, rs110862865, rs136289499, rs109033645, rs109206351, rs109126156, rs133952074, rs136196870, rs109161732, rs110956243, rs109757561, rs135273308, rs135114899, rs110676654, rs41585737, rs132864792, rs136727095, rs42725700, rs42845899, rs42846543	29	0.39
SRXN1	rs137780202	1	0.38
BOLA	rs136092545, rs109476334, rs109905817, rs133778695, rs109528441	5	0.38
NFATC4	rs29018687, rs110672259, rs132745513	3	0.37
ARHGAP25	rs110557491, rs135914685, rs109984248, rs132703816, rs136800085, rs110639278, rs133917922, rs110396768, rs110801095, rs110076686, rs110175417, rs110598252, rs109896046, rs137732541, rs110242967, rs134225791, rs110196671, rs108991474, rs135514086, rs133094747	20	0.37
MPDU1	rs42879465, rs42878726, rs134085221	3	0.37
ABCA3	rs42960720	1	0.37
PSEN2	rs135814026, rs135406561, rs134194763, rs29021598, rs110573052, rs109348957, rs109192474	7	0.35
PIM1	rs110659736, rs41795573	2	0.35
RAB15	rs43710096, rs110979600, rs133832435, rs134601683	4	0.35
PPM1F	rs133439814	1	0.35
MYH11	rs135017776	1	0.33
SUSD2	rs135270777	1	0.32
FAM214B	rs137282900	1	0.31
PNPLA2	rs134813792, rs43415132, rs136584128	3	0.31
PPM1D	rs109984248, rs134095631, rs134388814, rs135393467, rs132684582, rs136764192	6	0.30
CCL1	rs110456472, rs134388687	2	0.30

PTPRCAP	rs135914685, rs109940676, rs110545035, rs109488874, rs41612806, rs108964085, rs110297051, rs110102172, rs135514086, rs133094747, rs137552295, rs41646812	12	0.29
ALG14	rs110481483, rs134155084, rs135311765, rs133666409, rs134993302, rs109486557, rs134309048	7	0.28
ECE2	rs110129186	1	0.26
NDRG4	rs137461885, rs135699036	2	0.25
SEMA3F	rs133144838	1	0.25
SIRT6	rs137213606, rs135112808, rs135912109, rs135914685, rs109940676, rs137525867, rs109984248, rs132703816, rs136800085, rs110639278, rs133917922, rs43469885, rs110175417, rs110598252, rs109896046, rs137732541, rs108988328, rs110242967, rs134225791, rs110196671, rs108991474, rs135514086, rs133094747, rs110561011, rs134095631, rs137552295, rs136609253, rs132914250, rs41646812, rs137740028	30	0.24
WDR4	rs109940676, rs110639278, rs133917922, rs110242967, rs134225791, rs110196671, rs136326069, rs108991474, rs136478269, rs134279379, rs110481483, rs110162928, rs109777972, rs137552295, rs137740028	15	0.24
B2M	rs132972973	1	0.23
TMEM14A	rs134998649, rs133941859, rs133816334	3	0.23
EIF1AD	rs135914685, rs137525867, rs110545035, rs137740028, rs132684582, rs136764192	6	0.21
PALMD	rs133590893, rs132894811	2	0.20
GIPC2	rs109712684, rs137594086, rs110300068, rs110826573	4	0.20
DPH2	rs135061608, rs135520464, rs134767414, rs136478269, rs134279379	5	0.20
PLA2G7	rs137341074, rs134231394, rs136581229, rs134212794, rs41604174, rs109199422, rs41604172, rs133941093, rs110863284, rs110513609, rs109136782, rs135735289, rs110529321, rs133089170, rs109237975, rs109264240, rs110729420, rs109690540, rs110310028, rs109558921, rs109459969, rs109301246, rs109381466, rs109081026, rs134138017	25	0.20
SNAPC1	rs135914685, rs109940676, rs109984248, rs132703816, rs136800085, rs110639278, rs133917922, rs136609253	8	0.19
GSS	rs134128662	1	0.15
ZBTB5	rs43424685	1	0.14
CBX3	rs134436580	1	0.14
AQP3	rs134638989, rs134722778, rs133129824	3	0.11
DCAF12	rs133239609, rs136150528, rs133051353, rs137256713, rs136198552, rs135829650	6	0.10
TIGD7	rs42481686, rs42481672, rs137213606, rs135912109, rs135914685, rs109940676, rs137525867, rs109984248, rs110639278, rs133917922, rs43163609, rs43469885, rs110396768, rs110801095, rs110076686, rs110175417, rs110598252, rs109896046, rs137732541, rs109084991, rs110125895, rs110297051, rs110102172, rs135422302, rs108988328, rs110242967, rs134225791, rs110196671, rs136326069, rs108991474, rs135514086, rs133830598, rs133094747, rs133734177, rs109236363, rs110077164, rs135079996, rs109394236, rs134665677, rs136355161, rs42658653, rs136478269, rs134279379, rs134095631, rs41814665, rs109440367, rs136610099, rs110685681, rs109202970, rs110481483, rs110162928, rs29015079,	75	0.07

	rs109777972, rs110851849, rs109167287, rs134981779, rs134155084, rs135311765, rs133666409, rs134993302, rs109486557, rs134309048, rs133528596, rs136160933, rs133525912, rs133731074, rs137552295, rs110063718, rs132914250, rs41646812, rs137740028, rs132684582, rs136764192, rs43708380, rs136547282		

#M8

GS	SNP ID	Number of eQTLs	MM
ANXA1	rs110672259, rs132745513	2	0.89
MARVELD1	rs133097787, rs109504875, rs110686431, rs110225456, rs110170388, rs110672259, rs132745513	7	0.84
MFAP5	rs110279458, rs134407381	2	0.83
ISLR	rs110107165	1	0.82
AEBP1	rs110672259, rs132745513	2	0.81
PCDH18	rs134107947	1	0.79
LOXL2	rs133097787, rs109504875, rs110686431, rs110225456, rs110170388, rs110672259, rs132745513	7	0.78
DKK3	rs110672259, rs132745513	2	0.78
PI16	rs110879640, rs136906228, rs135120313, rs111017844, rs110343243, rs110172601	6	0.77
C3AR1	rs42797051, rs134222862	2	0.76
PLTP	rs137138701, rs42979165, rs110107165	3	0.76
NOV	rs134407381, rs136638558	2	0.76
TNC	rs110672259, rs132745513, rs109768101, rs137266670, rs135246597	5	0.75
C1QC	rs109705986	1	0.75
FRMD4B	rs137571674	1	0.74
CADM3	rs134033375, rs137571674, rs137193443, rs133236731, rs109434434	5	0.73
POSTN	rs109989341, rs134285331, rs109361638	3	0.72
POFUT1	rs109283156	1	0.72
ASPN	rs42821533, rs42470823	2	0.71
EFEMP1	rs41644369	1	0.71
MAMDC2	rs134443065	1	0.70
SFRP4	rs109014733	1	0.70
GPR34	rs42797051	1	0.70
ELN	rs43467652, rs43467654, rs134040217, rs137551818	4	0.69
GPNMB	rs136324176, rs132900853, rs134943975, rs136683910, rs43528002, rs135394759	6	0.68
PTMS	rs110672259, rs132745513	2	0.67
PI15	rs43355292	1	0.66
FMOD	rs109361638	1	0.66
SRC	rs135914685, rs109940676, rs109084991, rs110242967, rs134225791, rs110196671, rs41814665, rs109440367, rs137740028	9	0.65
CPQ	rs134407381, rs110066506, rs137788513, rs132758105, rs132950872	5	0.65

GPR137B	rs109142779	1	0.65
C1S	rs137386793	1	0.65
TUSC3	rs110183484, rs110691616, rs109672446, rs110768883, rs132748517, rs110304994, rs135885169, rs136809650, rs109416677, rs133129904, rs110722390	11	0.64
PHF19	rs109811851, rs43229085	2	0.64
TGIF1	rs134407381	1	0.63
THBS4	rs110668767	1	0.63
LAPTM4A	rs42021922	1	0.60
TENM3	rs137388629	1	0.60
NONO	rs108980319, rs109334365, rs41580349	3	0.60
EXT2	rs43704807	1	0.60
NPTXR	rs137213606, rs109940676, rs137525867, rs109984248, rs43469885, rs134930167, rs109168192, rs108988328, rs110242967, rs134225791, rs110196671, rs136326069, rs108991474, rs135514086, rs133094747, rs42023197, rs42023200, rs42023210, rs134095631, rs133058866, rs41814665, rs109440367, rs110685681, rs134155084, rs135311765, rs133666409, rs134993302, rs109486557, rs134309048, rs137552295, rs132914250, rs41646812, rs137740028, rs43708380	34	0.60
CC2D2A	rs41899523	1	0.59
TIAM1	rs137213606, rs135112808, rs109940676, rs109984248, rs132703816, rs136800085, rs110639278, rs133917922, rs134400660, rs110242967, rs134225791, rs110196671, rs135514086, rs133094747, rs110561011, rs42023200, rs134155084, rs135311765, rs133666409, rs134993302, rs109486557, rs134309048, rs137552295, rs136609253, rs43726953, rs43726967, rs132914250, rs41646812	28	0.58
PLA2G4A	rs110237127, rs110822591, rs110552553, rs137798166	4	0.57
GLMP	rs135914685, rs109984248, rs132703816, rs136800085, rs110639278, rs133917922, rs109084991, rs110242967, rs134225791, rs110196671, rs109440367, rs137740028	12	0.57
LOXL4	rs109418925	1	0.57
TRERF1	rs137571674, rs109434434	2	0.56
AP1S1	rs42008026	1	0.55
F3	rs42320898	1	0.55
GDA	rs109954073, rs134222862	2	0.55
PLVAP	rs132664554	1	0.54
ADCY3	rs135534252, rs42128371, rs109630523	3	0.54
LOXL3	rs110672259, rs132745513	2	0.54
CD5L	rs134611166, rs109129214	2	0.54
GANAB	rs136704898	1	0.53
FUT8	rs135724202, rs110267781, rs135900600, rs109736157, rs136007322, rs109433719, rs133769432, rs109543244, rs135507459, rs134048493	10	0.53
PREX1	rs109984248, rs110639278, rs133917922, rs110242967, rs134225791, rs110196671, rs134095631, rs137740028	8	0.53
SLC6A6	rs42420625, rs42420584, rs110625380, rs42420575, rs110988763, rs109378149, rs135828755, rs133179662, rs41670228, rs135214037, rs43535233, rs110778230, rs136727095, rs134386088, rs42725700, rs137120452,	25	0.52

	rs133147341, rs42726340, rs133509927, rs137530470, rs109043048, rs109142779, rs42845899, rs42846543, rs42087452		
ST6GAL1	rs134794466, rs136202090	2	0.52
MKI67	rs135206448	1	0.52
MLLT11	rs109077994	1	0.51
TMEM181	rs137000874, rs132697398, rs110133118, rs137351885, rs109749964	5	0.51
THBS2	rs136808582, rs134117055	2	0.51
HSD17B12	rs43383299	1	0.50
SERPINB8	rs135534252, rs42128371, rs135950065, rs134047088	4	0.50
NSDHL	rs43771111	1	0.50
KIT	rs110890760, rs133417288, rs133062502, rs134794466, rs136202090, rs134382468	6	0.48
PPM1M	rs137282900	1	0.48
CYB561	rs135914685, rs109440367, rs136609253, rs132684582, rs136764192	5	0.47
ADORA2B	rs134590244, rs41751194, rs137525867, rs109984248, rs132703816, rs136800085, rs110639278, rs133917922, rs43469885, rs110396768, rs110801095, rs110076686, rs110175417, rs110598252, rs109896046, rs137732541, rs109084991, rs108988328, rs110242967, rs134225791, rs110196671, rs133058866, rs134155084, rs135311765, rs133666409, rs134993302, rs109486557, rs134309048, rs137552295, rs137740028	30	0.47
CA5B	rs132876069	1	0.47
PLEKHA4	rs42590304	1	0.46
C1QTNF2	rs108988328	1	0.46
PRG4	rs134186102, rs42965727, rs135470403	3	0.45
PMM2	rs109900921	1	0.45
GPRC5B	rs42061772, rs110784434, rs135914650, rs41649636, rs109628654, rs109797232, rs134923731	7	0.44
ORMDL2	rs135914685, rs43163609, rs42367641, rs134095631, rs136610099, rs137415979	6	0.42
PIP4K2A	rs134095631, rs43726953, rs43726967	3	0.42
ARSB	rs134183339, rs134655709, rs132806081	3	0.41
SLC41A2	rs134098809, rs135932346, rs110118407, rs136335158, rs110534162, rs133671478, rs110753071, rs109267145, rs110531656, rs110691693, rs135241064	11	0.38
NR2F1	rs109130131, rs133338302, rs137726827, rs136449684, rs137414052, rs134226940, rs135706192, rs134020475, rs137585599, rs136174310, rs135062606, rs136196246, rs134528149, rs137756137, rs133552324, rs137416786, rs133131230, rs137182711, rs137587211, rs134637402, rs133432837, rs137353449, rs135798610, rs132976883, rs110576232, rs135464227, rs136211707, rs136877339, rs134597583, rs110879022, rs136790936, rs133505163, rs134996882, rs110800037, rs135481952, rs136646381, rs134587776	37	0.37
ASNS	rs132679084	1	0.37
CYP20A1	rs134721330	1	0.36
RBP1	rs109086298, rs134802067, rs110221626, rs135771377, rs110635609, rs132773879, rs136701923, rs135199890, rs135023705	9	0.36

KIAA1755	rs110805804, rs108938210, rs42032117, rs135387983, rs42032094, rs41642174, rs135430566	7	0.36
PTGDS	rs134887690, rs136715938	2	0.35
SLC2A1	rs110778230	1	0.35
IL33	rs109305478, rs135667132	2	0.35
CHI3L1	rs43054286	1	0.35
TTYH2	rs109744711	1	0.35
PLAT	rs134991491, rs135965367	2	0.34
SBSPON	rs134095631, rs109440367, rs132914250, rs132684582, rs136764192	5	0.33
P3H4	rs41900888, rs41900885	2	0.32
XRCC4	rs109460836	1	0.32
VMAC	rs133383461, rs135306853, rs135980529, rs137822955, rs137425890	5	0.32
SLC2A3	rs134595185	1	0.31
PTI	rs133760272, rs133683314	2	0.31
CAPRIN2	rs41569814, rs136915587	2	0.30
POLA2	rs134625376	1	0.29
PXYLP1	rs42343482	1	0.28
FEZ2	rs133880717	1	0.28
ARSA	rs43230751, rs43231337, rs137740028	3	0.28
ATG4C	rs133895481	1	0.28
PSPH	rs43435359, rs110647357, rs133473528	3	0.27
DMPK	rs133320513, rs137565648, rs109859725, rs109294975	4	0.27
RGMB	rs42108969	1	0.23
RCN2	rs134786139, rs135949030	2	0.23
SIX2	rs135535345, rs43222405, rs43222401, rs42101904, rs42101901	5	0.23
UCHL1	rs135225672, rs110593184, rs132882178	3	0.22
PRSS23	rs136003247, rs109283190, rs134576663, rs134069018	4	0.22
CLDN1	rs134163232, rs137626720, rs133474210, rs136172877, rs109300561, rs132989280	6	0.22
IFT27	rs110274393	1	0.22
BOLA-DQB	rs134510877, rs133707740, rs134857722, rs133360232, rs136760466, rs137652883, rs42089074, rs42089079, rs42089112, rs42089125, rs42097010	11	0.22
CEP170B	rs109811851, rs43229085	2	0.20
CTNS	rs137740028	1	0.17
MCM4	rs43230751, rs43231337, rs137213606, rs43297830, rs135112808, rs110557491, rs109940676, rs109984248, rs132703816, rs136800085, rs110639278, rs133917922, rs109084991, rs108988328, rs110242967, rs134225791, rs110196671, rs133734177, rs109236363, rs110077164, rs135079996, rs109394236, rs134665677, rs136355161, rs42658653, rs41814665, rs108974354, rs109440367, rs110685681, rs137552295	30	0.17
GNPNAT1	rs108946356	1	0.17
ARL10	rs41646812	1	0.16
TMEM98	rs109268270	1	0.16

TSPYL2	rs135914685, rs41814665, rs109440367, rs136547282	4	0.15
CYB5RL	rs109149575	1	0.14
PLP1	rs43631229	1	0.14
C8H9orf64	rs135914685, rs137525867, rs109984248, rs43163609, rs43469885, rs135514086, rs133094747, rs134095631, rs109145948, rs110685681, rs109202970, rs110481483, rs110162928, rs135796971, rs29015079, rs109777972, rs110851849, rs109167287, rs132739394, rs133782336, rs109609827, rs109101895, rs135628919, rs134981779, rs136525838, rs134155084, rs135311765, rs133666409, rs134993302, rs109486557, rs134309048, rs133528596, rs136160933, rs133525912, rs133731074, rs137552295, rs134388814, rs135393467, rs136609253, rs41646812, rs132684582, rs136764192	42	0.14
CYP4B1	rs135374316, rs109133471, rs110365597, rs137706254	4	0.14
NANP	rs110557491, rs135914685, rs109940676, rs43469885, rs110396768, rs110801095, rs110076686, rs109337245, rs108988328, rs110242967, rs134225791, rs110196671, rs110561011, rs134095631, rs137552295, rs132914250	16	0.12
UHRF1	rs110395895	1	0.08
PKMYT1	rs42883301, rs42883266, rs42883257, rs42883250, rs42883245, rs42882317	6	0.07
GDPGP1	rs134590244, rs41751194, rs137213606, rs135112808, rs135912109, rs110557491, rs135914685, rs109940676, rs109984248, rs132703816, rs136800085, rs110639278, rs133917922, rs43163609, rs43469885, rs108988328, rs109158392, rs110242967, rs134225791, rs110196671, rs136326069, rs108991474, rs135514086, rs133094747, rs110077164, rs110561011, rs136478269, rs134279379, rs134095631, rs109440367, rs110685681, rs109202970, rs110481483, rs110162928, rs135796971, rs29015079, rs109777972, rs110851849, rs136925245, rs109167287, rs132739394, rs133782336, rs109609827, rs109101895, rs135628919, rs134981779, rs136525838, rs134155084, rs135311765, rs137781930, rs133666409, rs134993302, rs109486557, rs134309048, rs137044334, rs133528596, rs136160933, rs133525912, rs133731074, rs137552295, rs134388814, rs135393467, rs132914250, rs41646812, rs137740028, rs132684582, rs136764192	67	0.04
ETV4	rs135514086, rs133094747	2	0.03

#M9

GS	SNP ID	Number of eQTLs	MM
ATF3	rs135613815	1	0.85
CTGF	rs110672259, rs132745513	2	0.85
CYR61	rs110672259, rs132745513	2	0.55
FOSL2	rs42239322	1	0.45
ID1	rs136607103, rs136694731	2	0.64
JOSD1	rs133821104, rs109155697, rs109580293	3	0.42
JUN	rs135446069	1	0.59
PPP1R15A	rs109611634, rs133828764	2	0.64
ZBTB48	rs109036198, rs110165235, rs135439773, rs110123180	4	0.50

#M17

GS	SNP ID	Number of eQTLs	MM
SETX	rs137236655, rs134905945	2	0.81
AQR	rs110434008	1	0.80
NEB	rs135092787	1	0.79
BRAF	rs110434008	1	0.78
PBRM1	rs111010838	1	0.77
CNOT1	rs109704475	1	0.76
MTF1	rs110434008	1	0.76
CDK12	rs43771111	1	0.73
ZZEF1	rs137349723, rs135086198	2	0.73
RALGAPB	rs111010838	1	0.72
PGAP1	rs110242967, rs134225791, rs110196671, rs108991474, rs110561011, rs137552295, rs132684582, rs136764192	8	0.72
UBXN7	rs43771111	1	0.72
STRN	rs111010838, rs110434008, rs134133810	3	0.71
ZNF654	rs109704475	1	0.71
ZNF451	rs109940676, rs110242967, rs134225791, rs110196671, rs136326069, rs108991474, rs109236363, rs110077164, rs135079996, rs109394236, rs134665677, rs136355161, rs42658653, rs110561011	14	0.69
PGM2	rs108980319, rs109334365, rs41580349	3	0.69
FBXO28	rs111010838	1	0.68
UTP20	rs110434008	1	0.67
DGKH	rs43415132	1	0.66
CDK13	rs111010838	1	0.66
DPH5	rs109394236, rs134665677	2	0.65
AR	rs110077164, rs110561011	2	0.64
TULP4	rs110610619, rs109927193, rs135955471, rs136662133, rs110181274, rs110052635, rs136325076, rs109428311,	19	0.64

	rs110449318, rs109604010, rs136063329, rs134221143, rs137000874, rs132697398, rs134110001, rs134672623, rs110133118, rs137351885, rs109749964		
CBX5	rs110434008	1	0.63
PREPL	rs43641148	1	0.62
RLF	rs109704475	1	0.62
RB1	rs109704475	1	0.60
PUM2	rs111010838	1	0.60
SP140L	rs136453218, rs135487439, rs136509631	3	0.58
STX17	rs132729161	1	0.58
DHX36	rs109704475	1	0.57
MTO1	rs110561011	1	0.55
RREB1	rs109202742, rs136843777	2	0.55
SETD1B	rs135061608, rs135520464, rs134767414, rs136478269, rs134279379	5	0.55
INPP4B	rs133167990, rs109613896, rs109550465, rs134009722	4	0.55
KIAA1551	rs109266309	1	0.55
DPY19L4	rs109704475	1	0.54
PDE3A	rs136536771	1	0.54
MAP4K5	rs109704475	1	0.53
PCGF5	rs109704475	1	0.53
ZFR	rs135848494, rs135465723, rs42605631	3	0.53
RALGAPA2	rs135061608, rs135520464, rs134767414, rs137110347	4	0.51
INO80	rs111010838	1	0.49
ACVR2A	rs109704475	1	0.48
CASZ1	rs137349723, rs133576521, rs135086198	3	0.48
TECPR2	rs136478269, rs134279379	2	0.48
RYR3	rs110402020	1	0.48
USP42	rs43771111, rs132684582, rs136764192	3	0.47
PLEC	rs42759118	1	0.47
SPRTN	rs109940676, rs110242967, rs134225791, rs110196671, rs109236363, rs110077164, rs135079996, rs109394236, rs134665677, rs136355161, rs42658653, rs134095631, rs132684582, rs136764192	14	0.47
NAPEPLD	rs137349723, rs135086198	2	0.47
ST8SIA5	rs110988763, rs133942318, rs137767832, rs133857779, rs133582460, rs136613449, rs136319392, rs133619698, rs134382634, rs136294542, rs134620797, rs137749121, rs109126156, rs109161732, rs110956243, rs137586132, rs133053112, rs110748721, rs109739082, rs110117548, rs109521826	21	0.44
DSTYK	rs136427596	1	0.43
PLEKHA8	rs134095631	1	0.43
ZNF432	rs110242967, rs134225791, rs110196671, rs110561011	4	0.42
STON2	rs132653901	1	0.42
ZNF407	rs111010838	1	0.42
SAAL1	rs136688415, rs43286577	2	0.40

ZSCAN20	rs136478269, rs134279379, rs43726953	3	0.40
ZNF184	rs137213606, rs135112808, rs135912109, rs109940676, rs109984248, rs110242967, rs134225791, rs110196671, rs136326069, rs108991474, rs109236363, rs110077164, rs135079996, rs109394236, rs134665677, rs136355161, rs42658653, rs110561011, rs136478269, rs134279379, rs134095631, rs110685681, rs110481483, rs110162928, rs134155084, rs135311765, rs133666409, rs134993302, rs109486557, rs134309048, rs137552295, rs134388814, rs135393467, rs132684582, rs136764192, rs43708380	36	0.35
AEBP2	rs43063713, rs111010838	2	0.34
PLAGL2	rs108965205	1	0.34
MAP3K9	rs109084991, rs110242967, rs134225791, rs110196671, rs136326069, rs108991474, rs110077164, rs136478269, rs134279379, rs109440367, rs137740028	11	0.27
TMED6	rs109236363, rs110077164, rs135079996, rs136355161, rs42658653, rs133058866, rs136609253	7	0.24
HMGCS1	rs109704475	1	0.22
PDK1	rs133281809	1	0.17

Supplementary Table 6. Summary of pathway analysis from ClueGo for hub genes.

GOTerm	Group Pvalue	Nr. Genes	Associated Genes Found
Pentose phosphate pathway	0.01	3	[FBP1, G6PD, TKT]
Ubiquitin mediated proteolysis	0.01	6	[BIRC6, HERC1, HERC2, HUWE1, ITCH, UBR5]
Lysine degradation	0.00	6	[ASH1L, KMT2A, KMT2C, KMT2D, LOC540197, PRDM2]
Proteoglycans in cancer	0.00	9	[CAV1, CD44, DCN, FGFR1, FN1, ITGB5, MRAS, MSN, MYC]
Central carbon metabolism in cancer	0.03	3	[FGFR1, G6PD, MYC]
Fatty acid elongation	0.02	3	[ELOVL5, ELOVL6, HACD2]
Biosynthesis of unsaturated fatty acids	0.02	3	[ELOVL5, ELOVL6, HACD2]
Hepatitis B	0.00	9	[CREB5, DDX58, FOS, IFIH1, IRF7, JUN, MYC, TGFB3, YWHAB]
Herpes simplex infection	0.00	9	[DDX58, EIF2AK2, FOS, IFIH1, IRF7, JUN, LOC100139670, OAS1Y, TNFRSF1A]
Colorectal cancer	0.00	4	[FOS, JUN, MYC, TGFB3]
Hepatitis C	0.00	6	[DDX58, EIF2AK2, IRF7, LOC100139670, OAS1Y, TNFRSF1A]
Hepatitis B	0.00	9	[CREB5, DDX58, FOS, IFIH1, IRF7, JUN, MYC, TGFB3, YWHAB]
Measles	0.00	7	[DDX58, EIF2AK2, IFIH1, IRF7, MSN, MX1, OAS1Y]
Influenza A	0.00	9	[DDX58, EIF2AK2, IFIH1, IRF7, JUN, MX1, OAS1Y, RSAD2, TNFRSF1A]
Herpes simplex infection	0.00	9	[DDX58, EIF2AK2, FOS, IFIH1, IRF7, JUN, LOC100139670, OAS1Y, TNFRSF1A]
Glycolysis / Gluconeogenesis	0.00	3	[FBP1, PCK1, PCK2]
Pyruvate metabolism	0.00	3	[ACACA, PCK1, PCK2]
PPAR signaling pathway	0.00	5	[ADIPOQ, FABP4, PCK1, PCK2, PLIN1]
AMPK signaling pathway	0.00	8	[ACACA, ADIPOQ, CREB5, FASN, FBP1, LIPE, PCK1, PCK2]
Insulin signaling pathway	0.00	7	[ACACA, FASN, FBP1, LIPE, PCK1, PCK2, PDE3B]
Adipocytokine signaling pathway	0.00	4	[ADIPOQ, PCK1, PCK2, TNFRSF1A]
Glucagon signaling pathway	0.00	6	[ACACA, CREB5, GNAQ, PCK1, PCK2, PDE3B]
Focal adhesion	0.00	10	[ARHGAP5, CAV1, COL1A1, COL1A2, COL4A1, COL4A2, FN1, ITGB5, JUN, PARVA]

ECM-receptor interaction	0.00	7	[CD44, COL1A1, COL1A2, COL4A1, COL4A2, FN1, ITGB5]
Platelet activation	0.00	8	[COL1A1, COL1A2, COL3A1, FERMT3, GNAI1, GNAI2, GNAQ, LCP2]
Relaxin signaling pathway	0.00	11	[COL1A1, COL1A2, COL3A1, COL4A1, COL4A2, CREB5, FOS, GNAI1, GNAI2, GNG2, JUN]
AGE-RAGE signaling pathway in diabetic complications	0.00	8	[COL1A1, COL1A2, COL3A1, COL4A1, COL4A2, FN1, JUN, TGFB3]
Protein digestion and absorption	0.00	5	[COL1A1, COL1A2, COL3A1, COL4A1, COL4A2]
Amoebiasis	0.00	9	[COL1A1, COL1A2, COL3A1, COL4A1, COL4A2, FN1, GNAQ, ITGB2, TGFB3]
Small cell lung cancer	0.00	5	[COL4A1, COL4A2, FN1, MYC, PTGS2]
Apoptosis	0.00	7	[ATM, CTSK, CTSS, FOS, JUN, SPTAN1, TNFRSF1A]
TGF-beta signaling pathway	0.00	4	[DCN, ID3, MYC, TGFB3]
Osteoclast differentiation	0.00	9	[CTSK, FOS, FOSB, FOSL2, JUN, JUNB, JUND, LCP2, TNFRSF1A]
IL-17 signaling pathway	0.00	5	[FOS, FOSB, JUN, JUND, PTGS2]
TNF signaling pathway	0.00	7	[CREB5, FOS, ITCH, JUN, JUNB, PTGS2, TNFRSF1A]
Dopaminergic synapse	0.00	7	[CREB5, FOS, GNAI1, GNAI2, GNAQ, GNG2, PPP1R1B]
Estrogen signaling pathway	0.00	6	[CREB5, FOS, GNAI1, GNAI2, GNAQ, JUN]
Cocaine addiction	0.00	6	[CREB5, FOSB, GNAI1, GNAI2, JUN, PPP1R1B]
Amphetamine addiction	0.00	5	[CREB5, FOS, FOSB, JUN, PPP1R1B]
Pertussis	0.00	5	[FOS, GNAI1, GNAI2, ITGB2, JUN]
Leishmaniasis	0.00	5	[FOS, ITGB2, JUN, PTGS2, TGFB3]
Chagas disease (American trypanosomiasis)	0.00	7	[FOS, GNAI1, GNAI2, GNAQ, JUN, TGFB3, TNFRSF1A]
Hepatitis B	0.00	9	[CREB5, DDX58, FOS, IFIH1, IRF7, JUN, MYC, TGFB3, YWHAB]
Colorectal cancer	0.00	4	[FOS, JUN, MYC, TGFB3]
Rheumatoid arthritis	0.00	5	[CTSK, FOS, ITGB2, JUN, TGFB3]
Apelin signaling pathway	0.00	8	[GNAI1, GNAI2, GNAQ, GNG2, LIPE, MRAS, PDE3B, PLIN1]
Platelet activation	0.00	8	[COL1A1, COL1A2, COL3A1, FERMT3, GNAI1, GNAI2, GNAQ, LCP2]
TNF signaling pathway	0.00	7	[CREB5, FOS, ITCH, JUN, JUNB, PTGS2, TNFRSF1A]
Leukocyte transendothelial migration	0.00	5	[ARHGAP5, GNAI1, GNAI2, ITGB2, MSN]
Circadian entrainment	0.00	5	[FOS, GNAI1, GNAI2, GNAQ, GNG2]

Cholinergic synapse	0.00	6	[CREB5, FOS, GNAI1, GNAI2, GNAQ, GNG2]
Serotonergic synapse	0.00	5	[GNAI1, GNAI2, GNAQ, GNG2, PTGS2]
Dopaminergic synapse	0.00	7	[CREB5, FOS, GNAI1, GNAI2, GNAQ, GNG2, PPP1R1B]
Long-term depression	0.00	3	[GNAI1, GNAI2, GNAQ]
Estrogen signaling pathway	0.00	6	[CREB5, FOS, GNAI1, GNAI2, GNAQ, JUN]
Regulation of lipolysis in adipocytes	0.00	7	[FABP4, GNAI1, GNAI2, LIPE, PDE3B, PLIN1, PTGS2]
Renin secretion	0.00	4	[GNAI1, GNAI2, GNAQ, PDE3B]
Relaxin signaling pathway	0.00	11	[COL1A1, COL1A2, COL3A1, COL4A1, COL4A2, CREB5, FOS, GNAI1, GNAI2, GNG2, JUN]
AGE-RAGE signaling pathway in diabetic complications	0.00	8	[COL1A1, COL1A2, COL3A1, COL4A1, COL4A2, FN1, JUN, TGFB3]
Gastric acid secretion	0.00	3	[GNAI1, GNAI2, GNAQ]
Protein digestion and absorption	0.00	5	[COL1A1, COL1A2, COL3A1, COL4A1, COL4A2]
Cocaine addiction	0.00	6	[CREB5, FOSB, GNAI1, GNAI2, JUN, PPP1R1B]
Amphetamine addiction	0.00	5	[CREB5, FOS, FOSB, JUN, PPP1R1B]
Morphine addiction	0.00	4	[GNAI1, GNAI2, GNG2, PDE3B]
Pertussis	0.00	5	[FOS, GNAI1, GNAI2, ITGB2, JUN]
Leishmaniasis	0.00	5	[FOS, ITGB2, JUN, PTGS2, TGFB3]
Chagas disease (American trypanosomiasis)	0.00	7	[FOS, GNAI1, GNAI2, GNAQ, JUN, TGFB3, TNFRSF1A]
Toxoplasmosis	0.00	5	[GNAI1, GNAI2, IL10RA, TGFB3, TNFRSF1A]
Amoebiasis	0.00	9	[COL1A1, COL1A2, COL3A1, COL4A1, COL4A2, FN1, GNAQ, ITGB2, TGFB3]
Colorectal cancer	0.00	4	[FOS, JUN, MYC, TGFB3]
Rheumatoid arthritis	0.00	5	[CTSK, FOS, ITGB2, JUN, TGFB3]

SUPPLEMENTARY MATERIAL

Interplay among miR-29 family, mineral metabolism, and gene regulation in muscle

Wellison Jarles da Silva Diniz[1,2,3], Priyanka Banerjee[2#], Gianluca Mazzoni[4#], Luiz Lehmann Coutinho[5], Aline Silva Mello Cesar[5], Juliana Afonso[1], Caio Fernando Gromboni[6], Ana Rita Araújo Nogueira[3], Haja N. Kadarmideen[2], Luciana Correia de Almeida Regitano[3*]

Supplementary Figure S1 Module-trait association analysis.

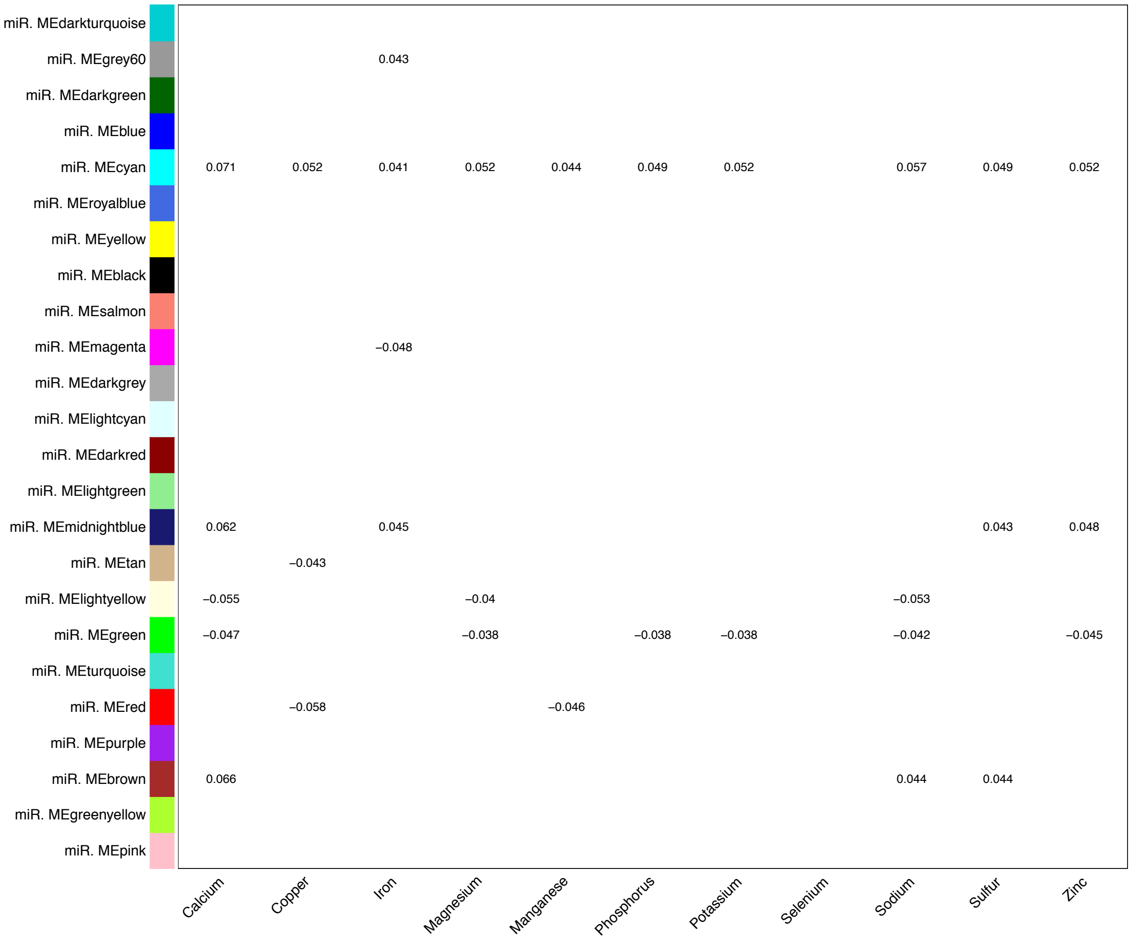

Modules are labeled by color on the y-axis and traits on the x-axis. For significantly associated modules, the coefficient from the linear model is given within the cell. Only associations with $p \leq 0.05$ are shown.

Supplementary Figure S2 Regulatory network of negative miRNA-mRNA pairs in Nelore muscle.

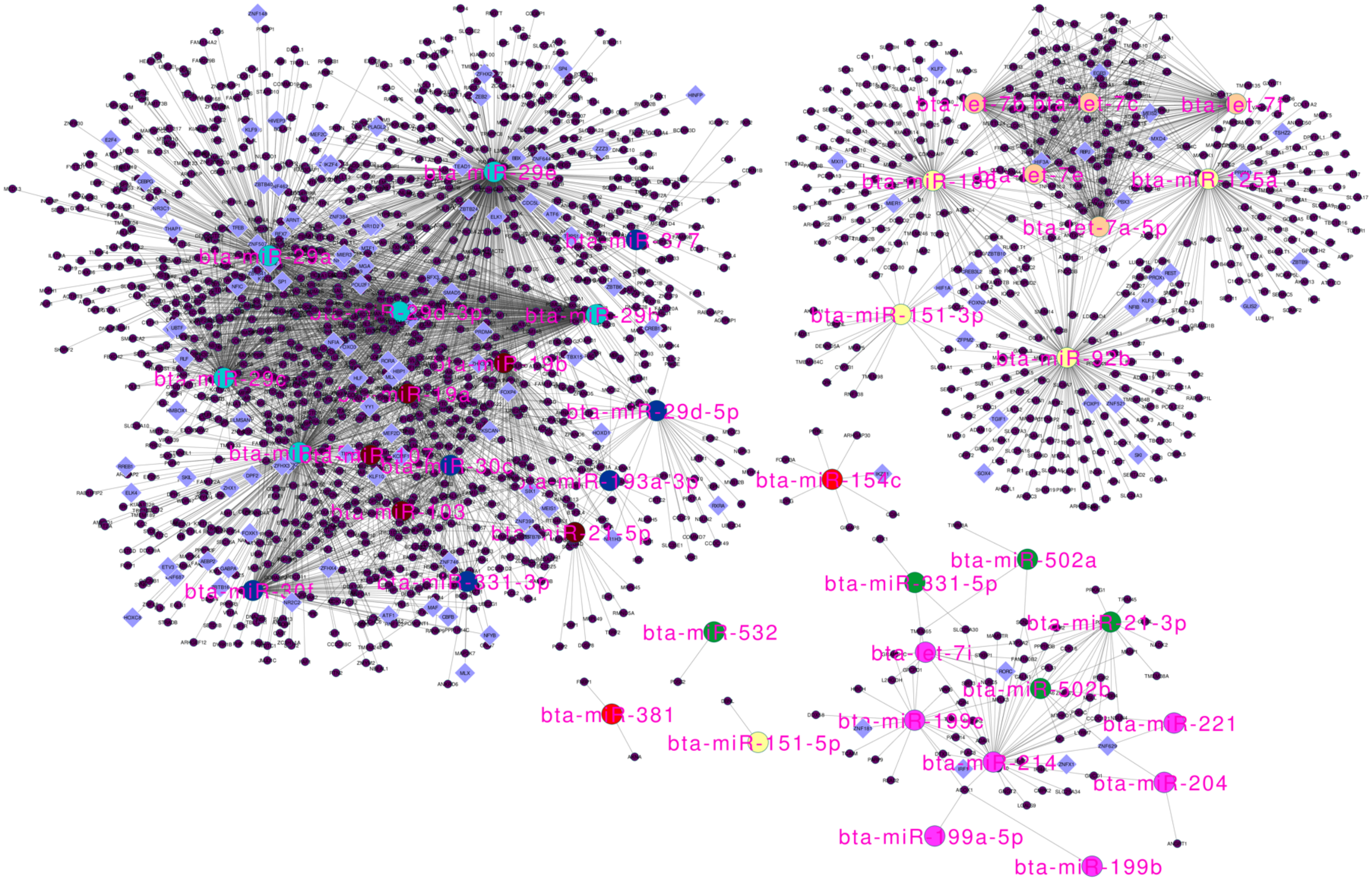

The edges are colored according to miRNA module (miR.MEbrown, miR.MEcyan, miR.MEgreen, miR.MElightyellow, miR.MEmagenta, miR.MEmidnightblue, miR.MEred, and miR.MEtan) Transcription factors are represented by lightpurple diamond shape.

Supplementary Table S1 Summary of the miRNA modules. Total of miRNAs and the proportion of variance explained by the module eigengene (MEs). MiRNA list and module membership (MM) for each selected module. Hub miRNAs are in bold. Spreadsheet tabs are divided by module.

Module	miRNAs	MES	Module	miRNAs	MEs
miR.MEblack	18	0.39	miR.MElightgreen	8	0.42
miR.MEblue	32	0.42	miR.MElightyellow	8	0.50
miR.MEbrown	25	0.35	miR.MEmagenta	17	0.41
miR.MEcyan	10	0.47	miR.MEmidnightblue	9	0.49
miR.MEdarkgreen	5	0.68	miR.MEpink	17	0.47
miR.MEdarkgrey	5	0.57	miR.MEpurple	15	0.51
miR.MEdarkred	5	0.51	miR.MEred	21	0.37
miR.MEdarkturquoise	5	0.53	miR.MEroyalblue	7	0.48
miR.MEgreen	23	0.29	miR.MEsalmon	12	0.51
miR.MEgreenyellow	15	0.39	miR.MEtan	12	0.43
miR.MEgrey60	8	0.54	miR.MEturquoise	34	0.37
miR.MElightcyan	8	0.53	miR.MEyellow	24	0.45

#miR.MEBrown

miRNA	MM	miRNA	MM
bta-miR-19b	**0.90**	bta-miR-145	0.55
bta-miR-19a	**0.89**	bta-miR-106b	0.51
bta-miR-103	**0.83**	bta-miR-93	0.48
bta-miR-107	**0.81**	bta-miR-190a	0.47
bta-miR-21-5p	**0.80**	bta-miR-28	0.46
bta-miR-20a	0.67	bta-miR-181c	0.44
bta-miR-22-5p	0.67	bta-miR-31	0.36
bta-miR-20b	0.64	bta-miR-2284ab	0.34
bta-miR-106a	0.63	bta-miR-2285by	0.34
bta-miR-17-5p	0.62	bta-miR-362-3p	0.33
bta-miR-301a	0.58	bta-miR-542-5p	0.32
bta-miR-455-5p	0.57	bta-miR-33b	0.25
bta-miR-345-5p	0.56		

#miR.MEcyan

miRNA	MM	miRNA	MM
bta-miR-29c	**0.87**	**bta-miR-29e**	**0.72**
bta-miR-29d-3p	**0.86**	bta-miR-499	0.49
bta-miR-29a	**0.80**	bta-miR-374b	0.48
bta-miR-29b	**0.78**	bta-miR-885	0.44
bta-miR-15a	**0.77**	bta-miR-628	0.42

#miR.MEgreen

miRNA	MM	miRNA	MM	miRNA	MM
bta-miR-502a	**0.94**	bta-miR-196b	0.57	bta-miR-483	0.26
bta-miR-502b	**0.93**	bta-miR-2320-5p	0.56	bta-miR-365-5p	0.25
bta-miR-21-3p	**0.78**	bta-miR-769	0.51	bta-miR-11984	0.24
bta-miR-331-5p	**0.76**	bta-miR-196a	0.50	bta-miR-2299-5p	0.23
bta-miR-532	**0.75**	bta-miR-24	0.49	bta-miR-652	0.22
bta-miR-504	0.64	bta-miR-148a	0.38	bta-miR-383	0.17
bta-miR-7180	0.61	bta-miR-503-3p	0.38	bta-miR-105a	0.16
bta-miR-197	0.60	bta-miR-345-3p	0.32		

#miR.MEgrey60

miRNA	MM	miRNA	MM	miRNA	MM
bta-miR-2285aw	**0.90**	**bta-miR-2285g**	**0.78**	bta-miR-2285b	0.65
bta-miR-2285cm	**0.90**	**bta-miR-32**	**0.75**	bta-miR-6123	0.44
bta-miR-2285c	**0.86**	bta-miR-182	0.41		

#miR.MElightyellow

miRNA	MM	miRNA	MM	miRNA	MM
bta-miR-125a	**0.90**	**bta-miR-186**	**0.72**	bta-miR-193a-5p	0.58
bta-miR-151-5p	**0.83**	**bta-miR-92b**	**0.71**	bta-miR-1246	0.36
bta-miR-151-3p	**0.72**	bta-miR-125b	0.69		

#miR.MEmagenta

miRNA	MM	miRNA	MM	miRNA	MM
bta-miR-199c	**0.91**	**bta-miR-204**	**0.71**	bta-miR-3431	0.48
bta-miR-199a-3p	**0.91**	**bta-miR-214**	**0.70**	bta-miR-497	0.46
bta-miR-199a-5p	**0.81**	bta-miR-130a	0.51	bta-miR-224	0.46
bta-let-7i	**0.79**	bta-miR-211	0.51	bta-miR-452	0.43
bta-miR-221	**0.73**	bta-miR-155	0.50	bta-miR-382	0.28
bta-miR-199b	**0.72**	bta-miR-335	0.50		

#miR.MEmidnightblue

miRNA	MM	miRNA	MM	miRNA	MM
bta-miR-30c	**0.84**	**bta-miR-877**	**0.73**	bta-miR-30b-5p	0.70
bta-miR-30f	**0.84**	**bta-miR-331-3p**	**0.71**	bta-miR-365-3p	0.53
bta-miR-193a-3p	**0.74**	**bta-miR-29d-5p**	**0.71**	bta-miR-1306	0.38

#miR.MEred

miRNA	MM	miRNA	MM	miRNA	MM
bta-miR-411a	**0.88**	bta-miR-380-3p	0.67	bta-miR-543	0.41
bta-miR-154c	**0.84**	bta-miR-432	0.66	bta-miR-450b	0.41
bta-miR-381	**0.81**	bta-miR-127	0.65	bta-miR-454	0.40
bta-miR-410	**0.76**	bta-miR-136	0.61	bta-miR-424-3p	0.40
bta-miR-487b	**0.76**	bta-miR-369-5p	0.58	bta-miR-654	0.38
bta-miR-493	0.70	bta-miR-495	0.47	bta-miR-450a	0.38
bta-miR-665	0.69	bta-miR-411c-5p	0.46	bta-miR-299	0.36

#miR.MEtan

miRNA	MM	miRNA	MM	miRNA	MM
bta-let-7c	**0.91**	**bta-let-7f**	**0.78**	bta-miR-222	0.55
bta-let-7e	**0.91**	bta-let-7d	0.59	bta-miR-3432a	0.56
bta-let-7b	**0.84**	bta-miR-11971	0.41	bta-miR-3432b	0.35
bta-let-7a-5p	**0.83**	bta-miR-15b	0.38	bta-miR-574	0.37

Supplementary Table S2 Summary of the miRNA target prediction (TargetScan) and full list of gene targets by module in Nelore muscle.

Module	miRNA	Total of genes from TargetScan	Intersection TargetScan and muscle expression data	miRNA Family
miR.MEbrown (Ca, Na, S)	bta-miR-19b	1233	976	mir-19
	bta-miR-19a	1233	976	mir-19
	bta-miR-103	730	557	mir-103
	bta-miR-107	730	557	mir-103
	bta-miR-21-5p	354	277	mir-21
		Unique targets	1591	
miR.MEcyan (Ca, Cu, Fe, K, Mg, Mn, P,Na, S, Zn)	bta-miR-29c	1176	901	mir-29
	bta-miR-29d-3p	1176	901	mir-29
	bta-miR-29a	2085	1471	mir-29
	bta-miR-29b	1176	901	mir-29
	bta-miR-15a	1380	1047	mir-15
	bta-miR-29e	2929	1978	mir-29
		Unique targets	3811	
miR.MEgreen (Ca, K, Mg, P,Na, Zn)	bta-miR-502a	207	156	mir-500
	bta-miR-502b	2010	1342	mir-500
	bta-miR-21-3p	4743	3322	mir-21
	bta-miR-331-5p	1799	1219	mir-331
	bta-miR-532	223	176	mir-188
		Unique targets	4646	
miR.MElightyellow (Ca, Mg, Na)	bta-miR-125a	846	647	mir-103
	bta-miR-151-5p	16	11	mir-28
	bta-miR-151-3p	97	80	mir-28
	bta-miR-186	852	650	mir-186
	bta-miR-92b	942	723	mir-25
		Unique targets	1788	
miR.MEmagenta (Fe)	bta-miR-199c	3310	2361	mir-199
	bta-miR-199a-3p	426	360	mir-199
	bta-miR-199a-5p	571	455	mir-199
	bta-let-7i	1104	830	let-7
	bta-miR-221	468	360	mir-221
	bta-miR-199b	571	455	mir-199
	bta-miR-204	732	547	mir-204
	bta-miR-214	5086	3449	mir-214
		Unique targets	5492	
miR.MEmidnightblue Cu, Fe, S, Zn)	bta-miR-30c	1463	1134	mir-30
	bta-miR-30f	1456	1134	mir-30
	bta-miR-193a-3p	263	209	mir-193
	bta-miR-877	99	74	mir-877
	bta-miR-331-3p	225	159	mir-331

	bta-miR-29d-5p	444	310	mir-29
		Unique targets	1707	
miR.MEred (Cu, Mg)	bta-miR-411a	138	111	mir-379
	bta-miR-154c	2416	1613	mir-154
	bta-miR-381	781	626	mir-154
	bta-miR-410	578	445	mir-154
	bta-miR-487b	16	13	mir-154
		Unique targets	2372	
miR.MEtan (Cu)	bta-let-7c	1104	830	let-7
	bta-let-7e	1104	830	let-7
	bta-let-7b	1104	830	let-7
	bta-let-7a-5p	1104	830	let-7
	bta-let-7f	1104	830	let-7
		Unique targets	830	
miR.MEgrey60 ** (Fe)	bta-miR-2285aw	No targets	-	*
	bta-miR-2285cm	No targets	-	*
	bta-miR-2285c	2791	1973	mir-2284
	bta-miR-2285g	2791	1973	mir-2284
	bta-miR-32	942	723	mir-32
		Unique targets	2461	

* Not available in miRBase** No correlation was identfied between miR.MEgrey60 ME and mRNA MEs.

Supplementary Table S3 Gene module trait association, gene list, and module membership for the 15 mRNA modules (Supplementary table 3 from chapter 2).

Module	Code - Diniz et al. (2019)	ME	Associated traits
MEblack	M7	0.23	Cr, IMF, Na
MEbrown	M13	0.25	WBSF7
MEcyan	M2	0.43	Cr
MEdarkgrey	M1	0.48	Cr, Co
MEdarkred	M3	0.46	Cr
MEdarkturquoise	M5	0.53	Mn, IMF, Fe, Ca, S, Zn, Na, P, Mg, K
MEgreen	M17	0.36	WBSF7, Co, Mn
MEgreenyellow	M14	0.23	Cr
MEgrey60	M11	0.36	Fe
MElightcyan	M23	0.41	IMF
MElightyellow	M4	0.25	Cr
MEorange	M9	0.39	Cr, IMF
MEroyalblue	M16	0.29	IMF
MEsalmon	M6	0.47	Cr, IMF
MEyellow	M8	0.30	Cr, IMF, Fe, Ca, S, Na, P, Mg, K

Supplementary Table S4 MiRNA-mRNA pairs from the TargetScan prediction and associated mRNAs modules intersection (negatively correlated miRNA-mRNA modules) in Nelore cattle.

GS	miRNA	Module	*GS*	miRNA	Module
AAK1	bta-miR-29a	miR.MEcyan	*CREB3L2*	bta-miR-186	miR.MElightyellow
AAK1	bta-miR-29e	miR.MEcyan	*CREB3L2*	bta-miR-92b	miR.MElightyellow
ABCF1	bta-miR-103	miR.MEbrown	*CREBBP*	bta-miR-29e	miR.MEcyan
ABCF1	bta-miR-107	miR.MEbrown	*CRK*	bta-miR-151-3p	miR.MElightyellow
ABCF1	bta-miR-15a	miR.MEcyan	*CRNKL1*	bta-miR-29e	miR.MEcyan
ABCF1	bta-miR-29e	miR.MEcyan	*CRNKL1*	bta-miR-29d-5p	miR.MEmidnightblue
ABHD2	bta-miR-186	miR.MElightyellow	*CRTC1*	bta-miR-29e	miR.MEcyan
ABL2	bta-miR-15a	miR.MEcyan	*CSDE1*	bta-miR-15a	miR.MEcyan
ABL2	bta-miR-29a	miR.MEcyan	*CSGALNACT2*	bta-miR-29a	miR.MEcyan
ABL2	bta-miR-29e	miR.MEcyan	*CSGALNACT2*	bta-miR-29b	miR.MEcyan
ACER2	bta-miR-125a	miR.MElightyellow	*CSGALNACT2*	bta-miR-29c	miR.MEcyan
ACER2	bta-let-7c	miR.MEtan	*CSGALNACT2*	bta-miR-29d-3p	miR.MEcyan
ACER2	bta-let-7e	miR.MEtan	*CTBP2*	bta-miR-29e	miR.MEcyan
ACER2	bta-let-7b	miR.MEtan	*CTIF*	bta-miR-29e	miR.MEcyan
ACER2	bta-let-7a-5p	miR.MEtan	*CTIF*	bta-miR-193a-3p	miR.MEmidnightblue
ACER2	bta-let-7f	miR.MEtan	*CTNNBL1*	bta-miR-15a	miR.MEcyan
ACVR2A	bta-miR-15a	miR.MEcyan	*CTNS*	bta-miR-186	miR.MElightyellow
ACVR2A	bta-miR-29b	miR.MEcyan	*CTNS*	bta-let-7c	miR.MEtan
ACVR2A	bta-miR-29c	miR.MEcyan	*CTNS*	bta-let-7e	miR.MEtan
ACVR2A	bta-miR-29d-3p	miR.MEcyan	*CTNS*	bta-let-7b	miR.MEtan
ACVR2A	bta-miR-29e	miR.MEcyan	*CTNS*	bta-let-7a-5p	miR.MEtan
ADAMTS17	bta-let-7c	miR.MEtan	*CTNS*	bta-let-7f	miR.MEtan
ADAMTS17	bta-let-7e	miR.MEtan	*CUL2*	bta-miR-15a	miR.MEcyan
ADAMTS17	bta-let-7b	miR.MEtan	*CUL2*	bta-miR-29e	miR.MEcyan
ADAMTS17	bta-let-7a-5p	miR.MEtan	*CUL2*	bta-miR-30c	miR.MEmidnightblue
ADAMTS17	bta-let-7f	miR.MEtan	*CUL2*	bta-miR-30f	miR.MEmidnightblue
ADAMTS20	bta-miR-29b	miR.MEcyan	*CUL3*	bta-miR-29e	miR.MEcyan
ADAMTS20	bta-miR-29c	miR.MEcyan	*CUL4A*	bta-miR-29a	miR.MEcyan
ADAMTS20	bta-miR-29d-3p	miR.MEcyan	*CYTH3*	bta-miR-29b	miR.MEcyan
AEBP2	bta-miR-15a	miR.MEcyan	*CYTH3*	bta-miR-29c	miR.MEcyan
AFF1	bta-miR-29e	miR.MEcyan	*CYTH3*	bta-miR-29d-3p	miR.MEcyan
AFF4	bta-miR-15a	miR.MEcyan	*DAAM1*	bta-miR-125a	miR.MElightyellow
AFF4	bta-miR-29a	miR.MEcyan	*DAAM1*	bta-miR-92b	miR.MElightyellow
AFF4	bta-miR-29b	miR.MEcyan	*DBNL*	bta-miR-151-5p	miR.MElightyellow
AFF4	bta-miR-29c	miR.MEcyan	*DCAKD*	bta-miR-29b	miR.MEcyan
AFF4	bta-miR-29d-3p	miR.MEcyan	*DCAKD*	bta-miR-29c	miR.MEcyan
AFF4	bta-miR-29e	miR.MEcyan	*DCAKD*	bta-miR-29d-3p	miR.MEcyan
AGO1	bta-miR-15a	miR.MEcyan	*DCAKD*	bta-miR-29e	miR.MEcyan
AGO1	bta-miR-29a	miR.MEcyan	*DCUN1D5*	bta-miR-29a	miR.MEcyan

AGO1	bta-miR-29b	miR.MEcyan	*DCUN1D5*	bta-miR-29b	miR.MEcyan
AGO1	bta-miR-29c	miR.MEcyan	*DCUN1D5*	bta-miR-29c	miR.MEcyan
AGO1	bta-miR-29d-3p	miR.MEcyan	*DCUN1D5*	bta-miR-29d-3p	miR.MEcyan
AGO1	bta-miR-29e	miR.MEcyan	*DCUN1D5*	bta-miR-29e	miR.MEcyan
AGO2	bta-miR-15a	miR.MEcyan	*DDX19B*	bta-miR-15a	miR.MEcyan
AGO2	bta-miR-29a	miR.MEcyan	*DDX19B*	bta-miR-30c	miR.MEmidnightblue
AGO2	bta-miR-29b	miR.MEcyan	*DDX19B*	bta-miR-30f	miR.MEmidnightblue
AGO2	bta-miR-29c	miR.MEcyan	*DDX20*	bta-miR-29e	miR.MEcyan
AGO2	bta-miR-29d-3p	miR.MEcyan	*DDX39A*	bta-miR-15a	miR.MEcyan
AGO2	bta-miR-29e	miR.MEcyan	*DDX46*	bta-miR-29b	miR.MEcyan
AGO2	bta-miR-30c	miR.MEmidnightblue	*DDX46*	bta-miR-29c	miR.MEcyan
AGO2	bta-miR-30f	miR.MEmidnightblue	*DDX46*	bta-miR-29d-3p	miR.MEcyan
AGO3	bta-miR-15a	miR.MEcyan	*DDX54*	bta-miR-15a	miR.MEcyan
AGO3	bta-miR-29a	miR.MEcyan	*DDX58*	bta-miR-199c	miR.MEmagenta
AGO3	bta-miR-29b	miR.MEcyan	*DEDD*	bta-miR-15a	miR.MEcyan
AGO3	bta-miR-29c	miR.MEcyan	*DEDD*	bta-miR-29b	miR.MEcyan
AGO3	bta-miR-29d-3p	miR.MEcyan	*DEDD*	bta-miR-29c	miR.MEcyan
AGO3	bta-miR-29e	miR.MEcyan	*DEDD*	bta-miR-29d-3p	miR.MEcyan
AGO4	bta-miR-15a	miR.MEcyan	*DENND4A*	bta-miR-15a	miR.MEcyan
AGO4	bta-miR-29e	miR.MEcyan	*DENND5B*	bta-miR-29a	miR.MEcyan
AGPAT5	bta-miR-19a	miR.MEbrown	*DENND5B*	bta-miR-29b	miR.MEcyan
AGPAT5	bta-miR-19b	miR.MEbrown	*DENND5B*	bta-miR-29c	miR.MEcyan
AGPAT5	bta-miR-29e	miR.MEcyan	*DENND5B*	bta-miR-29d-3p	miR.MEcyan
AIDA	bta-miR-92b	miR.MElightyellow	*DENR*	bta-miR-29a	miR.MEcyan
AKIRIN1	bta-miR-21-5p	miR.MEbrown	*DESI1*	bta-miR-15a	miR.MEcyan
AKIRIN1	bta-miR-15a	miR.MEcyan	*DESI1*	bta-miR-331-3p	miR.MEmidnightblue
AKIRIN1	bta-miR-30c	miR.MEmidnightblue	*DHX36*	bta-miR-29a	miR.MEcyan
AKIRIN1	bta-miR-30f	miR.MEmidnightblue	*DIMT1*	bta-miR-29e	miR.MEcyan
AKT3	bta-miR-125a	miR.MElightyellow	*DIP2B*	bta-miR-29b	miR.MEcyan
AKT3	bta-miR-151-3p	miR.MElightyellow	*DIP2B*	bta-miR-29c	miR.MEcyan
AKT3	bta-miR-186	miR.MElightyellow	*DIP2B*	bta-miR-29d-3p	miR.MEcyan
ANKFY1	bta-miR-15a	miR.MEcyan	*DKK1*	bta-miR-29a	miR.MEcyan
ANKFY1	bta-miR-29e	miR.MEcyan	*DKK3*	bta-miR-92b	miR.MElightyellow
ANKIB1	bta-miR-15a	miR.MEcyan	*DKK3*	bta-let-7c	miR.MEtan
ANKRD13C	bta-miR-19a	miR.MEbrown	*DKK3*	bta-let-7e	miR.MEtan
ANKRD13C	bta-miR-19b	miR.MEbrown	*DKK3*	bta-let-7b	miR.MEtan
ANKRD13C	bta-miR-29a	miR.MEcyan	*DKK3*	bta-let-7a-5p	miR.MEtan
ANKRD13C	bta-miR-29b	miR.MEcyan	*DKK3*	bta-let-7f	miR.MEtan
ANKRD13C	bta-miR-29c	miR.MEcyan	*DMD*	bta-miR-29e	miR.MEcyan
ANKRD13C	bta-miR-29d-3p	miR.MEcyan	*DNAJB2*	bta-miR-15a	miR.MEcyan
ANKRD13C	bta-miR-29e	miR.MEcyan	*DNAJC1*	bta-miR-29e	miR.MEcyan
ANKRD52	bta-miR-29a	miR.MEcyan	*DNAJC10*	bta-miR-29e	miR.MEcyan
ANKRD52	bta-miR-29b	miR.MEcyan	*DNAJC28*	bta-miR-29e	miR.MEcyan

ANKRD52	bta-miR-29c	miR.MEcyan	*DNAJC30*	bta-miR-29a	miR.MEcyan
ANKRD52	bta-miR-29d-3p	miR.MEcyan	*DNPEP*	bta-miR-29a	miR.MEcyan
ANKRD52	bta-miR-29e	miR.MEcyan	*DOCK5*	bta-miR-92b	miR.MElightyellow
AP5M1	bta-miR-29e	miR.MEcyan	*DPF2*	bta-miR-15a	miR.MEcyan
APBA1	bta-let-7c	miR.MEtan	*DPH1*	bta-miR-29a	miR.MEcyan
APBA1	bta-let-7e	miR.MEtan	*DPH3*	bta-miR-29a	miR.MEcyan
APBA1	bta-let-7b	miR.MEtan	*DPH5*	bta-miR-15a	miR.MEcyan
APBA1	bta-let-7a-5p	miR.MEtan	*DPP9*	bta-miR-15a	miR.MEcyan
APBA1	bta-let-7f	miR.MEtan	*DPP9*	bta-miR-331-3p	miR.MEmidnightblue
APPBP2	bta-miR-29b	miR.MEcyan	*DPY19L4*	bta-miR-15a	miR.MEcyan
APPBP2	bta-miR-29c	miR.MEcyan	*DSTYK*	bta-miR-29e	miR.MEcyan
APPBP2	bta-miR-29d-3p	miR.MEcyan	*DTWD2*	bta-miR-29a	miR.MEcyan
APPL1	bta-miR-29e	miR.MEcyan	*DTWD2*	bta-miR-29b	miR.MEcyan
AR	bta-miR-29e	miR.MEcyan	*DTWD2*	bta-miR-29c	miR.MEcyan
ARHGAP35	bta-miR-29a	miR.MEcyan	*DTWD2*	bta-miR-29d-3p	miR.MEcyan
ARHGAP35	bta-miR-29e	miR.MEcyan	*DTX4*	bta-miR-125a	miR.MElightyellow
ARHGAP35	bta-miR-877	miR.MEmidnightblue	*DTX4*	bta-let-7c	miR.MEtan
ARHGAP5	bta-miR-15a	miR.MEcyan	*DTX4*	bta-let-7e	miR.MEtan
ARHGAP5	bta-miR-29e	miR.MEcyan	*DTX4*	bta-let-7b	miR.MEtan
ARHGEF12	bta-miR-15a	miR.MEcyan	*DTX4*	bta-let-7a-5p	miR.MEtan
ARID2	bta-miR-29e	miR.MEcyan	*DTX4*	bta-let-7f	miR.MEtan
ARIH2	bta-miR-103	miR.MEbrown	*DUSP3*	bta-miR-29e	miR.MEcyan
ARIH2	bta-miR-107	miR.MEbrown	*DUSP6*	bta-miR-125a	miR.MElightyellow
ARIH2	bta-miR-29e	miR.MEcyan	*DUSP6*	bta-miR-92b	miR.MElightyellow
ARL8A	bta-miR-103	miR.MEbrown	*DYRK1B*	bta-miR-15a	miR.MEcyan
ARL8A	bta-miR-107	miR.MEbrown	*DZIP1*	bta-let-7c	miR.MEtan
ARL8A	bta-miR-19a	miR.MEbrown	*DZIP1*	bta-let-7e	miR.MEtan
ARL8A	bta-miR-19b	miR.MEbrown	*DZIP1*	bta-let-7b	miR.MEtan
ARL8A	bta-miR-29e	miR.MEcyan	*DZIP1*	bta-let-7a-5p	miR.MEtan
ARMC1	bta-miR-92b	miR.MElightyellow	*DZIP1*	bta-let-7f	miR.MEtan
ARMC10	bta-miR-186	miR.MElightyellow	*E2F4*	bta-miR-29a	miR.MEcyan
ARMC8	bta-miR-15a	miR.MEcyan	*EDEM1*	bta-miR-125a	miR.MElightyellow
ARMC8	bta-miR-29a	miR.MEcyan	*EDEM1*	bta-miR-186	miR.MElightyellow
ARMC8	bta-miR-29b	miR.MEcyan	*EDEM1*	bta-miR-92b	miR.MElightyellow
ARMC8	bta-miR-29c	miR.MEcyan	*EGLN1*	bta-miR-15a	miR.MEcyan
ARMC8	bta-miR-29d-3p	miR.MEcyan	*EIF2AK2*	bta-miR-199c	miR.MEmagenta
ARNT	bta-miR-29b	miR.MEcyan	*EIF2AK2*	bta-miR-214	miR.MEmagenta
ARNT	bta-miR-29c	miR.MEcyan	*EIF2B5*	bta-miR-15a	miR.MEcyan
ARNT	bta-miR-29d-3p	miR.MEcyan	*EIF2S2*	bta-miR-29a	miR.MEcyan
ARNT	bta-miR-29e	miR.MEcyan	*EIF2S2*	bta-miR-29b	miR.MEcyan
ARPC5L	bta-miR-103	miR.MEbrown	*EIF2S2*	bta-miR-29c	miR.MEcyan
ARPC5L	bta-miR-107	miR.MEbrown	*EIF2S2*	bta-miR-29d-3p	miR.MEcyan
ARRDC3	bta-miR-92b	miR.MElightyellow	*EIF2S2*	bta-miR-29e	miR.MEcyan

ASH1L	bta-miR-15a	miR.MEcyan	*EIF3J*	bta-miR-29a	miR.MEcyan
ASNA1	bta-miR-19a	miR.MEbrown	*EIF3J*	bta-miR-29b	miR.MEcyan
ASNA1	bta-miR-19b	miR.MEbrown	*EIF3J*	bta-miR-29c	miR.MEcyan
ASXL2	bta-miR-29a	miR.MEcyan	*EIF3J*	bta-miR-29d-3p	miR.MEcyan
ASXL2	bta-miR-29e	miR.MEcyan	*EIF4E2*	bta-miR-29a	miR.MEcyan
ATAD2B	bta-miR-29a	miR.MEcyan	*EIF4E2*	bta-miR-29b	miR.MEcyan
ATAD2B	bta-miR-29b	miR.MEcyan	*EIF4E2*	bta-miR-29c	miR.MEcyan
ATAD2B	bta-miR-29c	miR.MEcyan	*EIF4E2*	bta-miR-29d-3p	miR.MEcyan
ATAD2B	bta-miR-29d-3p	miR.MEcyan	*EIF4H*	bta-miR-15a	miR.MEcyan
ATAD2B	bta-miR-29e	miR.MEcyan	*EIF4H*	bta-miR-29e	miR.MEcyan
ATF7IP	bta-miR-29a	miR.MEcyan	*EIF5A*	bta-miR-15a	miR.MEcyan
ATG4D	bta-miR-19a	miR.MEbrown	*ELK1*	bta-miR-29a	miR.MEcyan
ATG4D	bta-miR-19b	miR.MEbrown	*ELK1*	bta-miR-29e	miR.MEcyan
ATP2A2	bta-miR-21-3p	miR.MEgreen	*ELMSAN1*	bta-miR-15a	miR.MEcyan
ATP2A2	bta-let-7i	miR.MEmagenta	*ELMSAN1*	bta-miR-29b	miR.MEcyan
ATP2A2	bta-miR-214	miR.MEmagenta	*ELMSAN1*	bta-miR-29c	miR.MEcyan
ATP2B2	bta-miR-19a	miR.MEbrown	*ELMSAN1*	bta-miR-29d-3p	miR.MEcyan
ATP2B2	bta-miR-19b	miR.MEbrown	*EMC10*	bta-miR-29a	miR.MEcyan
ATP2B2	bta-miR-15a	miR.MEcyan	*EMC10*	bta-miR-29e	miR.MEcyan
ATP2B2	bta-miR-29b	miR.MEcyan	*EMC2*	bta-miR-29e	miR.MEcyan
ATP2B2	bta-miR-29c	miR.MEcyan	*EMC8*	bta-miR-29e	miR.MEcyan
ATP2B2	bta-miR-29d-3p	miR.MEcyan	*EML4*	bta-miR-29b	miR.MEcyan
ATP2B2	bta-miR-29e	miR.MEcyan	*EML4*	bta-miR-29c	miR.MEcyan
ATP2B2	bta-miR-30c	miR.MEmidnightblue	*EML4*	bta-miR-29d-3p	miR.MEcyan
ATP2B2	bta-miR-30f	miR.MEmidnightblue	*EML4*	bta-miR-29e	miR.MEcyan
ATXN1	bta-miR-29b	miR.MEcyan	*ENHO*	bta-miR-29a	miR.MEcyan
ATXN1	bta-miR-29c	miR.MEcyan	*ENHO*	bta-miR-29b	miR.MEcyan
ATXN1	bta-miR-29d-3p	miR.MEcyan	*ENHO*	bta-miR-29c	miR.MEcyan
ATXN1L	bta-miR-15a	miR.MEcyan	*ENHO*	bta-miR-29d-3p	miR.MEcyan
ATXN1L	bta-miR-29a	miR.MEcyan	*ENTPD5*	bta-miR-92b	miR.MElightyellow
ATXN1L	bta-miR-29e	miR.MEcyan	*EPM2A*	bta-miR-29e	miR.MEcyan
AVL9	bta-miR-15a	miR.MEcyan	*ERC1*	bta-miR-29a	miR.MEcyan
AVL9	bta-miR-29a	miR.MEcyan	*ERC1*	bta-miR-29b	miR.MEcyan
AZIN1	bta-miR-186	miR.MElightyellow	*ERC1*	bta-miR-29c	miR.MEcyan
AZIN1	bta-miR-92b	miR.MElightyellow	*ERC1*	bta-miR-29d-3p	miR.MEcyan
B4GALT2	bta-miR-19a	miR.MEbrown	*ERGIC2*	bta-miR-29e	miR.MEcyan
B4GALT2	bta-miR-19b	miR.MEbrown	*ERI1*	bta-miR-29e	miR.MEcyan
B4GALT2	bta-miR-331-3p	miR.MEmidnightblue	*ERN1*	bta-miR-29e	miR.MEcyan
BACE1	bta-miR-19a	miR.MEbrown	*ESRP2*	bta-miR-29a	miR.MEcyan
BACE1	bta-miR-19b	miR.MEbrown	*ETNK1*	bta-miR-15a	miR.MEcyan
BACE1	bta-miR-15a	miR.MEcyan	*EVI5*	bta-miR-92b	miR.MElightyellow
BACE1	bta-miR-29a	miR.MEcyan	*EXOC7*	bta-miR-29b	miR.MEcyan
BACE1	bta-miR-29b	miR.MEcyan	*EXOC7*	bta-miR-29c	miR.MEcyan

BACE1	bta-miR-29c	miR.MEcyan
BACE1	bta-miR-29d-3p	miR.MEcyan
BACE1	bta-miR-29e	miR.MEcyan
BAZ2A	bta-miR-15a	miR.MEcyan
BAZ2A	bta-miR-29e	miR.MEcyan
BCAS3	bta-miR-19a	miR.MEbrown
BCAS3	bta-miR-19b	miR.MEbrown
BCAS3	bta-miR-21-5p	miR.MEbrown
BCAS3	bta-miR-29d-5p	miR.MEmidnightblue
BCKDK	bta-miR-103	miR.MEbrown
BCKDK	bta-miR-107	miR.MEbrown
BCL2L13	bta-miR-103	miR.MEbrown
BCL2L13	bta-miR-107	miR.MEbrown
BEND3	bta-miR-29e	miR.MEcyan
BEND3	bta-miR-30c	miR.MEmidnightblue
BEND3	bta-miR-30f	miR.MEmidnightblue
BLMH	bta-miR-103	miR.MEbrown
BLMH	bta-miR-107	miR.MEbrown
BLMH	bta-miR-29b	miR.MEcyan
BLMH	bta-miR-29c	miR.MEcyan
BLMH	bta-miR-29d-3p	miR.MEcyan
BNIP2	bta-miR-29e	miR.MEcyan
BPTF	bta-miR-15a	miR.MEcyan
BPTF	bta-miR-29a	miR.MEcyan
BRWD1	bta-miR-29a	miR.MEcyan
BRWD1	bta-miR-29b	miR.MEcyan
BRWD1	bta-miR-29c	miR.MEcyan
BRWD1	bta-miR-29d-3p	miR.MEcyan
BRWD1	bta-miR-29e	miR.MEcyan
BRWD3	bta-miR-29b	miR.MEcyan
BRWD3	bta-miR-29c	miR.MEcyan
BRWD3	bta-miR-29d-3p	miR.MEcyan
BTAF1	bta-miR-15a	miR.MEcyan
BTBD7	bta-miR-29a	miR.MEcyan
BTBD7	bta-miR-29b	miR.MEcyan
BTBD7	bta-miR-29c	miR.MEcyan
BTBD7	bta-miR-29d-3p	miR.MEcyan
BTF3L4	bta-miR-19a	miR.MEbrown
BTF3L4	bta-miR-19b	miR.MEbrown
CACNA2D1	bta-miR-15a	miR.MEcyan
CACNA2D1	bta-miR-29e	miR.MEcyan
CACUL1	bta-miR-15a	miR.MEcyan
CACUL1	bta-miR-29e	miR.MEcyan
EXOC7	bta-miR-29d-3p	miR.MEcyan
EXOC7	bta-miR-331-3p	miR.MEmidnightblue
EXOC8	bta-miR-29a	miR.MEcyan
EXOC8	bta-miR-29e	miR.MEcyan
EXOSC9	bta-miR-29a	miR.MEcyan
EXT2	bta-miR-186	miR.MElightyellow
FADS1	bta-miR-151-3p	miR.MElightyellow
FAF1	bta-miR-15a	miR.MEcyan
FAM114A2	bta-miR-29a	miR.MEcyan
FAM120A	bta-miR-29e	miR.MEcyan
FAM122A	bta-miR-15a	miR.MEcyan
FAM122A	bta-miR-29a	miR.MEcyan
FAM126A	bta-miR-186	miR.MElightyellow
FAM135A	bta-miR-15a	miR.MEcyan
FAM160B1	bta-miR-15a	miR.MEcyan
FAM160B1	bta-miR-29a	miR.MEcyan
FAM160B1	bta-miR-29e	miR.MEcyan
FAM160B2	bta-miR-21-3p	miR.MEgreen
FAM160B2	bta-let-7i	miR.MEmagenta
FAM160B2	bta-miR-214	miR.MEmagenta
FAM173B	bta-miR-29a	miR.MEcyan
FAM199X	bta-miR-15a	miR.MEcyan
FAM199X	bta-miR-29a	miR.MEcyan
FAM20B	bta-miR-29a	miR.MEcyan
FAM20B	bta-miR-29e	miR.MEcyan
FAM213A	bta-miR-29a	miR.MEcyan
FAM229B	bta-miR-29a	miR.MEcyan
FAM89B	bta-miR-29e	miR.MEcyan
FAM98C	bta-miR-29e	miR.MEcyan
FANCM	bta-miR-29a	miR.MEcyan
FAR1	bta-miR-29a	miR.MEcyan
FAXC	bta-miR-29a	miR.MEcyan
FAXC	bta-miR-29b	miR.MEcyan
FAXC	bta-miR-29c	miR.MEcyan
FAXC	bta-miR-29d-3p	miR.MEcyan
FAXC	bta-miR-29e	miR.MEcyan
FBN1	bta-miR-92b	miR.MElightyellow
FBXL18	bta-miR-29a	miR.MEcyan
FBXL18	bta-miR-29b	miR.MEcyan
FBXL18	bta-miR-29c	miR.MEcyan
FBXL18	bta-miR-29d-3p	miR.MEcyan
FBXO31	bta-miR-29e	miR.MEcyan
FBXO42	bta-miR-29b	miR.MEcyan

CALD1	bta-miR-151-3p	miR.MElightyellow	*FBXO42*	bta-miR-29c	miR.MEcyan
CALD1	bta-miR-92b	miR.MElightyellow	*FBXO42*	bta-miR-29d-3p	miR.MEcyan
CALM1	bta-miR-19a	miR.MEbrown	*FBXO7*	bta-miR-29a	miR.MEcyan
CALM1	bta-miR-19b	miR.MEbrown	*FBXW2*	bta-miR-29a	miR.MEcyan
CALM1	bta-miR-15a	miR.MEcyan	*FBXW2*	bta-miR-29b	miR.MEcyan
CALM1	bta-miR-193a-3p	miR.MEmidnightblue	*FBXW2*	bta-miR-29c	miR.MEcyan
CALU	bta-let-7c	miR.MEtan	*FBXW2*	bta-miR-29d-3p	miR.MEcyan
CALU	bta-let-7e	miR.MEtan	*FEM1A*	bta-miR-29a	miR.MEcyan
CALU	bta-let-7b	miR.MEtan	*FEM1B*	bta-miR-29a	miR.MEcyan
CALU	bta-let-7a-5p	miR.MEtan	*FEM1B*	bta-miR-29b	miR.MEcyan
CALU	bta-let-7f	miR.MEtan	*FEM1B*	bta-miR-29c	miR.MEcyan
CAND1	bta-miR-29b	miR.MEcyan	*FEM1B*	bta-miR-29d-3p	miR.MEcyan
CAND1	bta-miR-29c	miR.MEcyan	*FGFR1OP*	bta-miR-29e	miR.MEcyan
CAND1	bta-miR-29d-3p	miR.MEcyan	*FILIP1*	bta-miR-29e	miR.MEcyan
CAPZA2	bta-miR-103	miR.MEbrown	*FIP1L1*	bta-miR-29e	miR.MEcyan
CAPZA2	bta-miR-107	miR.MEbrown	*FKBP10*	bta-let-7c	miR.MEtan
CAPZA2	bta-miR-15a	miR.MEcyan	*FKBP10*	bta-let-7e	miR.MEtan
CARM1	bta-miR-103	miR.MEbrown	*FKBP10*	bta-let-7b	miR.MEtan
CARM1	bta-miR-107	miR.MEbrown	*FKBP10*	bta-let-7a-5p	miR.MEtan
CARM1	bta-miR-15a	miR.MEcyan	*FKBP10*	bta-let-7f	miR.MEtan
CASK	bta-miR-186	miR.MElightyellow	*FKBP14*	bta-miR-186	miR.MElightyellow
CASK	bta-miR-92b	miR.MElightyellow	*FKBP14*	bta-miR-92b	miR.MElightyellow
CAST	bta-miR-15a	miR.MEcyan	*FKBP4*	bta-miR-29a	miR.MEcyan
CBFB	bta-miR-30c	miR.MEmidnightblue	*FKBP4*	bta-miR-29b	miR.MEcyan
CBFB	bta-miR-30f	miR.MEmidnightblue	*FKBP4*	bta-miR-29c	miR.MEcyan
CC2D1A	bta-miR-19a	miR.MEbrown	*FKBP4*	bta-miR-29d-3p	miR.MEcyan
CC2D1A	bta-miR-19b	miR.MEbrown	*FKBP4*	bta-miR-29e	miR.MEcyan
CCDC6	bta-miR-19a	miR.MEbrown	*FKTN*	bta-miR-29e	miR.MEcyan
CCDC6	bta-miR-19b	miR.MEbrown	*FNIP2*	bta-miR-92b	miR.MElightyellow
CCDC6	bta-miR-15a	miR.MEcyan	*FOCAD*	bta-miR-29e	miR.MEcyan
CCDC6	bta-miR-30c	miR.MEmidnightblue	*FOXK1*	bta-miR-15a	miR.MEcyan
CCDC6	bta-miR-30f	miR.MEmidnightblue	*FOXN2*	bta-miR-186	miR.MElightyellow
CCNE1	bta-miR-103	miR.MEbrown	*FOXN2*	bta-miR-92b	miR.MElightyellow
CCNE1	bta-miR-107	miR.MEbrown	*FOXO3*	bta-miR-29b	miR.MEcyan
CCNE1	bta-miR-15a	miR.MEcyan	*FOXO3*	bta-miR-29c	miR.MEcyan
CCNYL1	bta-miR-103	miR.MEbrown	*FOXO3*	bta-miR-29d-3p	miR.MEcyan
CCNYL1	bta-miR-107	miR.MEbrown	*FOXO3*	bta-miR-29e	miR.MEcyan
CCNYL1	bta-miR-15a	miR.MEcyan	*FOXO3*	bta-miR-30c	miR.MEmidnightblue
CCNYL1	bta-miR-29b	miR.MEcyan	*FOXO3*	bta-miR-30f	miR.MEmidnightblue
CCNYL1	bta-miR-29c	miR.MEcyan	*FOXP4*	bta-miR-29e	miR.MEcyan
CCNYL1	bta-miR-29d-3p	miR.MEcyan	*FOXP4*	bta-miR-30c	miR.MEmidnightblue
CCSER2	bta-miR-29a	miR.MEcyan	*FOXP4*	bta-miR-30f	miR.MEmidnightblue
CCSER2	bta-miR-29b	miR.MEcyan	*FRAT2*	bta-miR-29a	miR.MEcyan

CCSER2	bta-miR-29c	miR.MEcyan
CCSER2	bta-miR-29d-3p	miR.MEcyan
CCSER2	bta-miR-29e	miR.MEcyan
CD164	bta-miR-19a	miR.MEbrown
CD164	bta-miR-19b	miR.MEbrown
CD164	bta-miR-15a	miR.MEcyan
CDC27	bta-miR-15a	miR.MEcyan
CDC37L1	bta-miR-103	miR.MEbrown
CDC37L1	bta-miR-107	miR.MEbrown
CDC37L1	bta-miR-15a	miR.MEcyan
CDC37L1	bta-miR-30c	miR.MEmidnightblue
CDC37L1	bta-miR-30f	miR.MEmidnightblue
CDC42BPA	bta-miR-29a	miR.MEcyan
CDC42BPA	bta-miR-29b	miR.MEcyan
CDC42BPA	bta-miR-29c	miR.MEcyan
CDC42BPA	bta-miR-29d-3p	miR.MEcyan
CDC42BPA	bta-miR-29e	miR.MEcyan
CDH11	bta-miR-186	miR.MElightyellow
CDK12	bta-miR-15a	miR.MEcyan
CDK13	bta-miR-29e	miR.MEcyan
CDK14	bta-miR-186	miR.MElightyellow
CDK14	bta-let-7c	miR.MEtan
CDK14	bta-let-7e	miR.MEtan
CDK14	bta-let-7b	miR.MEtan
CDK14	bta-let-7a-5p	miR.MEtan
CDK14	bta-let-7f	miR.MEtan
CDK19	bta-miR-125a	miR.MElightyellow
CDK6	bta-miR-186	miR.MElightyellow
CDV3	bta-miR-103	miR.MEbrown
CDV3	bta-miR-107	miR.MEbrown
CDV3	bta-miR-15a	miR.MEcyan
CDV3	bta-miR-29e	miR.MEcyan
CELF2	bta-miR-29a	miR.MEcyan
CELF2	bta-miR-29b	miR.MEcyan
CELF2	bta-miR-29c	miR.MEcyan
CELF2	bta-miR-29d-3p	miR.MEcyan
CEP350	bta-miR-29a	miR.MEcyan
CEP350	bta-miR-29e	miR.MEcyan
CHD2	bta-miR-15a	miR.MEcyan
CHD2	bta-miR-29e	miR.MEcyan
CHD6	bta-miR-15a	miR.MEcyan
CHD6	bta-miR-29e	miR.MEcyan
CHD7	bta-miR-15a	miR.MEcyan
FRAT2	bta-miR-29b	miR.MEcyan
FRAT2	bta-miR-29c	miR.MEcyan
FRAT2	bta-miR-29d-3p	miR.MEcyan
FRMD4A	bta-miR-29a	miR.MEcyan
FRMD4A	bta-miR-29b	miR.MEcyan
FRMD4A	bta-miR-29c	miR.MEcyan
FRMD4A	bta-miR-29d-3p	miR.MEcyan
FRY	bta-miR-15a	miR.MEcyan
FRZB	bta-miR-29e	miR.MEcyan
FUT11	bta-miR-29a	miR.MEcyan
FUT11	bta-miR-29b	miR.MEcyan
FUT11	bta-miR-29c	miR.MEcyan
FUT11	bta-miR-29d-3p	miR.MEcyan
FUT11	bta-miR-331-3p	miR.MEmidnightblue
FXN	bta-miR-29a	miR.MEcyan
FYTTD1	bta-miR-29a	miR.MEcyan
FZD7	bta-miR-29e	miR.MEcyan
G3BP1	bta-miR-29b	miR.MEcyan
G3BP1	bta-miR-29c	miR.MEcyan
G3BP1	bta-miR-29d-3p	miR.MEcyan
G3BP1	bta-miR-29e	miR.MEcyan
GABPA	bta-miR-15a	miR.MEcyan
GALNT1	bta-miR-29e	miR.MEcyan
GALNT4	bta-let-7c	miR.MEtan
GALNT4	bta-let-7e	miR.MEtan
GALNT4	bta-let-7b	miR.MEtan
GALNT4	bta-let-7a-5p	miR.MEtan
GALNT4	bta-let-7f	miR.MEtan
GAS2L3	bta-miR-92b	miR.MElightyellow
GAS7	bta-let-7c	miR.MEtan
GAS7	bta-let-7e	miR.MEtan
GAS7	bta-let-7b	miR.MEtan
GAS7	bta-let-7a-5p	miR.MEtan
GAS7	bta-let-7f	miR.MEtan
GCC2	bta-miR-15a	miR.MEcyan
GDE1	bta-miR-29e	miR.MEcyan
GDPD5	bta-miR-125a	miR.MElightyellow
GEMIN4	bta-miR-29e	miR.MEcyan
GID8	bta-miR-29a	miR.MEcyan
GID8	bta-miR-29b	miR.MEcyan
GID8	bta-miR-29c	miR.MEcyan
GID8	bta-miR-29d-3p	miR.MEcyan
GIMAP8	bta-miR-154c	miR.MEred

CHD7	bta-miR-29e	miR.MEcyan
CHM	bta-miR-29a	miR.MEcyan
CHMP1A	bta-miR-19a	miR.MEbrown
CHMP1A	bta-miR-19b	miR.MEbrown
CHMP4B	bta-miR-19a	miR.MEbrown
CHMP4B	bta-miR-19b	miR.MEbrown
CLCN5	bta-miR-15a	miR.MEcyan
CLCN5	bta-miR-29a	miR.MEcyan
CLCN5	bta-miR-29b	miR.MEcyan
CLCN5	bta-miR-29c	miR.MEcyan
CLCN5	bta-miR-29d-3p	miR.MEcyan
CLCN5	bta-miR-29e	miR.MEcyan
CLOCK	bta-miR-15a	miR.MEcyan
CLOCK	bta-miR-29a	miR.MEcyan
CNKSR2	bta-miR-15a	miR.MEcyan
CNKSR2	bta-miR-30c	miR.MEmidnightblue
CNKSR2	bta-miR-30f	miR.MEmidnightblue
CNOT7	bta-miR-19a	miR.MEbrown
CNOT7	bta-miR-19b	miR.MEbrown
CNOT7	bta-miR-29a	miR.MEcyan
COL1A2	bta-miR-92b	miR.MElightyellow
COL1A2	bta-let-7c	miR.MEtan
COL1A2	bta-let-7e	miR.MEtan
COL1A2	bta-let-7b	miR.MEtan
COL1A2	bta-let-7a-5p	miR.MEtan
COL1A2	bta-let-7f	miR.MEtan
COL4A3BP	bta-miR-15a	miR.MEcyan
COL4A3BP	bta-miR-29e	miR.MEcyan
COPS2	bta-miR-103	miR.MEbrown
COPS2	bta-miR-107	miR.MEbrown
COPS2	bta-miR-15a	miR.MEcyan
CORO2B	bta-miR-125a	miR.MElightyellow
CPEB1	bta-miR-92b	miR.MElightyellow
CPEB1	bta-let-7c	miR.MEtan
CPEB1	bta-let-7e	miR.MEtan
CPEB1	bta-let-7b	miR.MEtan
CPEB1	bta-let-7a-5p	miR.MEtan
CPEB1	bta-let-7f	miR.MEtan
CREBRF	bta-miR-15a	miR.MEcyan
CREBRF	bta-miR-29e	miR.MEcyan
CRLS1	bta-miR-21-3p	miR.MEgreen
CRLS1	bta-miR-214	miR.MEmagenta
CSNK1G2	bta-miR-103	miR.MEbrown
GIT1	bta-miR-15a	miR.MEcyan
GLOD4	bta-miR-29e	miR.MEcyan
GLYCTK	bta-miR-29b	miR.MEcyan
GLYCTK	bta-miR-29c	miR.MEcyan
GLYCTK	bta-miR-29d-3p	miR.MEcyan
GLYCTK	bta-miR-29e	miR.MEcyan
GMPR	bta-miR-29e	miR.MEcyan
GMPS	bta-miR-29e	miR.MEcyan
GNA13	bta-miR-15a	miR.MEcyan
GNA13	bta-miR-29b	miR.MEcyan
GNA13	bta-miR-29c	miR.MEcyan
GNA13	bta-miR-29d-3p	miR.MEcyan
GNA13	bta-miR-30c	miR.MEmidnightblue
GNA13	bta-miR-30f	miR.MEmidnightblue
GNL1	bta-miR-29a	miR.MEcyan
GNL1	bta-miR-29e	miR.MEcyan
GOLGA1	bta-miR-15a	miR.MEcyan
GOLGA1	bta-miR-29e	miR.MEcyan
GOLGA4	bta-miR-29e	miR.MEcyan
GORASP2	bta-miR-15a	miR.MEcyan
GPALPP1	bta-miR-29a	miR.MEcyan
GPALPP1	bta-miR-29e	miR.MEcyan
GPC4	bta-miR-29a	miR.MEcyan
GPM6A	bta-miR-92b	miR.MElightyellow
GPR107	bta-miR-29e	miR.MEcyan
GPR173	bta-miR-92b	miR.MElightyellow
GPR180	bta-miR-92b	miR.MElightyellow
GPSM2	bta-miR-29e	miR.MEcyan
GPX7	bta-let-7c	miR.MEtan
GPX7	bta-let-7e	miR.MEtan
GPX7	bta-let-7b	miR.MEtan
GPX7	bta-let-7a-5p	miR.MEtan
GPX7	bta-let-7f	miR.MEtan
GRAMD1C	bta-let-7i	miR.MEmagenta
GRAMD1C	bta-miR-199c	miR.MEmagenta
GRHPR	bta-miR-29e	miR.MEcyan
GSK3B	bta-miR-15a	miR.MEcyan
GSK3B	bta-miR-29b	miR.MEcyan
GSK3B	bta-miR-29c	miR.MEcyan
GSK3B	bta-miR-29d-3p	miR.MEcyan
GSTA4	bta-miR-29b	miR.MEcyan
GSTA4	bta-miR-29c	miR.MEcyan
GSTA4	bta-miR-29d-3p	miR.MEcyan

CSNK1G2	bta-miR-107	miR.MEbrown	*GSTK1*	bta-miR-331-5p	miR.MEgreen
CSNK1G2	bta-miR-29e	miR.MEcyan	*GTDC1*	bta-miR-29b	miR.MEcyan
CSNK2A1	bta-miR-19a	miR.MEbrown	*GTDC1*	bta-miR-29c	miR.MEcyan
CSNK2A1	bta-miR-19b	miR.MEbrown	*GTDC1*	bta-miR-29d-3p	miR.MEcyan
CSNK2A1	bta-miR-30c	miR.MEmidnightblue	*GTDC1*	bta-miR-30c	miR.MEmidnightblue
CSNK2A1	bta-miR-30f	miR.MEmidnightblue	*GTDC1*	bta-miR-30f	miR.MEmidnightblue
CSNK2A1	bta-miR-331-3p	miR.MEmidnightblue	*GTF3C4*	bta-miR-29a	miR.MEcyan
CTDSPL2	bta-miR-186	miR.MElightyellow	*GTPBP8*	bta-miR-29e	miR.MEcyan
CYB5R4	bta-miR-186	miR.MElightyellow	*GUCD1*	bta-miR-204	miR.MEmagenta
CYLD	bta-miR-15a	miR.MEcyan	*GUCD1*	bta-miR-214	miR.MEmagenta
DCAF10	bta-miR-15a	miR.MEcyan	*HCFC1*	bta-miR-29e	miR.MEcyan
DCAF10	bta-miR-29e	miR.MEcyan	*HEATR5A*	bta-miR-29a	miR.MEcyan
DCAF7	bta-miR-15a	miR.MEcyan	*HECTD4*	bta-miR-15a	miR.MEcyan
DCAF7	bta-miR-29e	miR.MEcyan	*HECTD4*	bta-miR-29e	miR.MEcyan
DCBLD2	bta-miR-186	miR.MElightyellow	*HERC4*	bta-miR-29e	miR.MEcyan
DCP1A	bta-miR-15a	miR.MEcyan	*HEXIM1*	bta-miR-29e	miR.MEcyan
DCP1A	bta-miR-29e	miR.MEcyan	*HEXIM1*	bta-miR-29d-5p	miR.MEmidnightblue
DCUN1D2	bta-miR-19a	miR.MEbrown	*HIF3A*	bta-let-7c	miR.MEtan
DCUN1D2	bta-miR-19b	miR.MEbrown	*HIF3A*	bta-let-7e	miR.MEtan
DDX6	bta-miR-29b	miR.MEcyan	*HIF3A*	bta-let-7b	miR.MEtan
DDX6	bta-miR-29c	miR.MEcyan	*HIF3A*	bta-let-7a-5p	miR.MEtan
DDX6	bta-miR-29d-3p	miR.MEcyan	*HIF3A*	bta-let-7f	miR.MEtan
DGCR8	bta-miR-19a	miR.MEbrown	*HINFP*	bta-miR-29e	miR.MEcyan
DGCR8	bta-miR-19b	miR.MEbrown	*HIST1H2BD*	bta-miR-29e	miR.MEcyan
DGKH	bta-miR-29a	miR.MEcyan	*HIVEP3*	bta-miR-29a	miR.MEcyan
DGKH	bta-miR-29b	miR.MEcyan	*HMBOX1*	bta-miR-15a	miR.MEcyan
DGKH	bta-miR-29c	miR.MEcyan	*HMBOX1*	bta-miR-29a	miR.MEcyan
DGKH	bta-miR-29d-3p	miR.MEcyan	*HMGB2*	bta-miR-186	miR.MElightyellow
DHRS3	bta-miR-19a	miR.MEbrown	*HMGCS1*	bta-miR-29b	miR.MEcyan
DHRS3	bta-miR-19b	miR.MEbrown	*HMGCS1*	bta-miR-29c	miR.MEcyan
DHX33	bta-miR-29e	miR.MEcyan	*HMGCS1*	bta-miR-29d-3p	miR.MEcyan
DHX40	bta-miR-186	miR.MElightyellow	*HNRNPL*	bta-miR-29e	miR.MEcyan
DICER1	bta-miR-15a	miR.MEcyan	*HOOK3*	bta-miR-29a	miR.MEcyan
DICER1	bta-miR-29a	miR.MEcyan	*HOOK3*	bta-miR-29b	miR.MEcyan
DICER1	bta-miR-29b	miR.MEcyan	*HOOK3*	bta-miR-29c	miR.MEcyan
DICER1	bta-miR-29c	miR.MEcyan	*HOOK3*	bta-miR-29d-3p	miR.MEcyan
DICER1	bta-miR-29d-3p	miR.MEcyan	*HOOK3*	bta-miR-29e	miR.MEcyan
DMXL1	bta-miR-29a	miR.MEcyan	*HOXC8*	bta-miR-15a	miR.MEcyan
DNAJA2	bta-miR-19a	miR.MEbrown	*HRAS*	bta-miR-29e	miR.MEcyan
DNAJA2	bta-miR-19b	miR.MEbrown	*IDS*	bta-miR-186	miR.MElightyellow
DNAJA2	bta-miR-21-5p	miR.MEbrown	*IFI44L*	bta-miR-214	miR.MEmagenta
DNAJA2	bta-miR-15a	miR.MEcyan	*IFRD2*	bta-miR-29e	miR.MEcyan
DNAL1	bta-miR-29a	miR.MEcyan	*IKZF4*	bta-miR-29a	miR.MEcyan

DNAL1	bta-miR-29b	miR.MEcyan	*IKZF4*	bta-miR-29e	miR.MEcyan
DNAL1	bta-miR-29c	miR.MEcyan	*IL17RA*	bta-miR-29a	miR.MEcyan
DNAL1	bta-miR-29d-3p	miR.MEcyan	*IL2RG*	bta-miR-154c	miR.MEred
DPYSL3	bta-let-7c	miR.MEtan	*INCENP*	bta-miR-29a	miR.MEcyan
DPYSL3	bta-let-7e	miR.MEtan	*ING2*	bta-miR-15a	miR.MEcyan
DPYSL3	bta-let-7b	miR.MEtan	*ING2*	bta-miR-29b	miR.MEcyan
DPYSL3	bta-let-7a-5p	miR.MEtan	*ING2*	bta-miR-29c	miR.MEcyan
DPYSL3	bta-let-7f	miR.MEtan	*ING2*	bta-miR-29d-3p	miR.MEcyan
DST	bta-miR-29e	miR.MEcyan	*INPP4B*	bta-miR-29e	miR.MEcyan
DUSP7	bta-miR-19a	miR.MEbrown	*INSR*	bta-miR-15a	miR.MEcyan
DUSP7	bta-miR-19b	miR.MEbrown	*IPMK*	bta-miR-29a	miR.MEcyan
DUSP7	bta-miR-193a-3p	miR.MEmidnightblue	*IPO7*	bta-miR-15a	miR.MEcyan
DUSP8	bta-miR-21-5p	miR.MEbrown	*IPO7*	bta-miR-29e	miR.MEcyan
DUT	bta-miR-19a	miR.MEbrown	*IPO8*	bta-miR-29a	miR.MEcyan
DUT	bta-miR-19b	miR.MEbrown	*IPO9*	bta-miR-15a	miR.MEcyan
DYNC1LI2	bta-miR-15a	miR.MEcyan	*IPO9*	bta-miR-29e	miR.MEcyan
DYNC1LI2	bta-miR-29e	miR.MEcyan	*IPO9*	bta-miR-877	miR.MEmidnightblue
DYNLL2	bta-miR-103	miR.MEbrown	*IRAK2*	bta-miR-15a	miR.MEcyan
DYNLL2	bta-miR-107	miR.MEbrown	*IRF1*	bta-miR-214	miR.MEmagenta
DYNLL2	bta-miR-19a	miR.MEbrown	*IRF2BP1*	bta-miR-15a	miR.MEcyan
DYNLL2	bta-miR-19b	miR.MEbrown	*IRF2BPL*	bta-miR-15a	miR.MEcyan
DYNLL2	bta-miR-15a	miR.MEcyan	*IRF2BPL*	bta-miR-29e	miR.MEcyan
DYNLL2	bta-miR-29a	miR.MEcyan	*IRF2BPL*	bta-miR-193a-3p	miR.MEmidnightblue
DYNLL2	bta-miR-29e	miR.MEcyan	*ISLR*	bta-let-7c	miR.MEtan
DYNLL2	bta-miR-193a-3p	miR.MEmidnightblue	*ISLR*	bta-let-7e	miR.MEtan
DYNLL2	bta-miR-331-3p	miR.MEmidnightblue	*ISLR*	bta-let-7b	miR.MEtan
EEA1	bta-miR-29a	miR.MEcyan	*ISLR*	bta-let-7a-5p	miR.MEtan
EEA1	bta-miR-29e	miR.MEcyan	*ISLR*	bta-let-7f	miR.MEtan
EGR3	bta-let-7c	miR.MEtan	*ITGAV*	bta-miR-29e	miR.MEcyan
EGR3	bta-let-7e	miR.MEtan	*ITPR1*	bta-miR-29e	miR.MEcyan
EGR3	bta-let-7b	miR.MEtan	*IYD*	bta-miR-29e	miR.MEcyan
EGR3	bta-let-7a-5p	miR.MEtan	*JMJD1C*	bta-miR-15a	miR.MEcyan
EGR3	bta-let-7f	miR.MEtan	*JMY*	bta-miR-29b	miR.MEcyan
EHD1	bta-miR-21-5p	miR.MEbrown	*JMY*	bta-miR-29c	miR.MEcyan
EIF2S1	bta-miR-103	miR.MEbrown	*JMY*	bta-miR-29d-3p	miR.MEcyan
EIF2S1	bta-miR-107	miR.MEbrown	*JOSD1*	bta-let-7c	miR.MEtan
EIF2S1	bta-miR-15a	miR.MEcyan	*JOSD1*	bta-let-7e	miR.MEtan
EIF2S1	bta-miR-29b	miR.MEcyan	*JOSD1*	bta-let-7b	miR.MEtan
EIF2S1	bta-miR-29c	miR.MEcyan	*JOSD1*	bta-let-7a-5p	miR.MEtan
EIF2S1	bta-miR-29d-3p	miR.MEcyan	*JOSD1*	bta-let-7f	miR.MEtan
EIF4A2	bta-miR-19a	miR.MEbrown	*KAT6B*	bta-miR-29a	miR.MEcyan
EIF4A2	bta-miR-19b	miR.MEbrown	*KATNBL1*	bta-miR-15a	miR.MEcyan
EIF4A2	bta-miR-29a	miR.MEcyan	*KATNBL1*	bta-miR-29a	miR.MEcyan

EIF4B	bta-miR-103	miR.MEbrown
EIF4B	bta-miR-107	miR.MEbrown
EIF4B	bta-miR-15a	miR.MEcyan
EIF4B	bta-miR-331-3p	miR.MEmidnightblue
EIF4E	bta-miR-19a	miR.MEbrown
EIF4E	bta-miR-19b	miR.MEbrown
EIF4E	bta-miR-15a	miR.MEcyan
EIF4E3	bta-miR-19a	miR.MEbrown
EIF4E3	bta-miR-19b	miR.MEbrown
EIF4E3	bta-miR-29b	miR.MEcyan
EIF4E3	bta-miR-29c	miR.MEcyan
EIF4E3	bta-miR-29d-3p	miR.MEcyan
EIF4E3	bta-miR-29e	miR.MEcyan
EIF4EBP2	bta-miR-29e	miR.MEcyan
ELK4	bta-miR-15a	miR.MEcyan
ELOVL6	bta-miR-125a	miR.MElightyellow
ELOVL6	bta-miR-186	miR.MElightyellow
ELOVL6	bta-miR-92b	miR.MElightyellow
EPC1	bta-miR-15a	miR.MEcyan
EPC1	bta-miR-29a	miR.MEcyan
EPC1	bta-miR-29b	miR.MEcyan
EPC1	bta-miR-29c	miR.MEcyan
EPC1	bta-miR-29d-3p	miR.MEcyan
EPC1	bta-miR-29e	miR.MEcyan
EPG5	bta-miR-29a	miR.MEcyan
EPG5	bta-miR-29e	miR.MEcyan
EPS15	bta-miR-19a	miR.MEbrown
EPS15	bta-miR-19b	miR.MEbrown
EPS15	bta-miR-29b	miR.MEcyan
EPS15	bta-miR-29c	miR.MEcyan
EPS15	bta-miR-29d-3p	miR.MEcyan
ERBB3	bta-miR-125a	miR.MElightyellow
ETF1	bta-miR-103	miR.MEbrown
ETF1	bta-miR-107	miR.MEbrown
ETV3	bta-miR-15a	miR.MEcyan
EVI5L	bta-miR-19a	miR.MEbrown
EVI5L	bta-miR-19b	miR.MEbrown
EVI5L	bta-miR-30c	miR.MEmidnightblue
EVI5L	bta-miR-30f	miR.MEmidnightblue
EXOC5	bta-miR-15a	miR.MEcyan
EXOC5	bta-miR-29a	miR.MEcyan
FAM104A	bta-miR-103	miR.MEbrown
FAM104A	bta-miR-107	miR.MEbrown
KATNBL1	bta-miR-29b	miR.MEcyan
KATNBL1	bta-miR-29c	miR.MEcyan
KATNBL1	bta-miR-29d-3p	miR.MEcyan
KCNB1	bta-miR-29e	miR.MEcyan
KCNJ12	bta-miR-29a	miR.MEcyan
KCNJ12	bta-miR-29b	miR.MEcyan
KCNJ12	bta-miR-29c	miR.MEcyan
KCNJ12	bta-miR-29d-3p	miR.MEcyan
KCNJ12	bta-miR-29e	miR.MEcyan
KCNJ12	bta-miR-30c	miR.MEmidnightblue
KCNJ12	bta-miR-30f	miR.MEmidnightblue
KCTD15	bta-miR-29a	miR.MEcyan
KCTD15	bta-miR-29b	miR.MEcyan
KCTD15	bta-miR-29c	miR.MEcyan
KCTD15	bta-miR-29d-3p	miR.MEcyan
KCTD15	bta-miR-29e	miR.MEcyan
KCTD20	bta-miR-29b	miR.MEcyan
KCTD20	bta-miR-29c	miR.MEcyan
KCTD20	bta-miR-29d-3p	miR.MEcyan
KCTD21	bta-miR-29b	miR.MEcyan
KCTD21	bta-miR-29c	miR.MEcyan
KCTD21	bta-miR-29d-3p	miR.MEcyan
KCTD3	bta-miR-29a	miR.MEcyan
KCTD3	bta-miR-29b	miR.MEcyan
KCTD3	bta-miR-29c	miR.MEcyan
KCTD3	bta-miR-29d-3p	miR.MEcyan
KCTD5	bta-miR-29a	miR.MEcyan
KCTD5	bta-miR-29b	miR.MEcyan
KCTD5	bta-miR-29c	miR.MEcyan
KCTD5	bta-miR-29d-3p	miR.MEcyan
KDM4B	bta-miR-29a	miR.MEcyan
KDM4B	bta-miR-29b	miR.MEcyan
KDM4B	bta-miR-29c	miR.MEcyan
KDM4B	bta-miR-29d-3p	miR.MEcyan
KDM5A	bta-miR-29e	miR.MEcyan
KDM5B	bta-miR-186	miR.MElightyellow
KDM6B	bta-miR-29b	miR.MEcyan
KDM6B	bta-miR-29c	miR.MEcyan
KDM6B	bta-miR-29d-3p	miR.MEcyan
KHNYN	bta-miR-125a	miR.MElightyellow
KIAA0100	bta-miR-29e	miR.MEcyan
KIAA0391	bta-miR-29a	miR.MEcyan
KIAA0391	bta-miR-29e	miR.MEcyan

FAM104A	bta-miR-19a	miR.MEbrown
FAM104A	bta-miR-19b	miR.MEbrown
FAM104A	bta-miR-30c	miR.MEmidnightblue
FAM104A	bta-miR-30f	miR.MEmidnightblue
FAM107B	bta-miR-125a	miR.MElightyellow
FAM117B	bta-miR-186	miR.MElightyellow
FAM117B	bta-miR-92b	miR.MElightyellow
FAM160A1	bta-miR-19a	miR.MEbrown
FAM160A1	bta-miR-19b	miR.MEbrown
FAM160A1	bta-miR-29e	miR.MEcyan
FAM46A	bta-miR-125a	miR.MElightyellow
FAM46A	bta-miR-92b	miR.MElightyellow
FAT4	bta-miR-125a	miR.MElightyellow
FBXO28	bta-miR-29b	miR.MEcyan
FBXO28	bta-miR-29c	miR.MEcyan
FBXO28	bta-miR-29d-3p	miR.MEcyan
FBXW7	bta-miR-15a	miR.MEcyan
FBXW7	bta-miR-29a	miR.MEcyan
FBXW7	bta-miR-29b	miR.MEcyan
FBXW7	bta-miR-29c	miR.MEcyan
FBXW7	bta-miR-29d-3p	miR.MEcyan
FBXW7	bta-miR-29e	miR.MEcyan
FGF7	bta-miR-186	miR.MElightyellow
FLOT2	bta-miR-103	miR.MEbrown
FLOT2	bta-miR-107	miR.MEbrown
FNDC3B	bta-miR-125a	miR.MElightyellow
FNDC3B	bta-miR-186	miR.MElightyellow
FNDC3B	bta-miR-92b	miR.MElightyellow
FOXP1	bta-miR-92b	miR.MElightyellow
FRS2	bta-miR-92b	miR.MElightyellow
FRYL	bta-miR-15a	miR.MEcyan
FRYL	bta-miR-29e	miR.MEcyan
FTO	bta-miR-21-5p	miR.MEbrown
FTO	bta-miR-29a	miR.MEcyan
FTO	bta-miR-29e	miR.MEcyan
FTO	bta-miR-30c	miR.MEmidnightblue
FTO	bta-miR-30f	miR.MEmidnightblue
FUBP1	bta-miR-15a	miR.MEcyan
FURIN	bta-miR-103	miR.MEbrown
FURIN	bta-miR-107	miR.MEbrown
FURIN	bta-miR-19a	miR.MEbrown
FURIN	bta-miR-19b	miR.MEbrown
FURIN	bta-miR-15a	miR.MEcyan
KIAA1328	bta-miR-15a	miR.MEcyan
KIAA1522	bta-miR-29e	miR.MEcyan
KIAA1522	bta-miR-30c	miR.MEmidnightblue
KIAA1522	bta-miR-30f	miR.MEmidnightblue
KIAA1549	bta-miR-15a	miR.MEcyan
KIAA1549	bta-miR-29a	miR.MEcyan
KIAA1549	bta-miR-29b	miR.MEcyan
KIAA1549	bta-miR-29c	miR.MEcyan
KIAA1549	bta-miR-29d-3p	miR.MEcyan
KIAA1549	bta-miR-29e	miR.MEcyan
KIDINS220	bta-miR-29e	miR.MEcyan
KIF1C	bta-miR-15a	miR.MEcyan
KIF1C	bta-miR-29e	miR.MEcyan
KIFAP3	bta-miR-29e	miR.MEcyan
KIN	bta-miR-29e	miR.MEcyan
KLC2	bta-miR-15a	miR.MEcyan
KLF11	bta-miR-29a	miR.MEcyan
KLHL21	bta-miR-29e	miR.MEcyan
KLHL24	bta-miR-29a	miR.MEcyan
KLHL24	bta-miR-29e	miR.MEcyan
KLHL25	bta-miR-29b	miR.MEcyan
KLHL25	bta-miR-29c	miR.MEcyan
KLHL25	bta-miR-29d-3p	miR.MEcyan
KLHL26	bta-miR-15a	miR.MEcyan
KLHL31	bta-miR-29e	miR.MEcyan
KMT2A	bta-miR-15a	miR.MEcyan
KMT2C	bta-miR-15a	miR.MEcyan
KMT2E	bta-miR-29e	miR.MEcyan
KRIT1	bta-miR-29e	miR.MEcyan
KSR1	bta-miR-29a	miR.MEcyan
KSR1	bta-miR-30c	miR.MEmidnightblue
KSR1	bta-miR-30f	miR.MEmidnightblue
L3MBTL2	bta-miR-29e	miR.MEcyan
LAMTOR3	bta-miR-15a	miR.MEcyan
LAMTOR3	bta-miR-29e	miR.MEcyan
LARP4B	bta-miR-29b	miR.MEcyan
LARP4B	bta-miR-29c	miR.MEcyan
LARP4B	bta-miR-29d-3p	miR.MEcyan
LDB3	bta-miR-29e	miR.MEcyan
LDHA	bta-miR-29a	miR.MEcyan
LDHA	bta-miR-29e	miR.MEcyan
LDLRAD4	bta-miR-92b	miR.MElightyellow
LHFPL2	bta-miR-186	miR.MElightyellow

FURIN	bta-miR-331-3p	miR.MEmidnightblue	*LHFPL2*	bta-miR-92b	miR.MElightyellow
GALNT7	bta-miR-125a	miR.MElightyellow	*LIFR*	bta-miR-29a	miR.MEcyan
GALNT7	bta-miR-92b	miR.MElightyellow	*LIG3*	bta-miR-29e	miR.MEcyan
GAN	bta-miR-15a	miR.MEcyan	*LMAN1*	bta-miR-29e	miR.MEcyan
GAN	bta-miR-29a	miR.MEcyan	*LMAN2L*	bta-miR-15a	miR.MEcyan
GAN	bta-miR-29b	miR.MEcyan	*LMAN2L*	bta-miR-29a	miR.MEcyan
GAN	bta-miR-29c	miR.MEcyan	*LMAN2L*	bta-miR-29e	miR.MEcyan
GAN	bta-miR-29d-3p	miR.MEcyan	*LMBRD2*	bta-miR-29e	miR.MEcyan
GAN	bta-miR-29e	miR.MEcyan	*LMTK2*	bta-miR-29a	miR.MEcyan
GGA1	bta-miR-19a	miR.MEbrown	*LMTK2*	bta-miR-29b	miR.MEcyan
GGA1	bta-miR-19b	miR.MEbrown	*LMTK2*	bta-miR-29c	miR.MEcyan
GGA1	bta-miR-29b	miR.MEcyan	*LMTK2*	bta-miR-29d-3p	miR.MEcyan
GGA1	bta-miR-29c	miR.MEcyan	*LNPEP*	bta-miR-15a	miR.MEcyan
GGA1	bta-miR-29d-3p	miR.MEcyan	*LNPEP*	bta-miR-29a	miR.MEcyan
GGA2	bta-miR-103	miR.MEbrown	*LNPEP*	bta-miR-29b	miR.MEcyan
GGA2	bta-miR-107	miR.MEbrown	*LNPEP*	bta-miR-29c	miR.MEcyan
GGA2	bta-miR-15a	miR.MEcyan	*LNPEP*	bta-miR-29d-3p	miR.MEcyan
GGA2	bta-miR-29a	miR.MEcyan	*LOX*	bta-miR-186	miR.MElightyellow
GHR	bta-miR-15a	miR.MEcyan	*LOXL4*	bta-let-7c	miR.MEtan
GID4	bta-miR-21-5p	miR.MEbrown	*LOXL4*	bta-let-7e	miR.MEtan
GID4	bta-miR-29a	miR.MEcyan	*LOXL4*	bta-let-7b	miR.MEtan
GLIS2	bta-miR-125a	miR.MElightyellow	*LOXL4*	bta-let-7a-5p	miR.MEtan
GLTP	bta-miR-125a	miR.MElightyellow	*LOXL4*	bta-let-7f	miR.MEtan
GMFB	bta-miR-186	miR.MElightyellow	*LPGAT1*	bta-miR-186	miR.MElightyellow
GNAQ	bta-miR-15a	miR.MEcyan	*LRP6*	bta-miR-15a	miR.MEcyan
GNAQ	bta-miR-29e	miR.MEcyan	*LRP6*	bta-miR-29b	miR.MEcyan
GNS	bta-miR-92b	miR.MElightyellow	*LRP6*	bta-miR-29c	miR.MEcyan
GNS	bta-let-7c	miR.MEtan	*LRP6*	bta-miR-29d-3p	miR.MEcyan
GNS	bta-let-7e	miR.MEtan	*LRP6*	bta-miR-29e	miR.MEcyan
GNS	bta-let-7b	miR.MEtan	*LRRC20*	bta-miR-29a	miR.MEcyan
GNS	bta-let-7a-5p	miR.MEtan	*LRRC28*	bta-miR-29a	miR.MEcyan
GNS	bta-let-7f	miR.MEtan	*LRRC58*	bta-miR-15a	miR.MEcyan
GPBP1	bta-miR-19a	miR.MEbrown	*LRRC58*	bta-miR-29a	miR.MEcyan
GPBP1	bta-miR-19b	miR.MEbrown	*LRRC58*	bta-miR-29b	miR.MEcyan
GPCPD1	bta-let-7i	miR.MEmagenta	*LRRC58*	bta-miR-29c	miR.MEcyan
GPCPD1	bta-miR-199c	miR.MEmagenta	*LRRC58*	bta-miR-29d-3p	miR.MEcyan
GPR63	bta-let-7c	miR.MEtan	*LSM14B*	bta-miR-29e	miR.MEcyan
GPR63	bta-let-7e	miR.MEtan	*LURAP1*	bta-miR-125a	miR.MElightyellow
GPR63	bta-let-7b	miR.MEtan	*LURAP1L*	bta-miR-125a	miR.MElightyellow
GPR63	bta-let-7a-5p	miR.MEtan	*LURAP1L*	bta-miR-92b	miR.MElightyellow
GPR63	bta-let-7f	miR.MEtan	*LYRM2*	bta-miR-29e	miR.MEcyan
GRAMD1B	bta-miR-125a	miR.MElightyellow	*LYSMD1*	bta-miR-29a	miR.MEcyan
GRAMD1B	bta-miR-92b	miR.MElightyellow	*LYSMD1*	bta-miR-29b	miR.MEcyan

GRB10	bta-miR-19a	miR.MEbrown	*LYSMD1*	bta-miR-29c	miR.MEcyan
GRB10	bta-miR-19b	miR.MEbrown	*LYSMD1*	bta-miR-29d-3p	miR.MEcyan
GRB10	bta-miR-29e	miR.MEcyan	*LYVE1*	bta-let-7c	miR.MEtan
GRB10	bta-miR-30c	miR.MEmidnightblue	*LYVE1*	bta-let-7e	miR.MEtan
GRB10	bta-miR-30f	miR.MEmidnightblue	*LYVE1*	bta-let-7b	miR.MEtan
GRM4	bta-miR-19a	miR.MEbrown	*LYVE1*	bta-let-7a-5p	miR.MEtan
GRM4	bta-miR-19b	miR.MEbrown	*LYVE1*	bta-let-7f	miR.MEtan
GRM4	bta-miR-29b	miR.MEcyan	*LZIC*	bta-miR-29a	miR.MEcyan
GRM4	bta-miR-29c	miR.MEcyan	*MAMSTR*	bta-miR-214	miR.MEmagenta
GRM4	bta-miR-29d-3p	miR.MEcyan	*MAN2A1*	bta-miR-92b	miR.MElightyellow
GSKIP	bta-miR-103	miR.MEbrown	*MAP2*	bta-miR-186	miR.MElightyellow
GSKIP	bta-miR-107	miR.MEbrown	*MAP2K4*	bta-miR-29e	miR.MEcyan
GSKIP	bta-miR-19a	miR.MEbrown	*MAP3K4*	bta-miR-15a	miR.MEcyan
GSKIP	bta-miR-19b	miR.MEbrown	*MAP3K7*	bta-miR-29e	miR.MEcyan
GSKIP	bta-miR-15a	miR.MEcyan	*MAP3K7CL*	bta-miR-29a	miR.MEcyan
GSKIP	bta-miR-30c	miR.MEmidnightblue	*MAP3K9*	bta-miR-15a	miR.MEcyan
GSKIP	bta-miR-30f	miR.MEmidnightblue	*MAP3K9*	bta-miR-29e	miR.MEcyan
GSTCD	bta-miR-15a	miR.MEcyan	*MAPKAPK2*	bta-miR-29e	miR.MEcyan
GTF2A1	bta-miR-29a	miR.MEcyan	*MARCH8*	bta-miR-92b	miR.MElightyellow
GTPBP1	bta-miR-29e	miR.MEcyan	*MARCH9*	bta-miR-15a	miR.MEcyan
HBP1	bta-miR-19a	miR.MEbrown	*MARK1*	bta-miR-92b	miR.MElightyellow
HBP1	bta-miR-19b	miR.MEbrown	*MARK3*	bta-miR-29a	miR.MEcyan
HBP1	bta-miR-29a	miR.MEcyan	*MARK3*	bta-miR-29b	miR.MEcyan
HBP1	bta-miR-29b	miR.MEcyan	*MARK3*	bta-miR-29c	miR.MEcyan
HBP1	bta-miR-29c	miR.MEcyan	*MARK3*	bta-miR-29d-3p	miR.MEcyan
HBP1	bta-miR-29d-3p	miR.MEcyan	*MARK3*	bta-miR-30c	miR.MEmidnightblue
HELZ	bta-miR-15a	miR.MEcyan	*MARK3*	bta-miR-30f	miR.MEmidnightblue
HELZ	bta-miR-29a	miR.MEcyan	*MARK4*	bta-miR-29e	miR.MEcyan
HELZ	bta-miR-29b	miR.MEcyan	*MASP1*	bta-miR-21-3p	miR.MEgreen
HELZ	bta-miR-29c	miR.MEcyan	*MASP1*	bta-miR-502b	miR.MEgreen
HELZ	bta-miR-29d-3p	miR.MEcyan	*MAT2B*	bta-miR-29e	miR.MEcyan
HELZ	bta-miR-29e	miR.MEcyan	*MAVS*	bta-miR-29a	miR.MEcyan
HIF1A	bta-miR-151-3p	miR.MElightyellow	*MAZ*	bta-miR-29b	miR.MEcyan
HIF1A	bta-miR-186	miR.MElightyellow	*MAZ*	bta-miR-29c	miR.MEcyan
HIF1A	bta-miR-92b	miR.MElightyellow	*MAZ*	bta-miR-29d-3p	miR.MEcyan
HLF	bta-miR-103	miR.MEbrown	*MBD5*	bta-miR-29a	miR.MEcyan
HLF	bta-miR-107	miR.MEbrown	*MBD5*	bta-miR-29b	miR.MEcyan
HLF	bta-miR-19a	miR.MEbrown	*MBD5*	bta-miR-29c	miR.MEcyan
HLF	bta-miR-19b	miR.MEbrown	*MBD5*	bta-miR-29d-3p	miR.MEcyan
HLF	bta-miR-29a	miR.MEcyan	*MBOAT2*	bta-miR-125a	miR.MElightyellow
HLF	bta-miR-29b	miR.MEcyan	*MBP*	bta-miR-29e	miR.MEcyan
HLF	bta-miR-29c	miR.MEcyan	*MBP*	bta-miR-29d-5p	miR.MEmidnightblue
HLF	bta-miR-29d-3p	miR.MEcyan	*MBTPS2*	bta-miR-15a	miR.MEcyan

HLF	bta-miR-30c	miR.MEmidnightblue	*MCC*	bta-miR-186	miR.MElightyellow
HLF	bta-miR-30f	miR.MEmidnightblue	*MCPH1*	bta-miR-29a	miR.MEcyan
HMGA1	bta-miR-103	miR.MEbrown	*MDN1*	bta-miR-15a	miR.MEcyan
HMGA1	bta-miR-107	miR.MEbrown	*MDN1*	bta-miR-29e	miR.MEcyan
HMGA1	bta-miR-15a	miR.MEcyan	*MED1*	bta-miR-15a	miR.MEcyan
HNRNPK	bta-miR-21-5p	miR.MEbrown	*MED1*	bta-miR-29e	miR.MEcyan
HNRNPK	bta-miR-29e	miR.MEcyan	*MED22*	bta-miR-29e	miR.MEcyan
HOXA10	bta-miR-103	miR.MEbrown	*MED28*	bta-miR-29e	miR.MEcyan
HOXA10	bta-miR-107	miR.MEbrown	*MEF2D*	bta-miR-29e	miR.MEcyan
HOXA10	bta-miR-15a	miR.MEcyan	*MEF2D*	bta-miR-30c	miR.MEmidnightblue
HOXA9	bta-miR-19a	miR.MEbrown	*MEF2D*	bta-miR-30f	miR.MEmidnightblue
HOXA9	bta-miR-19b	miR.MEbrown	*MEIS2*	bta-miR-125a	miR.MElightyellow
HOXA9	bta-miR-30c	miR.MEmidnightblue	*MEIS2*	bta-let-7c	miR.MEtan
HOXA9	bta-miR-30f	miR.MEmidnightblue	*MEIS2*	bta-let-7e	miR.MEtan
HOXD1	bta-miR-19a	miR.MEbrown	*MEIS2*	bta-let-7b	miR.MEtan
HOXD1	bta-miR-19b	miR.MEbrown	*MEIS2*	bta-let-7a-5p	miR.MEtan
HS3ST5	bta-miR-19a	miR.MEbrown	*MEIS2*	bta-let-7f	miR.MEtan
HS3ST5	bta-miR-19b	miR.MEbrown	*METAP2*	bta-miR-29a	miR.MEcyan
HSPBAP1	bta-miR-19a	miR.MEbrown	*METAP2*	bta-miR-29b	miR.MEcyan
HSPBAP1	bta-miR-19b	miR.MEbrown	*METAP2*	bta-miR-29c	miR.MEcyan
HSPBAP1	bta-miR-15a	miR.MEcyan	*METAP2*	bta-miR-29d-3p	miR.MEcyan
IGF1	bta-miR-186	miR.MElightyellow	*METAP2*	bta-miR-30c	miR.MEmidnightblue
IGF1	bta-let-7c	miR.MEtan	*METAP2*	bta-miR-30f	miR.MEmidnightblue
IGF1	bta-let-7e	miR.MEtan	*MFAP5*	bta-miR-151-3p	miR.MElightyellow
IGF1	bta-let-7b	miR.MEtan	*MGAT4A*	bta-miR-15a	miR.MEcyan
IGF1	bta-let-7a-5p	miR.MEtan	*MGAT4A*	bta-miR-29a	miR.MEcyan
IGF1	bta-let-7f	miR.MEtan	*MGAT4B*	bta-miR-29b	miR.MEcyan
IGF1R	bta-miR-15a	miR.MEcyan	*MGAT4B*	bta-miR-29c	miR.MEcyan
IGF2R	bta-miR-29e	miR.MEcyan	*MGAT4B*	bta-miR-29d-3p	miR.MEcyan
IGSF10	bta-miR-186	miR.MElightyellow	*MKLN1*	bta-miR-29a	miR.MEcyan
IL6R	bta-miR-29e	miR.MEcyan	*MKLN1*	bta-miR-29e	miR.MEcyan
IL6ST	bta-miR-29a	miR.MEcyan	*MLLT3*	bta-miR-29a	miR.MEcyan
IL6ST	bta-miR-29e	miR.MEcyan	*MLLT3*	bta-miR-29e	miR.MEcyan
INO80	bta-miR-29a	miR.MEcyan	*MLXIP*	bta-miR-29b	miR.MEcyan
INO80	bta-miR-29e	miR.MEcyan	*MLXIP*	bta-miR-29c	miR.MEcyan
INO80D	bta-miR-29b	miR.MEcyan	*MLXIP*	bta-miR-29d-3p	miR.MEcyan
INO80D	bta-miR-29c	miR.MEcyan	*MLXIP*	bta-miR-29e	miR.MEcyan
INO80D	bta-miR-29d-3p	miR.MEcyan	*MLXIP*	bta-miR-30c	miR.MEmidnightblue
INSIG1	bta-miR-92b	miR.MElightyellow	*MLXIP*	bta-miR-30f	miR.MEmidnightblue
IREB2	bta-miR-29a	miR.MEcyan	*MMP16*	bta-miR-92b	miR.MElightyellow
IREB2	bta-miR-29b	miR.MEcyan	*MOB1A*	bta-miR-186	miR.MElightyellow
IREB2	bta-miR-29c	miR.MEcyan	*MOCS2*	bta-miR-29e	miR.MEcyan
IREB2	bta-miR-29d-3p	miR.MEcyan	*MOCS2*	bta-miR-193a-3p	miR.MEmidnightblue

IREB2	bta-miR-29e	miR.MEcyan	*MPHOSPH9*	bta-miR-29e	miR.MEcyan
ITCH	bta-miR-29e	miR.MEcyan	*MPLKIP*	bta-miR-29e	miR.MEcyan
ITGB3	bta-miR-125a	miR.MElightyellow	*MSANTD3*	bta-miR-29a	miR.MEcyan
ITGB3	bta-let-7c	miR.MEtan	*MSANTD3*	bta-miR-29e	miR.MEcyan
ITGB3	bta-let-7e	miR.MEtan	*MSANTD4*	bta-miR-29e	miR.MEcyan
ITGB3	bta-let-7b	miR.MEtan	*MSRB1*	bta-miR-29e	miR.MEcyan
ITGB3	bta-let-7a-5p	miR.MEtan	*MSRB3*	bta-miR-29a	miR.MEcyan
ITGB3	bta-let-7f	miR.MEtan	*MT2A*	bta-miR-15a	miR.MEcyan
ITSN1	bta-miR-29e	miR.MEcyan	*MTR*	bta-miR-29a	miR.MEcyan
IVNS1ABP	bta-miR-19a	miR.MEbrown	*MTR*	bta-miR-29e	miR.MEcyan
IVNS1ABP	bta-miR-19b	miR.MEbrown	*MTRR*	bta-miR-29e	miR.MEcyan
JAG1	bta-miR-186	miR.MElightyellow	*MTUS1*	bta-miR-29e	miR.MEcyan
JPH1	bta-miR-21-5p	miR.MEbrown	*MXI1*	bta-miR-186	miR.MElightyellow
JPH1	bta-miR-15a	miR.MEcyan	*MYCBP*	bta-miR-29a	miR.MEcyan
JPH1	bta-miR-29a	miR.MEcyan	*MYCBP*	bta-miR-29e	miR.MEcyan
JPH1	bta-miR-29e	miR.MEcyan	*MYO5A*	bta-miR-92b	miR.MElightyellow
KALRN	bta-miR-92b	miR.MElightyellow	*MYO9A*	bta-miR-29e	miR.MEcyan
KAZN	bta-miR-186	miR.MElightyellow	*NAA25*	bta-miR-15a	miR.MEcyan
KBTBD8	bta-miR-29a	miR.MEcyan	*NADK2*	bta-miR-21-3p	miR.MEgreen
KBTBD8	bta-miR-29b	miR.MEcyan	*NAMPT*	bta-miR-29a	miR.MEcyan
KBTBD8	bta-miR-29c	miR.MEcyan	*NANOS1*	bta-miR-29a	miR.MEcyan
KBTBD8	bta-miR-29d-3p	miR.MEcyan	*NANOS1*	bta-miR-29b	miR.MEcyan
KBTBD8	bta-miR-29e	miR.MEcyan	*NANOS1*	bta-miR-29c	miR.MEcyan
KCMF1	bta-miR-103	miR.MEbrown	*NANOS1*	bta-miR-29d-3p	miR.MEcyan
KCMF1	bta-miR-107	miR.MEbrown	*NAPEPLD*	bta-miR-15a	miR.MEcyan
KCMF1	bta-miR-29a	miR.MEcyan	*NAPG*	bta-miR-15a	miR.MEcyan
KCMF1	bta-miR-331-3p	miR.MEmidnightblue	*NAPG*	bta-miR-29e	miR.MEcyan
KCNN3	bta-miR-29e	miR.MEcyan	*NARF*	bta-miR-29a	miR.MEcyan
KDM2A	bta-miR-29a	miR.MEcyan	*NARF*	bta-miR-29b	miR.MEcyan
KDM2A	bta-miR-29b	miR.MEcyan	*NARF*	bta-miR-29c	miR.MEcyan
KDM2A	bta-miR-29c	miR.MEcyan	*NARF*	bta-miR-29d-3p	miR.MEcyan
KDM2A	bta-miR-29d-3p	miR.MEcyan	*NARS*	bta-miR-29a	miR.MEcyan
KIAA1217	bta-miR-29a	miR.MEcyan	*NASP*	bta-miR-186	miR.MElightyellow
KIAA1468	bta-miR-29a	miR.MEcyan	*NBEAL1*	bta-miR-15a	miR.MEcyan
KIAA1958	bta-miR-29e	miR.MEcyan	*NBR1*	bta-miR-15a	miR.MEcyan
KIAA2013	bta-miR-19a	miR.MEbrown	*NBR1*	bta-miR-29a	miR.MEcyan
KIAA2013	bta-miR-19b	miR.MEbrown	*NCK1*	bta-miR-29a	miR.MEcyan
KIF1B	bta-miR-15a	miR.MEcyan	*NCK1*	bta-miR-29e	miR.MEcyan
KIF1B	bta-miR-29d-5p	miR.MEmidnightblue	*NCKAP1*	bta-miR-29a	miR.MEcyan
KIF3A	bta-miR-29a	miR.MEcyan	*NCKAP1*	bta-miR-29e	miR.MEcyan
KIF3B	bta-miR-92b	miR.MElightyellow	*NCKAP5L*	bta-miR-125a	miR.MElightyellow
KLF10	bta-miR-19a	miR.MEbrown	*NCOA1*	bta-miR-29e	miR.MEcyan
KLF10	bta-miR-19b	miR.MEbrown	*NCOA3*	bta-miR-29b	miR.MEcyan

KLF10	bta-miR-29a	miR.MEcyan	*NCOA3*	bta-miR-29c	miR.MEcyan
KLF10	bta-miR-30c	miR.MEmidnightblue	*NCOA3*	bta-miR-29d-3p	miR.MEcyan
KLF10	bta-miR-30f	miR.MEmidnightblue	*NCOR1*	bta-miR-29e	miR.MEcyan
KLF12	bta-miR-29b	miR.MEcyan	*NDST1*	bta-miR-29a	miR.MEcyan
KLF12	bta-miR-29c	miR.MEcyan	*NDST1*	bta-miR-29b	miR.MEcyan
KLF12	bta-miR-29d-3p	miR.MEcyan	*NDST1*	bta-miR-29c	miR.MEcyan
KLF3	bta-miR-125a	miR.MElightyellow	*NDST1*	bta-miR-29d-3p	miR.MEcyan
KLF3	bta-miR-92b	miR.MElightyellow	*NHEJ1*	bta-miR-29a	miR.MEcyan
KLF7	bta-miR-186	miR.MElightyellow	*NHLRC2*	bta-miR-29a	miR.MEcyan
KLF9	bta-miR-29a	miR.MEcyan	*NHLRC2*	bta-miR-29b	miR.MEcyan
KLHL20	bta-miR-29a	miR.MEcyan	*NHLRC2*	bta-miR-29c	miR.MEcyan
KLHL20	bta-miR-29e	miR.MEcyan	*NHLRC2*	bta-miR-29d-3p	miR.MEcyan
KLHL28	bta-miR-29a	miR.MEcyan	*NHLRC2*	bta-miR-29e	miR.MEcyan
KLHL28	bta-miR-29b	miR.MEcyan	*NINJ1*	bta-miR-29e	miR.MEcyan
KLHL28	bta-miR-29c	miR.MEcyan	*NKAIN1*	bta-miR-29b	miR.MEcyan
KLHL28	bta-miR-29d-3p	miR.MEcyan	*NKAIN1*	bta-miR-29c	miR.MEcyan
KLHL28	bta-miR-29e	miR.MEcyan	*NKAIN1*	bta-miR-29d-3p	miR.MEcyan
KMT2D	bta-miR-15a	miR.MEcyan	*NKIRAS2*	bta-miR-29a	miR.MEcyan
KPNA1	bta-miR-15a	miR.MEcyan	*NKIRAS2*	bta-miR-29b	miR.MEcyan
KPNA1	bta-miR-29a	miR.MEcyan	*NKIRAS2*	bta-miR-29c	miR.MEcyan
KPNA1	bta-miR-29b	miR.MEcyan	*NKIRAS2*	bta-miR-29d-3p	miR.MEcyan
KPNA1	bta-miR-29c	miR.MEcyan	*NKIRAS2*	bta-miR-331-3p	miR.MEmidnightblue
KPNA1	bta-miR-29d-3p	miR.MEcyan	*NLRC5*	bta-let-7i	miR.MEmagenta
KPNA4	bta-miR-15a	miR.MEcyan	*NLRC5*	bta-miR-214	miR.MEmagenta
KPNA4	bta-miR-29b	miR.MEcyan	*NMNAT2*	bta-miR-15a	miR.MEcyan
KPNA4	bta-miR-29c	miR.MEcyan	*NMNAT2*	bta-miR-29e	miR.MEcyan
KPNA4	bta-miR-29d-3p	miR.MEcyan	*NMT1*	bta-miR-29e	miR.MEcyan
KPNA4	bta-miR-29e	miR.MEcyan	*NOL11*	bta-miR-29e	miR.MEcyan
KRAS	bta-miR-15a	miR.MEcyan	*NPAT*	bta-miR-29e	miR.MEcyan
KRAS	bta-miR-29e	miR.MEcyan	*NPEPPS*	bta-miR-29e	miR.MEcyan
LATS2	bta-miR-92b	miR.MElightyellow	*NPR3*	bta-miR-186	miR.MElightyellow
LCLAT1	bta-miR-29e	miR.MEcyan	*NR3C1*	bta-miR-29a	miR.MEcyan
LCOR	bta-miR-15a	miR.MEcyan	*NSD1*	bta-miR-29a	miR.MEcyan
LCOR	bta-miR-29a	miR.MEcyan	*NSD1*	bta-miR-29b	miR.MEcyan
LCOR	bta-miR-29e	miR.MEcyan	*NSD1*	bta-miR-29c	miR.MEcyan
LMBR1	bta-miR-186	miR.MElightyellow	*NSD1*	bta-miR-29d-3p	miR.MEcyan
LPP	bta-miR-125a	miR.MElightyellow	*NSF*	bta-miR-92b	miR.MElightyellow
LRP11	bta-miR-19a	miR.MEbrown	*NSUN4*	bta-miR-21-3p	miR.MEgreen
LRP11	bta-miR-19b	miR.MEbrown	*NSUN4*	bta-miR-214	miR.MEmagenta
LRP11	bta-miR-29e	miR.MEcyan	*NSUN4*	bta-miR-221	miR.MEmagenta
LRRC14	bta-miR-103	miR.MEbrown	*NT5DC3*	bta-miR-29a	miR.MEcyan
LRRC14	bta-miR-107	miR.MEbrown	*NT5DC3*	bta-miR-29e	miR.MEcyan
LRRC14	bta-miR-15a	miR.MEcyan	*NT5DC3*	bta-miR-193a-3p	miR.MEmidnightblue

LRRC14	bta-miR-331-3p	miR.MEmidnightblue	*NT5DC3*	bta-miR-30c	miR.MEmidnightblue
LRRC15	bta-miR-103	miR.MEbrown	*NT5DC3*	bta-miR-30f	miR.MEmidnightblue
LRRC15	bta-miR-107	miR.MEbrown	*NTPCR*	bta-miR-29a	miR.MEcyan
LRRC15	bta-miR-15a	miR.MEcyan	*NTPCR*	bta-miR-29e	miR.MEcyan
LRRC15	bta-miR-29e	miR.MEcyan	*NUB1*	bta-miR-29e	miR.MEcyan
LSM12	bta-miR-19a	miR.MEbrown	*NUDCD1*	bta-miR-29a	miR.MEcyan
LSM12	bta-miR-19b	miR.MEbrown	*NUDT3*	bta-miR-29a	miR.MEcyan
LSM12	bta-miR-29e	miR.MEcyan	*NUDT3*	bta-miR-29e	miR.MEcyan
MAP1B	bta-miR-92b	miR.MElightyellow	*NUP153*	bta-miR-29a	miR.MEcyan
MAP2K6	bta-miR-103	miR.MEbrown	*NUP160*	bta-miR-29a	miR.MEcyan
MAP2K6	bta-miR-107	miR.MEbrown	*NUP160*	bta-miR-29b	miR.MEcyan
MAP2K6	bta-miR-15a	miR.MEcyan	*NUP160*	bta-miR-29c	miR.MEcyan
MAP2K6	bta-miR-29a	miR.MEcyan	*NUP160*	bta-miR-29d-3p	miR.MEcyan
MAP2K6	bta-miR-29b	miR.MEcyan	*NXN*	bta-miR-29a	miR.MEcyan
MAP2K6	bta-miR-29c	miR.MEcyan	*NXN*	bta-miR-29e	miR.MEcyan
MAP2K6	bta-miR-29d-3p	miR.MEcyan	*OARD1*	bta-miR-29e	miR.MEcyan
MAP2K6	bta-miR-29e	miR.MEcyan	*OBSCN*	bta-miR-29e	miR.MEcyan
MAP3K1	bta-miR-125a	miR.MElightyellow	*OLFML2A*	bta-miR-125a	miR.MElightyellow
MAP3K2	bta-miR-29b	miR.MEcyan	*OPA1*	bta-miR-29a	miR.MEcyan
MAP3K2	bta-miR-29c	miR.MEcyan	*OPA3*	bta-miR-29e	miR.MEcyan
MAP3K2	bta-miR-29d-3p	miR.MEcyan	*OSBPL11*	bta-miR-29a	miR.MEcyan
MAP3K2	bta-miR-29e	miR.MEcyan	*OSBPL3*	bta-miR-186	miR.MElightyellow
MAP4	bta-miR-15a	miR.MEcyan	*OSBPL8*	bta-miR-186	miR.MElightyellow
MAPK1IP1L	bta-let-7c	miR.MEtan	*OSBPL8*	bta-miR-92b	miR.MElightyellow
MAPK1IP1L	bta-let-7e	miR.MEtan	*OTUD6B*	bta-miR-29e	miR.MEcyan
MAPK1IP1L	bta-let-7b	miR.MEtan	*OXCT1*	bta-miR-29b	miR.MEcyan
MAPK1IP1L	bta-let-7a-5p	miR.MEtan	*OXCT1*	bta-miR-29c	miR.MEcyan
MAPK1IP1L	bta-let-7f	miR.MEtan	*OXCT1*	bta-miR-29d-3p	miR.MEcyan
MAPK6	bta-miR-19a	miR.MEbrown	*P4HA2*	bta-let-7c	miR.MEtan
MAPK6	bta-miR-19b	miR.MEbrown	*P4HA2*	bta-let-7e	miR.MEtan
MAPRE2	bta-miR-19a	miR.MEbrown	*P4HA2*	bta-let-7b	miR.MEtan
MAPRE2	bta-miR-19b	miR.MEbrown	*P4HA2*	bta-let-7a-5p	miR.MEtan
MAPRE2	bta-miR-29b	miR.MEcyan	*P4HA2*	bta-let-7f	miR.MEtan
MAPRE2	bta-miR-29c	miR.MEcyan	*PABPC4L*	bta-miR-125a	miR.MElightyellow
MAPRE2	bta-miR-29d-3p	miR.MEcyan	*PAIP1*	bta-miR-29e	miR.MEcyan
MBNL3	bta-miR-125a	miR.MElightyellow	*PAIP2*	bta-miR-29b	miR.MEcyan
MBNL3	bta-miR-92b	miR.MElightyellow	*PAIP2*	bta-miR-29c	miR.MEcyan
MCMBP	bta-miR-29b	miR.MEcyan	*PAIP2*	bta-miR-29d-3p	miR.MEcyan
MCMBP	bta-miR-29c	miR.MEcyan	*PAK1*	bta-miR-29e	miR.MEcyan
MCMBP	bta-miR-29d-3p	miR.MEcyan	*PAK2*	bta-miR-15a	miR.MEcyan
MECP2	bta-miR-29e	miR.MEcyan	*PAK2*	bta-miR-29e	miR.MEcyan
MECP2	bta-miR-29d-5p	miR.MEmidnightblue	*PAK3*	bta-miR-125a	miR.MElightyellow
MECP2	bta-miR-30c	miR.MEmidnightblue	*PAK3*	bta-miR-186	miR.MElightyellow

MECP2	bta-miR-30f	miR.MEmidnightblue	*PANX1*	bta-miR-29e	miR.MEcyan
MED13	bta-miR-29a	miR.MEcyan	*PAPOLG*	bta-miR-29a	miR.MEcyan
MEF2C	bta-miR-29a	miR.MEcyan	*PAPOLG*	bta-miR-29b	miR.MEcyan
MEF2C	bta-miR-29e	miR.MEcyan	*PAPOLG*	bta-miR-29c	miR.MEcyan
MEIS1	bta-miR-21-5p	miR.MEbrown	*PAPOLG*	bta-miR-29d-3p	miR.MEcyan
MEIS1	bta-miR-29d-5p	miR.MEmidnightblue	*PARD3*	bta-miR-29e	miR.MEcyan
MEIS1	bta-miR-331-3p	miR.MEmidnightblue	*PARD3B*	bta-miR-186	miR.MElightyellow
MEMO1	bta-miR-19a	miR.MEbrown	*PARG*	bta-miR-29a	miR.MEcyan
MEMO1	bta-miR-19b	miR.MEbrown	*PARG*	bta-miR-29b	miR.MEcyan
MFSD9	bta-miR-19a	miR.MEbrown	*PARG*	bta-miR-29c	miR.MEcyan
MFSD9	bta-miR-19b	miR.MEbrown	*PARG*	bta-miR-29d-3p	miR.MEcyan
MFSD9	bta-miR-29a	miR.MEcyan	*PARG*	bta-miR-29e	miR.MEcyan
MGA	bta-miR-29b	miR.MEcyan	*PBX3*	bta-let-7c	miR.MEtan
MGA	bta-miR-29c	miR.MEcyan	*PBX3*	bta-let-7e	miR.MEtan
MGA	bta-miR-29d-3p	miR.MEcyan	*PBX3*	bta-let-7b	miR.MEtan
MGA	bta-miR-29e	miR.MEcyan	*PBX3*	bta-let-7a-5p	miR.MEtan
MGAT5	bta-miR-125a	miR.MElightyellow	*PBX3*	bta-let-7f	miR.MEtan
MIB1	bta-miR-15a	miR.MEcyan	*PCM1*	bta-miR-29a	miR.MEcyan
MIB1	bta-miR-29a	miR.MEcyan	*PCMT1*	bta-miR-15a	miR.MEcyan
MIB1	bta-miR-29b	miR.MEcyan	*PCMT1*	bta-miR-29e	miR.MEcyan
MIB1	bta-miR-29c	miR.MEcyan	*PCYOX1*	bta-miR-29e	miR.MEcyan
MIB1	bta-miR-29d-3p	miR.MEcyan	*PDCD11*	bta-miR-15a	miR.MEcyan
MICAL2	bta-miR-19a	miR.MEbrown	*PDCD6IP*	bta-miR-15a	miR.MEcyan
MICAL2	bta-miR-19b	miR.MEbrown	*PDCD6IP*	bta-miR-29e	miR.MEcyan
MICAL2	bta-miR-29a	miR.MEcyan	*PDE10A*	bta-miR-186	miR.MElightyellow
MICAL2	bta-miR-29e	miR.MEcyan	*PDE10A*	bta-miR-92b	miR.MElightyellow
MID1IP1	bta-miR-19a	miR.MEbrown	*PDE3B*	bta-miR-186	miR.MElightyellow
MID1IP1	bta-miR-19b	miR.MEbrown	*PDE4B*	bta-miR-29a	miR.MEcyan
MIER1	bta-miR-186	miR.MElightyellow	*PDE4DIP*	bta-miR-29a	miR.MEcyan
MIER3	bta-miR-29a	miR.MEcyan	*PDE4DIP*	bta-miR-29e	miR.MEcyan
MIER3	bta-miR-29b	miR.MEcyan	*PDF*	bta-miR-29e	miR.MEcyan
MIER3	bta-miR-29c	miR.MEcyan	*PDGFC*	bta-miR-186	miR.MElightyellow
MIER3	bta-miR-29d-3p	miR.MEcyan	*PDK1*	bta-miR-29e	miR.MEcyan
MOB3B	bta-miR-103	miR.MEbrown	*PDS5B*	bta-miR-29a	miR.MEcyan
MOB3B	bta-miR-107	miR.MEbrown	*PDXDC1*	bta-miR-92b	miR.MElightyellow
MOB3B	bta-miR-15a	miR.MEcyan	*PEAK1*	bta-miR-29a	miR.MEcyan
MOB3B	bta-miR-29e	miR.MEcyan	*PEAK1*	bta-miR-29b	miR.MEcyan
MON2	bta-miR-29e	miR.MEcyan	*PEAK1*	bta-miR-29c	miR.MEcyan
MPRIP	bta-miR-29e	miR.MEcyan	*PEAK1*	bta-miR-29d-3p	miR.MEcyan
MRPL45	bta-miR-21-5p	miR.MEbrown	*PEAK1*	bta-miR-29e	miR.MEcyan
MRPL49	bta-miR-21-5p	miR.MEbrown	*PELI3*	bta-miR-15a	miR.MEcyan
MTF1	bta-miR-29a	miR.MEcyan	*PELI3*	bta-miR-29a	miR.MEcyan
MTF1	bta-miR-29e	miR.MEcyan	*PEX11B*	bta-miR-29e	miR.MEcyan

MTHFD1	bta-miR-21-3p	miR.MEgreen	*PEX19*	bta-miR-15a	miR.MEcyan
MTHFD1	bta-miR-502b	miR.MEgreen	*PFKFB3*	bta-miR-29e	miR.MEcyan
MTHFD1	bta-miR-214	miR.MEmagenta	*PGAP1*	bta-miR-29b	miR.MEcyan
MTMR10	bta-miR-29a	miR.MEcyan	*PGAP1*	bta-miR-29c	miR.MEcyan
MXD4	bta-miR-125a	miR.MElightyellow	*PGAP1*	bta-miR-29d-3p	miR.MEcyan
MXD4	bta-let-7c	miR.MEtan	*PGAP1*	bta-miR-29e	miR.MEcyan
MXD4	bta-let-7e	miR.MEtan	*PGAP2*	bta-miR-29a	miR.MEcyan
MXD4	bta-let-7b	miR.MEtan	*PGAP2*	bta-miR-29b	miR.MEcyan
MXD4	bta-let-7a-5p	miR.MEtan	*PGAP2*	bta-miR-29c	miR.MEcyan
MXD4	bta-let-7f	miR.MEtan	*PGAP2*	bta-miR-29d-3p	miR.MEcyan
MYNN	bta-miR-29e	miR.MEcyan	*PGM3*	bta-miR-186	miR.MElightyellow
NAA15	bta-miR-15a	miR.MEcyan	*PGP*	bta-miR-29b	miR.MEcyan
NAA15	bta-miR-29a	miR.MEcyan	*PGP*	bta-miR-29c	miR.MEcyan
NAA15	bta-miR-29e	miR.MEcyan	*PGP*	bta-miR-29d-3p	miR.MEcyan
NACC1	bta-miR-19a	miR.MEbrown	*PGP*	bta-miR-30c	miR.MEmidnightblue
NACC1	bta-miR-19b	miR.MEbrown	*PGP*	bta-miR-30f	miR.MEmidnightblue
NACC1	bta-miR-29d-5p	miR.MEmidnightblue	*PHC1*	bta-miR-29a	miR.MEcyan
NACC1	bta-miR-331-3p	miR.MEmidnightblue	*PHC1*	bta-miR-29b	miR.MEcyan
NBEA	bta-miR-29e	miR.MEcyan	*PHC1*	bta-miR-29c	miR.MEcyan
NCOA2	bta-miR-29e	miR.MEcyan	*PHC1*	bta-miR-29d-3p	miR.MEcyan
NF1	bta-miR-15a	miR.MEcyan	*PHC3*	bta-miR-15a	miR.MEcyan
NF1	bta-miR-29e	miR.MEcyan	*PHC3*	bta-miR-29a	miR.MEcyan
NFAT5	bta-miR-29a	miR.MEcyan	*PHC3*	bta-miR-29e	miR.MEcyan
NFAT5	bta-miR-29b	miR.MEcyan	*PHF2*	bta-miR-29e	miR.MEcyan
NFAT5	bta-miR-29c	miR.MEcyan	*PHF2*	bta-miR-29d-5p	miR.MEmidnightblue
NFAT5	bta-miR-29d-3p	miR.MEcyan	*PHF3*	bta-miR-29e	miR.MEcyan
NFIA	bta-miR-29a	miR.MEcyan	*PHF6*	bta-miR-29a	miR.MEcyan
NFIA	bta-miR-29b	miR.MEcyan	*PHKB*	bta-miR-29a	miR.MEcyan
NFIA	bta-miR-29c	miR.MEcyan	*PIAS1*	bta-miR-15a	miR.MEcyan
NFIA	bta-miR-29d-3p	miR.MEcyan	*PIAS1*	bta-miR-29a	miR.MEcyan
NFIA	bta-miR-29e	miR.MEcyan	*PIAS1*	bta-miR-29e	miR.MEcyan
NFIB	bta-miR-125a	miR.MElightyellow	*PIAS2*	bta-miR-15a	miR.MEcyan
NFIB	bta-miR-92b	miR.MElightyellow	*PIAS2*	bta-miR-29b	miR.MEcyan
NFIC	bta-miR-29b	miR.MEcyan	*PIAS2*	bta-miR-29c	miR.MEcyan
NFIC	bta-miR-29c	miR.MEcyan	*PIAS2*	bta-miR-29d-3p	miR.MEcyan
NFIC	bta-miR-29d-3p	miR.MEcyan	*PIAS2*	bta-miR-29e	miR.MEcyan
NHSL2	bta-miR-125a	miR.MElightyellow	*PIK3AP1*	bta-miR-92b	miR.MElightyellow
NIPBL	bta-miR-29a	miR.MEcyan	*PIK3IP1*	bta-let-7c	miR.MEtan
NMNAT1	bta-miR-103	miR.MEbrown	*PIK3IP1*	bta-let-7e	miR.MEtan
NMNAT1	bta-miR-107	miR.MEbrown	*PIK3IP1*	bta-let-7b	miR.MEtan
NMNAT1	bta-miR-15a	miR.MEcyan	*PIK3IP1*	bta-let-7a-5p	miR.MEtan
NPEPL1	bta-miR-19a	miR.MEbrown	*PIK3IP1*	bta-let-7f	miR.MEtan
NPEPL1	bta-miR-19b	miR.MEbrown	*PKIA*	bta-miR-29e	miR.MEcyan

NPEPL1	bta-miR-29e	miR.MEcyan	*PKNOX2*	bta-miR-29a	miR.MEcyan
NR1D2	bta-miR-29a	miR.MEcyan	*PKNOX2*	bta-miR-30c	miR.MEmidnightblue
NR1D2	bta-miR-29e	miR.MEcyan	*PKNOX2*	bta-miR-30f	miR.MEmidnightblue
NR1H3	bta-miR-19a	miR.MEbrown	*PLA2G12A*	bta-miR-29e	miR.MEcyan
NR1H3	bta-miR-19b	miR.MEbrown	*PLA2G15*	bta-let-7c	miR.MEtan
NR1H3	bta-miR-29d-5p	miR.MEmidnightblue	*PLA2G15*	bta-let-7e	miR.MEtan
NR2C2	bta-miR-15a	miR.MEcyan	*PLA2G15*	bta-let-7b	miR.MEtan
NR3C2	bta-miR-29a	miR.MEcyan	*PLA2G15*	bta-let-7a-5p	miR.MEtan
NRBF2	bta-miR-19a	miR.MEbrown	*PLA2G15*	bta-let-7f	miR.MEtan
NRBF2	bta-miR-19b	miR.MEbrown	*PLAGL2*	bta-miR-29a	miR.MEcyan
NRBF2	bta-miR-30c	miR.MEmidnightblue	*PLAGL2*	bta-miR-29e	miR.MEcyan
NRBF2	bta-miR-30f	miR.MEmidnightblue	*PLD3*	bta-let-7c	miR.MEtan
NRBP1	bta-miR-19a	miR.MEbrown	*PLD3*	bta-let-7e	miR.MEtan
NRBP1	bta-miR-19b	miR.MEbrown	*PLD3*	bta-let-7b	miR.MEtan
NRBP1	bta-miR-15a	miR.MEcyan	*PLD3*	bta-let-7a-5p	miR.MEtan
NRBP1	bta-miR-30c	miR.MEmidnightblue	*PLD3*	bta-let-7f	miR.MEtan
NRBP1	bta-miR-30f	miR.MEmidnightblue	*PLEKHA8*	bta-miR-29a	miR.MEcyan
NRK	bta-miR-92b	miR.MElightyellow	*PLEKHA8*	bta-miR-29b	miR.MEcyan
NRK	bta-let-7c	miR.MEtan	*PLEKHA8*	bta-miR-29c	miR.MEcyan
NRK	bta-let-7e	miR.MEtan	*PLEKHA8*	bta-miR-29d-3p	miR.MEcyan
NRK	bta-let-7b	miR.MEtan	*PLEKHM3*	bta-miR-29a	miR.MEcyan
NRK	bta-let-7a-5p	miR.MEtan	*PLEKHM3*	bta-miR-29e	miR.MEcyan
NRK	bta-let-7f	miR.MEtan	*POGLUT1*	bta-miR-29a	miR.MEcyan
NUP50	bta-miR-15a	miR.MEcyan	*POGZ*	bta-miR-29e	miR.MEcyan
NUP54	bta-miR-19a	miR.MEbrown	*POLE3*	bta-miR-29b	miR.MEcyan
NUP54	bta-miR-19b	miR.MEbrown	*POLE3*	bta-miR-29c	miR.MEcyan
OTUD4	bta-miR-15a	miR.MEcyan	*POLE3*	bta-miR-29d-3p	miR.MEcyan
OTUD4	bta-miR-29a	miR.MEcyan	*POLR1A*	bta-miR-29a	miR.MEcyan
OTUD4	bta-miR-29b	miR.MEcyan	*POLR1A*	bta-miR-29e	miR.MEcyan
OTUD4	bta-miR-29c	miR.MEcyan	*POU2F1*	bta-miR-15a	miR.MEcyan
OTUD4	bta-miR-29d-3p	miR.MEcyan	*POU2F1*	bta-miR-29a	miR.MEcyan
OTUD4	bta-miR-29e	miR.MEcyan	*POU2F1*	bta-miR-29e	miR.MEcyan
OTUD7B	bta-miR-15a	miR.MEcyan	*PPFIBP1*	bta-miR-29a	miR.MEcyan
OTUD7B	bta-miR-29a	miR.MEcyan	*PPM1B*	bta-miR-29e	miR.MEcyan
PAFAH1B2	bta-miR-15a	miR.MEcyan	*PPM1H*	bta-miR-125a	miR.MElightyellow
PAFAH1B2	bta-miR-29a	miR.MEcyan	*PPM1H*	bta-miR-92b	miR.MElightyellow
PAFAH1B2	bta-miR-29e	miR.MEcyan	*PPP1CB*	bta-miR-29e	miR.MEcyan
PANK3	bta-miR-29e	miR.MEcyan	*PPP1R1A*	bta-miR-29a	miR.MEcyan
PARM1	bta-miR-125a	miR.MElightyellow	*PPP1R3D*	bta-miR-29a	miR.MEcyan
PCBP1	bta-miR-21-5p	miR.MEbrown	*PPP1R3D*	bta-miR-29b	miR.MEcyan
PCBP2	bta-miR-21-5p	miR.MEbrown	*PPP1R3D*	bta-miR-29c	miR.MEcyan
PCDHA13	bta-miR-186	miR.MElightyellow	*PPP1R3D*	bta-miR-29d-3p	miR.MEcyan
PCGF2	bta-miR-103	miR.MEbrown	*PPP1R3D*	bta-miR-29d-5p	miR.MEmidnightblue

PCGF2	bta-miR-107	miR.MEbrown	*PPP1R3F*	bta-miR-15a	miR.MEcyan
PCGF5	bta-miR-15a	miR.MEcyan	*PPP1R9A*	bta-miR-29b	miR.MEcyan
PCGF5	bta-miR-29a	miR.MEcyan	*PPP1R9A*	bta-miR-29c	miR.MEcyan
PCGF5	bta-miR-29e	miR.MEcyan	*PPP1R9A*	bta-miR-29d-3p	miR.MEcyan
PDCD4	bta-miR-186	miR.MElightyellow	*PPP1R9A*	bta-miR-29e	miR.MEcyan
PDE3A	bta-miR-29b	miR.MEcyan	*PPP2R1B*	bta-miR-125a	miR.MElightyellow
PDE3A	bta-miR-29c	miR.MEcyan	*PPP3CB*	bta-miR-29a	miR.MEcyan
PDE3A	bta-miR-29d-3p	miR.MEcyan	*PPP3CB*	bta-miR-30c	miR.MEmidnightblue
PDE3A	bta-miR-29e	miR.MEcyan	*PPP3CB*	bta-miR-30f	miR.MEmidnightblue
PDE4D	bta-miR-29e	miR.MEcyan	*PRDM1*	bta-miR-125a	miR.MElightyellow
PDE4D	bta-miR-30c	miR.MEmidnightblue	*PRDM4*	bta-miR-15a	miR.MEcyan
PDE4D	bta-miR-30f	miR.MEmidnightblue	*PRDM4*	bta-miR-877	miR.MEmidnightblue
PDZD2	bta-miR-92b	miR.MElightyellow	*PREPL*	bta-miR-29e	miR.MEcyan
PDZD8	bta-miR-15a	miR.MEcyan	*PREX2*	bta-miR-29e	miR.MEcyan
PDZD8	bta-miR-29e	miR.MEcyan	*PRKCA*	bta-miR-29e	miR.MEcyan
PEG10	bta-let-7c	miR.MEtan	*PRKCZ*	bta-miR-29e	miR.MEcyan
PEG10	bta-let-7e	miR.MEtan	*PRKD3*	bta-miR-29e	miR.MEcyan
PEG10	bta-let-7b	miR.MEtan	*PRRC1*	bta-miR-125a	miR.MElightyellow
PEG10	bta-let-7a-5p	miR.MEtan	*PRRC2B*	bta-miR-29e	miR.MEcyan
PEG10	bta-let-7f	miR.MEtan	*PSKH1*	bta-miR-15a	miR.MEcyan
PFKM	bta-miR-21-5p	miR.MEbrown	*PSMA5*	bta-miR-15a	miR.MEcyan
PFKM	bta-miR-877	miR.MEmidnightblue	*PSMA5*	bta-miR-29e	miR.MEcyan
PHAX	bta-miR-19a	miR.MEbrown	*PSMC2*	bta-miR-29e	miR.MEcyan
PHAX	bta-miR-19b	miR.MEbrown	*PSTPIP2*	bta-miR-29e	miR.MEcyan
PHAX	bta-miR-29a	miR.MEcyan	*PTAR1*	bta-miR-29e	miR.MEcyan
PHF12	bta-miR-29a	miR.MEcyan	*PTPN11*	bta-miR-29a	miR.MEcyan
PHF12	bta-miR-29e	miR.MEcyan	*PTPN11*	bta-miR-29e	miR.MEcyan
PHF20	bta-miR-15a	miR.MEcyan	*PTPRF*	bta-miR-125a	miR.MElightyellow
PHF20	bta-miR-29e	miR.MEcyan	*PTPRK*	bta-miR-92b	miR.MElightyellow
PHF5A	bta-miR-103	miR.MEbrown	*PTPRM*	bta-miR-15a	miR.MEcyan
PHF5A	bta-miR-107	miR.MEbrown	*PTPRM*	bta-miR-29e	miR.MEcyan
PHIP	bta-miR-15a	miR.MEcyan	*PTRH2*	bta-miR-29b	miR.MEcyan
PHLPP2	bta-miR-15a	miR.MEcyan	*PTRH2*	bta-miR-29c	miR.MEcyan
PHLPP2	bta-miR-29a	miR.MEcyan	*PTRH2*	bta-miR-29d-3p	miR.MEcyan
PHLPP2	bta-miR-29b	miR.MEcyan	*PUF60*	bta-miR-15a	miR.MEcyan
PHLPP2	bta-miR-29c	miR.MEcyan	*PUM2*	bta-miR-29a	miR.MEcyan
PHLPP2	bta-miR-29d-3p	miR.MEcyan	*PUM2*	bta-miR-29e	miR.MEcyan
PHLPP2	bta-miR-29e	miR.MEcyan	*R3HDM4*	bta-miR-29b	miR.MEcyan
PI4KB	bta-miR-103	miR.MEbrown	*R3HDM4*	bta-miR-29c	miR.MEcyan
PI4KB	bta-miR-107	miR.MEbrown	*R3HDM4*	bta-miR-29d-3p	miR.MEcyan
PI4KB	bta-miR-15a	miR.MEcyan	*R3HDM4*	bta-miR-29e	miR.MEcyan
PIK3C2A	bta-miR-15a	miR.MEcyan	*RAB12*	bta-miR-29b	miR.MEcyan
PIK3CA	bta-miR-29b	miR.MEcyan	*RAB12*	bta-miR-29c	miR.MEcyan

PIK3CA	bta-miR-29c	miR.MEcyan
PIK3CA	bta-miR-29d-3p	miR.MEcyan
PIK3CB	bta-miR-92b	miR.MElightyellow
PIKFYVE	bta-miR-29e	miR.MEcyan
PITPNA	bta-miR-103	miR.MEbrown
PITPNA	bta-miR-107	miR.MEbrown
PITPNA	bta-miR-29b	miR.MEcyan
PITPNA	bta-miR-29c	miR.MEcyan
PITPNA	bta-miR-29d-3p	miR.MEcyan
PLAA	bta-miR-19a	miR.MEbrown
PLAA	bta-miR-19b	miR.MEbrown
PLCL2	bta-miR-19a	miR.MEbrown
PLCL2	bta-miR-19b	miR.MEbrown
PLD1	bta-miR-92b	miR.MElightyellow
PLEKHA1	bta-miR-15a	miR.MEcyan
PLEKHA1	bta-miR-29a	miR.MEcyan
PLEKHA1	bta-miR-29b	miR.MEcyan
PLEKHA1	bta-miR-29c	miR.MEcyan
PLEKHA1	bta-miR-29d-3p	miR.MEcyan
PLEKHA1	bta-miR-29e	miR.MEcyan
PLEKHF2	bta-miR-103	miR.MEbrown
PLEKHF2	bta-miR-107	miR.MEbrown
PLEKHF2	bta-miR-29b	miR.MEcyan
PLEKHF2	bta-miR-29c	miR.MEcyan
PLEKHF2	bta-miR-29d-3p	miR.MEcyan
PLXDC2	bta-miR-186	miR.MElightyellow
PLXDC2	bta-miR-92b	miR.MElightyellow
PLXNA4	bta-miR-151-3p	miR.MElightyellow
PLXNA4	bta-miR-186	miR.MElightyellow
PLXNA4	bta-let-7c	miR.MEtan
PLXNA4	bta-let-7e	miR.MEtan
PLXNA4	bta-let-7b	miR.MEtan
PLXNA4	bta-let-7a-5p	miR.MEtan
PLXNA4	bta-let-7f	miR.MEtan
PLXNC1	bta-let-7c	miR.MEtan
PLXNC1	bta-let-7e	miR.MEtan
PLXNC1	bta-let-7b	miR.MEtan
PLXNC1	bta-let-7a-5p	miR.MEtan
PLXNC1	bta-let-7f	miR.MEtan
POLR3D	bta-miR-19a	miR.MEbrown
POLR3D	bta-miR-19b	miR.MEbrown
POLR3D	bta-miR-29e	miR.MEcyan
POMGNT1	bta-miR-103	miR.MEbrown
RAB12	bta-miR-29d-3p	miR.MEcyan
RAB22A	bta-miR-29e	miR.MEcyan
RAB2A	bta-miR-29a	miR.MEcyan
RAB3D	bta-miR-125a	miR.MElightyellow
RAB3GAP1	bta-miR-29a	miR.MEcyan
RAB3GAP2	bta-miR-29e	miR.MEcyan
RAB9A	bta-miR-15a	miR.MEcyan
RABGAP1L	bta-miR-92b	miR.MElightyellow
RABGEF1	bta-miR-29a	miR.MEcyan
RABGEF1	bta-miR-29b	miR.MEcyan
RABGEF1	bta-miR-29c	miR.MEcyan
RABGEF1	bta-miR-29d-3p	miR.MEcyan
RAC1	bta-miR-29a	miR.MEcyan
RAC1	bta-miR-29d-5p	miR.MEmidnightblue
RAD9B	bta-miR-29e	miR.MEcyan
RAD9B	bta-miR-30c	miR.MEmidnightblue
RAD9B	bta-miR-30f	miR.MEmidnightblue
RALBP1	bta-miR-29a	miR.MEcyan
RALGAPA2	bta-miR-29e	miR.MEcyan
RALGAPB	bta-miR-29a	miR.MEcyan
RALGAPB	bta-miR-29e	miR.MEcyan
RANBP3	bta-miR-15a	miR.MEcyan
RANBP6	bta-miR-29e	miR.MEcyan
RAPGEF1	bta-miR-29e	miR.MEcyan
RB1	bta-miR-29e	miR.MEcyan
RBL2	bta-miR-29e	miR.MEcyan
RBM12	bta-miR-15a	miR.MEcyan
RBM12	bta-miR-29a	miR.MEcyan
RBM12	bta-miR-29e	miR.MEcyan
RCOR1	bta-miR-29b	miR.MEcyan
RCOR1	bta-miR-29c	miR.MEcyan
RCOR1	bta-miR-29d-3p	miR.MEcyan
REV3L	bta-miR-29a	miR.MEcyan
REV3L	bta-miR-29b	miR.MEcyan
REV3L	bta-miR-29c	miR.MEcyan
REV3L	bta-miR-29d-3p	miR.MEcyan
RFX3	bta-miR-15a	miR.MEcyan
RFX3	bta-miR-29e	miR.MEcyan
RFX7	bta-miR-29a	miR.MEcyan
RFX7	bta-miR-29b	miR.MEcyan
RFX7	bta-miR-29c	miR.MEcyan
RFX7	bta-miR-29d-3p	miR.MEcyan
RFX7	bta-miR-29e	miR.MEcyan

POMGNT1	bta-miR-107	miR.MEbrown	*RHBDD1*	bta-miR-29b	miR.MEcyan
PPARGC1B	bta-miR-29e	miR.MEcyan	*RHBDD1*	bta-miR-29c	miR.MEcyan
PPM1A	bta-miR-19a	miR.MEbrown	*RHBDD1*	bta-miR-29d-3p	miR.MEcyan
PPM1A	bta-miR-19b	miR.MEbrown	*RHOBTB2*	bta-miR-15a	miR.MEcyan
PPM1A	bta-miR-15a	miR.MEcyan	*RHOQ*	bta-miR-29e	miR.MEcyan
PPM1A	bta-miR-29a	miR.MEcyan	*RILPL1*	bta-miR-29a	miR.MEcyan
PPP1R12A	bta-miR-29e	miR.MEcyan	*RLF*	bta-miR-29a	miR.MEcyan
PPP1R15B	bta-miR-186	miR.MElightyellow	*RLF*	bta-miR-29b	miR.MEcyan
PPP1R3B	bta-miR-21-3p	miR.MEgreen	*RLF*	bta-miR-29c	miR.MEcyan
PPP1R3B	bta-miR-214	miR.MEmagenta	*RLF*	bta-miR-29d-3p	miR.MEcyan
PPP3R1	bta-miR-103	miR.MEbrown	*RNF10*	bta-miR-15a	miR.MEcyan
PPP3R1	bta-miR-107	miR.MEbrown	*RNF138*	bta-miR-151-3p	miR.MElightyellow
PPP3R1	bta-miR-30c	miR.MEmidnightblue	*RNF139*	bta-miR-29a	miR.MEcyan
PPP3R1	bta-miR-30f	miR.MEmidnightblue	*RNF14*	bta-miR-29a	miR.MEcyan
PPP6C	bta-miR-103	miR.MEbrown	*RNF14*	bta-miR-29e	miR.MEcyan
PPP6C	bta-miR-107	miR.MEbrown	*RNF141*	bta-miR-29b	miR.MEcyan
PPP6C	bta-miR-15a	miR.MEcyan	*RNF141*	bta-miR-29c	miR.MEcyan
PPP6C	bta-miR-29a	miR.MEcyan	*RNF141*	bta-miR-29d-3p	miR.MEcyan
PPP6C	bta-miR-29e	miR.MEcyan	*RNF144B*	bta-miR-15a	miR.MEcyan
PPP6C	bta-miR-30c	miR.MEmidnightblue	*RNF144B*	bta-miR-29a	miR.MEcyan
PPP6C	bta-miR-30f	miR.MEmidnightblue	*RNF144B*	bta-miR-29e	miR.MEcyan
PPP6R3	bta-miR-15a	miR.MEcyan	*RNF144B*	bta-miR-331-3p	miR.MEmidnightblue
PQLC1	bta-miR-103	miR.MEbrown	*RNF146*	bta-miR-29e	miR.MEcyan
PQLC1	bta-miR-107	miR.MEbrown	*RNF169*	bta-miR-29b	miR.MEcyan
PRKCE	bta-miR-29e	miR.MEcyan	*RNF169*	bta-miR-29c	miR.MEcyan
PRR14L	bta-miR-29a	miR.MEcyan	*RNF169*	bta-miR-29d-3p	miR.MEcyan
PRR14L	bta-miR-29b	miR.MEcyan	*RNF169*	bta-miR-29e	miR.MEcyan
PRR14L	bta-miR-29c	miR.MEcyan	*RNF185*	bta-miR-29a	miR.MEcyan
PRR14L	bta-miR-29d-3p	miR.MEcyan	*RNF19B*	bta-miR-29a	miR.MEcyan
PSAP	bta-miR-19a	miR.MEbrown	*RNF214*	bta-miR-29b	miR.MEcyan
PSAP	bta-miR-19b	miR.MEbrown	*RNF214*	bta-miR-29c	miR.MEcyan
PSD3	bta-miR-29e	miR.MEcyan	*RNF214*	bta-miR-29d-3p	miR.MEcyan
PSMB5	bta-miR-103	miR.MEbrown	*RNF217*	bta-miR-15a	miR.MEcyan
PSMB5	bta-miR-107	miR.MEbrown	*RNF217*	bta-miR-29a	miR.MEcyan
PSMB5	bta-miR-29e	miR.MEcyan	*RNF217*	bta-miR-29b	miR.MEcyan
PSMF1	bta-miR-103	miR.MEbrown	*RNF217*	bta-miR-29c	miR.MEcyan
PSMF1	bta-miR-107	miR.MEbrown	*RNF217*	bta-miR-29d-3p	miR.MEcyan
PTGES3	bta-miR-19a	miR.MEbrown	*RNF217*	bta-miR-30c	miR.MEmidnightblue
PTGES3	bta-miR-19b	miR.MEbrown	*RNF217*	bta-miR-30f	miR.MEmidnightblue
PTGES3	bta-miR-29e	miR.MEcyan	*RNF220*	bta-miR-29e	miR.MEcyan
PTP4A1	bta-miR-19a	miR.MEbrown	*RNF220*	bta-miR-30c	miR.MEmidnightblue
PTP4A1	bta-miR-19b	miR.MEbrown	*RNF220*	bta-miR-30f	miR.MEmidnightblue
PTP4A1	bta-miR-30c	miR.MEmidnightblue	*RNGTT*	bta-miR-29e	miR.MEcyan

PTP4A1	bta-miR-30f	miR.MEmidnightblue
PTPRD	bta-miR-92b	miR.MElightyellow
PURA	bta-miR-15a	miR.MEcyan
PURA	bta-miR-29a	miR.MEcyan
PURA	bta-miR-29b	miR.MEcyan
PURA	bta-miR-29c	miR.MEcyan
PURA	bta-miR-29d-3p	miR.MEcyan
PURB	bta-miR-15a	miR.MEcyan
PYGO1	bta-miR-29e	miR.MEcyan
QKI	bta-miR-15a	miR.MEcyan
QKI	bta-miR-29b	miR.MEcyan
QKI	bta-miR-29c	miR.MEcyan
QKI	bta-miR-29d-3p	miR.MEcyan
RAB11FIP2	bta-miR-15a	miR.MEcyan
RAB21	bta-miR-19a	miR.MEbrown
RAB21	bta-miR-19b	miR.MEbrown
RAB21	bta-miR-29a	miR.MEcyan
RAB4A	bta-miR-186	miR.MElightyellow
RAB5B	bta-miR-19a	miR.MEbrown
RAB5B	bta-miR-19b	miR.MEbrown
RAB5B	bta-miR-331-3p	miR.MEmidnightblue
RAB8B	bta-miR-125a	miR.MElightyellow
RAB8B	bta-miR-92b	miR.MElightyellow
RAD21	bta-miR-92b	miR.MElightyellow
RAD23B	bta-miR-19a	miR.MEbrown
RAD23B	bta-miR-19b	miR.MEbrown
RAD23B	bta-miR-15a	miR.MEcyan
RAD23B	bta-miR-30c	miR.MEmidnightblue
RAD23B	bta-miR-30f	miR.MEmidnightblue
RAF1	bta-miR-19a	miR.MEbrown
RAF1	bta-miR-19b	miR.MEbrown
RAF1	bta-miR-15a	miR.MEcyan
RALGPS2	bta-miR-125a	miR.MElightyellow
RAP2C	bta-miR-103	miR.MEbrown
RAP2C	bta-miR-107	miR.MEbrown
RAP2C	bta-miR-19a	miR.MEbrown
RAP2C	bta-miR-19b	miR.MEbrown
RAP2C	bta-miR-15a	miR.MEcyan
RAP2C	bta-miR-30c	miR.MEmidnightblue
RAP2C	bta-miR-30f	miR.MEmidnightblue
RASAL2	bta-miR-29b	miR.MEcyan
RASAL2	bta-miR-29c	miR.MEcyan
RASAL2	bta-miR-29d-3p	miR.MEcyan
ROBO1	bta-miR-92b	miR.MElightyellow
ROCK2	bta-miR-15a	miR.MEcyan
ROCK2	bta-miR-29a	miR.MEcyan
ROCK2	bta-miR-30c	miR.MEmidnightblue
ROCK2	bta-miR-30f	miR.MEmidnightblue
RPE	bta-miR-15a	miR.MEcyan
RPF1	bta-miR-29e	miR.MEcyan
RPP14	bta-miR-29e	miR.MEcyan
RPS6KA1	bta-miR-125a	miR.MElightyellow
RPS6KB1	bta-miR-29a	miR.MEcyan
RRAGA	bta-miR-15a	miR.MEcyan
RREB1	bta-miR-15a	miR.MEcyan
RSBN1	bta-miR-15a	miR.MEcyan
RSBN1L	bta-miR-29a	miR.MEcyan
RSF1	bta-miR-15a	miR.MEcyan
RSF1	bta-miR-29a	miR.MEcyan
RSF1	bta-miR-29e	miR.MEcyan
RWDD2B	bta-miR-29e	miR.MEcyan
SAMD12	bta-miR-186	miR.MElightyellow
SAMD12	bta-let-7c	miR.MEtan
SAMD12	bta-let-7e	miR.MEtan
SAMD12	bta-let-7b	miR.MEtan
SAMD12	bta-let-7a-5p	miR.MEtan
SAMD12	bta-let-7f	miR.MEtan
SAP130	bta-miR-29e	miR.MEcyan
SARM1	bta-miR-125a	miR.MElightyellow
SART3	bta-miR-29e	miR.MEcyan
SCAF11	bta-miR-29e	miR.MEcyan
SCD	bta-let-7c	miR.MEtan
SCD	bta-let-7e	miR.MEtan
SCD	bta-let-7b	miR.MEtan
SCD	bta-let-7a-5p	miR.MEtan
SCD	bta-let-7f	miR.MEtan
SCHIP1	bta-miR-29a	miR.MEcyan
SCHIP1	bta-miR-29b	miR.MEcyan
SCHIP1	bta-miR-29c	miR.MEcyan
SCHIP1	bta-miR-29d-3p	miR.MEcyan
SDK1	bta-let-7c	miR.MEtan
SDK1	bta-let-7e	miR.MEtan
SDK1	bta-let-7b	miR.MEtan
SDK1	bta-let-7a-5p	miR.MEtan
SDK1	bta-let-7f	miR.MEtan
SEC16A	bta-miR-15a	miR.MEcyan

RASAL2	bta-miR-29e	miR.MEcyan	*SEC23A*	bta-miR-29a	miR.MEcyan
RBBP6	bta-miR-15a	miR.MEcyan	*SEC23A*	bta-miR-29e	miR.MEcyan
RBM20	bta-miR-19a	miR.MEbrown	*SEC24A*	bta-miR-15a	miR.MEcyan
RBM20	bta-miR-19b	miR.MEbrown	*SEC24A*	bta-miR-29a	miR.MEcyan
RBM20	bta-miR-29e	miR.MEcyan	*SEH1L*	bta-miR-15a	miR.MEcyan
RBPJ	bta-miR-92b	miR.MElightyellow	*SEH1L*	bta-miR-29a	miR.MEcyan
RBPJ	bta-let-7c	miR.MEtan	*SEL1L*	bta-miR-29a	miR.MEcyan
RBPJ	bta-let-7e	miR.MEtan	*SENP5*	bta-miR-15a	miR.MEcyan
RBPJ	bta-let-7b	miR.MEtan	*SEPHS1*	bta-miR-29e	miR.MEcyan
RBPJ	bta-let-7a-5p	miR.MEtan	*SERBP1*	bta-miR-15a	miR.MEcyan
RBPJ	bta-let-7f	miR.MEtan	*SERBP1*	bta-miR-29a	miR.MEcyan
RDX	bta-miR-29a	miR.MEcyan	*SERBP1*	bta-miR-29b	miR.MEcyan
REEP3	bta-miR-125a	miR.MElightyellow	*SERBP1*	bta-miR-29c	miR.MEcyan
REST	bta-miR-125a	miR.MElightyellow	*SERBP1*	bta-miR-29d-3p	miR.MEcyan
REST	bta-miR-92b	miR.MElightyellow	*SERBP1*	bta-miR-29e	miR.MEcyan
RFFL	bta-let-7c	miR.MEtan	*SERINC5*	bta-miR-125a	miR.MElightyellow
RFFL	bta-let-7e	miR.MEtan	*SERTM1*	bta-miR-186	miR.MElightyellow
RFFL	bta-let-7b	miR.MEtan	*SETD3*	bta-miR-15a	miR.MEcyan
RFFL	bta-let-7a-5p	miR.MEtan	*SETD3*	bta-miR-29a	miR.MEcyan
RFFL	bta-let-7f	miR.MEtan	*SETD3*	bta-miR-30c	miR.MEmidnightblue
RICTOR	bta-miR-15a	miR.MEcyan	*SETD3*	bta-miR-30f	miR.MEmidnightblue
RICTOR	bta-miR-29a	miR.MEcyan	*SETDB1*	bta-miR-29a	miR.MEcyan
RLIM	bta-miR-15a	miR.MEcyan	*SFT2D2*	bta-miR-29e	miR.MEcyan
RLIM	bta-miR-29b	miR.MEcyan	*SFXN1*	bta-miR-92b	miR.MElightyellow
RLIM	bta-miR-29c	miR.MEcyan	*SFXN5*	bta-miR-15a	miR.MEcyan
RLIM	bta-miR-29d-3p	miR.MEcyan	*SFXN5*	bta-miR-29e	miR.MEcyan
RMND5A	bta-miR-21-5p	miR.MEbrown	*SGK3*	bta-miR-92b	miR.MElightyellow
RNF11	bta-miR-19a	miR.MEbrown	*SGMS1*	bta-miR-29a	miR.MEcyan
RNF11	bta-miR-19b	miR.MEbrown	*SH3GLB1*	bta-miR-29a	miR.MEcyan
RNF111	bta-miR-15a	miR.MEcyan	*SH3GLB1*	bta-miR-29b	miR.MEcyan
RNF111	bta-miR-29e	miR.MEcyan	*SH3GLB1*	bta-miR-29c	miR.MEcyan
RNF125	bta-miR-186	miR.MElightyellow	*SH3GLB1*	bta-miR-29d-3p	miR.MEcyan
RNF130	bta-miR-19a	miR.MEbrown	*SH3GLB1*	bta-miR-30c	miR.MEmidnightblue
RNF130	bta-miR-19b	miR.MEbrown	*SH3GLB1*	bta-miR-30f	miR.MEmidnightblue
RNF157	bta-miR-103	miR.MEbrown	*SH3RF2*	bta-miR-29a	miR.MEcyan
RNF157	bta-miR-107	miR.MEbrown	*SHOC2*	bta-miR-15a	miR.MEcyan
RORA	bta-miR-15a	miR.MEcyan	*SHOC2*	bta-miR-29e	miR.MEcyan
RORA	bta-miR-29a	miR.MEcyan	*SHPRH*	bta-miR-29b	miR.MEcyan
RORA	bta-miR-29b	miR.MEcyan	*SHPRH*	bta-miR-29c	miR.MEcyan
RORA	bta-miR-29c	miR.MEcyan	*SHPRH*	bta-miR-29d-3p	miR.MEcyan
RORA	bta-miR-29d-3p	miR.MEcyan	*SHROOM3*	bta-miR-29a	miR.MEcyan
RORA	bta-miR-29e	miR.MEcyan	*SHROOM3*	bta-miR-29e	miR.MEcyan
RPRD2	bta-miR-15a	miR.MEcyan	*SHROOM3*	bta-miR-331-3p	miR.MEmidnightblue

RPS6KA3	bta-miR-15a	miR.MEcyan	*SIAH1*	bta-miR-15a	miR.MEcyan
RPS6KA3	bta-miR-29b	miR.MEcyan	*SIAH1*	bta-miR-193a-3p	miR.MEmidnightblue
RPS6KA3	bta-miR-29c	miR.MEcyan	*SIDT2*	bta-miR-15a	miR.MEcyan
RPS6KA3	bta-miR-29d-3p	miR.MEcyan	*SIDT2*	bta-miR-29a	miR.MEcyan
RPS6KA3	bta-miR-29e	miR.MEcyan	*SIDT2*	bta-miR-29b	miR.MEcyan
RRAGC	bta-miR-186	miR.MElightyellow	*SIDT2*	bta-miR-29c	miR.MEcyan
RRAGD	bta-miR-19a	miR.MEbrown	*SIDT2*	bta-miR-29d-3p	miR.MEcyan
RRAGD	bta-miR-19b	miR.MEbrown	*SIDT2*	bta-miR-30c	miR.MEmidnightblue
RRAGD	bta-miR-29e	miR.MEcyan	*SIDT2*	bta-miR-30f	miR.MEmidnightblue
RSAD2	bta-miR-199c	miR.MEmagenta	*SIKE1*	bta-miR-29a	miR.MEcyan
RTN4RL1	bta-miR-19a	miR.MEbrown	*SIKE1*	bta-miR-29b	miR.MEcyan
RTN4RL1	bta-miR-19b	miR.MEbrown	*SIKE1*	bta-miR-29c	miR.MEcyan
RUNX1T1	bta-miR-186	miR.MElightyellow	*SIKE1*	bta-miR-29d-3p	miR.MEcyan
RUNX1T1	bta-miR-92b	miR.MElightyellow	*SIRPA*	bta-miR-92b	miR.MElightyellow
SAMD4A	bta-miR-15a	miR.MEcyan	*SIRT2*	bta-miR-29a	miR.MEcyan
SAMD4A	bta-miR-29b	miR.MEcyan	*SLC15A4*	bta-miR-15a	miR.MEcyan
SAMD4A	bta-miR-29c	miR.MEcyan	*SLC15A4*	bta-miR-29a	miR.MEcyan
SAMD4A	bta-miR-29d-3p	miR.MEcyan	*SLC20A1*	bta-let-7c	miR.MEtan
SBDS	bta-miR-103	miR.MEbrown	*SLC20A1*	bta-let-7e	miR.MEtan
SBDS	bta-miR-107	miR.MEbrown	*SLC20A1*	bta-let-7b	miR.MEtan
SBNO1	bta-miR-15a	miR.MEcyan	*SLC20A1*	bta-let-7a-5p	miR.MEtan
SBNO1	bta-miR-29e	miR.MEcyan	*SLC20A1*	bta-let-7f	miR.MEtan
SCN1B	bta-miR-19a	miR.MEbrown	*SLC22A23*	bta-miR-29e	miR.MEcyan
SCN1B	bta-miR-19b	miR.MEbrown	*SLC25A16*	bta-miR-92b	miR.MElightyellow
SCN4B	bta-miR-19a	miR.MEbrown	*SLC25A23*	bta-miR-29e	miR.MEcyan
SCN4B	bta-miR-19b	miR.MEbrown	*SLC25A53*	bta-miR-29a	miR.MEcyan
SCN4B	bta-miR-15a	miR.MEcyan	*SLC25A53*	bta-miR-29e	miR.MEcyan
SCN4B	bta-miR-29a	miR.MEcyan	*SLC35B4*	bta-miR-29a	miR.MEcyan
SCN4B	bta-miR-29e	miR.MEcyan	*SLC35B4*	bta-miR-29b	miR.MEcyan
SCOC	bta-miR-19a	miR.MEbrown	*SLC35B4*	bta-miR-29c	miR.MEcyan
SCOC	bta-miR-19b	miR.MEbrown	*SLC35B4*	bta-miR-29d-3p	miR.MEcyan
SCOC	bta-miR-15a	miR.MEcyan	*SLC35B4*	bta-miR-29e	miR.MEcyan
SCOC	bta-miR-29e	miR.MEcyan	*SLC35E2*	bta-miR-29e	miR.MEcyan
SDC2	bta-miR-103	miR.MEbrown	*SLC38A4*	bta-miR-29a	miR.MEcyan
SDC2	bta-miR-107	miR.MEbrown	*SLC38A4*	bta-miR-30c	miR.MEmidnightblue
SDC2	bta-miR-29e	miR.MEcyan	*SLC38A4*	bta-miR-30f	miR.MEmidnightblue
SDC2	bta-miR-30c	miR.MEmidnightblue	*SLC39A10*	bta-miR-15a	miR.MEcyan
SDC2	bta-miR-30f	miR.MEmidnightblue	*SLC39A10*	bta-miR-29a	miR.MEcyan
SEC61A2	bta-miR-19a	miR.MEbrown	*SLC39A9*	bta-miR-125a	miR.MElightyellow
SEC61A2	bta-miR-19b	miR.MEbrown	*SLC6A17*	bta-miR-125a	miR.MElightyellow
SEC61A2	bta-miR-29e	miR.MEcyan	*SLC7A1*	bta-miR-125a	miR.MElightyellow
SEC61A2	bta-miR-30c	miR.MEmidnightblue	*SLC7A8*	bta-miR-29a	miR.MEcyan
SEC61A2	bta-miR-30f	miR.MEmidnightblue	*SLC7A8*	bta-miR-29e	miR.MEcyan

SEC63	bta-miR-186	miR.MElightyellow
SEL1L3	bta-miR-19a	miR.MEbrown
SEL1L3	bta-miR-19b	miR.MEbrown
SEL1L3	bta-miR-15a	miR.MEcyan
SEMA4C	bta-miR-125a	miR.MElightyellow
SEMA4C	bta-let-7c	miR.MEtan
SEMA4C	bta-let-7e	miR.MEtan
SEMA4C	bta-let-7b	miR.MEtan
SEMA4C	bta-let-7a-5p	miR.MEtan
SEMA4C	bta-let-7f	miR.MEtan
SEMA4F	bta-miR-125a	miR.MElightyellow
SEMA4F	bta-let-7c	miR.MEtan
SEMA4F	bta-let-7e	miR.MEtan
SEMA4F	bta-let-7b	miR.MEtan
SEMA4F	bta-let-7a-5p	miR.MEtan
SEMA4F	bta-let-7f	miR.MEtan
SEMA6D	bta-miR-92b	miR.MElightyellow
SEPT7	bta-miR-151-3p	miR.MElightyellow
SEPT7	bta-miR-186	miR.MElightyellow
SERINC3	bta-miR-186	miR.MElightyellow
SESN1	bta-miR-15a	miR.MEcyan
SESN1	bta-miR-29b	miR.MEcyan
SESN1	bta-miR-29c	miR.MEcyan
SESN1	bta-miR-29d-3p	miR.MEcyan
SESN3	bta-miR-186	miR.MElightyellow
SESN3	bta-miR-92b	miR.MElightyellow
SESN3	bta-let-7c	miR.MEtan
SESN3	bta-let-7e	miR.MEtan
SESN3	bta-let-7b	miR.MEtan
SESN3	bta-let-7a-5p	miR.MEtan
SESN3	bta-let-7f	miR.MEtan
SESTD1	bta-miR-125a	miR.MElightyellow
SESTD1	bta-miR-186	miR.MElightyellow
SESTD1	bta-miR-92b	miR.MElightyellow
SETD1B	bta-miR-15a	miR.MEcyan
SETD5	bta-miR-29b	miR.MEcyan
SETD5	bta-miR-29c	miR.MEcyan
SETD5	bta-miR-29d-3p	miR.MEcyan
SF3A1	bta-miR-103	miR.MEbrown
SF3A1	bta-miR-107	miR.MEbrown
SF3A1	bta-miR-15a	miR.MEcyan
SGIP1	bta-miR-125a	miR.MElightyellow
SGIP1	bta-miR-92b	miR.MElightyellow
SLC9A7	bta-miR-92b	miR.MElightyellow
SLCO3A1	bta-miR-29e	miR.MEcyan
SLK	bta-miR-29a	miR.MEcyan
SLK	bta-miR-29b	miR.MEcyan
SLK	bta-miR-29c	miR.MEcyan
SLK	bta-miR-29d-3p	miR.MEcyan
SLX4IP	bta-miR-29a	miR.MEcyan
SLX4IP	bta-miR-29e	miR.MEcyan
SMAD2	bta-miR-15a	miR.MEcyan
SMAD2	bta-miR-29e	miR.MEcyan
SMAD3	bta-miR-15a	miR.MEcyan
SMAD3	bta-miR-29e	miR.MEcyan
SMARCA5	bta-miR-29e	miR.MEcyan
SMARCA5	bta-miR-30c	miR.MEmidnightblue
SMARCA5	bta-miR-30f	miR.MEmidnightblue
SMARCC1	bta-miR-29b	miR.MEcyan
SMARCC1	bta-miR-29c	miR.MEcyan
SMARCC1	bta-miR-29d-3p	miR.MEcyan
SMARCC1	bta-miR-29e	miR.MEcyan
SMC1A	bta-miR-29a	miR.MEcyan
SMC1A	bta-miR-29e	miR.MEcyan
SMC2	bta-miR-186	miR.MElightyellow
SMIM13	bta-miR-15a	miR.MEcyan
SMIM14	bta-miR-92b	miR.MElightyellow
SMU1	bta-miR-29e	miR.MEcyan
SNTB1	bta-miR-29a	miR.MEcyan
SNX1	bta-miR-29b	miR.MEcyan
SNX1	bta-miR-29c	miR.MEcyan
SNX1	bta-miR-29d-3p	miR.MEcyan
SNX1	bta-miR-30c	miR.MEmidnightblue
SNX1	bta-miR-30f	miR.MEmidnightblue
SNX2	bta-miR-186	miR.MElightyellow
SNX2	bta-miR-92b	miR.MElightyellow
SNX30	bta-miR-186	miR.MElightyellow
SNX33	bta-miR-15a	miR.MEcyan
SOBP	bta-miR-15a	miR.MEcyan
SOCS4	bta-miR-29e	miR.MEcyan
SORT1	bta-miR-15a	miR.MEcyan
SOX11	bta-miR-125a	miR.MElightyellow
SOX11	bta-miR-186	miR.MElightyellow
SOX11	bta-miR-92b	miR.MElightyellow
SP1	bta-miR-29a	miR.MEcyan
SP1	bta-miR-29b	miR.MEcyan

SH3BP5	bta-miR-103	miR.MEbrown
SH3BP5	bta-miR-107	miR.MEbrown
SH3BP5	bta-miR-15a	miR.MEcyan
SH3D19	bta-miR-92b	miR.MElightyellow
SH3RF3	bta-miR-19a	miR.MEbrown
SH3RF3	bta-miR-19b	miR.MEbrown
SH3RF3	bta-miR-29b	miR.MEcyan
SH3RF3	bta-miR-29c	miR.MEcyan
SH3RF3	bta-miR-29d-3p	miR.MEcyan
SIK2	bta-miR-92b	miR.MElightyellow
SIX1	bta-miR-19a	miR.MEbrown
SIX1	bta-miR-19b	miR.MEbrown
SIX1	bta-miR-30c	miR.MEmidnightblue
SIX1	bta-miR-30f	miR.MEmidnightblue
SKI	bta-miR-92b	miR.MElightyellow
SKIL	bta-miR-15a	miR.MEcyan
SLC24A3	bta-miR-92b	miR.MElightyellow
SLC25A34	bta-miR-214	miR.MEmagenta
SLC2A3	bta-miR-92b	miR.MElightyellow
SLC44A1	bta-miR-151-3p	miR.MElightyellow
SLC44A1	bta-miR-92b	miR.MElightyellow
SLC48A1	bta-miR-19a	miR.MEbrown
SLC48A1	bta-miR-19b	miR.MEbrown
SLC5A3	bta-miR-186	miR.MElightyellow
SLC8A1	bta-miR-92b	miR.MElightyellow
SLC9A2	bta-miR-19a	miR.MEbrown
SLC9A2	bta-miR-19b	miR.MEbrown
SMAD5	bta-miR-15a	miR.MEcyan
SMAD5	bta-miR-29e	miR.MEcyan
SMAD7	bta-miR-92b	miR.MElightyellow
SMARCA2	bta-miR-29b	miR.MEcyan
SMARCA2	bta-miR-29c	miR.MEcyan
SMARCA2	bta-miR-29d-3p	miR.MEcyan
SMCR8	bta-miR-29e	miR.MEcyan
SMTNL2	bta-miR-103	miR.MEbrown
SMTNL2	bta-miR-107	miR.MEbrown
SMTNL2	bta-miR-29a	miR.MEcyan
SMTNL2	bta-miR-29b	miR.MEcyan
SMTNL2	bta-miR-29c	miR.MEcyan
SMTNL2	bta-miR-29d-3p	miR.MEcyan
SMURF1	bta-miR-125a	miR.MElightyellow
SMURF1	bta-miR-92b	miR.MElightyellow
SMURF2	bta-miR-186	miR.MElightyellow
SP1	bta-miR-29c	miR.MEcyan
SP1	bta-miR-29d-3p	miR.MEcyan
SP1	bta-miR-29e	miR.MEcyan
SP140L	bta-miR-29e	miR.MEcyan
SP4	bta-miR-29e	miR.MEcyan
SPAG9	bta-miR-29e	miR.MEcyan
SPAST	bta-miR-29b	miR.MEcyan
SPAST	bta-miR-29c	miR.MEcyan
SPAST	bta-miR-29d-3p	miR.MEcyan
SPAST	bta-miR-30c	miR.MEmidnightblue
SPAST	bta-miR-30f	miR.MEmidnightblue
SPOP	bta-miR-29a	miR.MEcyan
SPR	bta-miR-29e	miR.MEcyan
SPRTN	bta-miR-29a	miR.MEcyan
SPRTN	bta-miR-29e	miR.MEcyan
SPTLC2	bta-miR-186	miR.MElightyellow
SQSTM1	bta-miR-29e	miR.MEcyan
SRD5A1	bta-miR-29e	miR.MEcyan
SRL	bta-miR-29e	miR.MEcyan
SRP72	bta-miR-15a	miR.MEcyan
SRPK1	bta-miR-15a	miR.MEcyan
SS18L1	bta-miR-29b	miR.MEcyan
SS18L1	bta-miR-29c	miR.MEcyan
SS18L1	bta-miR-29d-3p	miR.MEcyan
SSBP1	bta-miR-29e	miR.MEcyan
SSH2	bta-miR-29e	miR.MEcyan
SSR1	bta-miR-15a	miR.MEcyan
SSR1	bta-miR-30c	miR.MEmidnightblue
SSR1	bta-miR-30f	miR.MEmidnightblue
ST8SIA2	bta-miR-29e	miR.MEcyan
ST8SIA2	bta-miR-29d-5p	miR.MEmidnightblue
STARD10	bta-miR-29a	miR.MEcyan
STARD13	bta-miR-125a	miR.MElightyellow
STARD13	bta-miR-92b	miR.MElightyellow
STC1	bta-miR-125a	miR.MElightyellow
STK40	bta-miR-15a	miR.MEcyan
STON2	bta-miR-29a	miR.MEcyan
STON2	bta-miR-29e	miR.MEcyan
STRADB	bta-miR-15a	miR.MEcyan
STRN4	bta-miR-29a	miR.MEcyan
STRN4	bta-miR-29b	miR.MEcyan
STRN4	bta-miR-29c	miR.MEcyan
STRN4	bta-miR-29d-3p	miR.MEcyan

SNTB2	bta-miR-15a	miR.MEcyan	*STX17*	bta-miR-29a	miR.MEcyan
SNTB2	bta-miR-29a	miR.MEcyan	*STX17*	bta-miR-29b	miR.MEcyan
SNTB2	bta-miR-29b	miR.MEcyan	*STX17*	bta-miR-29c	miR.MEcyan
SNTB2	bta-miR-29c	miR.MEcyan	*STX17*	bta-miR-29d-3p	miR.MEcyan
SNTB2	bta-miR-29d-3p	miR.MEcyan	*STX17*	bta-miR-29e	miR.MEcyan
SNX11	bta-miR-103	miR.MEbrown	*STX4*	bta-miR-15a	miR.MEcyan
SNX11	bta-miR-107	miR.MEbrown	*STXBP1*	bta-miR-214	miR.MEmagenta
SNX11	bta-miR-21-5p	miR.MEbrown	*STXBP4*	bta-miR-29a	miR.MEcyan
SNX11	bta-miR-15a	miR.MEcyan	*STXBP4*	bta-miR-29e	miR.MEcyan
SNX11	bta-miR-29e	miR.MEcyan	*STXBP5*	bta-miR-15a	miR.MEcyan
SNX12	bta-miR-103	miR.MEbrown	*SUB1*	bta-miR-29a	miR.MEcyan
SNX12	bta-miR-107	miR.MEbrown	*SUB1*	bta-miR-29b	miR.MEcyan
SNX12	bta-miR-29e	miR.MEcyan	*SUB1*	bta-miR-29c	miR.MEcyan
SNX12	bta-miR-331-3p	miR.MEmidnightblue	*SUB1*	bta-miR-29d-3p	miR.MEcyan
SNX18	bta-miR-125a	miR.MElightyellow	*SUPT6H*	bta-miR-29e	miR.MEcyan
SNX18	bta-miR-186	miR.MElightyellow	*SYNE1*	bta-miR-29e	miR.MEcyan
SOCS5	bta-miR-151-3p	miR.MElightyellow	*SYNJ1*	bta-miR-15a	miR.MEcyan
SOCS5	bta-miR-186	miR.MElightyellow	*SYNJ1*	bta-miR-29e	miR.MEcyan
SOCS5	bta-miR-92b	miR.MElightyellow	*SYNRG*	bta-miR-15a	miR.MEcyan
SOCS6	bta-miR-15a	miR.MEcyan	*TADA2B*	bta-miR-29a	miR.MEcyan
SOCS6	bta-miR-30c	miR.MEmidnightblue	*TADA2B*	bta-miR-29e	miR.MEcyan
SOCS6	bta-miR-30f	miR.MEmidnightblue	*TADA2B*	bta-miR-30c	miR.MEmidnightblue
SOX4	bta-miR-92b	miR.MElightyellow	*TADA2B*	bta-miR-30f	miR.MEmidnightblue
SPATA2	bta-miR-19a	miR.MEbrown	*TAF1*	bta-miR-29e	miR.MEcyan
SPATA2	bta-miR-19b	miR.MEbrown	*TAF7*	bta-miR-29e	miR.MEcyan
SPATA2	bta-miR-29e	miR.MEcyan	*TAF8*	bta-miR-29e	miR.MEcyan
SPCS3	bta-miR-21-5p	miR.MEbrown	*TANC1*	bta-miR-29a	miR.MEcyan
SPCS3	bta-miR-29e	miR.MEcyan	*TANC1*	bta-miR-29b	miR.MEcyan
SPCS3	bta-miR-30c	miR.MEmidnightblue	*TANC1*	bta-miR-29c	miR.MEcyan
SPCS3	bta-miR-30f	miR.MEmidnightblue	*TANC1*	bta-miR-29d-3p	miR.MEcyan
SPEN	bta-miR-15a	miR.MEcyan	*TAP2*	bta-miR-199c	miR.MEmagenta
SPEN	bta-miR-29b	miR.MEcyan	*TAP2*	bta-miR-214	miR.MEmagenta
SPEN	bta-miR-29c	miR.MEcyan	*TBC1D15*	bta-miR-186	miR.MElightyellow
SPEN	bta-miR-29d-3p	miR.MEcyan	*TBC1D16*	bta-miR-125a	miR.MElightyellow
SPTSSA	bta-miR-19a	miR.MEbrown	*TBC1D20*	bta-miR-15a	miR.MEcyan
SPTSSA	bta-miR-19b	miR.MEbrown	*TBC1D30*	bta-miR-92b	miR.MElightyellow
SPTY2D1	bta-miR-29b	miR.MEcyan	*TBC1D7*	bta-miR-29b	miR.MEcyan
SPTY2D1	bta-miR-29c	miR.MEcyan	*TBC1D7*	bta-miR-29c	miR.MEcyan
SPTY2D1	bta-miR-29d-3p	miR.MEcyan	*TBC1D7*	bta-miR-29d-3p	miR.MEcyan
SRGAP1	bta-let-7c	miR.MEtan	*TBRG1*	bta-miR-15a	miR.MEcyan
SRGAP1	bta-let-7e	miR.MEtan	*TBRG1*	bta-miR-29e	miR.MEcyan
SRGAP1	bta-let-7b	miR.MEtan	*TBX15*	bta-miR-29e	miR.MEcyan
SRGAP1	bta-let-7a-5p	miR.MEtan	*TCAIM*	bta-miR-199c	miR.MEmagenta

SRGAP1	bta-let-7f	miR.MEtan	*TCEA3*	bta-miR-29e	miR.MEcyan
SRGAP2	bta-miR-125a	miR.MElightyellow	*TEAD1*	bta-miR-29a	miR.MEcyan
SRGAP2	bta-miR-186	miR.MElightyellow	*TEAD1*	bta-miR-29e	miR.MEcyan
SRGAP3	bta-let-7c	miR.MEtan	*TERF2IP*	bta-miR-29a	miR.MEcyan
SRGAP3	bta-let-7e	miR.MEtan	*TET2*	bta-miR-29a	miR.MEcyan
SRGAP3	bta-let-7b	miR.MEtan	*TET2*	bta-miR-29b	miR.MEcyan
SRGAP3	bta-let-7a-5p	miR.MEtan	*TET2*	bta-miR-29c	miR.MEcyan
SRGAP3	bta-let-7f	miR.MEtan	*TET2*	bta-miR-29d-3p	miR.MEcyan
SRPK2	bta-miR-92b	miR.MElightyellow	*TET2*	bta-miR-29e	miR.MEcyan
ST13	bta-miR-103	miR.MEbrown	*TEX261*	bta-miR-29a	miR.MEcyan
ST13	bta-miR-107	miR.MEbrown	*TEX261*	bta-miR-29d-5p	miR.MEmidnightblue
ST13	bta-miR-29e	miR.MEcyan	*TFEB*	bta-miR-29a	miR.MEcyan
ST6GAL1	bta-miR-125a	miR.MElightyellow	*TFEB*	bta-miR-29b	miR.MEcyan
STAG1	bta-miR-15a	miR.MEcyan	*TFEB*	bta-miR-29c	miR.MEcyan
STAG1	bta-miR-29e	miR.MEcyan	*TFEB*	bta-miR-29d-3p	miR.MEcyan
STAG2	bta-miR-29b	miR.MEcyan	*TGFB2*	bta-miR-92b	miR.MElightyellow
STAG2	bta-miR-29c	miR.MEcyan	*TGFBR1*	bta-miR-125a	miR.MElightyellow
STAG2	bta-miR-29d-3p	miR.MEcyan	*THAP1*	bta-miR-29a	miR.MEcyan
STAMBPL1	bta-miR-103	miR.MEbrown	*THAP2*	bta-miR-29a	miR.MEcyan
STAMBPL1	bta-miR-107	miR.MEbrown	*THAP6*	bta-miR-29a	miR.MEcyan
STAMBPL1	bta-miR-19a	miR.MEbrown	*THAP8*	bta-miR-29b	miR.MEcyan
STAMBPL1	bta-miR-19b	miR.MEbrown	*THAP8*	bta-miR-29c	miR.MEcyan
STAMBPL1	bta-miR-29e	miR.MEcyan	*THAP8*	bta-miR-29d-3p	miR.MEcyan
STRIP1	bta-miR-103	miR.MEbrown	*THUMPD1*	bta-miR-15a	miR.MEcyan
STRIP1	bta-miR-107	miR.MEbrown	*THUMPD1*	bta-miR-29e	miR.MEcyan
STRIP1	bta-miR-29e	miR.MEcyan	*TICAM2*	bta-miR-186	miR.MElightyellow
STRIP1	bta-miR-30c	miR.MEmidnightblue	*TIMM8A*	bta-miR-502a	miR.MEgreen
STRIP1	bta-miR-30f	miR.MEmidnightblue	*TM9SF4*	bta-miR-29a	miR.MEcyan
STRN	bta-miR-15a	miR.MEcyan	*TMCC1*	bta-miR-15a	miR.MEcyan
STRN	bta-miR-29b	miR.MEcyan	*TMCC1*	bta-miR-30c	miR.MEmidnightblue
STRN	bta-miR-29c	miR.MEcyan	*TMCC1*	bta-miR-30f	miR.MEmidnightblue
STRN	bta-miR-29d-3p	miR.MEcyan	*TMED5*	bta-miR-29e	miR.MEcyan
STRN	bta-miR-29e	miR.MEcyan	*TMED8*	bta-miR-15a	miR.MEcyan
STRN3	bta-miR-29a	miR.MEcyan	*TMED8*	bta-miR-29e	miR.MEcyan
STRN3	bta-miR-29b	miR.MEcyan	*TMEM104*	bta-miR-29a	miR.MEcyan
STRN3	bta-miR-29c	miR.MEcyan	*TMEM123*	bta-miR-29a	miR.MEcyan
STRN3	bta-miR-29d-3p	miR.MEcyan	*TMEM131*	bta-miR-29e	miR.MEcyan
STRN3	bta-miR-29e	miR.MEcyan	*TMEM168*	bta-miR-29a	miR.MEcyan
SULF1	bta-let-7c	miR.MEtan	*TMEM170B*	bta-miR-29e	miR.MEcyan
SULF1	bta-let-7e	miR.MEtan	*TMEM179B*	bta-miR-29b	miR.MEcyan
SULF1	bta-let-7b	miR.MEtan	*TMEM179B*	bta-miR-29c	miR.MEcyan
SULF1	bta-let-7a-5p	miR.MEtan	*TMEM179B*	bta-miR-29d-3p	miR.MEcyan
SULF1	bta-let-7f	miR.MEtan	*TMEM182*	bta-miR-29e	miR.MEcyan

SUN2	bta-miR-103	miR.MEbrown	*TMEM189*	bta-miR-15a	miR.MEcyan
SUN2	bta-miR-107	miR.MEbrown	*TMEM19*	bta-miR-29a	miR.MEcyan
SUN2	bta-miR-29e	miR.MEcyan	*TMEM201*	bta-miR-29a	miR.MEcyan
SUPT3H	bta-miR-186	miR.MElightyellow	*TMEM201*	bta-miR-29e	miR.MEcyan
SUZ12	bta-miR-15a	miR.MEcyan	*TMEM234*	bta-miR-29b	miR.MEcyan
SYDE2	bta-miR-15a	miR.MEcyan	*TMEM234*	bta-miR-29c	miR.MEcyan
SYNCRIP	bta-miR-29b	miR.MEcyan	*TMEM234*	bta-miR-29d-3p	miR.MEcyan
SYNCRIP	bta-miR-29c	miR.MEcyan	*TMEM248*	bta-miR-15a	miR.MEcyan
SYNCRIP	bta-miR-29d-3p	miR.MEcyan	*TMEM255A*	bta-miR-15a	miR.MEcyan
SYNCRIP	bta-miR-29e	miR.MEcyan	*TMEM255A*	bta-miR-29b	miR.MEcyan
SYNCRIP	bta-miR-877	miR.MEmidnightblue	*TMEM255A*	bta-miR-29c	miR.MEcyan
SYNGR1	bta-miR-103	miR.MEbrown	*TMEM255A*	bta-miR-29d-3p	miR.MEcyan
SYNGR1	bta-miR-107	miR.MEbrown	*TMEM255A*	bta-miR-29e	miR.MEcyan
SYNGR1	bta-miR-29a	miR.MEcyan	*TMEM33*	bta-miR-15a	miR.MEcyan
SYNGR1	bta-miR-29e	miR.MEcyan	*TMEM33*	bta-miR-29b	miR.MEcyan
SYNPO2	bta-miR-29e	miR.MEcyan	*TMEM33*	bta-miR-29c	miR.MEcyan
TAB3	bta-miR-15a	miR.MEcyan	*TMEM33*	bta-miR-29d-3p	miR.MEcyan
TAB3	bta-miR-29e	miR.MEcyan	*TMEM86A*	bta-miR-125a	miR.MElightyellow
TAOK1	bta-miR-15a	miR.MEcyan	*TMTC2*	bta-miR-125a	miR.MElightyellow
TAOK1	bta-miR-29a	miR.MEcyan	*TMTC3*	bta-miR-29b	miR.MEcyan
TARS	bta-miR-19a	miR.MEbrown	*TMTC3*	bta-miR-29c	miR.MEcyan
TARS	bta-miR-19b	miR.MEbrown	*TMTC3*	bta-miR-29d-3p	miR.MEcyan
TARS	bta-miR-29a	miR.MEcyan	*TMTC3*	bta-miR-29e	miR.MEcyan
TBC1D25	bta-miR-19a	miR.MEbrown	*TNFAIP8L3*	bta-let-7c	miR.MEtan
TBC1D25	bta-miR-19b	miR.MEbrown	*TNFAIP8L3*	bta-let-7e	miR.MEtan
TBC1D8	bta-miR-92b	miR.MElightyellow	*TNFAIP8L3*	bta-let-7b	miR.MEtan
TBKBP1	bta-miR-103	miR.MEbrown	*TNFAIP8L3*	bta-let-7a-5p	miR.MEtan
TBKBP1	bta-miR-107	miR.MEbrown	*TNFAIP8L3*	bta-let-7f	miR.MEtan
TBL1XR1	bta-miR-15a	miR.MEcyan	*TNPO3*	bta-miR-29a	miR.MEcyan
TERF2	bta-miR-21-5p	miR.MEbrown	*TNPO3*	bta-miR-29e	miR.MEcyan
TESK2	bta-miR-19a	miR.MEbrown	*TNPO3*	bta-miR-30c	miR.MEmidnightblue
TESK2	bta-miR-19b	miR.MEbrown	*TNPO3*	bta-miR-30f	miR.MEmidnightblue
TESK2	bta-miR-21-5p	miR.MEbrown	*TNRC18*	bta-miR-29b	miR.MEcyan
TFRC	bta-miR-103	miR.MEbrown	*TNRC18*	bta-miR-29c	miR.MEcyan
TFRC	bta-miR-107	miR.MEbrown	*TNRC18*	bta-miR-29d-3p	miR.MEcyan
TFRC	bta-miR-15a	miR.MEcyan	*TOB2*	bta-miR-29a	miR.MEcyan
TFRC	bta-miR-29e	miR.MEcyan	*TOB2*	bta-miR-29e	miR.MEcyan
TGFBR2	bta-miR-186	miR.MElightyellow	*TOR1AIP1*	bta-miR-29e	miR.MEcyan
TGFBR3	bta-let-7c	miR.MEtan	*TOX4*	bta-miR-29e	miR.MEcyan
TGFBR3	bta-let-7e	miR.MEtan	*TOX4*	bta-miR-331-3p	miR.MEmidnightblue
TGFBR3	bta-let-7b	miR.MEtan	*TPD52L2*	bta-miR-29e	miR.MEcyan
TGFBR3	bta-let-7a-5p	miR.MEtan	*TPK1*	bta-miR-29a	miR.MEcyan
TGFBR3	bta-let-7f	miR.MEtan	*TPK1*	bta-miR-29b	miR.MEcyan

TGIF1	bta-miR-92b	miR.MElightyellow	*TPK1*	bta-miR-29c	miR.MEcyan
TGOLN2	bta-miR-125a	miR.MElightyellow	*TPK1*	bta-miR-29d-3p	miR.MEcyan
THBS1	bta-let-7c	miR.MEtan	*TPK1*	bta-miR-29e	miR.MEcyan
THBS1	bta-let-7e	miR.MEtan	*TPM1*	bta-miR-29a	miR.MEcyan
THBS1	bta-let-7b	miR.MEtan	*TPM1*	bta-miR-29b	miR.MEcyan
THBS1	bta-let-7a-5p	miR.MEtan	*TPM1*	bta-miR-29c	miR.MEcyan
THBS1	bta-let-7f	miR.MEtan	*TPM1*	bta-miR-29d-3p	miR.MEcyan
THOC2	bta-miR-29e	miR.MEcyan	*TPMT*	bta-miR-29a	miR.MEcyan
THRA	bta-miR-103	miR.MEbrown	*TPR*	bta-miR-29e	miR.MEcyan
THRA	bta-miR-107	miR.MEbrown	*TRAF1*	bta-miR-29e	miR.MEcyan
THRA	bta-miR-19a	miR.MEbrown	*TRAF4*	bta-miR-29a	miR.MEcyan
THRA	bta-miR-19b	miR.MEbrown	*TRAF4*	bta-miR-29b	miR.MEcyan
THRA	bta-miR-29a	miR.MEcyan	*TRAF4*	bta-miR-29c	miR.MEcyan
THRA	bta-miR-29b	miR.MEcyan	*TRAF4*	bta-miR-29d-3p	miR.MEcyan
THRA	bta-miR-29c	miR.MEcyan	*TRIM13*	bta-miR-29e	miR.MEcyan
THRA	bta-miR-29d-3p	miR.MEcyan	*TRIM24*	bta-miR-29b	miR.MEcyan
THY1	bta-miR-125a	miR.MElightyellow	*TRIM24*	bta-miR-29c	miR.MEcyan
TLK1	bta-miR-15a	miR.MEcyan	*TRIM24*	bta-miR-29d-3p	miR.MEcyan
TMEM135	bta-miR-125a	miR.MElightyellow	*TRIM45*	bta-miR-21-3p	miR.MEgreen
TMEM184B	bta-miR-92b	miR.MElightyellow	*TRIM72*	bta-miR-29e	miR.MEcyan
TMEM259	bta-miR-103	miR.MEbrown	*TRIP11*	bta-miR-15a	miR.MEcyan
TMEM259	bta-miR-107	miR.MEbrown	*TRMT1L*	bta-miR-29a	miR.MEcyan
TMEM259	bta-miR-15a	miR.MEcyan	*TRPS1*	bta-miR-29e	miR.MEcyan
TMEM259	bta-miR-29b	miR.MEcyan	*TSN*	bta-miR-29e	miR.MEcyan
TMEM259	bta-miR-29c	miR.MEcyan	*TSPYL4*	bta-miR-29e	miR.MEcyan
TMEM259	bta-miR-29d-3p	miR.MEcyan	*TTC3*	bta-miR-29a	miR.MEcyan
TMEM65	bta-miR-331-5p	miR.MEgreen	*TTC4*	bta-miR-29e	miR.MEcyan
TMEM65	bta-miR-502a	miR.MEgreen	*TTC7A*	bta-miR-125a	miR.MElightyellow
TMEM65	bta-let-7i	miR.MEmagenta	*TTLL12*	bta-miR-29e	miR.MEcyan
TMEM65	bta-miR-199c	miR.MEmagenta	*TTLL12*	bta-miR-29d-5p	miR.MEmidnightblue
TNFAIP3	bta-miR-125a	miR.MElightyellow	*TXNL4A*	bta-miR-29a	miR.MEcyan
TNFAIP3	bta-let-7c	miR.MEtan	*TXNL4A*	bta-miR-29e	miR.MEcyan
TNFAIP3	bta-let-7e	miR.MEtan	*UBA3*	bta-miR-29e	miR.MEcyan
TNFAIP3	bta-let-7b	miR.MEtan	*UBAP1*	bta-miR-15a	miR.MEcyan
TNFAIP3	bta-let-7a-5p	miR.MEtan	*UBB*	bta-miR-29a	miR.MEcyan
TNFAIP3	bta-let-7f	miR.MEtan	*UBE2A*	bta-miR-29e	miR.MEcyan
TNFRSF1B	bta-miR-125a	miR.MElightyellow	*UBE2B*	bta-miR-15a	miR.MEcyan
TNFRSF1B	bta-let-7c	miR.MEtan	*UBE2B*	bta-miR-29e	miR.MEcyan
TNFRSF1B	bta-let-7e	miR.MEtan	*UBE2E1*	bta-miR-29a	miR.MEcyan
TNFRSF1B	bta-let-7b	miR.MEtan	*UBE2F*	bta-miR-29e	miR.MEcyan
TNFRSF1B	bta-let-7a-5p	miR.MEtan	*UBE2F*	bta-miR-30c	miR.MEmidnightblue
TNFRSF1B	bta-let-7f	miR.MEtan	*UBE2F*	bta-miR-30f	miR.MEmidnightblue
TNIP1	bta-miR-19a	miR.MEbrown	*UBE2G2*	bta-miR-29a	miR.MEcyan

TNIP1	bta-miR-19b	miR.MEbrown	*UBE2G2*	bta-miR-29e	miR.MEcyan
TNPO1	bta-miR-15a	miR.MEcyan	*UBE2Q1*	bta-miR-15a	miR.MEcyan
TNPO1	bta-miR-29a	miR.MEcyan	*UBE2V1*	bta-miR-15a	miR.MEcyan
TNPO1	bta-miR-29e	miR.MEcyan	*UBE2W*	bta-miR-15a	miR.MEcyan
TNRC6A	bta-miR-29e	miR.MEcyan	*UBE2W*	bta-miR-29e	miR.MEcyan
TNRC6B	bta-miR-15a	miR.MEcyan	*UBE2Z*	bta-miR-92b	miR.MElightyellow
TNRC6B	bta-miR-29a	miR.MEcyan	*UBFD1*	bta-miR-15a	miR.MEcyan
TNRC6B	bta-miR-29b	miR.MEcyan	*UBFD1*	bta-miR-29b	miR.MEcyan
TNRC6B	bta-miR-29c	miR.MEcyan	*UBFD1*	bta-miR-29c	miR.MEcyan
TNRC6B	bta-miR-29d-3p	miR.MEcyan	*UBFD1*	bta-miR-29d-3p	miR.MEcyan
TNRC6B	bta-miR-29e	miR.MEcyan	*UBR1*	bta-miR-29e	miR.MEcyan
TOR1B	bta-miR-19a	miR.MEbrown	*UBR4*	bta-miR-15a	miR.MEcyan
TOR1B	bta-miR-19b	miR.MEbrown	*UBR5*	bta-miR-29e	miR.MEcyan
TOR1B	bta-miR-29e	miR.MEcyan	*UBTF*	bta-miR-29b	miR.MEcyan
TOR1B	bta-miR-30c	miR.MEmidnightblue	*UBTF*	bta-miR-29c	miR.MEcyan
TOR1B	bta-miR-30f	miR.MEmidnightblue	*UBTF*	bta-miR-29d-3p	miR.MEcyan
TP53INP1	bta-miR-125a	miR.MElightyellow	*UBXN4*	bta-miR-29e	miR.MEcyan
TPCN1	bta-miR-92b	miR.MElightyellow	*UFL1*	bta-miR-29e	miR.MEcyan
TRABD2B	bta-miR-186	miR.MElightyellow	*UGGT1*	bta-miR-29e	miR.MEcyan
TRAF3	bta-miR-103	miR.MEbrown	*UHRF1BP1*	bta-miR-29a	miR.MEcyan
TRAF3	bta-miR-107	miR.MEbrown	*UHRF1BP1*	bta-miR-29e	miR.MEcyan
TRAF3	bta-miR-15a	miR.MEcyan	*UNG*	bta-miR-15a	miR.MEcyan
TRAF3	bta-miR-29a	miR.MEcyan	*URI1*	bta-miR-29a	miR.MEcyan
TRAF3	bta-miR-29b	miR.MEcyan	*USP24*	bta-miR-29e	miR.MEcyan
TRAF3	bta-miR-29c	miR.MEcyan	*USP31*	bta-miR-15a	miR.MEcyan
TRAF3	bta-miR-29d-3p	miR.MEcyan	*USP31*	bta-miR-29a	miR.MEcyan
TRAF3	bta-miR-29e	miR.MEcyan	*USP31*	bta-miR-29b	miR.MEcyan
TRAF3	bta-miR-30c	miR.MEmidnightblue	*USP31*	bta-miR-29c	miR.MEcyan
TRAF3	bta-miR-30f	miR.MEmidnightblue	*USP31*	bta-miR-29d-3p	miR.MEcyan
TRAK2	bta-miR-92b	miR.MElightyellow	*USP34*	bta-miR-29b	miR.MEcyan
TRAPPC8	bta-miR-29e	miR.MEcyan	*USP34*	bta-miR-29c	miR.MEcyan
TRIAP1	bta-miR-103	miR.MEbrown	*USP34*	bta-miR-29d-3p	miR.MEcyan
TRIAP1	bta-miR-107	miR.MEbrown	*USP37*	bta-miR-29b	miR.MEcyan
TRIM33	bta-miR-29e	miR.MEcyan	*USP37*	bta-miR-29c	miR.MEcyan
TSHZ2	bta-miR-125a	miR.MElightyellow	*USP37*	bta-miR-29d-3p	miR.MEcyan
TTC9	bta-miR-19a	miR.MEbrown	*USP46*	bta-miR-125a	miR.MElightyellow
TTC9	bta-miR-19b	miR.MEbrown	*USP9X*	bta-miR-29a	miR.MEcyan
TTC9	bta-miR-29a	miR.MEcyan	*USP9X*	bta-miR-29e	miR.MEcyan
TTC9	bta-miR-29b	miR.MEcyan	*VIPAS39*	bta-miR-29b	miR.MEcyan
TTC9	bta-miR-29c	miR.MEcyan	*VIPAS39*	bta-miR-29c	miR.MEcyan
TTC9	bta-miR-29d-3p	miR.MEcyan	*VIPAS39*	bta-miR-29d-3p	miR.MEcyan
TTC9	bta-miR-29e	miR.MEcyan	*VLDLR*	bta-miR-29a	miR.MEcyan
TTLL7	bta-miR-29e	miR.MEcyan	*VLDLR*	bta-miR-29e	miR.MEcyan

TXLNA	bta-miR-29b	miR.MEcyan
TXLNA	bta-miR-29c	miR.MEcyan
TXLNA	bta-miR-29d-3p	miR.MEcyan
TXLNA	bta-miR-29e	miR.MEcyan
TXLNG	bta-miR-15a	miR.MEcyan
TXLNG	bta-miR-29a	miR.MEcyan
TXLNG	bta-miR-29e	miR.MEcyan
UBE2D2	bta-miR-19a	miR.MEbrown
UBE2D2	bta-miR-19b	miR.MEbrown
UBE2D2	bta-miR-29e	miR.MEcyan
UBE2D2	bta-miR-30c	miR.MEmidnightblue
UBE2D2	bta-miR-30f	miR.MEmidnightblue
UBE2E3	bta-miR-103	miR.MEbrown
UBE2E3	bta-miR-107	miR.MEbrown
UBE2J1	bta-miR-15a	miR.MEcyan
UBE2J1	bta-miR-30c	miR.MEmidnightblue
UBE2J1	bta-miR-30f	miR.MEmidnightblue
UBE2R2	bta-miR-103	miR.MEbrown
UBE2R2	bta-miR-107	miR.MEbrown
UBE2R2	bta-miR-15a	miR.MEcyan
UBE2R2	bta-miR-29e	miR.MEcyan
UBE2R2	bta-miR-30c	miR.MEmidnightblue
UBE2R2	bta-miR-30f	miR.MEmidnightblue
UBE4A	bta-miR-15a	miR.MEcyan
UBE4A	bta-miR-29e	miR.MEcyan
UBL3	bta-miR-19a	miR.MEbrown
UBL3	bta-miR-19b	miR.MEbrown
UBL3	bta-miR-29e	miR.MEcyan
UBN2	bta-miR-15a	miR.MEcyan
UBN2	bta-miR-29b	miR.MEcyan
UBN2	bta-miR-29c	miR.MEcyan
UBN2	bta-miR-29d-3p	miR.MEcyan
UBXN7	bta-miR-29a	miR.MEcyan
UBXN7	bta-miR-29b	miR.MEcyan
UBXN7	bta-miR-29c	miR.MEcyan
UBXN7	bta-miR-29d-3p	miR.MEcyan
UBXN7	bta-miR-29e	miR.MEcyan
UCP3	bta-miR-19a	miR.MEbrown
UCP3	bta-miR-19b	miR.MEbrown
UCP3	bta-miR-29e	miR.MEcyan
UCP3	bta-miR-30c	miR.MEmidnightblue
UCP3	bta-miR-30f	miR.MEmidnightblue
UHMK1	bta-miR-15a	miR.MEcyan
VLDLR	bta-miR-877	miR.MEmidnightblue
VMA21	bta-miR-15a	miR.MEcyan
VMA21	bta-miR-29a	miR.MEcyan
VMA21	bta-miR-29e	miR.MEcyan
VPS13A	bta-miR-29a	miR.MEcyan
VPS13A	bta-miR-29b	miR.MEcyan
VPS13A	bta-miR-29c	miR.MEcyan
VPS13A	bta-miR-29d-3p	miR.MEcyan
VPS13A	bta-miR-29e	miR.MEcyan
VPS13B	bta-miR-29e	miR.MEcyan
VPS18	bta-miR-29a	miR.MEcyan
VPS18	bta-miR-29e	miR.MEcyan
VPS37C	bta-miR-15a	miR.MEcyan
VPS37C	bta-miR-29b	miR.MEcyan
VPS37C	bta-miR-29c	miR.MEcyan
VPS37C	bta-miR-29d-3p	miR.MEcyan
VSIG4	bta-miR-186	miR.MElightyellow
VTA1	bta-miR-15a	miR.MEcyan
VTA1	bta-miR-29b	miR.MEcyan
VTA1	bta-miR-29c	miR.MEcyan
VTA1	bta-miR-29d-3p	miR.MEcyan
VWA7	bta-miR-15a	miR.MEcyan
VWA7	bta-miR-29e	miR.MEcyan
WASL	bta-miR-15a	miR.MEcyan
WASL	bta-miR-29e	miR.MEcyan
WBP11	bta-miR-15a	miR.MEcyan
WBP11	bta-miR-29a	miR.MEcyan
WDR47	bta-miR-15a	miR.MEcyan
WDR70	bta-miR-29a	miR.MEcyan
WDR70	bta-miR-30c	miR.MEmidnightblue
WDR70	bta-miR-30f	miR.MEmidnightblue
WDR77	bta-miR-29e	miR.MEcyan
WDR82	bta-miR-15a	miR.MEcyan
WDR82	bta-miR-29e	miR.MEcyan
WDTC1	bta-miR-15a	miR.MEcyan
WHAMM	bta-miR-29e	miR.MEcyan
WIPF2	bta-miR-29a	miR.MEcyan
XIAP	bta-miR-29a	miR.MEcyan
XPOT	bta-miR-29a	miR.MEcyan
XPR1	bta-miR-15a	miR.MEcyan
XPR1	bta-miR-29e	miR.MEcyan
XRN1	bta-miR-29b	miR.MEcyan
XRN1	bta-miR-29c	miR.MEcyan

UHMK1	bta-miR-29e	miR.MEcyan	*XRN1*	bta-miR-29d-3p	miR.MEcyan
UHRF1BP1L	bta-miR-125a	miR.MElightyellow	*XRRA1*	bta-miR-29a	miR.MEcyan
UHRF1BP1L	bta-miR-186	miR.MElightyellow	*XRRA1*	bta-miR-29d-5p	miR.MEmidnightblue
ULK2	bta-miR-29e	miR.MEcyan	*XXYLT1*	bta-miR-29b	miR.MEcyan
USP12	bta-miR-15a	miR.MEcyan	*XXYLT1*	bta-miR-29c	miR.MEcyan
USP12	bta-miR-29e	miR.MEcyan	*XXYLT1*	bta-miR-29d-3p	miR.MEcyan
USP13	bta-miR-29a	miR.MEcyan	*YBX3*	bta-miR-29a	miR.MEcyan
USP13	bta-miR-29e	miR.MEcyan	*YBX3*	bta-miR-29b	miR.MEcyan
USP42	bta-miR-15a	miR.MEcyan	*YBX3*	bta-miR-29c	miR.MEcyan
USP42	bta-miR-29b	miR.MEcyan	*YBX3*	bta-miR-29d-3p	miR.MEcyan
USP42	bta-miR-29c	miR.MEcyan	*YTHDC2*	bta-miR-29a	miR.MEcyan
USP42	bta-miR-29d-3p	miR.MEcyan	*YTHDF1*	bta-miR-29e	miR.MEcyan
USP49	bta-miR-29a	miR.MEcyan	*YWHAE*	bta-miR-29b	miR.MEcyan
USP53	bta-miR-29a	miR.MEcyan	*YWHAE*	bta-miR-29c	miR.MEcyan
USP6NL	bta-miR-151-3p	miR.MElightyellow	*YWHAE*	bta-miR-29d-3p	miR.MEcyan
VANGL1	bta-miR-125a	miR.MElightyellow	*ZBTB24*	bta-miR-29e	miR.MEcyan
VAPA	bta-miR-19a	miR.MEbrown	*ZBTB40*	bta-miR-29b	miR.MEcyan
VAPA	bta-miR-19b	miR.MEbrown	*ZBTB40*	bta-miR-29c	miR.MEcyan
VAPA	bta-miR-29a	miR.MEcyan	*ZBTB40*	bta-miR-29d-3p	miR.MEcyan
VAPA	bta-miR-29e	miR.MEcyan	*ZBTB41*	bta-miR-29a	miR.MEcyan
VAPB	bta-miR-19a	miR.MEbrown	*ZBTB41*	bta-miR-29b	miR.MEcyan
VAPB	bta-miR-19b	miR.MEbrown	*ZBTB41*	bta-miR-29c	miR.MEcyan
VAPB	bta-miR-15a	miR.MEcyan	*ZBTB41*	bta-miR-29d-3p	miR.MEcyan
VAPB	bta-miR-29a	miR.MEcyan	*ZBTB6*	bta-miR-29e	miR.MEcyan
VAPB	bta-miR-29b	miR.MEcyan	*ZBTB9*	bta-miR-125a	miR.MElightyellow
VAPB	bta-miR-29c	miR.MEcyan	*ZC2HC1A*	bta-miR-92b	miR.MElightyellow
VAPB	bta-miR-29d-3p	miR.MEcyan	*ZC3H11A*	bta-miR-15a	miR.MEcyan
VAPB	bta-miR-29d-5p	miR.MEmidnightblue	*ZC3H13*	bta-miR-29e	miR.MEcyan
VAV3	bta-miR-125a	miR.MElightyellow	*ZC3H14*	bta-miR-29e	miR.MEcyan
VAV3	bta-let-7c	miR.MEtan	*ZCCHC14*	bta-miR-29e	miR.MEcyan
VAV3	bta-let-7e	miR.MEtan	*ZCCHC6*	bta-miR-15a	miR.MEcyan
VAV3	bta-let-7b	miR.MEtan	*ZDHHC14*	bta-miR-15a	miR.MEcyan
VAV3	bta-let-7a-5p	miR.MEtan	*ZDHHC14*	bta-miR-29a	miR.MEcyan
VAV3	bta-let-7f	miR.MEtan	*ZDHHC14*	bta-miR-29e	miR.MEcyan
VCP	bta-miR-103	miR.MEbrown	*ZDHHC14*	bta-miR-30c	miR.MEmidnightblue
VCP	bta-miR-107	miR.MEbrown	*ZDHHC14*	bta-miR-30f	miR.MEmidnightblue
VGLL3	bta-miR-186	miR.MElightyellow	*ZDHHC17*	bta-miR-29a	miR.MEcyan
VGLL3	bta-let-7c	miR.MEtan	*ZDHHC17*	bta-miR-29e	miR.MEcyan
VGLL3	bta-let-7e	miR.MEtan	*ZEB1*	bta-miR-29a	miR.MEcyan
VGLL3	bta-let-7b	miR.MEtan	*ZEB1*	bta-miR-29e	miR.MEcyan
VGLL3	bta-let-7a-5p	miR.MEtan	*ZEB2*	bta-miR-29e	miR.MEcyan
VGLL3	bta-let-7f	miR.MEtan	*ZFHX2*	bta-miR-29e	miR.MEcyan
VKORC1L1	bta-miR-19a	miR.MEbrown	*ZFHX3*	bta-miR-15a	miR.MEcyan

VKORC1L1	bta-miR-19b	miR.MEbrown	*ZFHX4*	bta-miR-15a	miR.MEcyan
VKORC1L1	bta-miR-29a	miR.MEcyan	*ZFX*	bta-miR-15a	miR.MEcyan
VKORC1L1	bta-miR-30c	miR.MEmidnightblue	*ZFX*	bta-miR-29a	miR.MEcyan
VKORC1L1	bta-miR-30f	miR.MEmidnightblue	*ZFX*	bta-miR-29b	miR.MEcyan
VPS37A	bta-miR-19a	miR.MEbrown	*ZFX*	bta-miR-29c	miR.MEcyan
VPS37A	bta-miR-19b	miR.MEbrown	*ZFX*	bta-miR-29d-3p	miR.MEcyan
VPS37A	bta-miR-29e	miR.MEcyan	*ZFYVE16*	bta-miR-29a	miR.MEcyan
VPS4A	bta-miR-103	miR.MEbrown	*ZKSCAN1*	bta-miR-15a	miR.MEcyan
VPS4A	bta-miR-107	miR.MEbrown	*ZKSCAN1*	bta-miR-29e	miR.MEcyan
VPS4A	bta-miR-15a	miR.MEcyan	*ZMYM4*	bta-miR-15a	miR.MEcyan
VPS4A	bta-miR-29e	miR.MEcyan	*ZNF148*	bta-miR-29a	miR.MEcyan
VTI1A	bta-miR-15a	miR.MEcyan	*ZNF181*	bta-miR-199c	miR.MEmagenta
WBP2	bta-miR-19a	miR.MEbrown	*ZNF24*	bta-miR-29b	miR.MEcyan
WBP2	bta-miR-19b	miR.MEbrown	*ZNF24*	bta-miR-29c	miR.MEcyan
WDFY3	bta-miR-29b	miR.MEcyan	*ZNF24*	bta-miR-29d-3p	miR.MEcyan
WDFY3	bta-miR-29c	miR.MEcyan	*ZNF24*	bta-miR-29e	miR.MEcyan
WDFY3	bta-miR-29d-3p	miR.MEcyan	*ZNF281*	bta-miR-29e	miR.MEcyan
WDR26	bta-miR-29a	miR.MEcyan	*ZNF282*	bta-miR-29a	miR.MEcyan
WDR26	bta-miR-29b	miR.MEcyan	*ZNF282*	bta-miR-29b	miR.MEcyan
WDR26	bta-miR-29c	miR.MEcyan	*ZNF282*	bta-miR-29c	miR.MEcyan
WDR26	bta-miR-29d-3p	miR.MEcyan	*ZNF282*	bta-miR-29d-3p	miR.MEcyan
WDR26	bta-miR-29e	miR.MEcyan	*ZNF319*	bta-miR-29a	miR.MEcyan
WIPI2	bta-miR-103	miR.MEbrown	*ZNF362*	bta-miR-15a	miR.MEcyan
WIPI2	bta-miR-107	miR.MEbrown	*ZNF362*	bta-miR-29b	miR.MEcyan
WIPI2	bta-miR-15a	miR.MEcyan	*ZNF362*	bta-miR-29c	miR.MEcyan
WNT4	bta-miR-103	miR.MEbrown	*ZNF362*	bta-miR-29d-3p	miR.MEcyan
WNT4	bta-miR-107	miR.MEbrown	*ZNF384*	bta-miR-29b	miR.MEcyan
WNT4	bta-miR-15a	miR.MEcyan	*ZNF384*	bta-miR-29c	miR.MEcyan
WNT4	bta-miR-29e	miR.MEcyan	*ZNF384*	bta-miR-29d-3p	miR.MEcyan
WSCD1	bta-miR-19a	miR.MEbrown	*ZNF384*	bta-miR-29e	miR.MEcyan
WSCD1	bta-miR-19b	miR.MEbrown	*ZNF398*	bta-miR-15a	miR.MEcyan
WSCD1	bta-miR-29a	miR.MEcyan	*ZNF398*	bta-miR-29d-5p	miR.MEmidnightblue
WSCD1	bta-miR-29e	miR.MEcyan	*ZNF451*	bta-miR-29a	miR.MEcyan
WWP1	bta-miR-19a	miR.MEbrown	*ZNF451*	bta-miR-29e	miR.MEcyan
WWP1	bta-miR-19b	miR.MEbrown	*ZNF462*	bta-miR-29a	miR.MEcyan
WWP1	bta-miR-21-5p	miR.MEbrown	*ZNF48*	bta-miR-15a	miR.MEcyan
WWP1	bta-miR-15a	miR.MEcyan	*ZNF507*	bta-miR-29a	miR.MEcyan
WWP1	bta-miR-29e	miR.MEcyan	*ZNF507*	bta-miR-29b	miR.MEcyan
WWP1	bta-miR-30c	miR.MEmidnightblue	*ZNF507*	bta-miR-29c	miR.MEcyan
WWP1	bta-miR-30f	miR.MEmidnightblue	*ZNF507*	bta-miR-29d-3p	miR.MEcyan
XKR8	bta-miR-21-5p	miR.MEbrown	*ZNF507*	bta-miR-29e	miR.MEcyan
XKR8	bta-miR-15a	miR.MEcyan	*ZNF579*	bta-miR-29e	miR.MEcyan
YIPF6	bta-miR-15a	miR.MEcyan	*ZNF592*	bta-miR-15a	miR.MEcyan

YTHDF2	bta-miR-29a	miR.MEcyan	*ZNF592*	bta-miR-29a	miR.MEcyan
YTHDF2	bta-miR-30c	miR.MEmidnightblue	*ZNF623*	bta-miR-29a	miR.MEcyan
YTHDF2	bta-miR-30f	miR.MEmidnightblue	*ZNF623*	bta-miR-29e	miR.MEcyan
YY1	bta-miR-19a	miR.MEbrown	*ZNF687*	bta-miR-15a	miR.MEcyan
YY1	bta-miR-19b	miR.MEbrown	*ZNF75A*	bta-miR-29a	miR.MEcyan
YY1	bta-miR-29a	miR.MEcyan	*ZNF793*	bta-miR-29e	miR.MEcyan
YY1	bta-miR-29b	miR.MEcyan	*ZNF830*	bta-miR-29a	miR.MEcyan
YY1	bta-miR-29c	miR.MEcyan	*ZNF879*	bta-miR-29e	miR.MEcyan
YY1	bta-miR-29d-3p	miR.MEcyan	*ZZZ3*	bta-miR-29e	miR.MEcyan
YY1	bta-miR-29d-5p	miR.MEmidnightblue	*ABHD6*	bta-miR-125a	miR.MElightyellow
YY1	bta-miR-30c	miR.MEmidnightblue	*ADM*	bta-miR-92b	miR.MElightyellow
YY1	bta-miR-30f	miR.MEmidnightblue	*ALKBH5*	bta-miR-193a-3p	miR.MEmidnightblue
ZBTB10	bta-miR-186	miR.MElightyellow	*ANKRA2*	bta-miR-30c	miR.MEmidnightblue
ZBTB10	bta-miR-92b	miR.MElightyellow	*ANKRA2*	bta-miR-30f	miR.MEmidnightblue
ZBTB16	bta-miR-15a	miR.MEcyan	*ANKRD6*	bta-miR-331-3p	miR.MEmidnightblue
ZBTB47	bta-miR-19a	miR.MEbrown	*AP1B1*	bta-miR-30c	miR.MEmidnightblue
ZBTB47	bta-miR-19b	miR.MEbrown	*AP1B1*	bta-miR-30f	miR.MEmidnightblue
ZBTB47	bta-miR-21-5p	miR.MEbrown	*AP3M2*	bta-miR-21-3p	miR.MEgreen
ZBTB47	bta-miR-29a	miR.MEcyan	*AP3M2*	bta-miR-214	miR.MEmagenta
ZBTB47	bta-miR-29b	miR.MEcyan	*ARHGAP22*	bta-miR-186	miR.MElightyellow
ZBTB47	bta-miR-29c	miR.MEcyan	*ARHGAP30*	bta-miR-154c	miR.MEred
ZBTB47	bta-miR-29d-3p	miR.MEcyan	*ARHGEF10*	bta-miR-92b	miR.MElightyellow
ZBTB7B	bta-miR-19a	miR.MEbrown	*ATXN3*	bta-miR-125a	miR.MElightyellow
ZBTB7B	bta-miR-19b	miR.MEbrown	*ATXN3*	bta-miR-186	miR.MElightyellow
ZDHHC18	bta-miR-19a	miR.MEbrown	*ATXN3*	bta-miR-92b	miR.MElightyellow
ZDHHC18	bta-miR-19b	miR.MEbrown	*B4GALT6*	bta-miR-125a	miR.MElightyellow
ZDHHC18	bta-miR-29d-5p	miR.MEmidnightblue	*BET1L*	bta-let-7c	miR.MEtan
ZDHHC3	bta-miR-103	miR.MEbrown	*BET1L*	bta-let-7e	miR.MEtan
ZDHHC3	bta-miR-107	miR.MEbrown	*BET1L*	bta-let-7b	miR.MEtan
ZDHHC3	bta-miR-29e	miR.MEcyan	*BET1L*	bta-let-7a-5p	miR.MEtan
ZDHHC3	bta-miR-29d-5p	miR.MEmidnightblue	*BET1L*	bta-let-7f	miR.MEtan
ZDHHC7	bta-miR-19a	miR.MEbrown	*CAB39L*	bta-miR-186	miR.MElightyellow
ZDHHC7	bta-miR-19b	miR.MEbrown	*CCDC149*	bta-miR-29d-5p	miR.MEmidnightblue
ZER1	bta-miR-19a	miR.MEbrown	*CDKN1B*	bta-miR-877	miR.MEmidnightblue
ZER1	bta-miR-19b	miR.MEbrown	*CLMP*	bta-miR-186	miR.MElightyellow
ZER1	bta-miR-15a	miR.MEcyan	*COL11A2*	bta-miR-125a	miR.MElightyellow
ZER1	bta-miR-29b	miR.MEcyan	*COMMD7*	bta-miR-29d-5p	miR.MEmidnightblue
ZER1	bta-miR-29c	miR.MEcyan	*CRTAP*	bta-let-7c	miR.MEtan
ZER1	bta-miR-29d-3p	miR.MEcyan	*CRTAP*	bta-let-7e	miR.MEtan
ZER1	bta-miR-29e	miR.MEcyan	*CRTAP*	bta-let-7b	miR.MEtan
ZFAND5	bta-miR-19a	miR.MEbrown	*CRTAP*	bta-let-7a-5p	miR.MEtan
ZFAND5	bta-miR-19b	miR.MEbrown	*CRTAP*	bta-let-7f	miR.MEtan
ZFAND5	bta-miR-29e	miR.MEcyan	*CRTC2*	bta-miR-193a-3p	miR.MEmidnightblue

ZFAND6	bta-miR-19a	miR.MEbrown	*CYP7B1*	bta-miR-151-3p	miR.MElightyellow
ZFAND6	bta-miR-19b	miR.MEbrown	*DACT1*	bta-miR-92b	miR.MElightyellow
ZFPM2	bta-miR-151-3p	miR.MElightyellow	*DESI2*	bta-miR-30c	miR.MEmidnightblue
ZFPM2	bta-miR-92b	miR.MElightyellow	*DESI2*	bta-miR-30f	miR.MEmidnightblue
ZFYVE26	bta-miR-29a	miR.MEcyan	*DSN1*	bta-miR-186	miR.MElightyellow
ZFYVE26	bta-miR-29b	miR.MEcyan	*DTX3L*	bta-miR-199c	miR.MEmagenta
ZFYVE26	bta-miR-29c	miR.MEcyan	*DTX3L*	bta-miR-214	miR.MEmagenta
ZFYVE26	bta-miR-29d-3p	miR.MEcyan	*EFHD2*	bta-let-7c	miR.MEtan
ZHX1	bta-miR-15a	miR.MEcyan	*EFHD2*	bta-let-7e	miR.MEtan
ZHX3	bta-miR-15a	miR.MEcyan	*EFHD2*	bta-let-7b	miR.MEtan
ZHX3	bta-miR-29e	miR.MEcyan	*EFHD2*	bta-let-7a-5p	miR.MEtan
ZMYM2	bta-miR-15a	miR.MEcyan	*EFHD2*	bta-let-7f	miR.MEtan
ZNF207	bta-miR-29a	miR.MEcyan	*EIF2B2*	bta-miR-29d-5p	miR.MEmidnightblue
ZNF521	bta-miR-92b	miR.MElightyellow	*ELFN2*	bta-miR-92b	miR.MElightyellow
ZNF609	bta-miR-15a	miR.MEcyan	*ESCO1*	bta-miR-30c	miR.MEmidnightblue
ZNF609	bta-miR-29b	miR.MEcyan	*ESCO1*	bta-miR-30f	miR.MEmidnightblue
ZNF609	bta-miR-29c	miR.MEcyan	*ESYT1*	bta-miR-125a	miR.MElightyellow
ZNF609	bta-miR-29d-3p	miR.MEcyan	*FAM210B*	bta-miR-193a-3p	miR.MEmidnightblue
ZNF609	bta-miR-29e	miR.MEcyan	*FAM210B*	bta-miR-30c	miR.MEmidnightblue
ZNF644	bta-miR-29e	miR.MEcyan	*FAM210B*	bta-miR-30f	miR.MEmidnightblue
ZNF654	bta-miR-15a	miR.MEcyan	*FAM53B*	bta-miR-30c	miR.MEmidnightblue
ZNF70	bta-miR-19a	miR.MEbrown	*FAM53B*	bta-miR-30f	miR.MEmidnightblue
ZNF70	bta-miR-19b	miR.MEbrown	*FNBP1*	bta-miR-381	miR.MEred
ZNF827	bta-miR-125a	miR.MElightyellow	*FRMD4B*	bta-miR-186	miR.MElightyellow
ZNF827	bta-miR-92b	miR.MElightyellow	*FRMD4B*	bta-let-7c	miR.MEtan
ZNRF1	bta-miR-19a	miR.MEbrown	*FRMD4B*	bta-let-7e	miR.MEtan
ZNRF1	bta-miR-19b	miR.MEbrown	*FRMD4B*	bta-let-7b	miR.MEtan
ZNRF1	bta-miR-29a	miR.MEcyan	*FRMD4B*	bta-let-7a-5p	miR.MEtan
ZNRF1	bta-miR-30c	miR.MEmidnightblue	*FRMD4B*	bta-let-7f	miR.MEtan
ZNRF1	bta-miR-30f	miR.MEmidnightblue	*FST*	bta-miR-92b	miR.MElightyellow
ZNRF2	bta-miR-103	miR.MEbrown	*FXR2*	bta-miR-877	miR.MEmidnightblue
ZNRF2	bta-miR-107	miR.MEbrown	*GALNT15*	bta-let-7c	miR.MEtan
ZNRF2	bta-miR-15a	miR.MEcyan	*GALNT15*	bta-let-7e	miR.MEtan
ZSWIM6	bta-miR-125a	miR.MElightyellow	*GALNT15*	bta-let-7b	miR.MEtan
AAR2	bta-miR-29a	miR.MEcyan	*GALNT15*	bta-let-7a-5p	miR.MEtan
AAR2	bta-miR-29b	miR.MEcyan	*GALNT15*	bta-let-7f	miR.MEtan
AAR2	bta-miR-29c	miR.MEcyan	*GALNT2*	bta-let-7c	miR.MEtan
AAR2	bta-miR-29d-3p	miR.MEcyan	*GALNT2*	bta-let-7e	miR.MEtan
ABCE1	bta-miR-29b	miR.MEcyan	*GALNT2*	bta-let-7b	miR.MEtan
ABCE1	bta-miR-29c	miR.MEcyan	*GALNT2*	bta-let-7a-5p	miR.MEtan
ABCE1	bta-miR-29d-3p	miR.MEcyan	*GALNT2*	bta-let-7f	miR.MEtan
ABHD13	bta-miR-29e	miR.MEcyan	*GCNT1*	bta-miR-125a	miR.MElightyellow
ACAP2	bta-miR-29e	miR.MEcyan	*GIPC1*	bta-let-7c	miR.MEtan

ACOX1	bta-miR-199a-5p	miR.MEmagenta	*GIPC1*	bta-let-7e	miR.MEtan
ACOX1	bta-miR-199b	miR.MEmagenta	*GIPC1*	bta-let-7b	miR.MEtan
ACOX1	bta-miR-199c	miR.MEmagenta	*GIPC1*	bta-let-7a-5p	miR.MEtan
ACOX1	bta-miR-214	miR.MEmagenta	*GIPC1*	bta-let-7f	miR.MEtan
ACP2	bta-miR-29e	miR.MEcyan	*GPATCH2*	bta-miR-125a	miR.MElightyellow
ACTC1	bta-miR-92b	miR.MElightyellow	*GXYLT1*	bta-miR-125a	miR.MElightyellow
ACTR1A	bta-miR-15a	miR.MEcyan	*HDAC5*	bta-miR-30c	miR.MEmidnightblue
ACTR1A	bta-miR-30c	miR.MEmidnightblue	*HDAC5*	bta-miR-30f	miR.MEmidnightblue
ACTR1A	bta-miR-30f	miR.MEmidnightblue	*HDAC5*	bta-miR-331-3p	miR.MEmidnightblue
ACTRT3	bta-miR-29a	miR.MEcyan	*ICK*	bta-miR-186	miR.MElightyellow
ADAM19	bta-miR-92b	miR.MElightyellow	*ICK*	bta-miR-92b	miR.MElightyellow
ADAMTS1	bta-let-7c	miR.MEtan	*ICK*	bta-let-7c	miR.MEtan
ADAMTS1	bta-let-7e	miR.MEtan	*ICK*	bta-let-7e	miR.MEtan
ADAMTS1	bta-let-7b	miR.MEtan	*ICK*	bta-let-7b	miR.MEtan
ADAMTS1	bta-let-7a-5p	miR.MEtan	*ICK*	bta-let-7a-5p	miR.MEtan
ADAMTS1	bta-let-7f	miR.MEtan	*ICK*	bta-let-7f	miR.MEtan
ADAMTS15	bta-miR-125a	miR.MElightyellow	*IFIT5*	bta-miR-214	miR.MEmagenta
ADAMTS15	bta-miR-151-3p	miR.MElightyellow	*IKZF1*	bta-miR-154c	miR.MEred
ADAMTS15	bta-let-7c	miR.MEtan	*IL13RA1*	bta-miR-186	miR.MElightyellow
ADAMTS15	bta-let-7e	miR.MEtan	*IL16*	bta-miR-125a	miR.MElightyellow
ADAMTS15	bta-let-7b	miR.MEtan	*ING1*	bta-miR-193a-3p	miR.MEmidnightblue
ADAMTS15	bta-let-7a-5p	miR.MEtan	*IQGAP2*	bta-miR-186	miR.MElightyellow
ADAMTS15	bta-let-7f	miR.MEtan	*IQGAP2*	bta-miR-92b	miR.MElightyellow
ADAMTS5	bta-let-7c	miR.MEtan	*IRS2*	bta-miR-92b	miR.MElightyellow
ADAMTS5	bta-let-7e	miR.MEtan	*ITGA8*	bta-miR-125a	miR.MElightyellow
ADAMTS5	bta-let-7b	miR.MEtan	*ITGA8*	bta-miR-92b	miR.MElightyellow
ADAMTS5	bta-let-7a-5p	miR.MEtan	*ITM2B*	bta-miR-92b	miR.MElightyellow
ADAMTS5	bta-let-7f	miR.MEtan	*KIAA1614*	bta-miR-186	miR.MElightyellow
ADAR	bta-miR-199c	miR.MEmagenta	*LMBR1L*	bta-miR-30c	miR.MEmidnightblue
ADAR	bta-miR-214	miR.MEmagenta	*LMBR1L*	bta-miR-30f	miR.MEmidnightblue
ADCY2	bta-miR-29a	miR.MEcyan	*LYRM7*	bta-miR-21-3p	miR.MEgreen
ADIPOQ	bta-miR-186	miR.MElightyellow	*LYRM7*	bta-miR-214	miR.MEmagenta
ADO	bta-miR-15a	miR.MEcyan	*MAMDC2*	bta-miR-125a	miR.MElightyellow
ADO	bta-miR-30c	miR.MEmidnightblue	*MAML2*	bta-miR-186	miR.MElightyellow
ADO	bta-miR-30f	miR.MEmidnightblue	*MARCKS*	bta-miR-186	miR.MElightyellow
ADRM1	bta-miR-29a	miR.MEcyan	*METTL24*	bta-miR-125a	miR.MElightyellow
ADSL	bta-miR-29a	miR.MEcyan	*METTL24*	bta-miR-186	miR.MElightyellow
ADSL	bta-miR-29e	miR.MEcyan	*MGLL*	bta-miR-21-3p	miR.MEgreen
AFF3	bta-miR-92b	miR.MElightyellow	*MGLL*	bta-miR-214	miR.MEmagenta
AGPS	bta-miR-15a	miR.MEcyan	*MLX*	bta-miR-331-3p	miR.MEmidnightblue
AGPS	bta-miR-29e	miR.MEcyan	*MVB12B*	bta-miR-29d-5p	miR.MEmidnightblue
AGTPBP1	bta-miR-29e	miR.MEcyan	*MYLK3*	bta-miR-21-3p	miR.MEgreen
AHCYL1	bta-miR-92b	miR.MElightyellow	*MYLK3*	bta-miR-199c	miR.MEmagenta

AHNAK	bta-miR-29e	miR.MEcyan	*MYLK3*	bta-miR-214	miR.MEmagenta
AIFM2	bta-miR-92b	miR.MElightyellow	*MYO10*	bta-miR-92b	miR.MElightyellow
AK1	bta-miR-29b	miR.MEcyan	*MYOZ3*	bta-miR-29d-5p	miR.MEmidnightblue
AK1	bta-miR-29c	miR.MEcyan	*MZT1*	bta-miR-30c	miR.MEmidnightblue
AK1	bta-miR-29d-3p	miR.MEcyan	*MZT1*	bta-miR-30f	miR.MEmidnightblue
AK3	bta-miR-502b	miR.MEgreen	*NIN*	bta-miR-125a	miR.MElightyellow
AK3	bta-miR-214	miR.MEmagenta	*NOL10*	bta-miR-29d-5p	miR.MEmidnightblue
AKAP11	bta-miR-151-3p	miR.MElightyellow	*NRAS*	bta-miR-186	miR.MElightyellow
AKAP13	bta-miR-125a	miR.MElightyellow	*NUMBL*	bta-miR-125a	miR.MElightyellow
AKR7A2	bta-miR-29e	miR.MEcyan	*NUMBL*	bta-let-7c	miR.MEtan
ALDOA	bta-miR-29e	miR.MEcyan	*NUMBL*	bta-let-7e	miR.MEtan
ALG8	bta-let-7c	miR.MEtan	*NUMBL*	bta-let-7b	miR.MEtan
ALG8	bta-let-7e	miR.MEtan	*NUMBL*	bta-let-7a-5p	miR.MEtan
ALG8	bta-let-7b	miR.MEtan	*NUMBL*	bta-let-7f	miR.MEtan
ALG8	bta-let-7a-5p	miR.MEtan	*NUP93*	bta-miR-29d-5p	miR.MEmidnightblue
ALG8	bta-let-7f	miR.MEtan	*NUS1*	bta-miR-186	miR.MElightyellow
ALPK3	bta-miR-29a	miR.MEcyan	*ORAI1*	bta-miR-877	miR.MEmidnightblue
ALPK3	bta-miR-30c	miR.MEmidnightblue	*PARP14*	bta-miR-199c	miR.MEmagenta
ALPK3	bta-miR-30f	miR.MEmidnightblue	*PARP14*	bta-miR-214	miR.MEmagenta
ALS2	bta-miR-29b	miR.MEcyan	*PARP9*	bta-miR-199c	miR.MEmagenta
ALS2	bta-miR-29c	miR.MEcyan	*PDE4C*	bta-miR-21-3p	miR.MEgreen
ALS2	bta-miR-29d-3p	miR.MEcyan	*PDE4C*	bta-miR-214	miR.MEmagenta
AMFR	bta-miR-29b	miR.MEcyan	*PDSS2*	bta-miR-532	miR.MEgreen
AMFR	bta-miR-29c	miR.MEcyan	*PGAM1*	bta-miR-92b	miR.MElightyellow
AMFR	bta-miR-29d-3p	miR.MEcyan	*PGM1*	bta-miR-30c	miR.MEmidnightblue
AMIGO1	bta-miR-15a	miR.MEcyan	*PGM1*	bta-miR-30f	miR.MEmidnightblue
AMOT	bta-miR-15a	miR.MEcyan	*PGPEP1*	bta-miR-21-3p	miR.MEgreen
AMOT	bta-miR-29b	miR.MEcyan	*PGPEP1*	bta-miR-502b	miR.MEgreen
AMOT	bta-miR-29c	miR.MEcyan	*PIK3R2*	bta-miR-30c	miR.MEmidnightblue
AMOT	bta-miR-29d-3p	miR.MEcyan	*PIK3R2*	bta-miR-30f	miR.MEmidnightblue
AMOT	bta-miR-29e	miR.MEcyan	*PKP4*	bta-miR-125a	miR.MElightyellow
AMOTL1	bta-miR-15a	miR.MEcyan	*PLAC8*	bta-miR-199c	miR.MEmagenta
AMOTL1	bta-miR-29e	miR.MEcyan	*PLAC8*	bta-miR-214	miR.MEmagenta
ANAPC10	bta-miR-29e	miR.MEcyan	*PRKAG1*	bta-miR-21-3p	miR.MEgreen
ANK1	bta-miR-29b	miR.MEcyan	*PROX1*	bta-miR-125a	miR.MElightyellow
ANK1	bta-miR-29c	miR.MEcyan	*PROX1*	bta-miR-92b	miR.MElightyellow
ANK1	bta-miR-29d-3p	miR.MEcyan	*PSME3*	bta-miR-30c	miR.MEmidnightblue
ANKRD13B	bta-miR-15a	miR.MEcyan	*PSME3*	bta-miR-30f	miR.MEmidnightblue
ANKRD13B	bta-miR-29a	miR.MEcyan	*PTPRE*	bta-miR-154c	miR.MEred
ANKRD13B	bta-miR-29b	miR.MEcyan	*RADIL*	bta-let-7c	miR.MEtan
ANKRD13B	bta-miR-29c	miR.MEcyan	*RADIL*	bta-let-7e	miR.MEtan
ANKRD13B	bta-miR-29d-3p	miR.MEcyan	*RADIL*	bta-let-7b	miR.MEtan
ANKRD13B	bta-miR-331-3p	miR.MEmidnightblue	*RADIL*	bta-let-7a-5p	miR.MEtan

ANO6	bta-miR-29e	miR.MEcyan	*RADIL*	bta-let-7f	miR.MEtan
ANTXR2	bta-miR-125a	miR.MElightyellow	*RANBP10*	bta-miR-30c	miR.MEmidnightblue
ANTXR2	bta-miR-186	miR.MElightyellow	*RANBP10*	bta-miR-30f	miR.MEmidnightblue
AP1G1	bta-miR-29a	miR.MEcyan	*RANBP9*	bta-miR-30c	miR.MEmidnightblue
AP1G1	bta-miR-29b	miR.MEcyan	*RANBP9*	bta-miR-30f	miR.MEmidnightblue
AP1G1	bta-miR-29c	miR.MEcyan	*RNF122*	bta-miR-30c	miR.MEmidnightblue
AP1G1	bta-miR-29d-3p	miR.MEcyan	*RNF122*	bta-miR-30f	miR.MEmidnightblue
AP1G1	bta-miR-29e	miR.MEcyan	*RNF34*	bta-miR-30c	miR.MEmidnightblue
AP1S1	bta-let-7c	miR.MEtan	*RNF34*	bta-miR-30f	miR.MEmidnightblue
AP1S1	bta-let-7e	miR.MEtan	*RORC*	bta-miR-502b	miR.MEgreen
AP1S1	bta-let-7b	miR.MEtan	*RORC*	bta-let-7i	miR.MEmagenta
AP1S1	bta-let-7a-5p	miR.MEtan	*RORC*	bta-miR-214	miR.MEmagenta
AP1S1	bta-let-7f	miR.MEtan	*RPA1*	bta-miR-30c	miR.MEmidnightblue
AP2A1	bta-miR-15a	miR.MEcyan	*RPA1*	bta-miR-30f	miR.MEmidnightblue
AP2A1	bta-miR-30c	miR.MEmidnightblue	*RTN2*	bta-miR-331-3p	miR.MEmidnightblue
AP2A1	bta-miR-30f	miR.MEmidnightblue	*RWDD4*	bta-miR-30c	miR.MEmidnightblue
AP2A1	bta-miR-331-3p	miR.MEmidnightblue	*RWDD4*	bta-miR-30f	miR.MEmidnightblue
AP4E1	bta-miR-29a	miR.MEcyan	*SAP30*	bta-miR-30c	miR.MEmidnightblue
AP4E1	bta-miR-29b	miR.MEcyan	*SAP30*	bta-miR-30f	miR.MEmidnightblue
AP4E1	bta-miR-29c	miR.MEcyan	*SCN2B*	bta-miR-502a	miR.MEgreen
AP4E1	bta-miR-29d-3p	miR.MEcyan	*SCN2B*	bta-miR-502b	miR.MEgreen
APBB2	bta-miR-29e	miR.MEcyan	*SCN2B*	bta-miR-214	miR.MEmagenta
APC	bta-miR-15a	miR.MEcyan	*SEMA4G*	bta-let-7c	miR.MEtan
APC	bta-miR-29a	miR.MEcyan	*SEMA4G*	bta-let-7e	miR.MEtan
APC	bta-miR-29b	miR.MEcyan	*SEMA4G*	bta-let-7b	miR.MEtan
APC	bta-miR-29c	miR.MEcyan	*SEMA4G*	bta-let-7a-5p	miR.MEtan
APC	bta-miR-29d-3p	miR.MEcyan	*SEMA4G*	bta-let-7f	miR.MEtan
APC	bta-miR-29e	miR.MEcyan	*SEPT11*	bta-miR-125a	miR.MElightyellow
APP	bta-miR-151-3p	miR.MElightyellow	*SLC23A2*	bta-miR-186	miR.MElightyellow
APP	bta-miR-186	miR.MElightyellow	*SLC25A30*	bta-miR-331-5p	miR.MEgreen
AQP4	bta-let-7i	miR.MEmagenta	*SLC25A30*	bta-miR-214	miR.MEmagenta
AQP4	bta-miR-199c	miR.MEmagenta	*SLC27A6*	bta-miR-21-3p	miR.MEgreen
AQP4	bta-miR-214	miR.MEmagenta	*SLC30A1*	bta-miR-186	miR.MElightyellow
AQR	bta-miR-29a	miR.MEcyan	*SLC35E1*	bta-miR-29d-5p	miR.MEmidnightblue
AQR	bta-miR-29e	miR.MEcyan	*SLC37A3*	bta-miR-92b	miR.MElightyellow
AREL1	bta-miR-29e	miR.MEcyan	*SLC38A9*	bta-miR-125a	miR.MElightyellow
ARF5	bta-miR-29a	miR.MEcyan	*SORL1*	bta-miR-92b	miR.MElightyellow
ARF5	bta-miR-29b	miR.MEcyan	*SPSB1*	bta-miR-186	miR.MElightyellow
ARF5	bta-miR-29c	miR.MEcyan	*SPSB1*	bta-miR-92b	miR.MElightyellow
ARF5	bta-miR-29d-3p	miR.MEcyan	*SSPN*	bta-miR-29d-5p	miR.MEmidnightblue
ARFGAP2	bta-miR-15a	miR.MEcyan	*SYT11*	bta-miR-186	miR.MElightyellow
ARFGEF2	bta-miR-29b	miR.MEcyan	*SYT11*	bta-let-7c	miR.MEtan
ARFGEF2	bta-miR-29c	miR.MEcyan	*SYT11*	bta-let-7e	miR.MEtan

ARFGEF2	bta-miR-29d-3p	miR.MEcyan	*SYT11*	bta-let-7b	miR.MEtan
ARHGAP17	bta-miR-29e	miR.MEcyan	*SYT11*	bta-let-7a-5p	miR.MEtan
ARHGAP20	bta-let-7c	miR.MEtan	*SYT11*	bta-let-7f	miR.MEtan
ARHGAP20	bta-let-7e	miR.MEtan	*TBC1D10B*	bta-miR-30c	miR.MEmidnightblue
ARHGAP20	bta-let-7b	miR.MEtan	*TBC1D10B*	bta-miR-30f	miR.MEmidnightblue
ARHGAP20	bta-let-7a-5p	miR.MEtan	*TLE3*	bta-miR-125a	miR.MElightyellow
ARHGAP20	bta-let-7f	miR.MEtan	*TLR5*	bta-let-7c	miR.MEtan
ARL14EP	bta-miR-29a	miR.MEcyan	*TLR5*	bta-let-7e	miR.MEtan
ARL4A	bta-miR-29a	miR.MEcyan	*TLR5*	bta-let-7b	miR.MEtan
ARL4A	bta-miR-30c	miR.MEmidnightblue	*TLR5*	bta-let-7a-5p	miR.MEtan
ARL4A	bta-miR-30f	miR.MEmidnightblue	*TLR5*	bta-let-7f	miR.MEtan
ARL5B	bta-miR-15a	miR.MEcyan	*TMEM110*	bta-let-7c	miR.MEtan
ARL5B	bta-miR-29b	miR.MEcyan	*TMEM110*	bta-let-7e	miR.MEtan
ARL5B	bta-miR-29c	miR.MEcyan	*TMEM110*	bta-let-7b	miR.MEtan
ARL5B	bta-miR-29d-3p	miR.MEcyan	*TMEM110*	bta-let-7a-5p	miR.MEtan
ARL5B	bta-miR-29e	miR.MEcyan	*TMEM110*	bta-let-7f	miR.MEtan
ARL8B	bta-miR-29a	miR.MEcyan	*TMEM246*	bta-miR-186	miR.MElightyellow
ASB8	bta-miR-29a	miR.MEcyan	*TMEM38A*	bta-miR-21-3p	miR.MEgreen
ASCC3	bta-miR-29e	miR.MEcyan	*TMEM98*	bta-miR-151-3p	miR.MElightyellow
ASPH	bta-miR-29e	miR.MEcyan	*TRAM2*	bta-miR-92b	miR.MElightyellow
ASPN	bta-miR-92b	miR.MElightyellow	*TRAM2*	bta-let-7c	miR.MEtan
ATF6	bta-miR-29e	miR.MEcyan	*TRAM2*	bta-let-7e	miR.MEtan
ATG12	bta-miR-29e	miR.MEcyan	*TRAM2*	bta-let-7b	miR.MEtan
ATG12	bta-miR-30c	miR.MEmidnightblue	*TRAM2*	bta-let-7a-5p	miR.MEtan
ATG12	bta-miR-30f	miR.MEmidnightblue	*TRAM2*	bta-let-7f	miR.MEtan
ATG9A	bta-miR-15a	miR.MEcyan	*TRIM25*	bta-miR-186	miR.MElightyellow
ATG9A	bta-miR-29a	miR.MEcyan	*TRMT5*	bta-miR-30c	miR.MEmidnightblue
ATG9A	bta-miR-29b	miR.MEcyan	*TRMT5*	bta-miR-30f	miR.MEmidnightblue
ATG9A	bta-miR-29c	miR.MEcyan	*TSPYL5*	bta-let-7c	miR.MEtan
ATG9A	bta-miR-29d-3p	miR.MEcyan	*TSPYL5*	bta-let-7e	miR.MEtan
ATMIN	bta-miR-29e	miR.MEcyan	*TSPYL5*	bta-let-7b	miR.MEtan
ATP11B	bta-miR-29e	miR.MEcyan	*TSPYL5*	bta-let-7a-5p	miR.MEtan
ATP2B4	bta-miR-186	miR.MElightyellow	*TSPYL5*	bta-let-7f	miR.MEtan
ATP6V0A2	bta-miR-29e	miR.MEcyan	*UBAC1*	bta-miR-30c	miR.MEmidnightblue
ATP6V1C1	bta-miR-29e	miR.MEcyan	*UBAC1*	bta-miR-30f	miR.MEmidnightblue
ATP6V1C1	bta-miR-30c	miR.MEmidnightblue	*UBR7*	bta-miR-30c	miR.MEmidnightblue
ATP6V1C1	bta-miR-30f	miR.MEmidnightblue	*UBR7*	bta-miR-30f	miR.MEmidnightblue
ATP9A	bta-miR-29a	miR.MEcyan	*VMAC*	bta-miR-125a	miR.MElightyellow
ATRN	bta-miR-29b	miR.MEcyan	*VPS33A*	bta-miR-30c	miR.MEmidnightblue
ATRN	bta-miR-29c	miR.MEcyan	*VPS33A*	bta-miR-30f	miR.MEmidnightblue
ATRN	bta-miR-29d-3p	miR.MEcyan	*VRK3*	bta-miR-29d-5p	miR.MEmidnightblue
ATRN	bta-miR-29e	miR.MEcyan	*WARS*	bta-miR-199c	miR.MEmagenta
ATXN2	bta-miR-15a	miR.MEcyan	*WARS*	bta-miR-214	miR.MEmagenta

ATXN2	bta-miR-29e	miR.MEcyan	*XK*	bta-miR-29d-5p	miR.MEmidnightblue
ATXN7L3B	bta-miR-15a	miR.MEcyan	*ZNF629*	bta-miR-502b	miR.MEgreen
ATXN7L3B	bta-miR-331-3p	miR.MEmidnightblue	*ZNF629*	bta-miR-204	miR.MEmagenta
AUP1	bta-miR-29a	miR.MEcyan	*ZNF629*	bta-miR-214	miR.MEmagenta
AVEN	bta-miR-15a	miR.MEcyan	*ZNF629*	bta-miR-221	miR.MEmagenta
AVEN	bta-miR-30c	miR.MEmidnightblue	*ZNF672*	bta-miR-21-3p	miR.MEgreen
AVEN	bta-miR-30f	miR.MEmidnightblue	*ZNF672*	bta-miR-214	miR.MEmagenta
AXL	bta-miR-92b	miR.MElightyellow	*ADAM10*	bta-miR-92b	miR.MElightyellow
B4GALT1	bta-miR-125a	miR.MElightyellow	*ADCY3*	bta-miR-92b	miR.MElightyellow
BACE2	bta-let-7c	miR.MEtan	*ADCY5*	bta-miR-125a	miR.MElightyellow
BACE2	bta-let-7e	miR.MEtan	*ADCY5*	bta-miR-186	miR.MElightyellow
BACE2	bta-let-7b	miR.MEtan	*ANGPTL2*	bta-miR-92b	miR.MElightyellow
BACE2	bta-let-7a-5p	miR.MEtan	*ANGPTL2*	bta-let-7c	miR.MEtan
BACE2	bta-let-7f	miR.MEtan	*ANGPTL2*	bta-let-7e	miR.MEtan
BAG5	bta-miR-15a	miR.MEcyan	*ANGPTL2*	bta-let-7b	miR.MEtan
BAP1	bta-miR-29a	miR.MEcyan	*ANGPTL2*	bta-let-7a-5p	miR.MEtan
BBX	bta-miR-29e	miR.MEcyan	*ANGPTL2*	bta-let-7f	miR.MEtan
BCCIP	bta-miR-29e	miR.MEcyan	*ANKRD50*	bta-miR-125a	miR.MElightyellow
BCDIN3D	bta-miR-29e	miR.MEcyan	*ANPEP*	bta-miR-125a	miR.MElightyellow
BCL2	bta-miR-15a	miR.MEcyan	*ATP10D*	bta-miR-125a	miR.MElightyellow
BCL2	bta-miR-29a	miR.MEcyan	*BGN*	bta-miR-92b	miR.MElightyellow
BCL9	bta-miR-92b	miR.MElightyellow	*C1QTNF3*	bta-miR-125a	miR.MElightyellow
BCLAF1	bta-miR-29a	miR.MEcyan	*CDKN2AIP*	bta-miR-186	miR.MElightyellow
BCORL1	bta-miR-29a	miR.MEcyan	*CDR2L*	bta-miR-125a	miR.MElightyellow
BCORL1	bta-miR-29b	miR.MEcyan	*CDR2L*	bta-miR-186	miR.MElightyellow
BCORL1	bta-miR-29c	miR.MEcyan	*CHERP*	bta-miR-186	miR.MElightyellow
BCORL1	bta-miR-29d-3p	miR.MEcyan	*CKAP4*	bta-miR-186	miR.MElightyellow
BLOC1S1	bta-miR-29a	miR.MEcyan	*CPM*	bta-miR-125a	miR.MElightyellow
BLOC1S5	bta-miR-29e	miR.MEcyan	*CTTNBP2*	bta-miR-92b	miR.MElightyellow
BLZF1	bta-miR-29e	miR.MEcyan	*DENND5A*	bta-miR-151-3p	miR.MElightyellow
BMI1	bta-miR-29e	miR.MEcyan	*DOCK1*	bta-miR-92b	miR.MElightyellow
BOD1L1	bta-miR-29e	miR.MEcyan	*DPY19L1*	bta-miR-125a	miR.MElightyellow
BPGM	bta-miR-29a	miR.MEcyan	*DUSP1*	bta-let-7c	miR.MEtan
BRD7	bta-miR-29a	miR.MEcyan	*DUSP1*	bta-let-7e	miR.MEtan
BROX	bta-miR-29a	miR.MEcyan	*DUSP1*	bta-let-7b	miR.MEtan
BSDC1	bta-miR-15a	miR.MEcyan	*DUSP1*	bta-let-7a-5p	miR.MEtan
BSDC1	bta-miR-29b	miR.MEcyan	*DUSP1*	bta-let-7f	miR.MEtan
BSDC1	bta-miR-29c	miR.MEcyan	*EFEMP1*	bta-miR-186	miR.MElightyellow
BSDC1	bta-miR-29d-3p	miR.MEcyan	*FUT8*	bta-miR-186	miR.MElightyellow
BSDC1	bta-miR-29e	miR.MEcyan	*GFPT2*	bta-miR-92b	miR.MElightyellow
BTBD11	bta-miR-29e	miR.MEcyan	*GNAI1*	bta-miR-186	miR.MElightyellow
BTBD9	bta-miR-29e	miR.MEcyan	*GOLGA5*	bta-miR-125a	miR.MElightyellow
BTBD9	bta-miR-29d-5p	miR.MEmidnightblue	*HERPUD2*	bta-miR-186	miR.MElightyellow

BTC	bta-miR-29a	miR.MEcyan	*HERPUD2*	bta-miR-92b	miR.MElightyellow
BTC	bta-miR-29e	miR.MEcyan	*IDH1*	bta-miR-92b	miR.MElightyellow
C1GALT1	bta-miR-29a	miR.MEcyan	*INTS7*	bta-miR-125a	miR.MElightyellow
C1GALT1	bta-miR-29e	miR.MEcyan	*LIPA*	bta-miR-125a	miR.MElightyellow
CA5B	bta-miR-186	miR.MElightyellow	*LOXL1*	bta-miR-125a	miR.MElightyellow
CACNA2D2	bta-miR-29e	miR.MEcyan	*LRRC1*	bta-miR-92b	miR.MElightyellow
CACNB1	bta-miR-15a	miR.MEcyan	*MAF*	bta-miR-30c	miR.MEmidnightblue
CALM3	bta-miR-29a	miR.MEcyan	*MAF*	bta-miR-30f	miR.MEmidnightblue
CALM3	bta-miR-29b	miR.MEcyan	*MAP2K7*	bta-miR-331-3p	miR.MEmidnightblue
CALM3	bta-miR-29c	miR.MEcyan	*MTA3*	bta-miR-92b	miR.MElightyellow
CALM3	bta-miR-29d-3p	miR.MEcyan	*NFYB*	bta-miR-30c	miR.MEmidnightblue
CALN1	bta-miR-21-3p	miR.MEgreen	*NFYB*	bta-miR-30f	miR.MEmidnightblue
CALN1	bta-let-7i	miR.MEmagenta	*NRF1*	bta-miR-92b	miR.MElightyellow
CALN1	bta-miR-214	miR.MEmagenta	*OSBPL5*	bta-miR-92b	miR.MElightyellow
CASP9	bta-miR-186	miR.MElightyellow	*PCOLCE2*	bta-miR-92b	miR.MElightyellow
CBL	bta-miR-29e	miR.MEcyan	*PDP2*	bta-miR-186	miR.MElightyellow
CBR4	bta-miR-21-3p	miR.MEgreen	*PMM2*	bta-miR-125a	miR.MElightyellow
CBR4	bta-miR-502b	miR.MEgreen	*POFUT2*	bta-miR-186	miR.MElightyellow
CBR4	bta-miR-214	miR.MEmagenta	*PPT1*	bta-miR-125a	miR.MElightyellow
CBX5	bta-miR-15a	miR.MEcyan	*PRKAR2B*	bta-miR-92b	miR.MElightyellow
CBX5	bta-miR-29a	miR.MEcyan	*PTPRU*	bta-miR-125a	miR.MElightyellow
CBX5	bta-miR-29b	miR.MEcyan	*PTPRU*	bta-let-7c	miR.MEtan
CBX5	bta-miR-29c	miR.MEcyan	*PTPRU*	bta-let-7e	miR.MEtan
CBX5	bta-miR-29d-3p	miR.MEcyan	*PTPRU*	bta-let-7b	miR.MEtan
CBX5	bta-miR-29e	miR.MEcyan	*PTPRU*	bta-let-7a-5p	miR.MEtan
CCDC121	bta-miR-21-3p	miR.MEgreen	*PTPRU*	bta-let-7f	miR.MEtan
CCDC121	bta-miR-214	miR.MEmagenta	*PXDC1*	bta-miR-186	miR.MElightyellow
CCDC28A	bta-miR-15a	miR.MEcyan	*QPCT*	bta-miR-92b	miR.MElightyellow
CCDC28A	bta-miR-29a	miR.MEcyan	*RRBP1*	bta-miR-92b	miR.MElightyellow
CCDC80	bta-miR-151-3p	miR.MElightyellow	*SBK1*	bta-miR-30c	miR.MEmidnightblue
CCDC80	bta-miR-186	miR.MElightyellow	*SBK1*	bta-miR-30f	miR.MEmidnightblue
CCDC88C	bta-miR-15a	miR.MEcyan	*SCARF2*	bta-miR-125a	miR.MElightyellow
CCNT1	bta-miR-15a	miR.MEcyan	*SERPINF1*	bta-miR-92b	miR.MElightyellow
CCNT1	bta-miR-29e	miR.MEcyan	*SERTAD2*	bta-miR-92b	miR.MElightyellow
CD55	bta-miR-186	miR.MElightyellow	*SGPP1*	bta-miR-92b	miR.MElightyellow
CD84	bta-miR-154c	miR.MEred	*SH3RF1*	bta-miR-186	miR.MElightyellow
CDC5L	bta-miR-29e	miR.MEcyan	*SIPA1L3*	bta-miR-186	miR.MElightyellow
CDK16	bta-miR-214	miR.MEmagenta	*SLC1A5*	bta-miR-125a	miR.MElightyellow
CDS2	bta-miR-125a	miR.MElightyellow	*SLC39A6*	bta-miR-92b	miR.MElightyellow
CDYL2	bta-miR-29a	miR.MEcyan	*SMC6*	bta-miR-186	miR.MElightyellow
CEBPG	bta-miR-29a	miR.MEcyan	*SPRYD7*	bta-miR-30c	miR.MEmidnightblue
CENPB	bta-miR-29a	miR.MEcyan	*SPRYD7*	bta-miR-30f	miR.MEmidnightblue
CENPI	bta-miR-29e	miR.MEcyan	*TMEM184C*	bta-miR-151-3p	miR.MElightyellow

CEP128	bta-miR-29e	miR.MEcyan	*TRIM36*	bta-miR-92b	miR.MElightyellow
CEP57	bta-miR-186	miR.MElightyellow	*TRPC1*	bta-miR-186	miR.MElightyellow
CEP85	bta-miR-15a	miR.MEcyan	*TWF1*	bta-miR-92b	miR.MElightyellow
CEP85L	bta-miR-15a	miR.MEcyan	*UBE2G1*	bta-miR-30c	miR.MEmidnightblue
CEP85L	bta-miR-29a	miR.MEcyan	*UBE2G1*	bta-miR-30f	miR.MEmidnightblue
CEP85L	bta-miR-29b	miR.MEcyan	*XYLT2*	bta-miR-92b	miR.MElightyellow
CEP85L	bta-miR-29c	miR.MEcyan	*ANGPT1*	bta-miR-204	miR.MEmagenta
CEP85L	bta-miR-29d-3p	miR.MEcyan	*CCNK*	bta-miR-30c	miR.MEmidnightblue
CEP97	bta-miR-29a	miR.MEcyan	*CCNK*	bta-miR-30f	miR.MEmidnightblue
CEP97	bta-miR-29b	miR.MEcyan	*DLGAP4*	bta-miR-30c	miR.MEmidnightblue
CEP97	bta-miR-29c	miR.MEcyan	*DLGAP4*	bta-miR-30f	miR.MEmidnightblue
CEP97	bta-miR-29d-3p	miR.MEcyan	*GNGT2*	bta-miR-214	miR.MEmagenta
CERCAM	bta-let-7c	miR.MEtan	*HIBCH*	bta-miR-199c	miR.MEmagenta
CERCAM	bta-let-7e	miR.MEtan	*IGF2*	bta-let-7c	miR.MEtan
CERCAM	bta-let-7b	miR.MEtan	*IGF2*	bta-let-7e	miR.MEtan
CERCAM	bta-let-7a-5p	miR.MEtan	*IGF2*	bta-let-7b	miR.MEtan
CERCAM	bta-let-7f	miR.MEtan	*IGF2*	bta-let-7a-5p	miR.MEtan
CERS1	bta-miR-15a	miR.MEcyan	*IGF2*	bta-let-7f	miR.MEtan
CERS1	bta-miR-29b	miR.MEcyan	*IGF2BP2*	bta-miR-877	miR.MEmidnightblue
CERS1	bta-miR-29c	miR.MEcyan	*IGFN1*	bta-miR-193a-3p	miR.MEmidnightblue
CERS1	bta-miR-29d-3p	miR.MEcyan	*L2HGDH*	bta-let-7i	miR.MEmagenta
CGGBP1	bta-miR-29e	miR.MEcyan	*L2HGDH*	bta-miR-199c	miR.MEmagenta
CHD9	bta-miR-15a	miR.MEcyan	*LGALS9*	bta-miR-214	miR.MEmagenta
CHD9	bta-miR-29e	miR.MEcyan	*NSUN2*	bta-miR-29d-5p	miR.MEmidnightblue
CHMP4C	bta-miR-29a	miR.MEcyan	*PAK4*	bta-miR-193a-3p	miR.MEmidnightblue
CHMP4C	bta-miR-29e	miR.MEcyan	*PAK4*	bta-miR-30c	miR.MEmidnightblue
CHMP6	bta-miR-29b	miR.MEcyan	*PAK4*	bta-miR-30f	miR.MEmidnightblue
CHMP6	bta-miR-29c	miR.MEcyan	*PEX11A*	bta-miR-29d-5p	miR.MEmidnightblue
CHMP6	bta-miR-29d-3p	miR.MEcyan	*PPP1R14C*	bta-miR-30c	miR.MEmidnightblue
CHN1	bta-miR-29e	miR.MEcyan	*PPP1R14C*	bta-miR-30f	miR.MEmidnightblue
CKAP5	bta-miR-29e	miR.MEcyan	*PTGR2*	bta-miR-214	miR.MEmagenta
CLASP1	bta-miR-15a	miR.MEcyan	*RCN2*	bta-let-7c	miR.MEtan
CLCC1	bta-miR-125a	miR.MElightyellow	*RCN2*	bta-let-7e	miR.MEtan
CLCC1	bta-miR-186	miR.MElightyellow	*RCN2*	bta-let-7b	miR.MEtan
CLCN3	bta-miR-15a	miR.MEcyan	*RCN2*	bta-let-7a-5p	miR.MEtan
CLCN3	bta-miR-29e	miR.MEcyan	*RCN2*	bta-let-7f	miR.MEtan
CLCN3	bta-miR-29d-5p	miR.MEmidnightblue	*RXRA*	bta-miR-29d-5p	miR.MEmidnightblue
CLCN3	bta-miR-30c	miR.MEmidnightblue	*SCARA3*	bta-let-7c	miR.MEtan
CLCN3	bta-miR-30f	miR.MEmidnightblue	*SCARA3*	bta-let-7e	miR.MEtan
CLDN1	bta-miR-186	miR.MElightyellow	*SCARA3*	bta-let-7b	miR.MEtan
CLDN1	bta-let-7c	miR.MEtan	*SCARA3*	bta-let-7a-5p	miR.MEtan
CLDN1	bta-let-7e	miR.MEtan	*SCARA3*	bta-let-7f	miR.MEtan
CLDN1	bta-let-7b	miR.MEtan	*SIRT3*	bta-miR-214	miR.MEmagenta

CLDN1	bta-let-7a-5p	miR.MEtan	*SLC9A9*	bta-let-7c	miR.MEtan
CLDN1	bta-let-7f	miR.MEtan	*SLC9A9*	bta-let-7e	miR.MEtan
CLIC4	bta-miR-125a	miR.MElightyellow	*SLC9A9*	bta-let-7b	miR.MEtan
CLPB	bta-miR-29e	miR.MEcyan	*SLC9A9*	bta-let-7a-5p	miR.MEtan
CLSTN2	bta-miR-29a	miR.MEcyan	*SLC9A9*	bta-let-7f	miR.MEtan
CLSTN2	bta-miR-29e	miR.MEcyan	*SMAP1*	bta-miR-30c	miR.MEmidnightblue
CLYBL	bta-miR-21-3p	miR.MEgreen	*SMAP1*	bta-miR-30f	miR.MEmidnightblue
CMAS	bta-miR-29e	miR.MEcyan	*TMED2*	bta-miR-30c	miR.MEmidnightblue
CMPK2	bta-miR-214	miR.MEmagenta	*TMED2*	bta-miR-30f	miR.MEmidnightblue
CNBP	bta-miR-29e	miR.MEcyan	*TNFSF10*	bta-miR-214	miR.MEmagenta
CNBP	bta-miR-193a-3p	miR.MEmidnightblue	*TRIOBP*	bta-let-7c	miR.MEtan
CNIH4	bta-miR-29e	miR.MEcyan	*TRIOBP*	bta-let-7e	miR.MEtan
CNNM4	bta-miR-125a	miR.MElightyellow	*TRIOBP*	bta-let-7b	miR.MEtan
CNNM4	bta-miR-92b	miR.MElightyellow	*TRIOBP*	bta-let-7a-5p	miR.MEtan
CNTN1	bta-miR-92b	miR.MElightyellow	*TRIOBP*	bta-let-7f	miR.MEtan
COG1	bta-miR-29a	miR.MEcyan	*UBE2O*	bta-miR-30c	miR.MEmidnightblue
COG5	bta-miR-29a	miR.MEcyan	*UBE2O*	bta-miR-30f	miR.MEmidnightblue
COL14A1	bta-let-7c	miR.MEtan	*ZNF746*	bta-miR-30c	miR.MEmidnightblue
COL14A1	bta-let-7e	miR.MEtan	*ZNF746*	bta-miR-30f	miR.MEmidnightblue
COL14A1	bta-let-7b	miR.MEtan	*ZNFX1*	bta-miR-214	miR.MEmagenta
COL14A1	bta-let-7a-5p	miR.MEtan	*ATF1*	bta-miR-30c	miR.MEmidnightblue
COL14A1	bta-let-7f	miR.MEtan	*ATF1*	bta-miR-30f	miR.MEmidnightblue
COL1A1	bta-miR-186	miR.MElightyellow	*BECN1*	bta-miR-30c	miR.MEmidnightblue
COL1A1	bta-let-7c	miR.MEtan	*BECN1*	bta-miR-30f	miR.MEmidnightblue
COL1A1	bta-let-7e	miR.MEtan	*BTBD10*	bta-miR-30c	miR.MEmidnightblue
COL1A1	bta-let-7b	miR.MEtan	*BTBD10*	bta-miR-30f	miR.MEmidnightblue
COL1A1	bta-let-7a-5p	miR.MEtan	*CCDC9*	bta-miR-29d-5p	miR.MEmidnightblue
COL1A1	bta-let-7f	miR.MEtan	*CTPS1*	bta-miR-30c	miR.MEmidnightblue
COL3A1	bta-let-7c	miR.MEtan	*CTPS1*	bta-miR-30f	miR.MEmidnightblue
COL3A1	bta-let-7e	miR.MEtan	*EI24*	bta-miR-29d-5p	miR.MEmidnightblue
COL3A1	bta-let-7b	miR.MEtan	*GNG7*	bta-miR-331-3p	miR.MEmidnightblue
COL3A1	bta-let-7a-5p	miR.MEtan	*GNPDA1*	bta-miR-30c	miR.MEmidnightblue
COL3A1	bta-let-7f	miR.MEtan	*GNPDA1*	bta-miR-30f	miR.MEmidnightblue
COL5A1	bta-miR-92b	miR.MElightyellow	*LETM1*	bta-miR-29d-5p	miR.MEmidnightblue
COL5A2	bta-let-7c	miR.MEtan	*MYH14*	bta-miR-29d-5p	miR.MEmidnightblue
COL5A2	bta-let-7e	miR.MEtan	*PPID*	bta-miR-30c	miR.MEmidnightblue
COL5A2	bta-let-7b	miR.MEtan	*PPID*	bta-miR-30f	miR.MEmidnightblue
COL5A2	bta-let-7a-5p	miR.MEtan	*RAB7A*	bta-miR-30c	miR.MEmidnightblue
COL5A2	bta-let-7f	miR.MEtan	*RAB7A*	bta-miR-30f	miR.MEmidnightblue
COMMD10	bta-miR-29a	miR.MEcyan	*SIAH2*	bta-miR-30c	miR.MEmidnightblue
COPS7B	bta-miR-15a	miR.MEcyan	*SIAH2*	bta-miR-30f	miR.MEmidnightblue
COPS7B	bta-miR-30c	miR.MEmidnightblue	*SLC7A10*	bta-miR-30c	miR.MEmidnightblue
COPS7B	bta-miR-30f	miR.MEmidnightblue	*SLC7A10*	bta-miR-30f	miR.MEmidnightblue

CPSF7	bta-miR-29b	miR.MEcyan	*SYN1*	bta-miR-193a-3p	miR.MEmidnightblue
CPSF7	bta-miR-29c	miR.MEcyan	*UBE2D4*	bta-miR-29d-5p	miR.MEmidnightblue
CPSF7	bta-miR-29d-3p	miR.MEcyan	*YPEL5*	bta-miR-30c	miR.MEmidnightblue
CRBN	bta-miR-29e	miR.MEcyan	*YPEL5*	bta-miR-30f	miR.MEmidnightblue
CREB1	bta-miR-29e	miR.MEcyan	*AKNA*	bta-miR-381	miR.MEred

GS	MM	GS	MM	GS	MM	GS	MM
AAK1	0.85	*EPM2A*	0.65	*MYO10*	0.42	*SLC20A1*	0.66
AAR2	0.38	*EPS15*	0.52	*MYO5A*	0.73	*SLC22A23*	0.30
ABCE1	0.68	*ERBB3*	0.20	*MYO9A*	0.64	*SLC23A2*	0.79
ABCF1	0.74	*ERC1*	0.48	*MYOZ3*	0.56	*SLC24A3*	0.67
ABHD13	0.43	*ERGIC2*	0.38	*MZT1*	0.37	*SLC25A16*	0.39
ABHD2	0.40	*ERI1*	0.13	*NAA15*	0.71	*SLC25A23*	0.15
ABHD6	0.42	*ERN1*	0.47	*NAA25*	0.76	*SLC25A30*	0.62
ABL2	0.68	*ESCO1*	0.54	*NACC1*	0.36	*SLC25A34*	0.58
ACAP2	0.71	*ESRP2*	0.25	*NADK2*	0.52	*SLC25A53*	0.24
ACER2	0.64	*ESYT1*	0.78	*NAMPT*	0.57	*SLC27A6*	0.62
ACOX1	0.51	*ETF1*	0.68	*NANOS1*	0.43	*SLC2A3*	0.31
ACP2	0.53	*ETNK1*	0.50	*NAPEPLD*	0.47	*SLC30A1*	0.46
ACTC1	0.26	***ETV3***	0.56	*NAPG*	0.65	*SLC35B4*	0.40
ACTR1A	0.26	*EVI5*	0.62	*NARF*	0.18	*SLC35E1*	0.52
ACTRT3	0.51	*EVI5L*	0.67	*NARS*	0.35	*SLC35E2*	0.42
ACVR2A	0.48	*EXOC5*	0.56	*NASP*	0.28	*SLC37A3*	0.43
ADAM10	0.70	*EXOC7*	0.54	*NBEA*	0.52	*SLC38A4*	0.11
ADAM19	0.33	*EXOC8*	0.60	*NBEAL1*	0.77	*SLC38A9*	0.38
ADAMTS1	0.71	*EXOSC9*	0.28	*NBR1*	0.57	*SLC39A10*	0.55
ADAMTS15	0.35	*EXT2*	0.60	*NCK1*	0.58	*SLC39A6*	0.69
ADAMTS17	0.54	*FADS1*	0.40	*NCKAP1*	0.71	*SLC39A9*	0.54
ADAMTS20	0.47	*FAF1*	0.73	*NCKAP5L*	0.35	*SLC44A1*	0.55
ADAMTS5	0.45	*FAM104A*	0.07	*NCOA1*	0.62	*SLC48A1*	0.71
ADAR	0.74	*FAM107B*	0.62	*NCOA2*	0.74	*SLC5A3*	0.65
ADCY2	0.64	*FAM114A2*	0.51	*NCOA3*	0.79	*SLC6A17*	0.14
ADCY3	0.54	*FAM117B*	0.61	*NCOR1*	0.73	*SLC7A1*	0.39
ADCY5	0.63	*FAM120A*	0.47	*NDST1*	0.45	*SLC7A10*	0.22
ADIPOQ	0.90	*FAM122A*	0.46	*NF1*	0.85	*SLC7A8*	0.33
ADM	0.66	*FAM126A*	0.58	***NFAT5***	0.83	*SLC8A1*	0.59
ADO	0.53	*FAM135A*	0.57	***NFIA***	0.39	*SLC9A2*	0.52
ADRM1	0.73	*FAM160A1*	0.21	***NFIB***	0.40	*SLC9A7*	0.38
ADSL	0.48	*FAM160B1*	0.77	***NFIC***	0.67	*SLC9A9*	0.65
AEBP2	0.34	*FAM160B2*	0.55	***NFYB***	0.23	*SLCO3A1*	0.49
AFF1	0.83	*FAM173B*	0.49	*NHEJ1*	0.42	*SLK*	0.59
AFF3	0.57	*FAM199X*	0.85	*NHLRC2*	0.66	*SLX4IP*	0.30

AFF4	0.84	*FAM20B*	0.29	*NHSL2*	0.67	***SMAD2***	0.37
AGO1	0.58	*FAM210B*	0.36	*NIN*	0.83	***SMAD3***	0.48
AGO2	0.72	*FAM213A*	0.55	*NINJ1*	0.27	***SMAD5***	0.77
AGO3	0.73	*FAM229B*	0.34	*NIPBL*	0.88	*SMAD7*	0.10
AGO4	0.43	*FAM46A*	0.85	*NKAIN1*	0.40	*SMAP1*	0.45
AGPAT5	0.72	*FAM53B*	0.55	*NKIRAS2*	0.59	*SMARCA2*	0.39
AGPS	0.52	*FAM89B*	0.60	*NLRC5*	0.62	*SMARCA5*	0.74
AGTPBP1	0.15	*FAM98C*	0.58	*NMNAT1*	0.64	*SMARCC1*	0.47
AHCYL1	0.58	*FANCM*	0.64	*NMNAT2*	0.43	*SMC1A*	0.83
AHNAK	0.65	*FAR1*	0.64	*NMT1*	0.68	*SMC2*	0.60
AIDA	0.59	*FAT4*	0.82	*NOL10*	0.28	*SMC6*	0.60
AIFM2	0.55	*FAXC*	0.57	*NOL11*	0.48	*SMCR8*	0.46
AK1	0.84	*FBN1*	0.78	*NPAT*	0.62	*SMIM13*	0.40
AK3	0.50	*FBXL18*	0.58	*NPEPL1*	0.76	*SMIM14*	0.71
AKAP11	0.68	*FBXO28*	0.68	*NPEPPS*	0.67	*SMTNL2*	0.61
AKAP13	0.74	*FBXO31*	0.72	*NPR3*	0.21	*SMU1*	0.39
AKIRIN1	0.44	*FBXO42*	0.59	***NR1D2***	0.36	*SMURF1*	0.54
AKNA	0.68	*FBXO7*	0.37	***NR1H3***	0.64	*SMURF2*	0.66
AKR7A2	0.25	*FBXW2*	0.29	***NR2C2***	0.70	*SNTB1*	0.53
AKT3	0.83	*FBXW7*	0.28	***NR3C1***	0.58	*SNTB2*	0.72
ALDOA	0.83	*FCGR3A*	0.75	*NR3C2*	0.57	*SNX1*	0.49
ALG8	0.24	*FEM1A*	0.79	*NRAS*	0.39	*SNX11*	0.30
ALKBH5	0.86	*FEM1B*	0.65	*NRBF2*	0.21	*SNX12*	0.31
ALPK3	0.71	*FGF7*	0.61	*NRBP1*	0.70	*SNX18*	0.23
ALS2	0.50	*FGFR1OP*	0.39	*NRF1*	0.22	*SNX2*	0.33
AMFR	0.49	*FILIP1*	0.68	*NRK*	0.42	*SNX30*	0.48
AMIGO1	0.48	*FIP1L1*	0.40	*NSD1*	0.82	*SNX33*	0.46
AMOT	0.44	*FKBP10*	0.81	*NSF*	0.25	*SOBP*	0.26
AMOTL1	0.57	*FKBP14*	0.61	*NSUN2*	0.55	*SOCS4*	0.58
ANAPC10	0.26	*FKBP4*	0.70	*NSUN4*	0.51	*SOCS5*	0.44
ANGPT1	0.59	*FKTN*	0.49	*NT5DC3*	0.23	*SOCS6*	0.72
ANGPTL2	0.70	*FLOT2*	0.71	*NTPCR*	0.50	*SORL1*	0.25
ANK1	0.65	*FNBP1*	0.80	*NUB1*	0.32	*SORT1*	0.56
ANKFY1	0.52	*FNDC3B*	0.79	*NUDCD1*	0.23	*SOX11*	0.15
ANKIB1	0.55	*FNIP2*	0.50	*NUDT3*	0.58	***SOX4***	0.44
ANKRA2	0.27	*FOCAD*	0.43	*NUMBL*	0.53	***SP1***	0.68
ANKRD13B	0.40	***FOXK1***	0.56	*NUP153*	0.67	*SP140L*	0.58
ANKRD13C	0.10	***FOXN2***	0.51	*NUP160*	0.47	***SP4***	0.53
ANKRD50	0.69	***FOXO3***	0.70	*NUP50*	0.63	*SPAG9*	0.74
ANKRD52	0.55	***FOXP1***	0.57	*NUP54*	0.34	*SPAST*	0.43
ANKRD6	0.48	***FOXP4***	0.37	*NUP93*	0.19	*SPATA2*	0.64
ANO6	0.76	*FRAT2*	0.31	*NUS1*	0.29	*SPCS3*	0.37
ANPEP	0.58	*FRMD4A*	0.48	*NXN*	0.52	*SPEN*	0.81

ANTXR2	0.87	*FRMD4B*	0.74	*OARD1*	0.34	*SPOP*	0.59
AP1B1	0.25	*FRS2*	0.62	*OBSCN*	0.31	*SPR*	0.05
AP1G1	0.69	*FRY*	0.65	*OLFML2A*	0.51	*SPRTN*	0.47
AP1S1	0.55	*FRYL*	0.74	*OPA1*	0.32	*SPRYD7*	0.29
AP2A1	0.61	*FRZB*	0.18	*OPA3*	0.24	*SPSB1*	0.45
AP3M2	0.50	*FST*	0.34	*ORAI1*	0.49	*SPTLC2*	0.66
AP4E1	0.62	*FTO*	0.36	*OSBPL11*	0.33	*SPTSSA*	0.25
AP5M1	0.60	*FUBP1*	0.57	*OSBPL3*	0.44	*SPTY2D1*	0.55
APBA1	0.51	*FURIN*	0.42	*OSBPL5*	0.57	*SQSTM1*	0.65
APBB2	0.42	*FUT11*	0.26	*OSBPL8*	0.63	*SRD5A1*	0.27
APC	0.75	*FUT8*	0.53	*OTUD4*	0.74	*SRGAP1*	0.69
APP	0.83	*FXN*	0.65	*OTUD6B*	0.40	*SRGAP2*	0.71
APPBP2	0.55	*FXR2*	0.67	*OTUD7B*	0.66	*SRGAP3*	0.54
APPL1	0.66	*FYTTD1*	0.49	*OXCT1*	0.27	*SRL*	0.56
AQP4	0.60	*FZD7*	0.41	*P4HA2*	0.41	*SRP72*	0.48
AQR	0.80	*G3BP1*	0.64	*PABPC4L*	0.53	*SRPK1*	0.61
AR	0.64	***GABPA***	0.41	*PAFAH1B2*	0.60	*SRPK2*	0.50
AREL1	0.51	*GALNT1*	0.37	*PAIP1*	0.86	*SS18L1*	0.17
ARF5	0.26	*GALNT15*	0.46	*PAIP2*	0.65	*SSBP1*	0.53
ARFGAP2	0.55	*GALNT2*	0.57	*PAK1*	0.27	*SSH2*	0.56
ARFGEF2	0.76	*GALNT4*	0.47	*PAK2*	0.49	*SSPN*	0.53
ARHGAP17	0.58	*GALNT7*	0.62	*PAK3*	0.47	*SSR1*	0.34
ARHGAP20	0.46	*GAN*	0.77	*PAK4*	0.52	*ST13*	0.64
ARHGAP22	0.26	*GAS2L3*	0.46	*PANK3*	0.78	*ST6GAL1*	0.52
ARHGAP30	0.90	*GAS7*	0.74	*PANX1*	0.43	*ST8SIA2*	0.20
ARHGAP35	0.74	*GCC2*	0.64	*PAPOLG*	0.55	*STAG1*	0.48
ARHGAP5	0.81	*GCNT1*	0.34	*PARD3*	0.52	*STAG2*	0.71
ARHGEF10	0.68	*GDE1*	0.65	*PARD3B*	0.52	*STAMBPL1*	0.33
ARHGEF12	0.77	*GDPD5*	0.20	*PARG*	0.56	*STARD10*	0.43
ARID2	0.75	*GEMIN4*	0.57	*PARM1*	0.15	*STARD13*	0.66
ARIH2	0.83	*GFPT2*	0.53	*PARP14*	0.92	*STC1*	0.29
ARL14EP	0.44	*GGA1*	0.64	*PARP9*	0.79	*STK40*	0.55
ARL4A	0.14	*GGA2*	0.51	***PBX3***	0.71	*STON2*	0.42
ARL5B	0.58	*GHR*	0.46	*PCBP1*	0.84	*STRADB*	0.47
ARL8A	0.56	*GID4*	0.74	*PCBP2*	0.64	*STRIP1*	0.12
ARL8B	0.56	*GID8*	0.54	*PCDHA13*	0.51	*STRN*	0.71
ARMC1	0.15	*GIMAP8*	0.57	*PCGF2*	0.36	*STRN3*	0.68
ARMC10	0.41	*GIPC1*	0.39	*PCGF5*	0.53	*STRN4*	0.67
ARMC8	0.66	*GIT1*	0.28	*PCM1*	0.56	*STX17*	0.58
ARNT	0.69	***GLIS2***	0.66	*PCMT1*	0.73	*STX4*	0.71
ARPC5L	0.63	*GLOD4*	0.32	*PCOLCE2*	0.60	*STXBP1*	0.65
ARRDC3	0.22	*GLTP*	0.33	*PCYOX1*	0.54	*STXBP4*	0.68
ASB8	0.59	*GLYCTK*	0.22	*PDCD11*	0.43	*STXBP5*	0.44

ASCC3	0.61	*GMFB*	0.67	*PDCD4*	0.33	*SUB1*	0.35
ASH1L	0.94	*GMPR*	0.66	*PDCD6IP*	0.46	*SULF1*	0.82
ASNA1	0.81	*GMPS*	0.48	*PDE10A*	0.27	*SUN2*	0.24
ASPH	0.47	*GNA13*	0.53	*PDE3A*	0.54	*SUPT3H*	0.23
ASPN	0.71	*GNAI1*	0.93	*PDE3B*	0.89	*SUPT6H*	0.50
ASXL2	0.84	*GNAQ*	0.84	*PDE4B*	0.22	*SUZ12*	0.47
ATAD2B	0.71	*GNG7*	0.34	*PDE4C*	0.65	*SYDE2*	0.48
ATF1	0.66	*GNGT2*	0.40	*PDE4D*	0.78	*SYN1*	0.19
ATF6	0.60	*GNL1*	0.17	*PDE4DIP*	0.60	*SYNCRIP*	0.77
ATF7IP	0.75	*GNPDA1*	0.16	*PDF*	0.59	*SYNE1*	0.71
ATG12	0.24	*GNS*	0.45	*PDGFC*	0.69	*SYNGR1*	0.36
ATG4D	0.60	*GOLGA1*	0.52	*PDK1*	0.17	*SYNJ1*	0.50
ATG9A	0.68	*GOLGA4*	0.56	*PDP2*	0.82	*SYNPO2*	0.69
ATMIN	0.47	*GOLGA5*	0.19	*PDS5B*	0.72	*SYNRG*	0.50
ATP10D	0.68	*GORASP2*	0.52	*PDSS2*	0.38	*SYT11*	0.52
ATP11B	0.60	*GPALPP1*	0.43	*PDXDC1*	0.57	*TAB3*	0.64
ATP2A2	0.69	*GPATCH2*	0.46	*PDZD2*	0.63	*TADA2B*	0.57
ATP2B2	0.48	*GPBP1*	0.36	*PDZD8*	0.47	*TAF1*	0.77
ATP2B4	0.80	*GPC4*	0.32	*PEAK1*	0.69	*TAF7*	0.34
ATP6V0A2	0.58	*GPCPD1*	0.52	*PEG10*	0.33	*TAF8*	0.50
ATP6V1C1	0.33	*GPM6A*	0.41	*PELI3*	0.57	*TANC1*	0.59
ATP9A	0.50	*GPR107*	0.80	*PEX11A*	0.43	*TAOK1*	0.69
ATRN	0.70	*GPR173*	0.50	*PEX11B*	0.42	*TAP2*	0.52
ATXN1	0.75	*GPR180*	0.27	*PEX19*	0.81	*TARS*	0.46
ATXN1L	0.64	*GPR63*	0.66	*PFKFB3*	0.43	*TBC1D10B*	0.66
ATXN2	0.59	*GPSM2*	0.31	*PFKM*	0.68	*TBC1D15*	0.16
ATXN3	0.62	*GPX7*	0.75	*PGAM1*	0.63	*TBC1D16*	0.46
ATXN7L3B	0.57	*GRAMD1B*	0.20	*PGAP1*	0.72	*TBC1D20*	0.08
AUP1	0.59	*GRAMD1C*	0.43	*PGAP2*	0.40	*TBC1D25*	0.48
AVEN	0.63	*GRB10*	0.29	*PGM1*	0.75	*TBC1D30*	0.35
AVL9	0.51	*GRHPR*	0.43	*PGM3*	0.21	*TBC1D7*	0.15
AXL	0.85	*GRM4*	0.44	*PGP*	0.67	*TBC1D8*	0.25
AZIN1	0.16	*GSK3B*	0.68	*PGPEP1*	0.48	*TBKBP1*	0.48
B4GALT1	0.62	*GSKIP*	0.23	*PHAX*	0.30	*TBL1XR1*	0.48
B4GALT2	0.58	*GSTA4*	0.15	*PHC1*	0.50	*TBRG1*	0.73
B4GALT6	0.31	*GSTCD*	0.31	*PHC3*	0.88	***TBX15***	0.59
BACE1	0.14	*GSTK1*	0.44	*PHF12*	0.36	*TCAIM*	0.60
BACE2	0.55	*GTDC1*	0.47	*PHF2*	0.76	*TCEA3*	0.68
BAG5	0.38	*GTF2A1*	0.58	*PHF20*	0.51	***TEAD1***	0.65
BAP1	0.64	*GTF3C4*	0.76	*PHF3*	0.68	*TERF2*	0.07
BAZ2A	0.75	*GTPBP1*	0.24	*PHF5A*	0.53	*TERF2IP*	0.39
BBX	0.75	*GTPBP8*	0.39	*PHF6*	0.56	*TESK2*	0.25
BCAS3	0.40	*GUCD1*	0.54	*PHIP*	0.84	*TET2*	0.48

BCCIP	0.64	*GXYLT1*	0.70	*PHKB*	0.69	*TEX261*	0.34
BCDIN3D	0.11	***HBP1***	0.11	*PHLPP2*	0.53	***TFEB***	0.74
BCKDK	0.61	*HCFC1*	0.56	*PI4KB*	0.51	*TFRC*	0.23
BCL2	0.41	*HDAC5*	0.13	*PIAS1*	0.52	*TGFB2*	0.41
BCL2L13	0.65	*HEATR5A*	0.75	*PIAS2*	0.49	*TGFBR1*	0.48
BCL9	0.39	*HECTD4*	0.76	*PIK3AP1*	0.25	*TGFBR2*	0.73
BCLAF1	0.56	*HELZ*	0.86	*PIK3C2A*	0.66	*TGFBR3*	0.75
BCORL1	0.46	*HERC4*	0.53	*PIK3CA*	0.72	***TGIF1***	0.63
BECN1	0.25	*HERPUD2*	0.40	*PIK3CB*	0.23	*TGOLN2*	0.37
BEND3	0.37	*HEXIM1*	0.44	*PIK3IP1*	0.46	***THAP1***	0.39
BET1L	0.35	*HIBCH*	0.48	*PIK3R2*	0.28	*THAP2*	0.24
BGN	0.82	***HIF1A***	0.66	*PIKFYVE*	0.70	*THAP6*	0.43
BLMH	0.67	***HIF3A***	0.63	*PITPNA*	0.23	*THAP8*	0.22
BLOC1S1	0.71	***HINFP***	0.43	*PKIA*	0.33	*THBS1*	0.66
BLOC1S5	0.21	*HIST1H2BD*	0.53	***PKNOX2***	0.29	*THOC2*	0.66
BLZF1	0.56	***HIVEP3***	0.33	*PKP4*	0.54	***THRA***	0.70
BMI1	0.65	***HLF***	0.62	*PLA2G12A*	0.39	*THUMPD1*	0.67
BNIP2	0.81	***HMBOX1***	0.85	*PLA2G15*	0.20	*THY1*	0.86
BOD1L1	0.78	*HMGA1*	0.71	*PLAA*	0.69	*TICAM2*	0.31
BPGM	0.65	*HMGB2*	0.43	*PLAC8*	0.40	*TIMM8A*	0.54
BPTF	0.91	*HMGCS1*	0.22	***PLAGL2***	0.34	*TLE3*	0.65
BRD7	0.44	*HNRNPK*	0.24	*PLCL2*	0.71	*TLK1*	0.52
BROX	0.46	*HNRNPL*	0.30	*PLD1*	0.57	*TLR5*	0.33
BRWD1	0.75	*HOOK3*	0.85	*PLD3*	0.43	*TM9SF4*	0.38
BRWD3	0.82	*HOXA10*	0.53	*PLEKHA1*	0.53	*TMCC1*	0.41
BSDC1	0.30	*HOXA9*	0.34	*PLEKHA8*	0.43	*TMED2*	0.33
BTAF1	0.81	***HOXC8***	0.66	*PLEKHF2*	0.15	*TMED5*	0.47
BTBD10	0.58	***HOXD1***	0.51	*PLEKHM3*	0.53	*TMED8*	0.36
BTBD11	0.57	*HRAS*	0.76	*PLXDC2*	0.74	*TMEM104*	0.24
BTBD7	0.66	*HS3ST5*	0.07	*PLXNA4*	0.63	*TMEM110*	0.79
BTBD9	0.41	*HSPBAP1*	0.21	*PLXNC1*	0.39	*TMEM123*	0.50
BTC	0.54	*ICK*	0.70	*PMM2*	0.45	*TMEM131*	0.52
BTF3L4	0.27	*IDH1*	0.78	*POFUT2*	0.53	*TMEM135*	0.47
C1GALT1	0.57	*IDS*	0.55	*POGLUT1*	0.48	*TMEM168*	0.46
C1QTNF3	0.53	*IFI44L*	0.89	*POGZ*	0.66	*TMEM170B*	0.70
CA5B	0.47	*IFIT5*	0.73	*POLE3*	0.70	*TMEM179B*	0.37
CAB39L	0.49	*IFRD2*	0.62	*POLR1A*	0.51	*TMEM182*	0.43
CACNA2D1	0.53	*IGF1*	0.61	*POLR3D*	0.64	*TMEM184B*	0.44
CACNA2D2	0.42	*IGF1R*	0.53	*POMGNT1*	0.63	*TMEM184C*	0.20
CACNB1	0.59	*IGF2*	0.63	***POU2F1***	0.75	*TMEM189*	0.23
CACUL1	0.45	*IGF2BP2*	0.24	*PPARGC1B*	0.51	*TMEM19*	0.55
CALD1	0.80	*IGF2R*	0.57	*PPFIBP1*	0.51	*TMEM201*	0.23
CALM1	0.68	*IGFN1*	0.27	*PPID*	0.44	*TMEM234*	0.44

CALM3	0.86	*IGSF10*	0.62	*PPM1A*	0.66	*TMEM246*	0.35
CALN1	0.39	***IKZF1***	0.77	*PPM1B*	0.40	*TMEM248*	0.44
CALU	0.73	***IKZF4***	0.59	*PPM1H*	0.58	*TMEM255A*	0.22
CAND1	0.74	*IL13RA1*	0.76	*PPP1CB*	0.47	*TMEM259*	0.60
CAPZA2	0.55	*IL16*	0.60	*PPP1R12A*	0.59	*TMEM33*	0.63
CARM1	0.66	*IL17RA*	0.23	*PPP1R14C*	0.54	*TMEM38A*	0.66
CASK	0.50	*IL2RG*	0.54	*PPP1R15B*	0.27	*TMEM65*	0.58
CASP9	0.39	*IL6R*	0.63	*PPP1R1A*	0.81	*TMEM86A*	0.52
CAST	0.42	*IL6ST*	0.62	*PPP1R3B*	0.57	*TMEM98*	0.16
CBFB	0.50	*INCENP*	0.43	*PPP1R3D*	0.35	*TMTC2*	0.63
CBL	0.74	*ING1*	0.66	*PPP1R3F*	0.37	*TMTC3*	0.66
CBR4	0.62	*ING2*	0.38	*PPP1R9A*	0.60	*TNFAIP3*	0.44
CBX5	0.63	*INO80*	0.49	*PPP2R1B*	0.46	*TNFAIP8L3*	0.63
CC2D1A	0.49	*INO80D*	0.82	*PPP3CB*	0.72	*TNFRSF1B*	0.59
CCDC121	0.43	*INPP4B*	0.55	*PPP3R1*	0.55	*TNFSF10*	0.63
CCDC149	0.47	*INSIG1*	0.38	*PPP6C*	0.56	*TNIP1*	0.53
CCDC28A	0.26	*INSR*	0.41	*PPP6R3*	0.62	*TNPO1*	0.68
CCDC6	0.59	*INTS7*	0.41	*PPT1*	0.74	*TNPO3*	0.65
CCDC80	0.77	*IPMK*	0.44	*PQLC1*	0.34	*TNRC18*	0.49
CCDC88C	0.69	*IPO7*	0.71	***PRDM1***	0.27	*TNRC6A*	0.71
CCDC9	0.23	*IPO8*	0.63	***PRDM4***	0.31	*TNRC6B*	0.90
CCNE1	0.50	*IPO9*	0.58	*PREPL*	0.62	*TOB2*	0.29
CCNK	0.56	*IQGAP2*	0.83	*PREX2*	0.75	*TOR1AIP1*	0.60
CCNT1	0.72	*IRAK2*	0.26	*PRKAG1*	0.46	*TOR1B*	0.22
CCNYL1	0.54	*IREB2*	0.72	*PRKAR2B*	0.55	*TOX4*	0.50
CCSER2	0.64	***IRF1***	0.74	*PRKCA*	0.53	*TP53INP1*	0.44
CD164	0.24	*IRF2BP1*	0.69	*PRKCE*	0.38	*TPCN1*	0.34
CD55	0.59	*IRF2BPL*	0.29	*PRKCZ*	0.56	*TPD52L2*	0.42
CD84	0.72	*IRS2*	0.36	*PRKD3*	0.54	*TPK1*	0.18
CDC27	0.59	*ISLR*	0.82	***PROX1***	0.34	*TPM1*	0.82
CDC37L1	0.54	*ITCH*	0.80	*PRR14L*	0.68	*TPMT*	0.47
CDC42BPA	0.74	*ITGA8*	0.49	*PRRC1*	0.56	*TPR*	0.83
CDC5L	0.43	*ITGAV*	0.55	*PRRC2B*	0.68	*TRABD2B*	0.72
CDH11	0.75	*ITGB3*	0.74	*PSAP*	0.29	*TRAF1*	0.12
CDK12	0.73	*ITM2B*	0.69	*PSD3*	0.48	*TRAF3*	0.22
CDK13	0.66	*ITPR1*	0.65	*PSKH1*	0.75	*TRAF4*	0.31
CDK14	0.64	*ITSN1*	0.59	*PSMA5*	0.46	*TRAK2*	0.68
CDK16	0.38	*IVNS1ABP*	0.46	*PSMB5*	0.77	*TRAM2*	0.67
CDK19	0.58	*IYD*	0.34	*PSMC2*	0.77	*TRAPPC8*	0.70
CDK6	0.72	*JAG1*	0.60	*PSME3*	0.72	*TRIAP1*	0.61
CDKN1B	0.33	*JMJD1C*	0.66	*PSMF1*	0.44	*TRIM13*	0.33
CDKN2AIP	0.32	*JMY*	0.51	*PSTPIP2*	0.65	*TRIM24*	0.44
CDR2L	0.63	*JOSD1*	0.59	*PTAR1*	0.74	*TRIM25*	0.60

CDS2	0.64	*JPH1*	0.69	*PTGES3*	0.54	*TRIM33*	0.56
CDV3	0.53	*KALRN*	0.31	*PTGR2*	0.57	*TRIM36*	0.14
CDYL2	0.23	*KAT6B*	0.70	*PTP4A1*	0.62	*TRIM45*	0.47
CEBPG	0.33	*KATNBL1*	0.41	*PTPN11*	0.61	*TRIM72*	0.50
CELF2	0.61	*KAZN*	0.52	*PTPRD*	0.56	*TRIOBP*	0.29
CENPB	0.62	*KBTBD8*	0.52	*PTPRE*	0.61	*TRIP11*	0.78
CENPI	0.43	***KCMF1***	0.83	*PTPRF*	0.64	*TRMT1L*	0.54
CEP128	0.42	*KCNB1*	0.61	*PTPRK*	0.49	*TRMT5*	0.03
CEP350	0.93	*KCNJ12*	0.79	*PTPRM*	0.39	*TRPC1*	0.53
CEP57	0.19	*KCNN3*	0.60	*PTPRU*	0.28	***TRPS1***	0.59
CEP85	0.03	*KCTD15*	0.07	*PTRH2*	0.45	***TSHZ2***	0.77
CEP85L	0.65	*KCTD20*	0.33	*PUF60*	0.67	*TSN*	0.59
CEP97	0.69	*KCTD21*	0.38	*PUM2*	0.60	*TSPYL4*	0.39
CERCAM	0.65	*KCTD3*	0.48	*PURA*	0.63	*TSPYL5*	0.38
CERS1	0.27	*KCTD5*	0.28	*PURB*	0.48	*TTC3*	0.51
CGGBP1	0.45	*KDM2A*	0.53	*PXDC1*	0.58	*TTC4*	0.53
CHD2	0.51	*KDM4B*	0.37	*PYGO1*	0.55	*TTC7A*	0.59
CHD6	0.68	*KDM5A*	0.87	*QKI*	0.51	*TTC9*	0.40
CHD7	0.49	*KDM5B*	0.38	*QPCT*	0.51	*TTLL12*	0.54
CHD9	0.86	*KDM6B*	0.42	*R3HDM4*	0.39	*TTLL7*	0.62
CHERP	0.04	*KHNYN*	0.30	*RAB11FIP2*	0.76	*TWF1*	0.41
CHM	0.52	*KIAA0100*	0.73	*RAB12*	0.66	*TXLNA*	0.58
CHMP1A	0.55	*KIAA0391*	0.18	*RAB21*	0.49	*TXLNG*	0.67
CHMP4B	0.66	*KIAA1217*	0.65	*RAB22A*	0.58	*TXNL4A*	0.62
CHMP4C	0.07	*KIAA1328*	0.46	*RAB2A*	0.39	*UBA3*	0.43
CHMP6	0.57	*KIAA1468*	0.33	*RAB3D*	0.24	*UBAC1*	0.61
CHN1	0.10	*KIAA1522*	0.09	*RAB3GAP1*	0.42	*UBAP1*	0.62
CKAP4	0.73	*KIAA1549*	0.52	*RAB3GAP2*	0.74	*UBB*	0.67
CKAP5	0.49	*KIAA1614*	0.51	*RAB4A*	0.39	*UBE2A*	0.70
CLASP1	0.67	*KIAA1958*	0.69	*RAB5B*	0.59	*UBE2B*	0.51
CLCC1	0.30	*KIAA2013*	0.70	*RAB7A*	0.57	*UBE2D2*	0.75
CLCN3	0.30	*KIDINS220*	0.59	*RAB8B*	0.55	*UBE2D4*	0.70
CLCN5	0.39	*KIF1B*	0.87	*RAB9A*	0.29	*UBE2E1*	0.47
CLDN1	0.22	*KIF1C*	0.76	*RABGAP1L*	0.47	*UBE2E3*	0.57
CLIC4	0.73	*KIF3A*	0.68	*RABGEF1*	0.45	*UBE2F*	0.56
CLMP	0.80	*KIF3B*	0.48	*RAC1*	0.74	*UBE2G1*	0.67
CLOCK	0.67	*KIFAP3*	0.31	*RAD21*	0.44	*UBE2G2*	0.43
CLPB	0.69	*KIN*	0.47	*RAD23B*	0.71	*UBE2J1*	0.71
CLSTN2	0.48	*KLC2*	0.73	*RAD9B*	0.54	*UBE2O*	0.55
CLYBL	0.51	***KLF10***	0.45	*RADIL*	0.21	*UBE2Q1*	0.59
CMAS	0.38	*KLF11*	0.35	*RAF1*	0.83	*UBE2R2*	0.56
CMPK2	0.80	***KLF12***	0.64	*RALBP1*	0.53	*UBE2V1*	0.77
CNBP	0.66	***KLF3***	0.58	*RALGAPA2*	0.51	*UBE2W*	0.44

CNIH4	0.46	***KLF7***	0.73	*RALGAPB*	0.72	*UBE2Z*	0.25
CNKSR2	0.66	***KLF9***	0.56	*RALGPS2*	0.36	*UBE4A*	0.61
CNNM4	0.31	*KLHL20*	0.32	*RANBP10*	0.54	*UBFD1*	0.64
CNOT7	0.58	*KLHL21*	0.28	*RANBP3*	0.75	*UBL3*	0.35
CNTN1	0.78	*KLHL24*	0.49	*RANBP6*	0.37	*UBN2*	0.80
COG1	0.61	*KLHL25*	0.46	*RANBP9*	0.72	*UBR1*	0.84
COG5	0.47	*KLHL26*	0.26	*RAP2C*	0.16	*UBR4*	0.76
COL11A2	0.13	*KLHL28*	0.71	*RAPGEF1*	0.72	*UBR5*	0.82
COL14A1	0.86	*KLHL31*	0.57	*RASAL2*	0.53	*UBR7*	0.37
COL1A1	0.86	*KMT2A*	0.88	*RB1*	0.60	***UBTF***	0.36
COL1A2	0.88	*KMT2C*	0.88	*RBBP6*	0.59	*UBXN4*	0.60
COL3A1	0.84	*KMT2D*	0.86	*RBL2*	0.58	*UBXN7*	0.72
COL4A3BP	0.48	*KMT2E*	0.75	*RBM12*	0.53	*UCP3*	0.41
COL5A1	0.87	*KPNA1*	0.81	*RBM20*	0.47	*UFL1*	0.55
COL5A2	0.89	*KPNA4*	0.83	***RBPJ***	0.63	*UGGT1*	0.79
COMMD10	0.40	*KRAS*	0.59	*RCN2*	0.23	*UHMK1*	0.82
COMMD7	0.58	*KRIT1*	0.29	*RCOR1*	0.46	*UHRF1BP1*	0.52
COPS2	0.56	*KSR1*	0.27	*RDX*	0.56	*UHRF1BP1L*	0.57
COPS7B	0.27	*L2HGDH*	0.73	*REEP3*	0.84	*ULK2*	0.48
CORO2B	0.58	*L3MBTL2*	0.11	***REST***	0.55	*UNG*	0.69
CPEB1	0.41	*LAMTOR3*	0.52	*REV3L*	0.63	*URI1*	0.44
CPM	0.60	*LARP4B*	0.53	*RFFL*	0.44	*USP12*	0.35
CPSF7	0.66	*LATS2*	0.38	***RFX3***	0.41	*USP13*	0.73
CRBN	0.64	*LCLAT1*	0.36	***RFX7***	0.60	*USP24*	0.68
CREB1	0.71	*LCOR*	0.85	*RHBDD1*	0.10	*USP31*	0.63
CREB3L2	0.81	*LDB3*	0.34	*RHOBTB2*	0.48	*USP34*	0.84
CREBBP	0.71	*LDHA*	0.73	*RHOQ*	0.53	*USP37*	0.75
CREBRF	0.64	*LDLRAD4*	0.32	*RICTOR*	0.68	*USP42*	0.47
CRK	0.60	*LETM1*	0.25	*RILPL1*	0.50	*USP46*	0.68
CRLS1	0.65	*LGALS9*	0.74	***RLF***	0.62	*USP49*	0.44
CRNKL1	0.51	*LHFPL2*	0.84	*RLIM*	0.59	*USP53*	0.60
CRTAP	0.67	*LIFR*	0.70	*RMND5A*	0.58	*USP6NL*	0.55
CRTC1	0.44	*LIG3*	0.28	*RNF10*	0.62	*USP9X*	0.77
CRTC2	0.35	*LIPA*	0.61	*RNF11*	0.65	*VANGL1*	0.48
CSDE1	0.72	*LMAN1*	0.75	*RNF111*	0.67	*VAPA*	0.82
CSGALNACT2	0.42	*LMAN2L*	0.34	*RNF122*	0.10	*VAPB*	0.57
CSNK1G2	0.61	*LMBR1*	0.23	*RNF125*	0.76	*VAV3*	0.69
CSNK2A1	0.71	*LMBR1L*	0.50	*RNF130*	0.55	*VCP*	0.75
CTBP2	0.32	*LMBRD2*	0.77	*RNF138*	0.33	*VGLL3*	0.64
CTDSPL2	0.61	*LMTK2*	0.69	*RNF139*	0.28	*VIPAS39*	0.23
CTIF	0.26	*LNPEP*	0.69	*RNF14*	0.55	*VKORC1L1*	0.23
CTNNBL1	0.37	*LOX*	0.73	*RNF141*	0.48	*VLDLR*	0.44
CTNS	0.17	*LOXL1*	0.71	*RNF144B*	0.55	*VMA21*	0.41

CTPS1	0.11	*LOXL4*	0.57	*RNF146*	0.49	*VMAC*	0.32
CTTNBP2	0.56	*LPGAT1*	0.74	*RNF157*	0.71	*VPS13A*	0.76
CUL2	0.50	*LPP*	0.57	*RNF169*	0.36	*VPS13B*	0.84
CUL3	0.74	*LRP11*	0.18	*RNF185*	0.59	*VPS18*	0.48
CUL4A	0.72	*LRP6*	0.67	*RNF19B*	0.52	*VPS33A*	0.13
CYB5R4	0.08	*LRRC1*	0.40	*RNF214*	0.69	*VPS37A*	0.46
CYLD	0.69	*LRRC14*	0.20	*RNF217*	0.56	*VPS37C*	0.28
CYP7B1	0.48	*LRRC15*	0.16	*RNF220*	0.72	*VPS4A*	0.87
CYTH3	0.65	*LRRC20*	0.46	*RNF34*	0.32	*VRK3*	0.29
DAAM1	0.49	*LRRC28*	0.77	*RNGTT*	0.36	*VSIG4*	0.73
DACT1	0.56	*LRRC58*	0.70	*ROBO1*	0.50	*VTA1*	0.54
DBNL	0.33	*LSM12*	0.82	*ROCK2*	0.78	*VTI1A*	0.47
DCAF10	0.58	*LSM14B*	0.52	***RORA***	0.69	*VWA7*	0.36
DCAF7	0.51	*LURAP1*	0.34	***RORC***	0.43	*WARS*	0.72
DCAKD	0.10	*LURAP1L*	0.51	*RPA1*	0.29	*WASL*	0.46
DCBLD2	0.56	*LYRM2*	0.35	*RPE*	0.58	*WBP11*	0.68
DCP1A	0.57	*LYRM7*	0.75	*RPF1*	0.47	*WBP2*	0.71
DCUN1D2	0.30	*LYSMD1*	0.67	*RPP14*	0.60	*WDFY3*	0.72
DCUN1D5	0.38	*LYVE1*	0.62	*RPRD2*	0.68	*WDR26*	0.69
DDX19B	0.60	*LZIC*	0.37	*RPS6KA1*	0.14	*WDR47*	0.56
DDX20	0.28	***MAF***	0.32	*RPS6KA3*	0.41	*WDR70*	0.38
DDX39A	0.40	*MAMDC2*	0.70	*RPS6KB1*	0.73	*WDR77*	0.25
DDX46	0.57	*MAML2*	0.71	*RRAGA*	0.37	*WDR82*	0.38
DDX54	0.69	*MAMSTR*	0.56	*RRAGC*	0.28	*WDTC1*	0.64
DDX58	0.86	*MAN2A1*	0.73	*RRAGD*	0.70	*WHAMM*	0.52
DDX6	0.63	*MAP1B*	0.83	*RRBP1*	0.78	*WIPF2*	0.51
DEDD	0.74	*MAP2*	0.57	***RREB1***	0.55	*WIPI2*	0.60
DENND4A	0.57	*MAP2K4*	0.62	*RSAD2*	0.90	*WNT4*	0.39
DENND5A	0.70	*MAP2K6*	0.34	*RSBN1*	0.53	*WSCD1*	0.19
DENND5B	0.51	*MAP2K7*	0.54	*RSBN1L*	0.49	*WWP1*	0.58
DENR	0.57	*MAP3K1*	0.56	*RSF1*	0.80	*XIAP*	0.54
DESI1	0.32	*MAP3K2*	0.56	*RTN2*	0.78	*XK*	0.52
DESI2	0.60	*MAP3K4*	0.59	*RTN4RL1*	0.36	*XKR8*	0.15
DGCR8	0.27	*MAP3K7*	0.58	*RUNX1T1*	0.71	*XPOT*	0.40
DGKH	0.66	*MAP3K7CL*	0.26	*RWDD2B*	0.65	*XPR1*	0.55
DHRS3	0.56	*MAP3K9*	0.27	*RWDD4*	0.49	*XRN1*	0.67
DHX33	0.66	*MAP4*	0.55	***RXRA***	0.71	*XRRA1*	0.33
DHX36	0.57	*MAPK1IP1L*	0.57	*SAMD12*	0.60	*XXYLT1*	0.16
DHX40	0.32	*MAPK6*	0.54	*SAMD4A*	0.44	*XYLT2*	0.12
DICER1	0.78	*MAPKAPK2*	0.64	*SAP130*	0.42	***YBX3***	0.68
DIMT1	0.41	*MAPRE2*	0.52	*SAP30*	0.28	*YIPF6*	0.45
DIP2B	0.71	*MARCH8*	0.39	*SARM1*	0.55	*YPEL5*	0.37
DKK1	0.07	*MARCH9*	0.37	*SART3*	0.25	*YTHDC2*	0.55

DKK3	0.78	*MARCKS*	0.66	*SBDS*	0.49	*YTHDF1*	0.72
DLGAP4	0.63	*MARK1*	0.51	*SBK1*	0.10	*YTHDF2*	0.61
DMD	0.72	*MARK3*	0.65	*SBNO1*	0.81	*YWHAE*	0.61
DMXL1	0.91	*MARK4*	0.46	*SCAF11*	0.84	***YY1***	0.57
DNAJA2	0.34	*MASP1*	0.70	*SCARA3*	0.74	***ZBTB10***	0.60
DNAJB2	0.45	*MAT2B*	0.19	*SCARF2*	0.59	***ZBTB16***	0.41
DNAJC1	0.31	*MAVS*	0.71	*SCD*	0.73	***ZBTB24***	0.12
DNAJC10	0.13	*MAZ*	0.73	*SCHIP1*	0.43	***ZBTB40***	0.44
DNAJC28	0.40	*MBD5*	0.52	*SCN1B*	0.81	***ZBTB41***	0.69
DNAJC30	0.23	*MBNL3*	0.84	*SCN2B*	0.42	*ZBTB47*	0.36
DNAL1	0.46	*MBOAT2*	0.47	*SCN4B*	0.46	***ZBTB6***	0.54
DNPEP	0.50	*MBP*	0.29	*SCOC*	0.41	***ZBTB7B***	0.66
DOCK1	0.87	*MBTPS2*	0.48	*SDC2*	0.23	***ZBTB9***	0.14
DOCK5	0.59	*MCC*	0.57	*SDK1*	0.66	*ZC2HC1A*	0.42
DPF2	0.62	*MCMBP*	0.40	*SEC16A*	0.48	*ZC3H11A*	0.63
DPH1	0.56	*MCPH1*	0.24	*SEC23A*	0.43	*ZC3H13*	0.69
DPH3	0.56	*MDN1*	0.83	*SEC24A*	0.67	*ZC3H14*	0.61
DPH5	0.65	*MECP2*	0.45	*SEC61A2*	0.43	*ZCCHC14*	0.61
DPP9	0.53	*MED1*	0.85	*SEC63*	0.57	*ZCCHC6*	0.81
DPY19L1	0.31	*MED13*	0.91	*SEH1L*	0.39	*ZDHHC14*	0.24
DPY19L4	0.54	*MED22*	0.46	*SEL1L*	0.59	*ZDHHC17*	0.59
DPYSL3	0.56	*MED28*	0.26	*SEL1L3*	0.60	*ZDHHC18*	0.45
DSN1	0.14	***MEF2C***	0.33	*SEMA4C*	0.48	*ZDHHC3*	0.31
DST	0.80	***MEF2D***	0.63	*SEMA4F*	0.61	*ZDHHC7*	0.58
DSTYK	0.43	***MEIS1***	0.25	*SEMA4G*	0.33	***ZEB1***	0.57
DTWD2	0.51	***MEIS2***	0.63	*SEMA6D*	0.44	***ZEB2***	0.56
DTX3L	0.74	*MEMO1*	0.58	*SENP5*	0.78	*ZER1*	0.51
DTX4	0.14	*METAP2*	0.64	*SEPHS1*	0.49	*ZFAND5*	0.20
DUSP1	0.35	*METTL24*	0.46	*SEPT11*	0.31	*ZFAND6*	0.58
DUSP3	0.65	*MFAP5*	0.83	*SEPT7*	0.33	***ZFHX2***	0.33
DUSP6	0.76	*MFSD9*	0.21	*SERBP1*	0.58	***ZFHX3***	0.74
DUSP7	0.37	***MGA***	0.75	*SERINC3*	0.67	***ZFHX4***	0.84
DUSP8	0.33	*MGAT4A*	0.37	*SERINC5*	0.52	***ZFPM2***	0.60
DUT	0.55	*MGAT4B*	0.34	*SERPINF1*	0.87	*ZFX*	0.78
DYNC1LI2	0.64	*MGAT5*	0.75	*SERTAD2*	0.40	*ZFYVE16*	0.73
DYNLL2	0.49	*MGLL*	0.42	*SERTM1*	0.46	*ZFYVE26*	0.49
DYRK1B	0.57	*MIB1*	0.76	*SESN1*	0.42	***ZHX1***	0.65
DZIP1	0.73	*MICAL2*	0.41	*SESN3*	0.50	***ZHX3***	0.43
E2F4	0.72	*MID1IP1*	0.34	*SESTD1*	0.61	***ZKSCAN1***	0.70
EDEM1	0.61	***MIER1***	0.75	*SETD1B*	0.55	*ZMYM2*	0.74
EEA1	0.77	***MIER3***	0.61	*SETD3*	0.71	*ZMYM4*	0.61
EFEMP1	0.71	*MKLN1*	0.71	*SETD5*	0.80	***ZNF148***	0.71
EFHD2	0.70	*MLLT3*	0.37	*SETDB1*	0.51	***ZNF181***	0.38

EGLN1	0.58	***MLX***	0.46	*SF3A1*	0.39	*ZNF207*	0.52
EGR3	0.49	***MLXIP***	0.67	*SFT2D2*	0.62	***ZNF24***	0.73
EHD1	0.46	*MMP16*	0.80	*SFXN1*	0.43	*ZNF281*	0.39
EI24	0.43	*MOB1A*	0.77	*SFXN5*	0.12	*ZNF282*	0.29
EIF2AK2	0.85	*MOB3B*	0.23	*SGIP1*	0.57	*ZNF319*	0.21
EIF2B2	0.36	*MOCS2*	0.39	*SGK3*	0.17	*ZNF362*	0.34
EIF2B5	0.64	*MON2*	0.64	*SGMS1*	0.24	***ZNF384***	0.63
EIF2S1	0.66	*MPHOSPH9*	0.54	*SGPP1*	0.45	***ZNF398***	0.32
EIF2S2	0.84	*MPLKIP*	0.25	*SH3BP5*	0.56	*ZNF451*	0.69
EIF3J	0.65	*MPRIP*	0.73	*SH3D19*	0.70	***ZNF462***	0.72
EIF4A2	0.75	*MRPL45*	0.76	*SH3GLB1*	0.40	*ZNF48*	0.31
EIF4B	0.59	*MRPL49*	0.53	*SH3RF1*	0.33	***ZNF507***	0.64
EIF4E	0.52	*MSANTD3*	0.29	*SH3RF2*	0.49	***ZNF521***	0.41
EIF4E2	0.49	*MSANTD4*	0.22	*SH3RF3*	0.20	*ZNF579*	0.49
EIF4E3	0.13	*MSRB1*	0.60	*SHOC2*	0.45	*ZNF592*	0.43
EIF4EBP2	0.72	*MSRB3*	0.71	*SHPRH*	0.83	*ZNF609*	0.74
EIF4H	0.45	*MT2A*	0.16	*SHROOM3*	0.15	*ZNF623*	0.18
EIF5A	0.85	*MTA3*	0.41	*SIAH1*	0.31	***ZNF629***	0.39
ELFN2	0.35	***MTF1***	0.76	*SIAH2*	0.36	***ZNF644***	0.76
ELK1	0.71	*MTHFD1*	0.77	*SIDT2*	0.36	*ZNF654*	0.71
ELK4	0.79	*MTMR10*	0.58	*SIK2*	0.52	*ZNF672*	0.60
ELMSAN1	0.31	*MTR*	0.67	*SIKE1*	0.75	***ZNF687***	0.16
ELOVL6	0.86	*MTRR*	0.56	*SIPA1L3*	0.50	*ZNF70*	0.44
EMC10	0.74	*MTUS1*	0.71	*SIRPA*	0.35	***ZNF746***	0.30
EMC2	0.37	*MVB12B*	0.37	*SIRT2*	0.85	*ZNF75A*	0.61
EMC8	0.72	***MXD4***	0.52	*SIRT3*	0.71	*ZNF793*	0.46
EML4	0.49	***MXI1***	0.15	***SIX1***	0.53	*ZNF827*	0.32
ENHO	0.33	*MYCBP*	0.35	***SKI***	0.28	*ZNF830*	0.17
ENTPD5	0.20	*MYH14*	0.23	***SKIL***	0.56	*ZNF879*	0.26
EPC1	0.53	*MYLK3*	0.61	*SLC15A4*	0.30	***ZNFX1***	0.85
EPG5	0.76	*MYNN*	0.50	*SLC1A5*	0.61	*ZNRF1*	0.66

Supplementary Table S5 Summary of pathway analysis from ClueGo for target genes clustered into the correlated modules from Nelore muscle co-expression network. Spreadsheet tabs are divided by module.

#miR.MEbrown

GOTerm	Group Pvalue	Nr. Genes	Associated Genes Found
Autophagy	0.0121	6	[ATG4D, EIF2S1, NRBF2, RAF1, RRAGD, WIPI2]
Protein processing in endoplasmic reticulum	0.0103	7	[DNAJA2, EIF2S1, PLAA, RAD23B, SEC61A2, UBE2D2, VCP]
Endocytosis	0.0001	12	[ARPC5L, CAPZA2, CHMP1A, CHMP4B, EHD1, EPS15, RAB5B, SNX12, TFRC, VPS37A, VPS4A, WWP1]
Ferroptosis	0.0277	3	[PCBP1, PCBP2, TFRC]
Long-term potentiation	0.0423	3	[CALM1, PPP3R1, RAF1]

#miR.MEcyan

GOTerm	Group PValue	Nr. Genes	Associated Genes Found
RNA transport	0.00031	21	[DDX20, EIF2B5, EIF2S1, EIF2S2, EIF3J, EIF4A2, EIF4B, EIF4E, EIF4E2, EIF4EBP2, GEMIN4, NUP153, NUP160, NUP50, PAIP1, PHAX, RPP14, SEH1L, THOC2, TPR, XPOT]
ErbB signaling pathway	0.00033	15	[ABL2, BTC, CBL, ELK1, GSK3B, HRAS, KRAS, MAP2K4, NCK1, PAK1, PAK2, PIK3CA, PRKCA, RAF1, RPS6KB1]
Autophagy	0.00026	19	[ATG12, ATG9A, BCL2, EIF2S1, HRAS, IGF1R, ITPR1, KRAS, LOC524719, MAP3K7, PIK3CA, RAF1, RPS6KB1, RRAGA, RRAGD, SH3GLB1, STX17, ULK2, WIPI2]
Protein processing in endoplasmic reticulum	0.00027	22	[AMFR, ATF6, BCL2, DNAJA2, DNAJB2, DNAJC1, DNAJC10, EIF2S1, LMAN1, LOC524719, MBTPS2, RAD23B, RNF185, SEC23A, SEC24A, SEC61A2, SEL1L, SSR1, UBE2D2, UBE2G2, UBE2J1, UGGT1]
Endocytosis	0.00000	38	[ACAP2, AP2A1, ARF5, ARFGAP2, ARFGEF2, CAPZA2, CBL, CHMP4C, CHMP6, CYTH3, EEA1, EPS15, GIT1, HRAS, IGF1R, IGF2R, ITCH, PARD3, PDCD6IP, PRKCZ, PSD3, RAB11FIP2, RAB22A, SH3GLB1, SMAD2, SMAD3, SNX1, SNX12, TFRC, UBB, VPS37A, VPS37C, VPS4A, VTA1, WASL, WIPF2, WWP1, ZFYVE16]
mTOR signaling pathway	0.00000	26	[ATP6V1C1, EIF4B, EIF4E, EIF4E2, FZD7, GRB10, GSK3B, HRAS, IGF1R, INSR, KRAS, LAMTOR3, LRP6, PIK3CA, PRKCA, RAF1, RICTOR, RPS6KA3, RPS6KB1, RRAGA, RRAGD, SEH1L, STRADB, TBC1D7, ULK2, WNT4]
Neurotrophin signaling pathway	0.00017	19	[BCL2, CALM1, CALM3, FOXO3, GSK3B, HRAS, IRAK2, KIDINS220, KRAS, MAPKAPK2, PIK3CA, PRDM4, PTPN11, RAC1, RAF1, RAPGEF1, RPS6KA3, SORT1, YWHAE]

Insulin signaling pathway	0.00004	22	[CALM1, CALM3, CBL, EIF4E, EIF4E2, ELK1, EXOC7, GSK3B, HRAS, INSR, KRAS, PHKB, PIK3CA, PPP1CB, PPP1R3D, PPP1R3F, PRKCZ, RAF1, RAPGEF1, RHOQ, RPS6KB1, SOCS4]
Thyroid hormone signaling pathway	0.00055	16	[CREBBP, GSK3B, HRAS, ITGAV, KRAS, MED1, MED13, NCOA1, NCOA2, NCOA3, NCOR1, PIK3CA, PRKCA, RAF1, THRA, WNT4]
Renal cell carcinoma	0.00025	13	[ARNT, CREBBP, CUL2, EGLN1, HRAS, KRAS, PAK1, PAK2, PIK3CA, PTPN11, RAC1, RAF1, RAPGEF1]
HIF-1 signaling pathway	0.00022	16	[ARNT, BCL2, CREBBP, CUL2, EGLN1, EIF4E, EIF4E2, IGF1R, IL6R, INSR, PDK1, PFKFB3, PIK3CA, PRKCA, RPS6KB1, TFRC]
Ubiquitin mediated proteolysis	0.00000	28	[ANAPC10, CBL, CDC27, CUL2, CUL3, CUL4A, FBXW7, HERC4, ITCH, PIAS1, PIAS2, RHOBTB2, SIAH1, UBA3, UBE2A, UBE2B, UBE2D2, UBE2E1, UBE2F, UBE2G2, UBE2J1, UBE2Q1, UBE2R2, UBE2W, UBE4A, UBR5, WWP1, XIAP]
Long-term potentiation	0.00030	13	[CALM1, CALM3, CREBBP, GNAQ, HRAS, ITPR1, KRAS, PPP1CB, PPP1R1A, PPP3CB, PRKCA, RAF1, RPS6KA3]
GnRH signaling pathway	0.00030	14	[ADCY2, CALM1, CALM3, ELK1, GNAQ, HRAS, ITPR1, KRAS, MAP2K4, MAP2K6, MAP3K2, MAP3K4, PRKCA, RAF1]
Oxytocin signaling pathway	0.00030	19	[ADCY2, CACNA2D1, CACNA2D2, CACNB1, CALM1, CALM3, ELK1, GNAQ, HRAS, ITPR1, KCNJ12, KRAS, MEF2C, PPP1CB, PPP1R12A, PPP3CB, PRKCA, RAF1, ROCK2]
Signaling pathways regulating pluripotency of stem cells	0.00001	20	[ACVR2A, APC, BMI1, FZD7, GSK3B, HRAS, IGF1R, IL6ST, KRAS, LIFR, PCGF5, PIK3CA, RAF1, SETDB1, SKIL, SMAD2, SMAD3, SMAD5, WNT4, ZFHX3]
Pathways in cancer	0.00001	51	[ADCY2, APC, APPL1, AR, ARHGEF12, ARNT, BCL2, CALM1, CALM3, CBL, CCDC6, CCNE1, CREBBP, CTBP2, CUL2, EGLN1, ELK1, EML4, FRAT2, FZD7, GNA13, GNAQ, GSK3B, GSTA4, HRAS, IGF1R, IL6R, IL6ST, ITGAV, KRAS, LRP6, NCOA1, NCOA3, PIK3CA, PRKCA, RAC1, RAF1, RALBP1, RB1, ROCK2, RPS6KB1, SMAD2, SMAD3, SP1, TPR, TRAF1, TRAF3, TRAF4, WNT4, XIAP, ZBTB16]
Hepatocellular carcinoma	0.00001	22	[APC, ARID2, BRD7, ELK1, FRAT2, FZD7, GSK3B, GSTA4, HRAS, IGF1R, KRAS, LRP6, PIK3CA, PRKCA, RAF1, RB1, RPS6KB1, SMAD2, SMAD3, SMARCA2, SMARCC1, WNT4]

#miR.MElightyellow

GOTerm	Group PValue	Nr. Genes	Associated Genes Found
Sphingolipid signaling pathway	0.0012	9	[ACER2, AKT3, GNAI1, NRAS, PIK3CB, PLD1, PPP2R1B, SGPP1, SPTLC2]
TGF-beta signaling pathway	0.0001	9	[FST, PPP2R1B, SMAD7, SMURF1, SMURF2, TGFB2, TGFBR1, TGFBR2, TGIF1]
Focal adhesion	0.0006	12	[AKT3, COL1A1, COL1A2, CRK, DOCK1, IGF1, ITGA8, ITGB3, PAK3, PDGFC, PIK3CB, VAV3]
Renal cell carcinoma	0.0003	7	[AKT3, CRK, HIF1A, NRAS, PAK3, PIK3CB, TGFB2]
Chronic myeloid leukemia	0.0003	8	[AKT3, CDK6, CRK, NRAS, PIK3CB, TGFB2, TGFBR1, TGFBR2]
Longevity regulating pathway	0.0000	10	[ADCY3, ADCY5, ADIPOQ, AKT3, CREB3L2, IGF1, IRS2, NRAS, PIK3CB, SESN3]
Longevity regulating pathway	0.0000	7	[ADCY3, ADCY5, AKT3, IGF1, IRS2, NRAS, PIK3CB]
Apelin signaling pathway	0.0000	10	[ADCY3, ADCY5, AKT3, GNAI1, JAG1, NRAS, NRF1, PDE3B, SLC8A1, TGFBR1]
Progesterone-mediated oocyte maturation	0.0000	9	[ADCY3, ADCY5, AKT3, CPEB1, GNAI1, IGF1, PDE3B, PIK3CB, RPS6KA1]
Regulation of lipolysis in adipocytes	0.0000	7	[ADCY3, ADCY5, AKT3, GNAI1, IRS2, PDE3B, PIK3CB]
Relaxin signaling pathway	0.0000	11	[ADCY3, ADCY5, AKT3, COL1A1, COL1A2, CREB3L2, GNAI1, NRAS, PIK3CB, TGFBR1, TGFBR2]

#miR.MEmidnightblue

GOTerm	Group PValue	Nr. Genes	Associated Genes Found
cGMP-PKG signaling pathway	0.0023	7	[ATP2B2, CALM1, GNA13, MEF2D, PPP3CB, PPP3R1, ROCK2]
Ubiquitin mediated proteolysis	0.0000	10	[CUL2, SIAH1, UBE2D2, UBE2D4, UBE2F, UBE2G1, UBE2J1, UBE2O, UBE2R2, WWP1]
Protein processing in endoplasmic reticulum	0.0018	8	[MAP2K7, RAD23B, SEC61A2, SSR1, UBE2D2, UBE2D4, UBE2G1, UBE2J1]
Insulin resistance	0.0028	6	[CRTC2, MLX, MLXIP, NR1H3, PIK3R2, PPP1R3D]
Fc epsilon RI signaling pathway	0.0026	3	[MAP2K7, PIK3R2, RAC1]
Neurotrophin signaling pathway	0.0026	6	[CALM1, FOXO3, MAP2K7, PIK3R2, PRDM4, RAC1]
Kaposi's sarcoma-associated herpesvirus infection	0.0026	9	[BECN1, CALM1, GNG7, MAP2K7, PIK3R2, PPP3CB, PPP3R1, RAC1, TRAF3]

#miR.MEmidnightblue

GOTerm	Group Pvalue	Nr. Genes	Associated Genes Found
Mucin type O-glycan biosynthesis	0.0023	3	[GALNT15, GALNT2, GALNT4]
p53 signaling pathway	0.0068	3	[IGF1, SESN3, THBS1]
Notch signaling pathway	0.0044	3	[DTX4, NUMBL, RBPJ]
ECM-receptor interaction	0.0030	4	[COL1A1, COL1A2, ITGB3, THBS1]
Protein digestion and absorption	0.0017	5	[COL14A1, COL1A1, COL1A2, COL3A1, COL5A2]